LIÈGE université
Sciences Appliquées

Strategic outline and sizing of district heating networks using a geographic information system

A thesis submitted in partial fulfillment of the requirements
for the degree of Doctor of Philosphy (Phd) in Engineering Science

by

Thibaut RÉSIMONT

Supervisor: Pierre DEWALLEF

DOCTORAL COLLEGE IN AEROSPACE AND MECHANICS

DECEMBER 2021

LIÈGE université
Sciences Appliquées

Strategic outline and sizing of district heating networks using a geographic information system

A thesis submitted in partial fulfillment of the requirements
for the degree of Doctor of Philosphy (Phd) in Engineering Science

by

Thibaut RÉSIMONT

Supervisor: Pierre DEWALLEF

DOCTORAL COLLEGE IN AEROSPACE AND MECHANICS

DECEMBER 2021

Strategic outline and sizing of district heating networks using a geographic information system.

Thermodynamics Laboratory
Aerospace and Mechanical Engineering Department
Faculty of Applied Sciences - University of Liège
Allée de la Découverte 17
B-4000, Liège (BELGIUM)
thibaut.resimont13@gmail.com
+32 498 79 95 36

Members of the Examination Committee:

Pr. Dr. Ir. Pierre Dewallef, *Supervisor*
(University of Liège, Belgium)

Pr. Dr. Ir. Grégoire Léonard
(University of Liège, Belgium)

Pr. Dr. Ir. Quentin Louveaux
(University of Liège, Belgium)

Pr. Dr. Ir. François Maréchal
(Ecole Polytechnique Fédérale de Lausanne, Switzerland)

Pr. Dr. Ir. Sylvain Quoilin
(KU Leuven, Belgium)

Pr. Dr. Ir. Sigrid Reiter
(University of Liège, Belgium)

Pr. Dr. Ir. Pascal Stabat
(Mines ParisTech, France)

"*It is every man's obligation to put back into the world at least the equivalent of what he takes out of it.*"

Albert Einstein

Abstract

The implementation of district heating networks into cities is a main topic in European Union policy plannings looking for sustainable solutions to reduce CO_2 emissions and improve global energy efficiency of heating systems. Compared to decentralized heating production units, district heating networks provide higher energy efficiencies due to larger units' sizes. However, their development into cities is generally limited by high initial investment costs and a long return on investment period. Therefore, policymakers and investors are reserved about new district heating networks projects because of the risks associated with the profitability of the project.

The development of optimization methods intended to draft efficient systems using heating consumption profiles into a prescribed geographic area are useful in this purpose. A Multi-Period Mixed Integer Linear Programming (MILP) model for the optimal outline and sizing of a third generation district heating network based on a Geographic Information System (GIS) is described in this thesis. The optimal outline aims to determine the location of the heating sources and the pipes into the network while the optimal sizing aims to size the pipes and the heating sources (including thermal storage solutions). This model can be used as a decision tool based on the maximization of the net cash flow (NCF) generated by the system from user-defined economic and physical parameters. This methodology aims to be applicable for a large range of problem sizes from small-scale to large-scale case studies while guarantying numerical robustness and fast solutions. This thesis provides new insights for the optimization of heating network systems:

1. A global review of the district heating network sector regarding the advantages, the technical breakthroughs and the economic features of these heating networks. Existing optimization models for heating networks are compared to identify their main attributes and to highlight the novelty and the benefits of this work compared to the existing ones.

2. Implementation of a decision tool based on a methodology enabling to design any new heating network from scratch based on a geographic information system and user-defined economic and urbanistic parameters.

3. Applications of the methodology to small-scale and large-scale case studies to show the replicability of the decision tool to a large range of heating networks.

4. Optimized heating networks from the decision tool are modelled in a dynamic way to illustrate the limits of the decision tool and its lack of accuracy regarding the physics of the system.

Keywords: District Heating, Energy Integration, Geographic Information System, Heat Storage, Mixed Integer Linear Programming, Multi-period, Optimization, Outline, Sizing.

Résumé

L'implémentation de réseaux de chaleur dans les villes est une problématique importante abordée par la politique énergétique de l'Union européenne à la recherche de solutions durables pour réduire les émissions de CO_2 et améliorer l'efficacité énergétique globale des systèmes de chauffage. Par rapport aux unités de production de chaleur décentralisées, les réseaux de chaleur offrent une efficacité énergétique plus élevée en raison de la plus grande taille des unités de production utilisées. Cependant, leur développement dans les villes est généralement limité par des coûts d'investissement initiaux élevés. Les investisseurs publics ou privés ont peur d'investir dans le cadre de nouveaux projets de réseaux en raison des risques liés à la rentabilité de ce type de projets.

Le développement de méthodes d'optimisation visant à tracer et dimensionner ces réseaux à partir de profils de consommation de chaleur donnés est utile à cette fin. Un modèle de programmation linéaire en nombres entiers mixtes sur plusieurs périodes (MILP) pour le tracé et dimensionnement optimal d'un réseau de chaleur de troisième génération basé sur un système d'information géographique (SIG) est développé dans cette thèse. Le tracé optimal vise à déterminer l'emplacement des sources de chaleur et des conduites au sein du réseau tandis que le dimensionnement optimal vise à dimensionner les conduites et les sources de chaleur (incluant des solutions de stockage thermique). Ce modèle peut être utilisé comme un outil de décision basé sur la maximisation du cash flow net généré par le réseau à partir de paramètres définis par l'utilisateur de l'outil. Cette méthodologie vise à être applicable à une large gamme de tailles de problèmes tout en garantissant une robustesse numérique et des solutions rapides. Cette thèse apporte de nouvelles pistes pour l'optimisation des réseaux de distribution de chaleur :

1. Une revue globale de la filière des réseaux de chaleur concernant leurs atouts, les avancées techniques dans le domaine et les aspects économiques liés à ces réseaux. Les modèles existants d'optimisation sont comparés afin d'identifier leurs principales caractéristiques et de mettre en évidence la nouveauté et les bénéfices de ce travail par rapport aux travaux existants.

2. Une implémentation d'un outil d'aide à la décision permettant de concevoir tout nouveau projet de réseau de chaleur à partir d'un système d'information géographique et de paramètres économiques et urbanistiques définis par l'utilisateur de l'outil.

3. Des applications de la méthodologie à des études de cas à petite et grande échelle pour montrer la réplicabilité de l'outil d'aide à la décision à une large gamme de réseaux de chaleur.

4. Les réseaux de chaleur optimisés à partir de l'outil de décision sont modélisés de manière dynamique pour illustrer les limites de l'outil de décision et son manque de précision vis-à-vis de la physique du système.

Mots-clés: Réseaux de chaleur, Intégration énergétique, SIG, Stockage thermique, MILP, Multi-période, Optimisation, Tracé, Dimensionnement.

Acknowledgements

At the end of this PhD journey, there are several people I would like to thank, people without whom I would not be at this stage after this 4-year adventure. Firstly, I would like to express my gratitude to my supervisor, Pr. Pierre Dewallef, which offered me the opportunity to start a PhD linked to a research project I worked on.

Regarding this research project, I would like to thank the European Union and the Walloon region which funded the VERDIR Tropical Plant Factory (Project EcoSystemPass) project with the European Funds for Regional Development (EFRD). This on the field project was an opportunity to give sense to my research and to share it with a broad public. About sharing my research and learning from other people, I also get in mind all the enriching encounters I have made during conferences, summer schools and events like "Ma Thèse en 180 secondes": cheers to all these interesting discussions about research but mostly to all these more relaxing moments spent in a friendly atmosphere with you.

But above all, I would like to thank people who supported me everyday during these 4 years. This thesis would have not been the same at all without you. A first thought comes to me obviously for my team mates working in the Thermodynamics laboratory. Thanks Marcelo, Ber' and Sam for helping me to keep the motivation to end up this thesis. Thanks also to Oli, Rémi, Sergio and all my other team mates with whom I keep such good memories from our adventures and team buildings. From the Chapiteau party to the gala dinners in conferences, I will keep a lot of good souvenirs. Thanks also to Richie, little Bernie and hombre José for all the funny moments and discussions we shared together around a cup of coffee. A particular attention and huge thanks is also dedicated to my colleagues helping me so much about the content of my work. Thanks Kévin for all your support and knowledge that you provided to me and more generally to the lab. Thanks also to Olivier for your high-quality work provided in the frame of the research project we worked on together. And also a big thanks to Eva for your valuable support during this last year helping me to finalize this thesis.

Saving the best for last, I want really to thank with all of my heart my mother and Pauline without whom I would not be who I am today and I would have not accomplished all I have accomplished today. Thanks for your unconditional support and presence helping me to face some difficult circumstances.

Thibaut Résimont

List of Publications

- Résimont, T; Louveaux, Q; Dewallef, P. Optimization Tool for the Strategic Outline and Sizing of District Heating Networks Using a Geographic Information System. In: *Energies*, vol. 14, p. 5575, Sep. 2021. ISSN: 1996-1073. DOI: *10.3390/en14175575*

- Résimont, T; Thomé, O; Joskin, E, Dewallef, P. Tool for the Optimization of the Sizing and the Outline of District Heating Networks using a Geographic Information System: Application to a Real Case Study. In: *Proceedings of ECOS 2021 – The 34th International Conference On Efficiency, Cost, Optimization, Simulation and Environmental Impact of Energy Systems*. 2021.

- Résimont, T; Altes-Buch, Q; Sartor K; Dewallef, P. Economic and environmental comparison of a centralized and a decentralized heating production for. In: *Proceedings of SSB 2018 – The 10th International Conference On System Simulation in Buildings*. 2018.

- Résimont, T; Sartor, K; Dewallef, P. Thermo-Economic Evaluation of a Virtual District Heating Network Using Dynamic Simulation. In: *Proceedings of ECOS 2018 – The 31st International Conference On Efficiency, Cost, Optimization, Simulation and Environmental Impact of Energy Systems*. 2018.

- Sartor, K; Dickes, R; Résimont, T; Dewallef, P. Experimental validation of heat transport modeling in large solar thermal plant. In: *Proceedings of ECOS 2018 – The 31st International Conference On Efficiency, Cost, Optimization, Simulation and Environmental Impact of Energy Systems*. 2018.

Contents

Abstract vii

Résumé ix

Acknowledgements xi

Contents iii

List of Figures vii

List of Tables xi

List of Acronyms xiii

List of Symbols xv

List of Subscripts xvii

1 Introduction 1
- 1.1 Context . . . 1
- 1.2 Principle of the district heating network . . . 5
  - 1.2.1 Heating production and storage units . . . 9
  - 1.2.2 Heating consumers . . . 13
    - 1.2.2.1 Pricing models applied to the heating consumers 14
  - 1.2.3 Pipes . . . 19
  - 1.2.4 Pros and cons of district heating networks . . . 21
- 1.3 Problem statement . . . 22
  - 1.3.1 Literature review . . . 24
- 1.4 Manuscript overview . . . 37

2 Presentation of the decision tool 39
- 2.1 Inputs - Assessment of the heating demands . . . 42
  - 2.1.1 Collection of annual heating demand data . . . 42
  - 2.1.2 Generation of hourly heating demands profiles . . . 43
- 2.2 Preprocessing - Selection of representative periods for heat demands 45
- 2.3 Optimization model . . . 49
  - 2.3.1 Quick reminder on mathematical optimization . . . 49
    - 2.3.1.1 Linear optimization . . . 50
  - 2.3.2 Sets . . . 52
  - 2.3.3 Constraints . . . 53

2.3.3.1 Energy balance at the vertices and the edges of the graph . . . 53
2.3.3.2 Maximum thermal capacity at the edges and vertices of the graph . . . 67
2.3.3.3 Link between pipes over some edges of the graph 71
2.3.4 Objective function . . . 72
2.3.4.1 Capital expenditures (CAPEX) . . . 73
2.3.4.2 Operating expenditures (OPEX) . . . 76
2.3.4.3 Heating revenues . . . 80
2.4 Outputs . . . 81
2.4.1 Mapping into the Geographic Information System . . . 81
2.4.2 Specific cost . . . 82
2.4.3 Net Present Value . . . 83
2.4.4 Savings of CO_2 emissions . . . 83
2.4.5 Repartition of the pipes diameters . . . 84
2.5 Conclusion . . . 85

3 Tests of the decision tool on a small-scale theoretical case study 89
3.1 Description of the case study . . . 89
3.1.1 Definition of the scenarios . . . 91
3.1.2 Dwellings models . . . 93
3.2 Influence of the heating demand of the neighbourhood . . . 97
3.3 Influence of the heating sales price r_{heat} . . . 103
3.4 Influence of the connection rate p_j . . . 105
3.5 Influence of the actualization rate a . . . 107
3.6 Influence of the limited pipe diameters into the streets . . . 109
3.7 Influence of the limited thermal capacities at the heating power plants . . . 111
3.8 Influence of the selection of the representative days on the optimal solution and the computation time . . . 113
3.9 Integration of thermal storages solutions . . . 114
3.9.1 Limitation on the heating capacity . . . 116
3.9.2 Variable heating production costs using heat pumps . . . 120
3.9.3 Limitation on the heating availability with solar collectors 123
3.9.4 CAPEX of the heating sources . . . 126
3.9.5 Location of the thermal storage . . . 127
3.10 Outline and sizing of a heating network from a blank sheet . . . 130
3.11 Comparison of a centralized and a decentralized heating production scenario . . . 134
3.12 Comparison of the linear and piecewise linear optimization formulations . . . 137
3.13 Conclusion . . . 139

4 Calibration of the optimization model from dynamic simulations 141
4.1 Description of the dynamic model . . . 142
4.1.1 Piping model . . . 142
4.1.1.1 Finite Volume Model . . . 143
4.1.1.2 Plug Flow Model . . . 145

4.1.1.3 Comparison of the finite volume and plug flow method . . . 147
4.1.2 Heating source model . . . 150
4.1.3 Substation model . . . 150
4.2 Dynamic simulations of the theoretical case study . . . 151
4.2.1 Heat losses for a 90-60°C operating network . . . 152
4.2.1.1 Calibration on the parameters for the assessment of the heat losses . . . 154
4.2.1.2 Temperature profiles over the network . . . 156
4.3 Conclusion . . . 158

5 Application of the decision tool to a large-scale real case study 159
5.1 Introduction . . . 160
5.2 Case Study . . . 160
5.2.1 Influence of the heating sales price on the network . . . 161
5.2.2 Influence of the connection rate on the network . . . 163
5.2.3 Influence of the greenhouse as a new heating consumer on the network . . . 164
5.2.4 Integration of new heating consumers on the available building surface . . . 165
5.3 Influence of the combined heat and power plant on the heating network . . . 167
5.4 Conclusion . . . 169

6 Conclusions and perspectives 171

A Optimization variables 179

B Parameters of the pieceiwse linearization 180

C Data for heating technologies in district heating networks 181

D Data for pipes 183

E Substations costs 184

F Parameters of the heat pumps 185

G Features of the dwellings of the case study 186

H Repartition of the dwellings over the different scenarios of the theoretical case study 187

I Coordinates of the nodes of the test case 192

Bibliography 193

List of Figures

1.1 Breakdown of the greenhouse gases emissions among the different sectors in the world in 2016 [1]. 1
1.2 Breakdown of the final energy demand among the different sectors in Belgium in 2015 [2]. 2
1.3 Heating context in European Union [3, 4]. 2
1.4 Breakdown of the energy mix by technology and by country into the EU27 [3]. 3
1.5 Illustrative scheme of a district heating network. 5
1.6 Evolution of district heating from first to fourth generation networks [12]. 7
1.7 Principle of a 5th generation heating and cooling network (Paris-Saclay thermal energy network) [16]. 8
1.8 Fuels mix into CHP in 2017 in EU [20]. 9
1.9 Geothermal resources in EU in 2020 [23]. 10
1.10 Waste treatment in EU between 1996 and 2018 [34]. 11
1.11 Review of the existing storage technologies [13]. 12
1.12 Costs for different existing thermal storages [41]. 13
1.13 Aggregation effect over a district heating network. 14
1.14 A substation and its main components [42]. 15
1.15 Operating principle of a calorimeter [43]. 15
1.16 Billing of heat consumption to a consumer for a heating period (adapted from [45]). 18
1.17 Pipes of a district heating network. 20
1.18 Illustration of the EcoSystemPass research project. 23

2.1 Methodology of the decision tool for the strategic planning of a district heating network project. 41
2.2 Readjusted methodology for the selection of representative time periods for a given year. 47
2.3 Selection of representative time periods. 48
2.4 Simplex algorithm [86]. 51
2.5 Branch-and-bound algorithm [86]. 51
2.6 Graph representation of a neighbourhood of 16 streets with 13 intersections. 52
2.7 Energy balances at the vertices and the edges of the graph 53
2.8 Physical representation of a 2-pipes distribution system. 55
2.9 Geometry of the pipes of a heating network. 55
2.10 Reynolds number as a function of the power flow. 56
2.11 Heat losses into the pipes as a function of the power flows. 58
2.12 Characterization of the heat losses. 58

2.13 Heat losses for each pipe diameter over the whole range of power flows. . . . 59
2.14 Picewise linear approximation of the heat losses as a function of their maximum power flows. . . . 60
2.15 Definition of intra and inter-periods for the representation of the thermal storage units. . . . 62
2.16 Thermal resistances linked to a thermal storage. . . . 64
2.17 Characterization of the thermal storages. . . . 67
2.18 Solar radiation over a solar panel inclined with an angle i and an orientation γ. . . . 68
2.19 Solar time coordinate system. . . . 70
2.20 Solar capacity in Liège. . . . 70
2.21 Pipes costs from manufacturer's data 74
2.22 Substations costs. . . . 76
2.23 COP for heat pumps using a polynomial model for an air-to-water heat pump with water at 90°C. . . . 79
2.24 Heating production cost with a heat pump 80
2.25 Mapping into a Geographic Information System. . . . 82
2.26 Comparison of the specific cost with a gas boiler or a heating network. 82
2.27 Net Present Value of a project over 30 years. . . . 83
2.28 Repartition of the pipes diameters into the heating network. . . . 84

3.1 Case Study with 16 streets and 3 potential existing heating sources. 90
3.2 Yearly heating demands for the 4 different scenarios. . . . 92
3.3 Consumptions over 1 week for the Scenario 2. . . . 92
3.4 Consumptions of the greenhouse and the poorly thermally insulated dwellings. . . . 93
3.5 Division of the detached (D) dwellings into zones: first (left) and second (right) floors. . . . 94
3.6 Total consumption over a reference year of the different dwellings. 95
3.7 Dwellings heating load profiles as a function of the outdoor temperature. . . . 96
3.8 Gas prices in the European Union [107]. . . . 97
3.9 Outline of the heating network for the 4 scenarios. . . . 98
3.10 Pipes diameters for the 2 first scenarios. . . . 99
3.11 Pipes diameters for Scenarios 2 and 3. . . . 100
3.12 Pipes diameters for Scenarios 3 and 4. . . . 100
3.13 Net Present Value of the project for the 4 scenarios. . . . 101
3.14 Outline of the heating network project with a decrease of the heating sales price from 0.07€/kWh to 0.04€/kWh. . . . 104
3.15 Net Present Value of the heating network project with a decrease of the heating sales price. . . . 105
3.16 Outline of the heating network project with a decrease of the connection rate. . . . 106
3.17 Net Present Value of the heating network project for Scenario 3 with a decrease of the connection rate. . . . 107
3.18 Outline of the network for different actualization rates. . . . 108
3.19 CAPEX and OPEX actualization factors. . . . 109

3.20 Outline of the heating network project with a zero diameter constraint at edges e_6 and e_{22}. 110
3.21 Outline of the heating network project with a limitation on the heating capacity. 111
3.22 Repartition of the diameters with a limitation on the heating capacity. 112
3.23 Influence of the thermal storage on the outline of the heating network project with a limitation on the heating capacity of 2.5 MW_{th} 116
3.24 Loading and unloading of the thermal storage compared to the heating demand of the network with a limited capacity of 2.5 MW_{th}.117
3.25 Influence of the thermal storage on the outline of the heating network project with a limitation on the heating capacity of 1.25 MW_{th}.118
3.26 Loading and unloading of the thermal storage compared to the heating demand of the network with a limted capacity of 1.25 MW_{th}.119
3.27 Outline of the heating network project for a scenario with a heat pump capacity of 10 MW_{th}. 120
3.28 Link between the levels of the thermal storage and the heating production costs. 121
3.29 Outline of a heating network with solar collectors and a thermal storage. 123
3.30 Outline with solar collectors of 100 000 m^2. 124
3.31 Storage dynamics with 10 000 m^2 solar collectors and a thermal storage. 125
3.32 Outline of the heating network with different CAPEX for the heating sources. 126
3.33 Outline of the heating network project for a scenario with a heat pump and thermal storage at node v_1 or v_{13}. 128
3.34 Repartition of the diameters for a scenario with a heat pump and thermal storage at node v_1 or v_{13}. 129
3.35 Optimal outline for a new heating network starting from a "blank sheet". 131
3.36 Dynamics of the heating production for an available surface of 1 000 m^2 without thermal storage. 132
3.37 Dynamics of the heating production for an available surface of 1 000 m^2 with thermal storage. 133
3.38 Load Duration Curve for the different heating production technologies. 135
3.39 Evolution of the Net Present Value of the project over 50 years. . 136
3.40 Pipes diameters for both formulations. 137
3.41 Load Duration Curve of the studied neighbourhood. 138

4.1 Finite Volume Method. 143
4.2 Principle of the Plug Flow Method. 146
4.3 Case study: 1km long pipe with an increase of temperature of 10°C at the inlet. 147
4.4 Evolution of the temperature with a finite volume model in *Dymola* for different discretization scales. 148
4.5 Evolution of the temperature with a PFM in Dymola. 148

4.6 Model of pipes with heat losses in *Dymola*. 149
4.7 Model for the heating source. 150
4.8 Map of the optimal network sized by the decision tool. 151
4.9 Dynamic model of the optimal network sized by the decision tool. 152
4.10 Comparison of the heat losses with the optimization model and the dynamic simulations. 152
4.11 Results with the calibrated optimization model. 155
4.12 Temperature decrease along the network for nominal conditions. . 156
4.13 Temperature profile along different branches of the network. . . . 157

5.1 Representation of the case study of Herstal. 160
5.2 Outline of the network for different heating sales prices. 161
5.3 Number of connected streets for different heating sales prices. . . 162
5.4 Influence on the net present value of the project for a heating sales price of (a) 0.07€/kWh (b) 0.05€/kWh. 163
5.5 Outline of the network for different connection rates. 163
5.6 Number of streets connected to the network for a connection rate from 80% to 20%. 164
5.7 Optimal network with the inclusion of a new neighourhood. . . . 166
5.8 Diagram of the combined heat and power plant of Intradel (Herstal, Belgium). 167

List of Tables

1.1 Standardized district heating pipes sizes. 21
1.2 Comparison of optimization methods from a literature review . . 26
1.3 Non-exhaustive review of optimization models for district heating networks. 27

2.1 Categories of dwellings for the residential and tertiary sector. . . . 42
2.2 Categories of optimization techniques. 50
2.3 CAPEX and OPEX over the lifetime of the project 73

3.1 Main features of the dwellings constitutive of the case study . . . 90
3.2 Properties of the power plants 93
3.3 Comparison of the 4 initial scenarios. 98
3.4 Economic comparison of Senario 3 with a decrease of the heating sales price from 0.07€/kWh to 0.04€/kWh. 103
3.5 Economic comparison of Scenario 3 with a decrease of the connection rate from 100% to 40%. 106
3.6 Economic comparison with for different actualization rates. 108
3.7 Economic comparison of Scenario 3 with a limitation on the pipes diameters linking nodes v_4 and v_9. 110
3.8 Economic comparison with a limitation on heating capacity of 2.5 MW_{th} at each power plant. 112
3.9 Comparison of the model with 8760H and 144H. 113
3.10 Comparison for a limited heating capacity of 2.5 MW_{th}. 116
3.11 Economic comparison for a limited heating capacity of 1.25 MW_{th}. 118
3.12 Economic comparison with 10 MW_{th} heat pumps and a thermal storage. 121
3.13 Economic comparison with a maximum heat pump capacity of 50 MW_{th}. 122
3.14 Economic comparison with solar collectors and thermal storage. . 124
3.15 Economic comparison with solar collectors of 100 000 m^2. 125
3.16 Economic comparison with CAPEX = 600 €/kW. 127
3.17 Economic comparison with CAPEX = 1 000 €/kW. 127
3.18 Comparison with thermal storage at node v_1 or v_{13}. 128
3.19 Economic comparison of Scenario 3 starting from scratch. 131
3.20 Capital expenses for gas boilers. 134
3.21 Operating expenses for gas boilers. 135
3.22 Comparison of the costs and CO_2 emissions with a centralized and decentralized heating production scenario for a 30 years lifetime project. 135

3.23 Comparison of the model with a purely linear and piecewise linear formulation for 144H. 138

4.1 Computational performance with Finite Volume Model (FVM) and Plug Flow Model (PFM). 149
4.2 Comparison of the heat losses with the optimization model and the dynamic simulations. 153
4.3 Comparison of the results with the initial and the calibrated optimization model. 154
4.4 Comparison of the heat losses with the calibrated optimization model and the dynamic simulations. 155

5.1 Influence of the greenhouse on the economic outputs 164
5.2 Influence of the size of the greenhouse on the economic outputs . 165
5.3 Influence of the integration of a new neighbourhood. 166
5.4 Influence of the greenhouse on the economic outputs 168

A.1 Continuous and discrete variables of the problem. 179

B.1 Parameters of the piecewise linearization of the pipes costs and heat losses 180

C.1 Heating technologies data [4, 98, 109]. 182

D.1 Pipes costs as a function of their diameters 183

E.1 Substations costs 184

F.1 Heat pump parameters for a Daikin Altherma heat pump 185

G.1 Features of the dwellings constitutive of the case study 186

H.1 Repartition of the dwellings for Scenario 1. 188
H.2 Repartition of the dwellings for Scenario 2. 189
H.3 Repartition of the dwellings for Scenario 3. 190
H.4 Repartition of the dwellings for Scenario 4. 191

I.1 Coordinates of the nodes of the theoretical case study in Chapter 3.192

List of Acronyms

ATES	**A**quifer **T**hermal **E**nergy **S**torage
BTES	**B**orehole **T**hermal **E**nergy **S**torage
CAPEX	**CAP**ital **EX**penditure
CF	**C**apacity **F**actor
CHP	**C**ombined **H**eat and **P**ower
COP	**C**oefficient **O**f **P**erformance
DSM	**D**emand **S**ide **M**anagement
EU	**E**uropean **U**nion
FWR	**F**rame to **W**indows **R**atio
GIS	**G**eographic **I**nformation **S**ystem
LF	**L**oad **F**actor
MILP	**M**ixed **I**nteger **L**inear **P**rogramming
MINLP	**M**ixed **I**nteger **N**on **L**inear **P**rogramming
NCF	**N**et **C**ash **F**low
NPV	**N**et **P**resent **V**alue
OPEX	**OP**erating **EX**penditure
PEI	**P**rimary **E**nergy **I**mport
PLR	**P**art **L**oad **R**atio
PTES	**P**it **T**hermal **E**nergy **S**torage
TES	**T**hermal **E**nergy **S**torage
TF	**T**ransfer **F**unction
VAT	**V**alue-**A**dded **T**ax

List of Symbols

Symbol	Name	Unit
A	area	m^2
a	actualization rate	- or %
b	choice or not of a power range	0 or 1
C	costs	€
C	thermal capacity	J/K
c	specific costs	$\frac{€}{kWh}$ or $\frac{€}{kW}$
c_p	specific heat capacity	$\frac{J}{kg.K}$
D	diameter	m
e	total enthalpy	J/kg
F	solar or shading factor	-
f	actualization factor	- or %
G	solar irradiation	$\frac{kWh}{m^2}$
g	gravity acceleration	$\frac{m^2}{s}$
H	height or depth	m
h	angular height	°,"
h	enthalpy	J/kg
i	inclination of a solar panel	°
k	thermal conductivity	$\frac{W}{m.K}$
L	length	m
l	pipe location into a city or not	0 or 1
m	mandatory building of a pipe	0 or 1
$\dot{m}$	mass flow rate	$\frac{kg}{s}$
N_{years}	lifetime of the project	years
N_{repr}	number of representative periods	-
P	Pressure	Pa
$\dot{P}$	power flow	kW
p	connection ratio of consumers to a street	- or %
Q	heating content	kWh
$\dot{Q}$	heating demand or production	kW
R	revenues	€
R	thermal resistance	K/W
r	specific revenues	$\frac{€}{kWh}$
S	spacing between 2 pipes	m
T	temperature	°C or K
th	thickness insulation	m
U	internal energy	J
u	use or not of a pipe	0 or 1

V	volume	m^3
v	velocity	$\frac{m}{s}$
$\dot{W}$	pumping power	kW
w	weight of a time period	-
x	building or not of a pipe	0 or 1
y	coefficients of a linear regression	[0,1]
z	azimut or relative height	°'" or m
α	heat losses coefficient	-
ΔP	pressure losses	Pa
ΔT	temperature difference	K or °C
Δt	duration of a timestep	h
δ	declination of the Earth	°'"
η	efficiency	-
γ	orientation angle	°'"
λ	friction factor	-
ω	solar time	°'"
ϕ	geographic latitude	°'"
ρ	density	$\frac{kg}{m^3}$
θ	temperature difference	°C or K
τ	thermal time constant	s
ξ	geographic longitude	°'"

List of Subscripts

a	dwelling type
$avail$	available
$build$	building
DHN	District Heating Network
$diam$	diameter
$elec$	electricity
eq	equivalent
ex	exhaust
fl	full-load
$friction, reg$	regular friction
$friction, sing$	singular friction
gd	ground
geo	geometric
HP	Heat Pump
i	vertex ID
in	incoming
inf	air infiltrations
ins	insulation
int	internal gains
j	edge ID
l	dwelling ID
m	heating technology ID
nom	nominal
$load$	loading
$loss$	heat losses
max	maximum
out	outcoming
p	pressure
pl	part-load
$prod$	production
rad	radial
$repr$	representative
s	cross-section
sol	solar
sto	storage
su	supply
sub	substation
sur	surroundings
t	timestep

tech	technology
tot	total
TU	Terminal Units
unload	unloading
V	volume
vent	ventilation
w	water
wd	day of the week

To Pauline and my mother.

Chapter 1

Introduction

"The best time to plant a tree was 20 years ago. The second best time is now."

—Chinese Proverb

1.1 Context

In the context of current environmental problems, issues related to the energy transition are of paramount importance for the upcoming years. The question of energy policy to meet these challenges concerns all parts of the population: political decision-makers, industrial leaders and citizens. The establishment of international agreements, like the *COP 21* agreements, between different nations on the basis of concrete objectives (e.g. the reduction of greenhouse gases emissions through the decarbonization of the energy sector) to be achieved for various time horizons is therefore a first solution to these environmental issues.

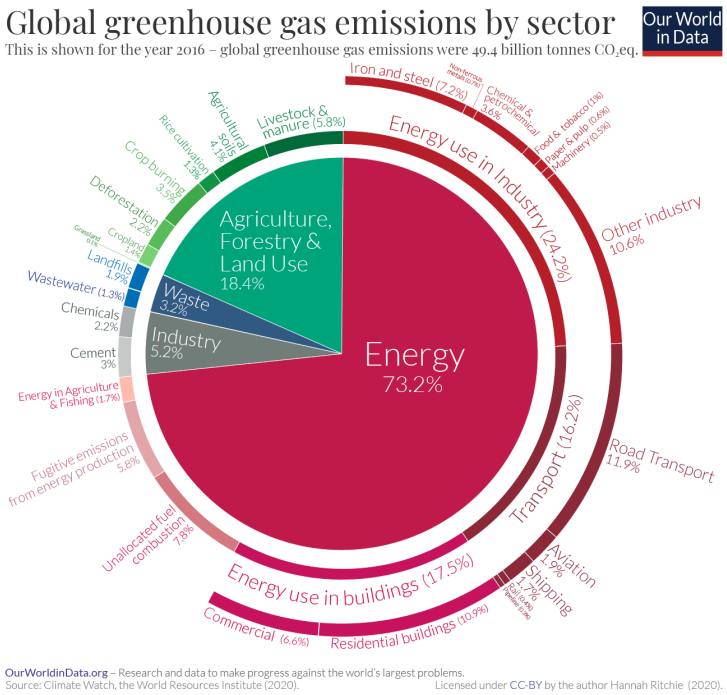

FIGURE 1.1: Breakdown of the greenhouse gases emissions among the different sectors in the world in 2016 [1].

The reduction of greenhouse gases (GHG) emissions is indeed one of the key factors in today's society in order to respond to short and medium-term climate issues. In the energy sector, this reduction of GHG emissions requires a shift from the use of conventional fossil fuels (oil, gas and coal) to renewable energy sources (solar, biomass, waste incineration, etc.) while a significant part of greenhouse gases emissions comes from the energy sector [1] (as illustrated in Figure 1.1 for the year 2016). Therefore, it is essential to focus on this sector in order to find solutions to reduce GHG emissions. The current problem lies in the fact that renewable energy production relies mainly on the electricity sector. The heating production sector, standing for approximately 50% of the final energy demand in Europe in 2015 [2] (cf. Figure 1.2 for Belgium), also seems worth considering. As illustrated in Figure 1.3, the current heating energy mix in the European Union (EU) relies mainly on fossil fuels [3] while several heating production alternatives with low carbon emissions exist [4].

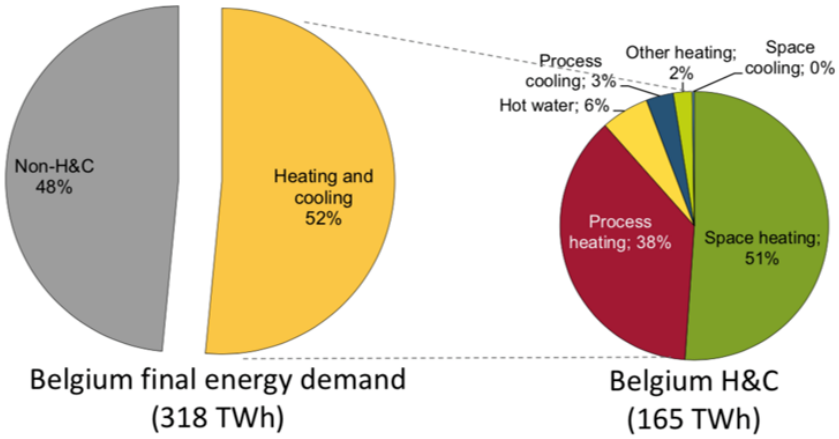

FIGURE 1.2: Breakdown of the final energy demand among the different sectors in Belgium in 2015 [2].

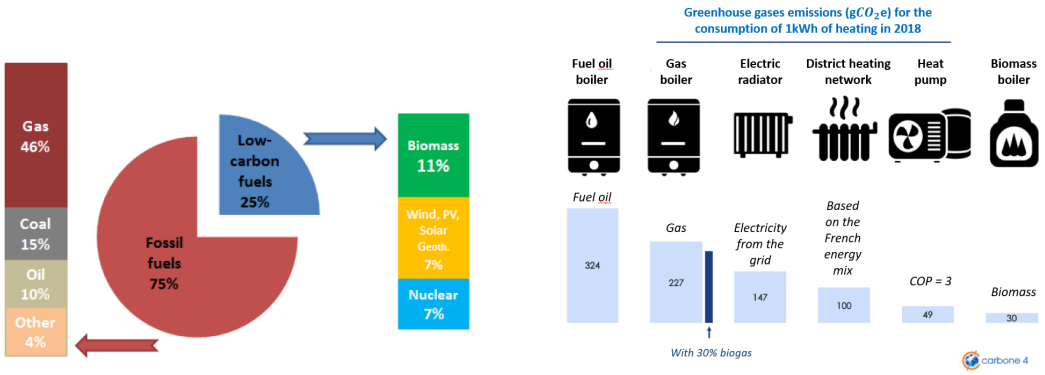

(a) Heating production in EU by technology in 2015

(b) Greenhouse gases emissions by technology

FIGURE 1.3: Heating context in European Union [3, 4].

Moreover, despite the reduction in heating consumption in buildings, this heating demand is going to increase in the upcoming years due to a growing demographic trend that is increasingly concentrated in cities [5]. In order to increase the energy share into the energy mix from low-carbon sources, the Member States of the European Union have adopted renewable energy quota targets to be achieved through the *National Renewable Energy Action Plans* [6] in their energy mix. These *National Renewable Energy Action Plans* determine the action plans undertaken by the different EU countries to achieve their individual targets in the electricity, heating and mobility sectors. These action plans also discuss the policy measures to set up at local, regional and national level to achieve these targets. As illustrated in Figure 1.4, the share of district heating technology used in the national energy mix of each country tends to be higher in the Scandinavian countries, which have already developed more intensively the use of district networks in their heating and cooling solutions.

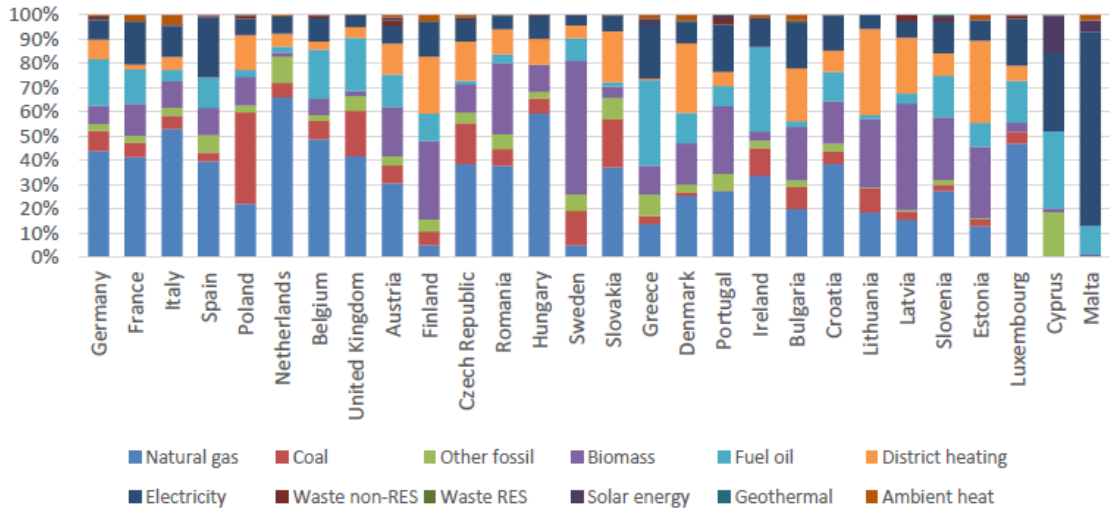

FIGURE 1.4: Breakdown of the energy mix by technology and by country into the EU27 [3].

Denmark, for example, illustrates this trend by having replaced part of its natural gas consumption by the introduction of biomass as an energy source and by the significant share of heat supply with district heating networks. This combination of biomass and heating networks therefore makes it possible to reduce the share of natural gas consumption in their energy mix compared with countries such as Belgium, France or Germany, where the share of natural gas in the energy mix is over 40 %. This global transition towards lower carbon emission district heating systems through a partial decarbonisation of the energy mix could reduce CO_2 emissions by up to 58% by 2050, allowing to limit the temperature increase only between 2 to 3°C [7]. Moreover, the political support given by the European Union in terms of financing for energy efficiency in the heating and cooling sector is not negligible: the European Structural and Investment Fund (ESIF) will allocate €19 billion to support energy efficiency and €6 billion to support renewable energy and district heating networks [3].

Heating technologies with low-carbon emissions like heat pumps and biomass boilers are promising for the future energy framework. However, these technologies at the small-scale level have a quite variable efficiency due to the fluctuation of the heating production to satisfy a variable heating demand over the year. This directly affects the total heating production cost. Better efficiencies are reached with large-scale units integrated into heating networks and combined with thermal storage units. Moreover, district heating makes it possible to create synergies between different energy carriers like heat and electricity by integrating locally residual heating resources such as waste incineration units for example or heat pumps using the electricity surplus from renewable electricity sources. However, these solutions require a large initial investment cost which is supported from public authorities or participatory financing to be viable [8]. These district heating networks could therefore be one of the means to respond to the energy transition that is expected over the next few years.

District heating networks appear thus to be a viable solution for the future but are not yet widely implemented in urban communities because of their relatively high initial investment costs. The building of district heating networks requires large fundings for the implementation of projects whose primary purpose is the installation of pipes to provide the heat produced at prescribed heating sources to the consumers by means of a heat transfer fluid. These site works, in addition to the considerable time required for their completion and the possible opposition of citizens to their implementation, are responsible for long-term investments for investors interested in investigating the field of district heating networks. In an attempt to promote investment in these networks in urban communities, the development of decision tools for the outline and sizing of district heating networks might be useful in order to guarantee a certain return on investment to the investors involved in the development of these new urban heating communities compared to the current conventional means of decentralised heating production such as gas and oil-fired boilers.

Heating networks are not very common in Belgium, especially in Wallonia, and remain very small-scale networks (up to 1km). As previously explained, the main barrier to the development of these networks relies on the large part of the initial investment cost. A simple and robust tool allowing a private operator or a local authority to estimate the opportunities for exploiting non-conventional and renewable energy sources, as well as their economic and environmental impact, would be a powerful incentive to develop this type of technology in Wallonia. It would also make it possible to test the influence, at the scale of Wallonia, of different policies to support heating networks. For this purpose, the *EcoSystemPass* project has been funded by the *European Regional Development Fund (ERDF)* to implement a decision support tool dedicated to the simulation and multi-scale energy optimisation of urban agriculture sites in a first phase and, in a second phase, to extend it to urban sites. This decision support tool aims for defining the best synergy scenarios between the available energy sources and the heating consumers by integrating different energy transport and conversion techniques.

1.2 Principle of the district heating network

District heating networks provide heat for space heating and domestic hot water in the residential, public and industrial sectors. The heat is produced centrally from one or several existing heating sources and distributed to the consumers thanks to a heat transfer fluid (generally water) flowing through pipes buried into the ground. The heating sources feeding these networks are of several types: combined heat and power (CHP) plants producing heat and electricity simultaneously, gas or biomass boilers for heating only, waste heat from industrial processes, geothermal sources, solar heat, heat from waste incineration or heat pumps. District heating networks enable significant primary energy savings through large-scale energy production. However, these technologies are generally associated with significant heat losses due to the distribution network between heating producers and consumers. In order to minimise these heat losses that are proportional to the distance between heating producers and consumers and the diameters of the pipes, district heating networks are of greater interest in densely populated (and therefore energy-dense) urban areas [9]. A schematic illustration of a district heating network is shown in Figure 1.5.

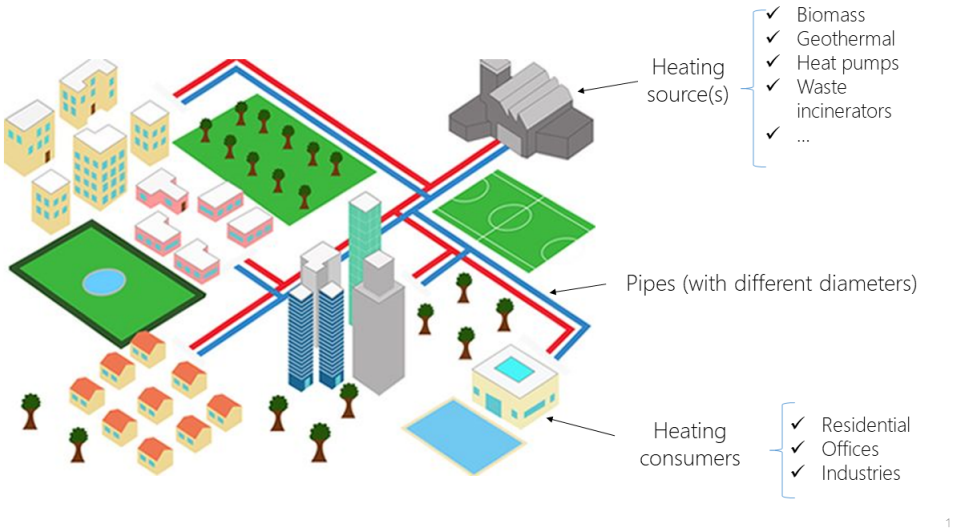

FIGURE 1.5: Illustrative scheme of a district heating network.

These networks have been involved in the energy sector for over a century and have undergone a significant technological breakthrough since their introduction as illustrated in Figure 1.6. The first generation of district heating networks was developed from 1880 in the United States using coal-based heating sources for the production of high-pressure steam distributed in concrete pipes. This high-temperature steam induced a lot of heat losses into the pipes such that from the 1930s, a transition to second generation district heating networks took place [10].

These second-generation district heating networks used coal and oil as fuels to provide pressurized hot water (instead of steam) at temperatures between

100 and 150°C. The main novelty of these networks was the introduction of cogeneration plants which increase the overall energy efficiency of the system while decreasing the temperature levels in the network and thus indirectly reducing heat losses along the network pipes. These networks were strongly developed between the 1930s and 1970s, especially after the Second World War in the communist Soviet countries, with the idea of an energy community [11].

These networks, based solely on the idea of a competitive solution in terms of heating price and not on the energy efficiency, have been replaced by third-generation heating networks. These networks are the networks currently in place in most countries already equipped with heating networks since they date from the early 1970s. The introduction of this new generation of networks was justified by the two consecutive oil crises of 1973 and 1979 and was particularly marked in the Scandinavian countries. The main goal of this type of network was then to increase the overall energy efficiency of the system by further reducing the temperature levels within the network (below 100°C) while using local energy resources (such as biomass in Sweden or waste incinerators in Denmark for example). Some networks even use renewable resources such as solar or geothermal energy. A novelty linked to this generation of networks is also based on the use of pre-fabricated and pre-insulated pipes that are directly buried into the ground .

With the increasing introduction of renewable energies into the energy market, a transition is currently taking place towards fourth generation heating networks. This fourth generation of networks tends to meet the environmental objectives set by national and international directives such as the adoption of the draft climate agreement of the COP21. These networks aim to integrate a large share of renewable energies into the heating mix by promoting synergies between the electricity and heating sectors. These new generation networks can therefore integrate a very wide range of heating sources, from renewable energies to waste heat [1], providing low temperature heat enabling to reduce heat losses along pipes and promoting the use of intermittent energy during time periods when this energy is available and not used for other applications [12].

For example, electricity from wind generation during the night is little used because the electricity demand is low during this time period. Currently, this electricity is dispatched in other countries with an electricity demand or stored in batteries to be reused at times when the electricity demand is high. This electricity storage in conventional batteries has a large cost and could be replaced by thermal storage using heat pumps that convert this electricity into heat which would then be stored as hot water in thermal storage tanks. This solution can be economically and environmentally interesting knowing that the cost of thermal storage in the form of sensitive energy is between 0.1 €/kWh and 10 €/kWh [13] whereas the cost of a conventional electricity storage with a lithium-ion battery is about 200 €/kWh [14]. The main problem with these synergy scenarios concerns the proper management of these fourth generation heating networks including

[1] Waste heat is heat from industrial processes that can be recovered and reused free of charge (waste incinerators, industrial processes, data centers, ...).

many intermittent heating sources that have to meet a global energy demand over the network throughout the year. The sizing, design and control of these networks is therefore essential for their operation in order to ensure optimal energy flexibility [15].

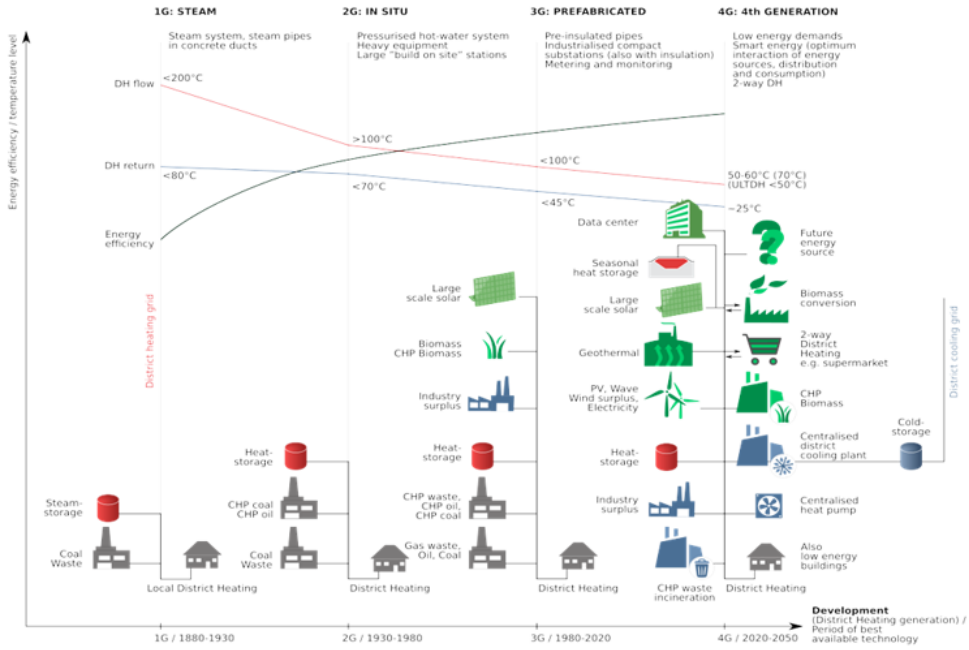

FIGURE 1.6: Evolution of district heating from first to fourth generation networks [12].

Several studies also mention fifth-generation district combined heating and cooling networks using ultra-low temperature grids to limit heat losses and prevent energy waste within the network. As illustrated in Figure 1.7 [16], the network is built as a closed loop system where heating and cooling heat exchanges occur simultaneously into the system. Heated buildings provide cold to the network while cooled buildings and industrial processes provide their excess heat to the network. These kinds of networks enable to provide some synergies between different buildings constitutive of the network. The ultra-low temperature (generally below 30°C) operation of these networks enables to directly use various low-temperature waste heat sources including shallow geothermal energy, waste heat from industrial processes or sewage water for example. The heating demand is then satisfied by using local boosters like heat pumps to increase the available heating load to the required temperature level for each building [17].

These kinds of networks are covered in the literature only since a few years but are very promising for future new heating and cooling network projects. Some 5th generation thermal networks are already in operation in Europe [18] to cover both heating and cooling demands of buildings by means of distributed heat pumps installed at the substations of the network. However, these networks generally require specific consumers with a relatively low temperature heating demand (below 60°C). This 5th generation technology is therefore tailored for

new neighbourhoods characterized by buildings with low-temperature heating demands.

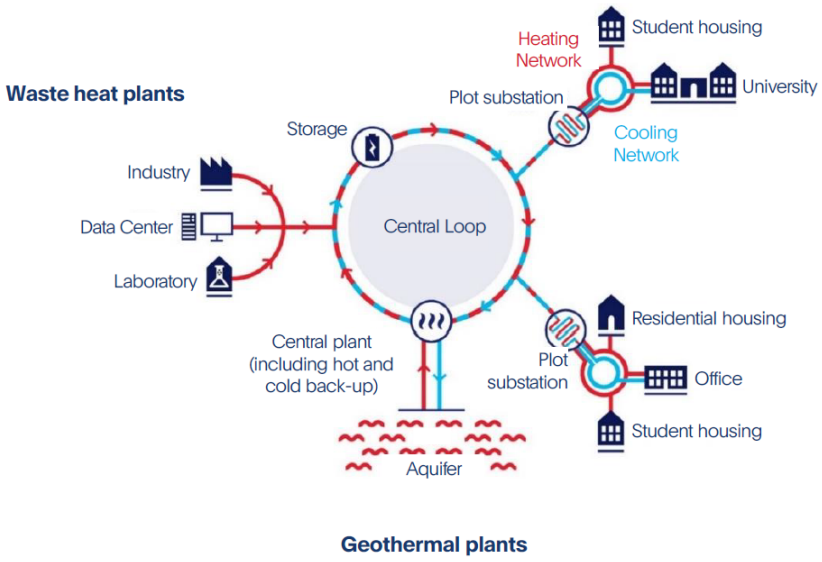

FIGURE 1.7: Principle of a 5th generation heating and cooling network (Paris-Saclay thermal energy network) [16].

In the frame of this thesis, a focus on third and potentially fourth generation heating networks is provided for their optimal outline and sizing. Indeed, the decision support tool linked to the *EcoSystemPass* project mentioned previously aims to help industries specialized for the implementation of mainly third generation heating networks to draw out and design in an optimal way these heating networks into a new geographic area. Initially, the tool is dedicated to a project in a township of Liège (Herstal) in Belgium by connecting a future greenhouse dedicated to the production of molecules of pharmaceutical interest to an existing waste incinerator through a new heating network project. This case study of a new heating network project is used in this thesis as a basis for the development of an open-source optimization platform for the integration of renewable energy sources through heating networks for the energy supply of various types of users. This optimization platform looks for promoting the development of energy communities taking into account a set of parameters like the heating sales price or the connection rate of users to a network for example.

Due to the heating profile of the studied neighbourhood in the *EcoSystemPass* project based on an existing building stock mainly made up of old poorly insulated dwellings requiring large temperature levels (around 80°C) for heating, fifth generation heating networks would not fit as the most suitable technology for the required application. Indeed, the main goal of the project is to implement a heating network to supply space heating and domestic hot water demands of an existing building stock mainly made up of old residential dwellings. Moreover, the use of a fifth generation thermal network would require local heat pumps with a large temperature difference between the cold and the hot source implying low coefficients of performance for these boosting units. Finally, the industrial

group *Coriance*, in charge of the sizing and building of the future heating network for the *EcoSystemPass* project, implements conventional third generation heating networks such that the decision tool developed in this thesis is initially focused on this generation of networks. Before detailing the goals of the decision tool developed in this thesis, a brief description of the components related to district heating networks is presented in the next section.

1.2.1 Heating production and storage units

District heating networks can use a large range of heating sources such as production units using fossil fuels or biomass as fuel, cogeneration plants, geothermal energy, heat from waste incineration or heat pumps [19]. The integration of heating technologies using renewable energies is also of particular interest for the development of renewable heating networks. These renewable networks could help to the decarbonization of the heating sector while integrating renewable intermittent energy sources.

Heat-only boilers

These boilers are only dedicated to the production of heat in the form of pressurized hot water using different types of fuels such as fossil fuels (natural gas or oil), biomass or residual waste treated in waste incinerators.

Combined heat and power (CHP)

Cogeneration plants simultaneously produce heat and electricity from an energy source. The advantage of cogeneration aims to make the most efficient use of the energy available within the energy source in order to achieve a better overall efficiency of energy production (i.e. to produce a maximum amount of useful energy in the form of heat and electricity based on the energy available within the source). The kind of sources used by these production units come in a variety of forms making it possible to obtain a diversified energy mix, as illustrated in Figure 1.8 [20].

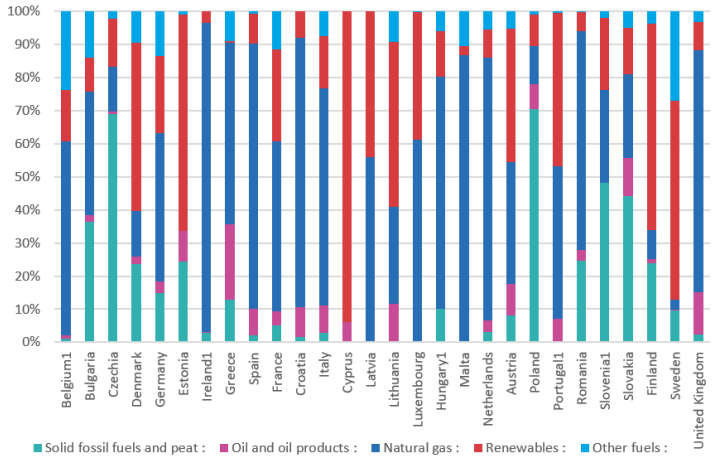

FIGURE 1.8: Fuels mix into CHP in 2017 in EU [20].

In order to meet environmental requirements while becoming energy independent from fossil fuels, some countries are beginning to look for these cogeneration plants using biomass as fuel with district heating networks. For example, Sweden is a heavy user of biomass (due to its large available resources) in cogeneration plants such as the Stockholm, Lund and Södertälje power plants [21].

Geothermal sources

Geothermal energy consists in exploiting the energy available within the earth's crust via a fluid that recovers this heat to produce heat and possibly electricity. Within the framework of district heating networks, geothermal sources can be suitable for supplying heat. The main advantages of geothermal sources are their zero CO_2 emissions while having a constant operating regime (this renewable energy is indeed not intermittent since it is available all over the year, day and night). However, the investment costs related to these geothermal sources are relatively high, particularly in cities. Geothermal energy is nevertheless a source to consider, knowing that 25% of the European population lives in urban areas where geothermal resources are available [22]. A graphical illustration of the geothermal resources available in the European Union is proposed in Figure 1.9 [23].

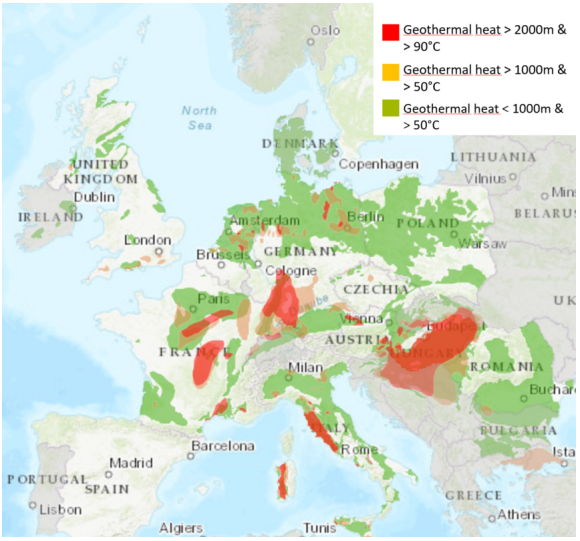

FIGURE 1.9: Geothermal resources in EU in 2020 [23].

Solar heat

Solar energy can also be exploited on a large scale for heating production through the use of solar collectors which focus the solar rays at a specific point to heat a fluid that will then be used as a heat transfer fluid to supply a district heating network or thermal storage (i.e., hot water tanks). This kind of heating production, even if it is used in some heating networks such as the Marstal heating network in Denmark [24], has many disadvantages. This energy source is

intermittent and requires large areas available for the installation of solar collectors, ideally in areas with a lot of sunshine all over the year [25]. Another form of solar heat can use a combination of photovoltaic panels combined to heat pumps.

Heat pumps

Heat pumps are energy-efficient units that make it possible to use many low-temperature heating sources to produce heat at a prescribed temperature level based on the heating consumer demand [26]. These heat pumps can also be used to locally raise the temperature level within the network to meet specific demands of some heating consumers (e.g. hospitals or industries that have heating demands with higher temperature levels) [27]. Heat pumps have the potential to include intermittent renewable energies producing electricity like solar photovoltaic panels which can be used to feed the heat pumps to produce heat stored in thermal storages [28] or used directly to feed a heating network [29].

Industrial waste heat sources

District heating networks can use waste heat (in the form of flue gases or cooling water) from industrial processes as a heating source. Heat recovery boilers or heat exchangers can be used to recover the waste heat contained into these flue gases to supply a heating network. Different kinds of waste heat sources are used for the supply of district heating networks: data centres [30], steel production plants [31] or kraft pulp mills [32] for example. Waste incinerators also produce heat in a continuous way to supply it to a large range of dwellings. Many examples exist worldwide and future projects using these incinerators as heating sources are being developed, such as the Brescia incinerator in Italy and the Copenhagen incinerator in Denmark [33]. The heating network for the *EcoSystemPass* project studied in this thesis also focuses on a waste incinerator as main heating source in a township of Liège (Herstal) in Belgium. This heating source is increasingly justified in the European context due to the growing share of municipal waste that is incinerated instead of being buried, as shown in Figure 1.10 [34].

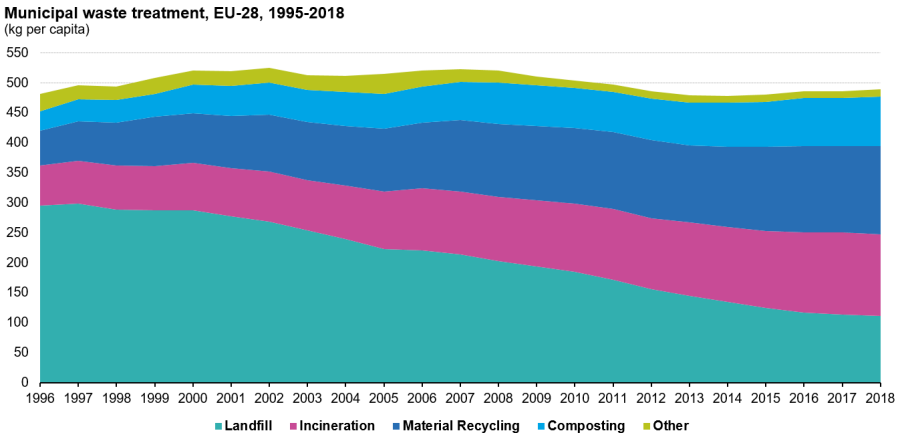

FIGURE 1.10: Waste treatment in EU between 1996 and 2018 [34].

Thermal heat storages

In order to include intermittent heating sources like solar heating or heating sources with a variable heating production cost like heat pumps, thermal heat storages can be used to shift the time at which energy is consumed. The heating storage can thus provide a solution to shift the heating production from non economically to economically interesting periods. This optimal heating production planning requires the use of thermal storage units [35]. These thermal storage units are interesting compared to electricity storage units thanks to their low specific costs (cf. Section 1.2).

The most common type of thermal energy storage (TES) consits of water storage into tanks or pits (PTES) [36]. These units can be above the ground or buried a few meters into the ground. Other underground water storage technologies (UTES) exist like borehole thermal energy storages (BTES) [37] or aquifer thermal energy storages (ATES) [38] for bigger depths beyond 100 meters. These storages are more dedicated to seasonal energy storage by storing heat during the summer and supplying this stored heat during high heating demand periods in winter. An alternative kind of heat storage relies on the buildings' thermal inertia. The flexible use of building inertia could be used to provide heat by shifting the heating supply planning in an optimal way [39]. This kind of heating storage has the advantage to be flexible but its storage capacity remains smaller than the use of pit thermal energy storages. All these storages rely on the use of the sensible heat of water.

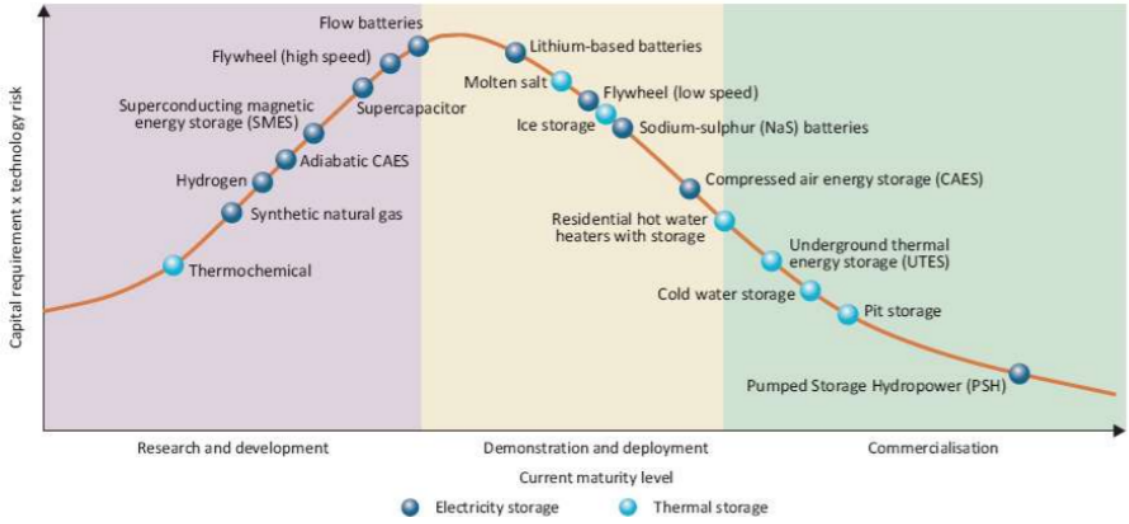

FIGURE 1.11: Review of the existing storage technologies [13].

In this thesis, the tank storage is considered as the main storage technology into the decision tool because of its technological maturity (cf. Figure 1.11), its easy implementation, its low cost and its flexibility for daily thermal storage [13]. Due to the fact that the underground thermal storage is quite dependent on the available kind of ground for the heating network project, underground thermal storage solutions are not considered into this thesis. However, the reader should be aware that this assumption benefits daily storage instead of seasonal storage

because of the larger thermal losses with tank thermal storages above the ground than underground thermal storages. It can also be observed from Figure 1.11 that other storage technologies are developed at the research and development or demonstration stage. However, these technologies are not considered into this thesis because they are not yet available at a commercial stage.

Storage tanks have a vertical cylindrical form, are made up of steel and are often located near the heating sources. These storages have different sizes based on the size of the heating network: they can be sized from a few hundred cubic meters to tens of thousands cubic meters [40]. As mentioned before, one of the advantages of the pit and tank storage technologies relies on its low cost with large-scale systems. A review of the existing systems and their specific costs for pit and tank storages as well as underground thermal storages is represented in Figure 1.12 [41]. It can be observed that the cheapest solution for large-scale systems is the underground thermal storage. However, this solution can only be applied to very large-scale thermal storages such that this solution can not be generalized to any size of heating network project. The tank storage is thus picked up as the main solution for thermal storages into the network even though its specific cost is slightly larger than with underground thermal storages.

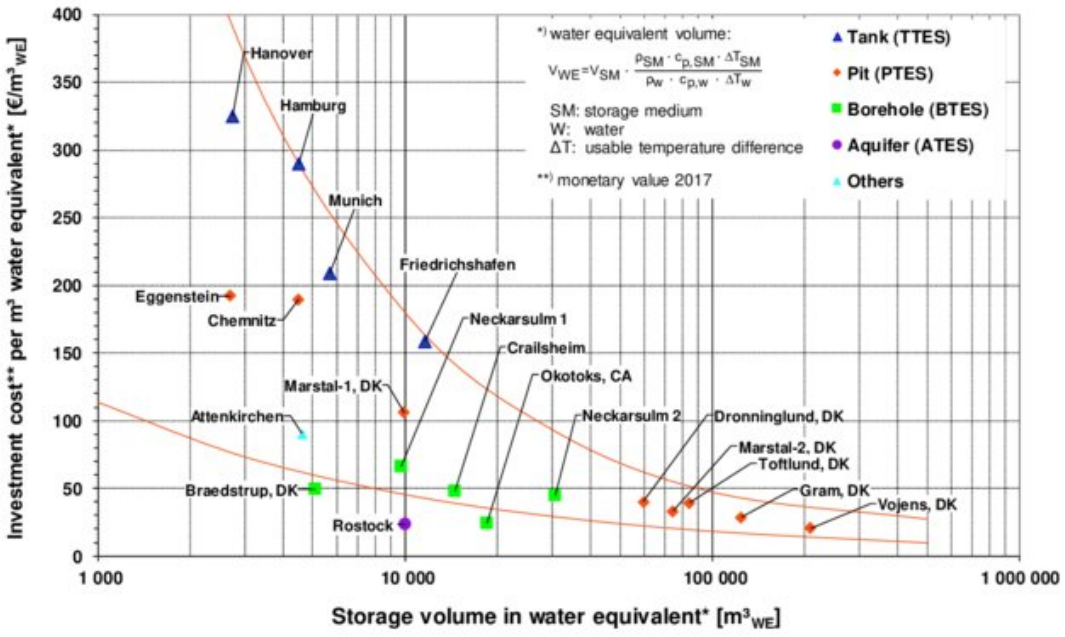

FIGURE 1.12: Costs for different existing thermal storages [41].

1.2.2 Heating consumers

Heating networks link the above-mentioned heating sources to the consumers, each of which having a very specific heating demand profile. These consumers can be residential dwellings like houses and apartments, businesses, industries or public buildings. Their heating demands are usually time-variable and

complementary such that the total heating load over the heating network is generally lower than separate individual heating loads. This aggregation effect can reduce the peak demand over the network, as shown in Figure 1.13.

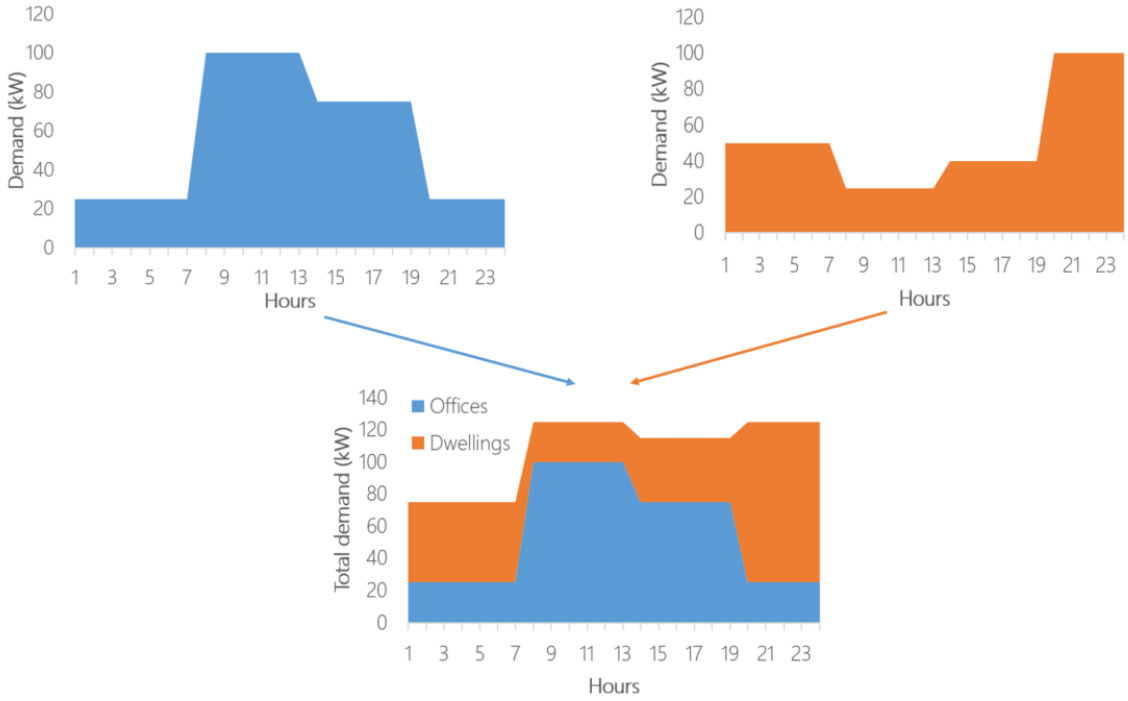

FIGURE 1.13: Aggregation effect over a district heating network.

This aggregation effect enables to get a total heating demand which is more constant over time as compared to the sum of the individual heating demands. This enables to save primary energy used for heating production dispatching the heating production in a better way thanks to dwellings with different heating demand profiles. These heating consumers are one of the key players of a heating network project because they indirectly finance the network infrastructure by buying heat to the network operator. Heating sales revenues can thus counterbalance capital and operating expenses to ensure profitability for the heating network project. A quick overview of the pricing models for district heating is presented in the following.

1.2.2.1 Pricing models applied to the heating consumers

Heating sales to the consumers are the main way to recover the initial investments spent for the building and operation of the network. As explained previously, the heat is supplied to the consumers through the network thanks to a primary circuit of pipes carrying the heat transfer fluid from the heating sources to the consumers. This fluid from the primary circuit then feeds substations located at consumer's places. As shown in Figure 1.14 [42], these substations use the heat content of the heat transfer fluid from the primary circuit to heat water in a secondary circuit. This secondary circuit aims to supply heat to the

consumers and is regulated from temperature and flow rate sensors.

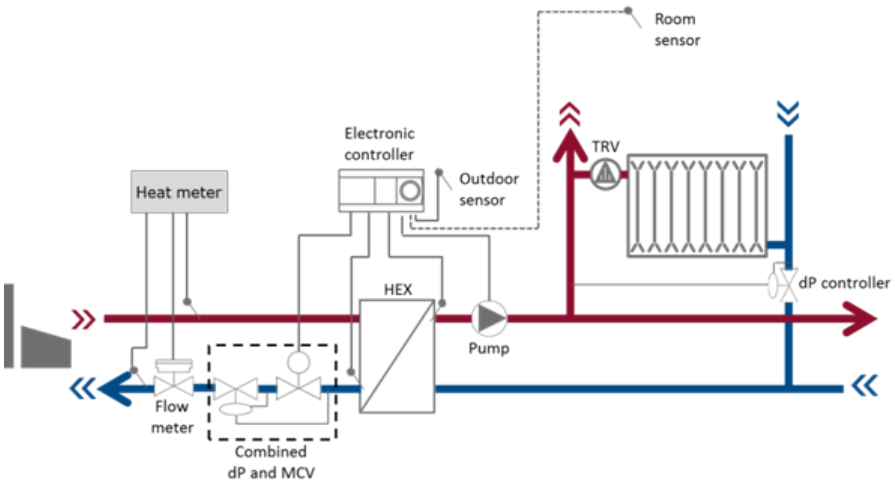

FIGURE 1.14: A substation and its main components [42].

In order to quantify the heat consumed by each user connected to a substation, the use of heat meters computes the energy consumed from the water mass flow rate and the temperature decrease measured in the primary circuit. As shown in Figure 1.15 [43], two temperature sensors are placed upstream and downstream of the consumer supply on the primary circuit to measure the temperature decrease at the primary circuit. A flowmeter is also set up to measure the water mass flow rate into the primary circuit. Based on these measurements, the heat meter computes instantly the amount of consumed heat.

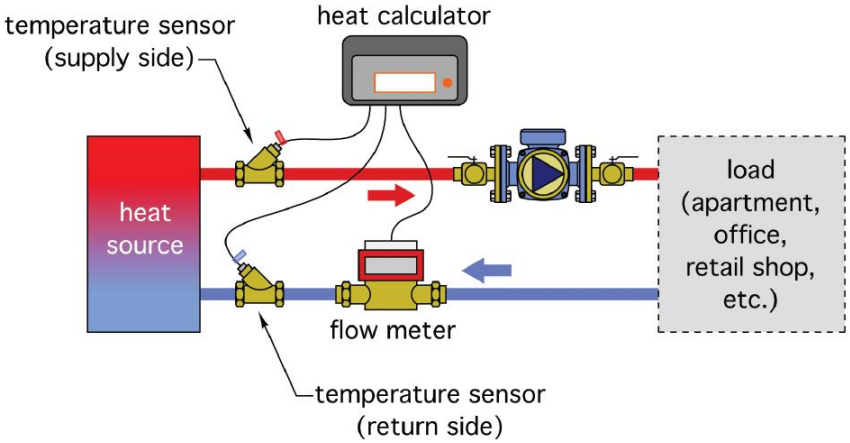

FIGURE 1.15: Operating principle of a calorimeter [43].

This heating consumption amount remains the main component for the pricing of heating sales. The heating supply is based on contracts between network operators and consumers. It is important to note that the form of these contracts come in a variety of forms from one heating network project to another. The pricing models come in a variety of form specific to each application. Even within the same heating network, several different pricing models can be applied by

the network operator depending on the type of customers. The details of these contracts are not set out in this thesis but a general review of the main existing pricing structures is proposed in the following section. Pricing contracts can be classified according to two main types of models: models based on investment and operating expenditures and models based on market prices [44].

Pricing models based on capital and operating expenditures

These models price the sold heat from the total annual costs of the network (including capital and operating expenditures) with a prescribed return on investment defined by the several stakeholders involved into these heating networks. The risks related to this model are twofold:

1. In the case of a monopolistic network structure, the sales prices can be adjusted quite flexibly by the network operators by increasing the profit margin freely and indefinitely if no legal framework for regulating sales prices is provided. The sales price paid by consumers could thus become far too high compared to the cost price of the network in a market mainly dominated by a monopoly.

2. On the other hand, in a competitive market with multiple heat supply alternatives, a model based solely on network costs and expected return on investment that does not take competition into account can lead to market share losses and become unprofitable.

A purely cost-based model exists and can be implemented in monopolistic configurations where the network operator has sufficient control over the market. However, this type of model is quite scarce in practice and is therefore frequently combined with a market-based pricing model.

Pricing models based on market prices

These models price heating sales from market prices of alternative heating supply solutions (mainly the gas suppliers). The objective aims to set a price competitive compared to these alternatives while trying to remain economically profitable for the network operator. This kind of model can obviously only be used in a market where competition is sufficiently developed to get pricing benchmarks. Two kinds of pricing based on market prices exist:

1. Pricing **directly** based on market prices:
   Heating sales price are continuously based on the market prices offered by competitors such that formulas linking the competitive market prices to the heating sales prices are used. The advantage of this method relies on the ensurance to always remain competitive on the heating market.

2. Pricing **indirectly** based on market prices:
   The heating sales price is no longer set continuously based on market prices but only predefined annually from average price estimates established by

competitors. A more accurate model that takes into account monthly consumption and includes the predefined annual selling price then determines the monthly selling price of heat.

The main drawback of this type of model is that it is based solely on market competition but does not necessarily ensure the profitability of the network. In practice, more complex pricing structures combining cost-based and market price models therefore exist in order to be simultaneously profitable and competitive in the market. These models must be established on a case-by-case basis and include certain key elements.

Key elements in the design of pricing models

Pricing models come in a variety of forms and can vary widely from one application to another. It is therefore essential to determine the key elements common to any viable pricing model. In the literature, the following main criteria are considered for the viability of a pricing model [33]:

- ✓ Competitive prices adapted to market **and** operating conditions:
  Variable operating costs are higher during peak demand periods and lower during base load periods. If the heating sales price is prescribed constant over the year without taking into account market and operating conditions, the sales price for the peak load would be too low and the sales price for the base load would be too high. This scenario can lead consumers to install their own base load heating unit and buy only the under-priced peak load leading to a non-viable pricing solution for the heating network operator.

- ✓ Tariffs based on the usage capacity subscribed to the network by consumers:
  This criterion seeks to favour consumers with a large heating demand who are more economically viable than consumers with a smaller heating demand. These consumers provide a base-load heating demand over the network with lower production costs than the peak heating production to satisfy smaller consumers. These big heating consumers can therefore be rewarded with a lower overall heating sales price than smaller consumers.

- ✓ Tariffs partially independent of the level of heating demand:
  The 2 previous criteria are mainly based on the level of heating consumption of network's users to establish a pricing model. However, some maintenance and network extension costs have also to be covered by all the users regardless of their consumption level. The pricing model must therefore also include these costs in the billing.

From these 3 criteria, network operators define pricing contracts with a fixed connection fee, a fixed capacity subscription fee and a variable charge based on the heating consumption over a prescribed time period. The variable price charge based on heating consumption is computed from heat meters enabling to price

directly heat based on market and operating conditions. Regarding the capacity subscription fee, it aims to reward large consumers subscribing to a larger heating capacity increasing the total heating demand of the network and thus reducing the financial risks incurred by the network operator. This fixed capacity subscription fee encourages all the users to subscribe to a maximum heating capacity in order to reduce their bill. This subscribed capacity represents the average heating consumption over a full year (of 8760 hours) and is calculated as follows:

$$\text{Subscribed capacity [kW]} = \frac{\text{Annual subscribed energy [kWh]}}{8760 \text{ [h]}}$$

Consumers are then clustered by categories according to their subscribed capacity to set a sales price specific to each category of consumers by assigning a revision coefficient depending on the category to which they belong. Consumers with a large subscribed capacity have a lower revision coefficient since the pricing model seeks to reward these customers. Finally, a fixed annual grid connection fee, independent on the heating demand and subscribed capacity of the consumer, ensures the maintenance and operational expenses linked to the network. A generic billing model for the heating sales is proposed in Figure 1.16 based on the heating network market in France [45].

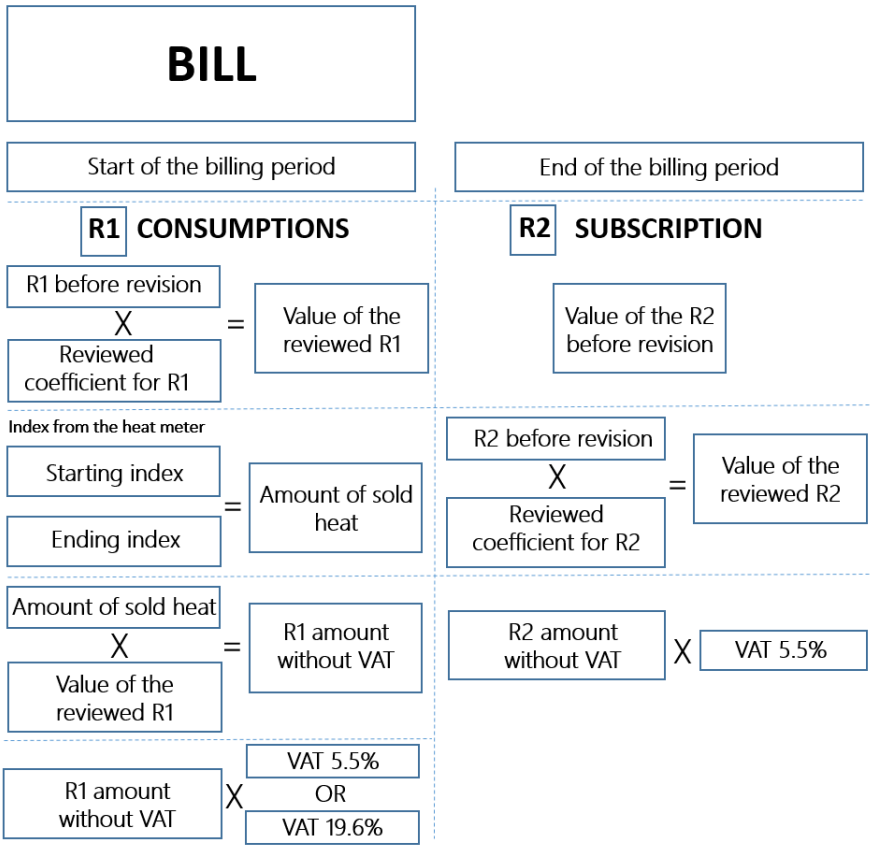

FIGURE 1.16: Billing of heat consumption to a consumer for a heating period (adapted from [45]).

The billing relies on a variable price component ($R1$) and a fixed price component ($R2$). The revision coefficient of $R1$ mainly takes into account the energy mix used for the heating production and the market prices. In the case of a network with a diversified energy mix, the pricing of the total consumption in kWh for a user is computed according to a weighted average of the part of the costs of the different fuels used into the heating mix. For example, considering a heating network with 2 heating sources A and B used proportionnally according to $\%_A$ and $\%_B$ with respective costs Cost_A and Cost_B in €/kWh, the revised coefficient can be computed as follows:

$$\text{R1 coefficient [€/kWh]} = \%_A \,.\, \text{Cost}_A + \%_B \,.\, \text{Cost}_B$$

Multiplying the heating amount measured by a heat meter over the current billing period by this coefficient then gives the total amount without value-added tax (VAT) to be paid by the consumer. The applied VAT rate depends on the energy mix used during the current heating period for the heating production. The applied VAT is generally 19.6% but may be reduced to 5.5% if the energy mix is based on at least 50% of renewable energy [2] and residual heat. Concerning the fixed part of the fee, it includes the fixed annual fee for the connection to the network and an annual capacity subscription fee where the revision coefficient depends on the capacity subscribed by the user.

Pricing model considered in this thesis

In this thesis, a pricing model only based on market prices is used considering the gas market as the main competitor for heating supply. This pricing model is used because one of the goals of this thesis is to highlight the economic benefits of district heating networks compared to conventional heating energy careers like gas. Therefore, a purely competitive pricing scheme is used as a comparison to show to policy-makers the potential interest of heating networks for a prescribed heating sales price. For sake of simplicity, a unique heating sales price is considered for all the consumers over the network even though it has been previously explained that the heating sales price is partially dependent on the heating demand of each consumer and also of the kind of consumers. Even if a single heating sales price is considered, the optimization formulation presented in Chapter 2 makes possible to prescribe a different heating sales price for each potential consumer (street) of the network.

1.2.3 Pipes

The last components of the network are the pipes connecting the heating sources to the consumers by carrying the heat transfer fluid. These pipes, generally made up of steel surrounded by a polyurethane foam for third generation heating networks, are usually buried into the ground and therefore require major worksites within cities to dig the trenches to install them. The investment

[2] Renewable and recovery energies include most energy carriers except nuclear, oil, gas and coal.

costs for these pipes take a significant part of the initial investment costs and must be taken into account when designing a new heating network project. This important capital cost component into a heating network project has been illustrated by [46] with more than 50% of the total costs dedicated only to the trenching and the pipes.

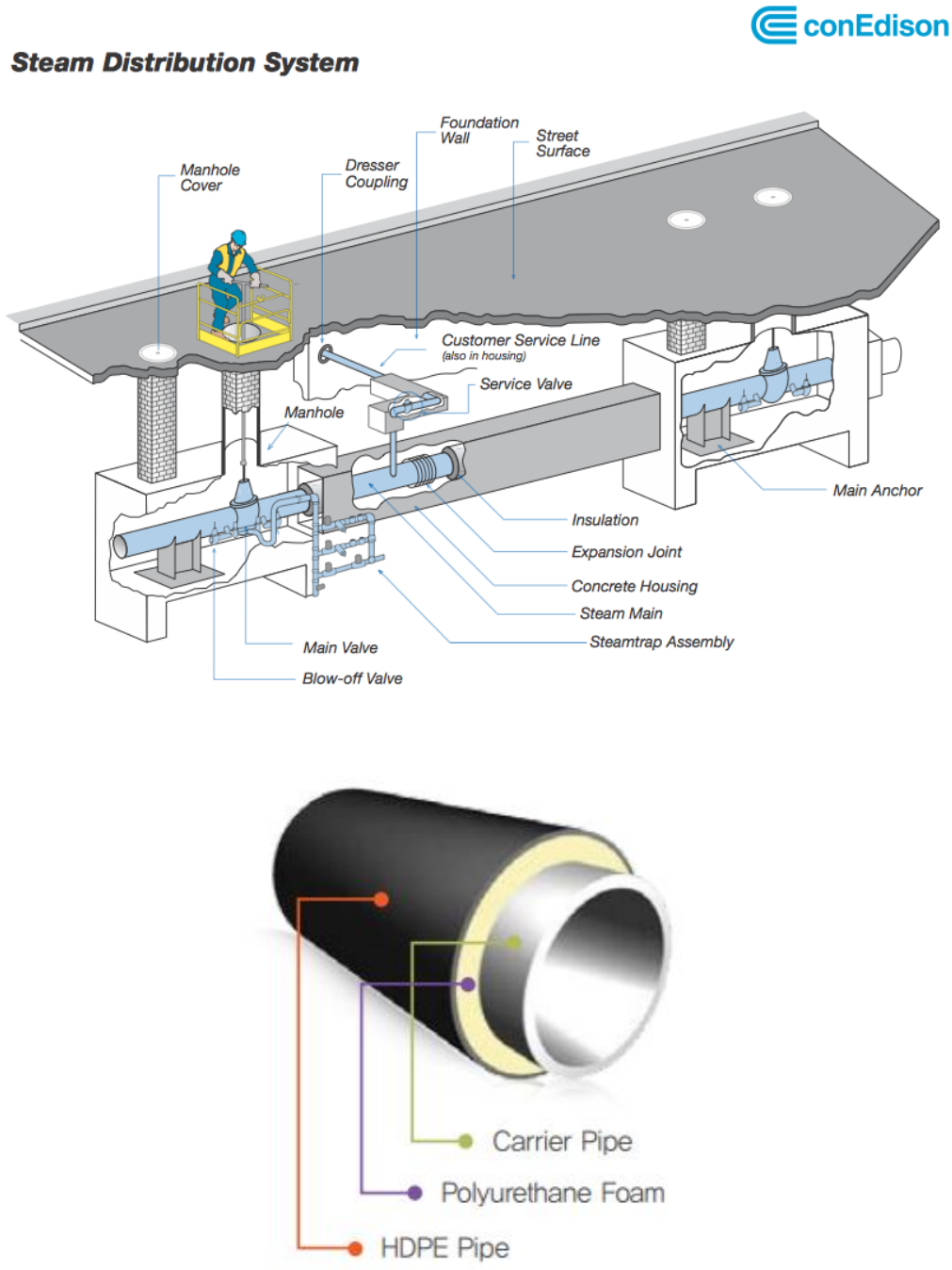

FIGURE 1.17: Pipes of a district heating network.

These pipes have standardized diameters defined by pipes manufacturers. These standardized diameters are summarized in Table 1.1. These pipes have

an average cost dependent on their diameters such that these costs, which take an important part into the total capital costs, have to be considered for the implementation of new heating networks. These costs will be detailed in Chapter 2.

TABLE 1.1: Standardized district heating pipes sizes.

DN (mm)	Steel pipe diameter (mm)	Insulation thickness (mm)
20	26.9	2.6
25	33.7	3.2
32	42.4	3.2
40	48.3	3.2
50	60.3	3.2
65	76.1	3.2
80	88.9	3.2
100	114.3	3.6
125	139.7	3.6
150	168.3	4.0
200	219.1	4.5
250	273.0	5.0
300	323.9	5.6
350	355.6	5.6
400	406.4	6.3
450	457.2	6.3
500	508.0	6.3
550	558.8	6.3
600	610.0	7.1
700	711.0	8.0
800	813.0	8.8
900	914.0	10.0
1000	1016.0	10.0

1.2.4 Pros and cons of district heating networks

Large-scale heating networks can supply the heating needs of large cities with a variety of heating production sources. Compared to decentralized heating production units, district networks offer some advantages but also some disadvantages [7]:

- ✓ Lower heating production costs than with decentralized heating production units thanks to economies of scale and an aggregation effect;
- ✓ The availability for using diversified fuels and heating sources with a lower exergy (waste heat from industrial processes for example);
- ✓ A reduced environmental impact by monitoring pollutant emissions and reducing CO_2 emissions with respect to smaller individual installations;

- ✓ Combined heat and power production through cogeneration plants for a better overall energy efficiency of the system;
- ✓ An integration of renewable and local resources into the energy mix thanks for example to the inclusion of the vector of electricity for the heating production using a heating network combined with the use of thermal storages;
- ✓ Ease of use for heating consumers who do not have to worry about heating production but can simply consider the heat supply as a service provided by a network operator (just like electricity);
- × **Large initial investment costs which have to be funded by investors and/or public authorities**;
- × Substantial heat losses along the network requiring the production of more heat than the heating demand of the consumers ;
- × Short-term flexibility which is not always easy to manage in the case of centralized production systems.

Despite numerous advantages linked to district heating networks, there are some constraints linked to the development of this technology into the heating sector. This thesis is going to try for helping to promote the development of the heating network technology thanks to the use of specific tools assessing precisely the economic (and environmental) interest or not of a district heating network within a specific area.

1.3 Problem statement

The development of heating networks in urban communities is increasingly being studied at the scientific level for their environmental benefits while investors and policy makers are cautious about new investments in district heating network technology because of their large initial investment costs for their implementation into cities. Numerous studies within the European Union have already demonstrated the technical and environmental viability of the heating network technology (especially those embedding renewable energy sources) [47]. However, the economic factors are generally neglected although they are of paramount importance for investors and political decision-makers. This thesis aims therefore to address this issue by implementing a decision tool dedicated to the investors and policy-makers for the optimization of the outline and the sizing of third generation district heating networks in order to maximize the net cash flow linked to a new heating network project.

The development of the decision tool is based on the *EcoSystemPass* research project linked to a refurbishment project of an unused industrial zone into an urban agriculture site with a greenhouse. As illustrated in Figure 1.18, this refurbishment project initially aims to connect the future greenhouse with a piping system to an existing waste incinerator operated by *Veolia* for providing heating needs to the greenhouse. In the frame of this project, the company *Coriance* [48]

specialized in the implementation of third generation heating networks has been assigned to design a heating network in the neighbourhood of the waste incinerator. In parallel to this refurbishment project, the *EcoSystemPass* research project has therefore been launched to help companies like *Coriance* to draw out and size in an optimal way heating network projects. The main goal of this project is to develop a decision tool to help industrials and policymakers to promote heating network projects into small-size but also large-size neighbourhoods. This decision tool has to take into account economic parameters (project lifetime, actualization rate and heating sales price) as well as urbanistic parameters (space into the ground and available heating capacity in the neighbourhood). Finally, it was expected that the decision tool can help policy makers to identify interesting consumers to connect to a new network project while prescribing the connection of some of them if it is required for political reasons for example.

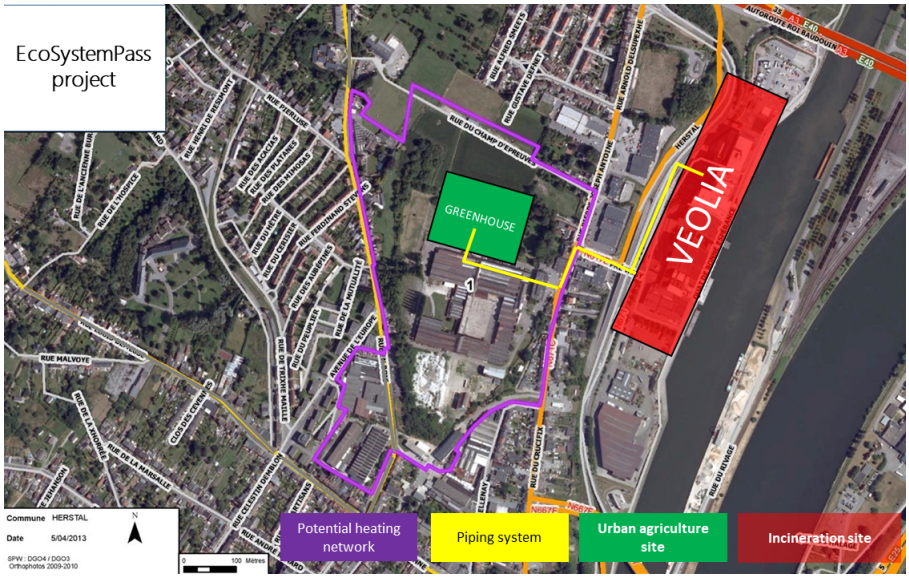

FIGURE 1.18: Illustration of the EcoSystemPass research project.

Based on this project, research groups have worked on different tasks linked to the site refurbishment:

- Compute the heating demands of the greenhouse using a dynamic model customizable for different kinds of culture into the greenhouse;
- Assess the heating demands of the dwellings constitutive of the neighbourhood surrounding the waste incinerator and the future greenhouse;
- **Implement an optimization method for urban energy planning with heating network projects into cities taking into account different economic and urbanistic parameters for the optimal outline and sizing of third and potentially fourth generation heating network projects**;
- Define a GIS-based visualization software to draw out the optimal network and show some results from the outputs of the optimization method.

The optimization method which is part of the global project is mainly presented into this thesis. To help the reader for understanding the decision tool into its global structure, the other tasks will also be quickly explained in the following. This aims to highlight the main inputs data used for the implementation of the optimization method and to explain how the visualization platform has been developed as an output of the global structure of the project. However, before presenting into details the optimization method developed in this thesis, a literature review based on the requirements of the *EcoSystemPass* research project for the optimal outline and sizing of heating networks is achieved to analyse the features of each model and their main characteristics compared to the expected characteristics of the new optimization model.

1.3.1 Literature review

District heating networks are of increasing interest in the field of scientific research because of their potential in the framework of the energy transition. Many studies are performed about the dynamic modelling and predictive control of operating district heating networks while other researches are related to the optimization of the outline and the sizing of these networks. A non-exhaustive literature review based on the main goals of the *EcoSystemPass* research project is proposed in the following. The main comparison criteria for optimization methods available in the literature are therefore based on the two main goals of the project: provide an optimal outline and sizing of any new heating network project into a prescribed geographic area defined in a geographic information system. Defining an outline for a new network consists of picking up which streets have to be connected to the network or not to guarantee the economic profitability of the project. It also includes the selection of the optimal pipes diameters to put into the streets if they are connected to the network. Regarding the sizing of the network, the decision tool determines where the heating sources and thermal storage units have to be installed and how they have to be sized to optimally design the heating network. For this project, third generation heating networks are mainly considered by the industrial client. However, from an academic point of view, the decision tool also looks for being applicable to fourth generation heating networks in the future by tuning some parameters of the tool as a function of the temperature level into the network.

Among numerous studies about district heating optimization, Apostolou [49] develops a methodology based on a mixed integer non-linear (MINLP) optimization approach minimizing the total costs of the system for the integration and the design of heating and cooling sources into a new district heating or cooling project. A MINLP formulation based on the minimization of the total costs is also developed by Mertz [50] for the outline and the whole sizing of a district heating project with the specificity to design the kind of connection between consumers (either parallel or in cascade). Roland [51] implements a mixed-integer nonlinear optimization model taking into account with a high level of details all the hydraulic and thermal effects based on the Euler momentum and thermal energy equations. Blommaert [52]

develops an adjoint-based numerical strategy to enable large-scale nonlinear thermo-economical network optimization for finding the best topology, pipe diameter choices, and operation parameters for realistic district heating networks.

Multi-objective non-linear optimization problems based on heuristic formulations are also developed to minimize total costs combined with a minimization of the CO2 emissions [53–56] or the share of primary energy import into the network [57]. These optimization formulations have a high level of complexity enabling to provide a detailed modelling of the system but their non-linearity does not ensure a unique optimal solution for the problem and their complexity limits the application scale to optimization problems with a small number of streets into the potential network.

Mixed Integer Linear Programming formulations optimizing the design and operation of district heating systems [58, 59] are also developed but do not consider the potential outline of a new district heating network project. These models are useful to assess the optimal use of existing energy sources but the important aspect of building or not pipes and power plants at given locations is missing. Another kind of optimization models taking into account the optimization of the outline of the heating network exists in the literature. Some of these models [60–62] define the optimal outline of a potential network by choosing the consumers to connect to it but are based on existing heating power plants with prescribed fixed capacities. The sizing of new potential heating plants is not included in these models.

Haikarainen [63], Soderman [64] and Lambert [65] develop MILP approaches combining the optimization of the outline and the design/operation of the network but validate their models only on small-scale test cases which are not connected to any geographic information system. Dorfner [66], Girardin [67] and Unternährer [68] implement an optimization formulation based on a geographic information system and combining both the outline and the design of a potential new heating network project. However, these models do not include thermal storage capacities into the outline of the network.

Finally, some methods are also available as commercial softwares or additional plug-ins of a geographic information system directly usable by any user for urban energy planning linked to heating network projects. The open-source decision support software *SigOpti* [69] looks for helping cities and network operators to optimally size a new heating network into a geographic information system. Based on a network outline defined by the user of the software, *SigOpti* provides the least expensive solution based from a global cost analysis in terms of network sizing (pipe diameters and flow rates) as well as in terms of heating production selection and sizing (gas, biomass, geothermal energy, ...). The software *URBio* also provides a tool for urban energy planning by identifying optimal energy strategies as well as insights into the urban layout, distribution and size of buildings [70]. This tool helps to define master plans for urban plannings in new neighbourhoods by selecting the kind

of buildings to build and by sizing the energy system linked to the neighbourhood.

TABLE 1.2: Comparison of optimization methods from a literature review

Authors	**Objective Function**	**Linear**	**Outline**	**Sizing/ Operation**	**Multi-period**	**Storage**	**GIS**
Apostolou [49]	min C_{tot}	×	✓	✓	✓	✓	×
Bertrand [58]	max *profits*	✓	×	✓	✓	×	✓
Blommaert [52]	min C_{tot}	×	✓	✓	×	×	✓
Bordin [60]	max *profits*	✓	✓	×	×	×	×
Dorfner [66]	min C_{tot}	✓	✓	✓	✓	×	✓
Falke [53]	min C_{tot} & CO_2	×	✓	×	✓	✓	×
Fazlollahi [54]	min C_{tot} & CO_2	×	✓	✓	✓	✓	✓
Girardin [67]	min C_{tot}	✓	✓	✓	×	×	✓
Haikarainen [63]	min C_{tot}	✓	✓	✓	✓	✓	×
Jebamalai [61]	min C_{tot}	✓	✓	×	✓	✓	✓
Lambert [65]	max *NCF*	✓	✓	✓	✓	×	×
Mertz [50]	min C_{tot}	×	✓	✓	×	×	×
Molyneaux [55]	min C_{tot} & CO_2	×	×	✓	×	×	×
Omu [59]	min C_{tot}	✓	×	✓	✓	✓	×
Roland [51]	max *NCF*	×	✓	×	×	×	×
Samsatli [62]	min C_{tot}	✓	×	✓	✓	✓	×
SigOpti [69]	min C_{tot}	✓	×	✓	×	×	✓
Soderman [64]	min C_{tot}	✓	✓	✓	✓	✓	×
Unternährer [68]	min C_{tot}	✓	✓	✓	✓	×	✓
URBio [70]	min C_{tot} or CO_2	✓	≈	✓	✓	×	✓
van der Heijde [57]	min C_{tot} & *PEI*	✓	×	✓	✓	✓	×
Weber [56]	min C_{tot} & CO_2	×	✓	✓	✓	✓	✓
Model in this thesis	max *NCF*	✓	✓	✓	✓	✓	✓

A summary of the main features of the different optimization models mentioned above is presented in Table 1.2. It can be observed that all the presented models do not complete all the features listed in Table 1.2. The contribution of this thesis with the new model described in the following chapter is to fill in all the features presented in Table 1.2. The 3 main features combined in this new model are the following:

1. A MILP model applicable at the street level to small-scale cases with a neighbourhood of a few streets to large-scale problems including heating network projects into cities. The linearity of the model ensures to provide a unique solution to the optimization problem and to guarantee robustness for the use of the tool by an external user.

2. A model combining both the optimization of the outline and the sizing/operation of the network. The optimization of the outline enables to draw out any new heating network project from scratch by choosing the location of streets where pipes can be built and which heating plants to use or to build. The optimization of the sizing/operation is useful to size the pipes and the heating plants and storages capacities.

3. A model that can be connected to a geographic information system such that the optimization procedure can be easily replicated to any new geographic area with potential interesting heating consumers to connect to a network.

Table 1.3: Non-exhaustive review of optimization models for district heating networks.

Authors	**Methodology**	**Summary**
Apostolou (2018) [71]	Single-objective Multi-period MINLP	Optimization model for the design of networks and energy conversion means using energy integration techniques. This model is applied to the design of industrial heat exchanger networks. The goal of the model is to be able to deal with the geographical and temporal scales enabling to assess the consequences of heating load fluctuations on the heating production units while defining the network layout. The optimization model therefore allows the outline and design of networks that take advantage of potential synergies.
Bertrand (2019) [58]	Single-objective Multi-period MILP connected to a GIS	Optimization model providing a framework to simultaneously optimize the multi-period exchange of waste heat between regional heating sources and consumers as well as the selection of the backup heating technologies. From cost data for the prescribed heating sources and the pipes to connect from the sources to the consumers, the design is optimized by maximising the profits from the network. The model takes into account fluctuations of temperature levels and heat loads between different periods for the heating sources providing a pre-design of the waste heating network considering standard pipes diameters.

continued ...

... continued

Authors	Methodology	Summary
Blommaert (2020) [52]	Single-objective single-period MINLP	Adjoint-based numerical strategy to enable large-scale nonlinear thermo-economical network optimization for finding the best topology, pipe diameter choices, and operation parameters for realistic district heating networks. The optimization problem aims for minimizing the cost associated with the installed network piping and the installed pump capacity while meeting the thermal demand of all consumers. The model is based on mass, momentum and energy equations which imply non-linear equations. The algorithm is tested by designing a fictitious district heating network with 160 consumers. As a proof-of-concept, the network is optimized for minimal investment cost and pumping power, while keeping the heat supplied to the consumers within a thermal comfort range of 5%.
Bordin (2016) [60]	Single-objective Single-period MILP connected to a GIS	Optimization model developed for the outline of district heating networks. The goal of the model is to select an optimal set of new users to be connected to an existing heating network while maximizing revenues and minimizing infrastructure and operational costs. The model considers steady-state conditions for the hydraulic system and takes into account physical constraints like the pressure levels into the system. The model is applied to a real case study with an existing heating network of 4.3 kilometers long in a town in Emilia-Romagna (Italy).

continued ...

... continued

Authors	Methodology	Summary
Dorfner (2014) [66]	Single-objective Multi-period MILP connected to a GIS	Optimization model for the outline and sizing of a district heating network. The optimization formulation relies on a mixed-integer linear programming model based on a graph representation of the studied geographic area. The model aims to optimize the outline and the sizing of the network while being connected to a geographic information system. Heating demands of buildings are aggregated along the streets. Heating sources are picked up from a set of available heating sources limited with a prescribed heating capacity. The model is validated on a case study in Munich using a district heating extension planning as reference.
Falke (2016) [53]	Multi-objective Multi-period MINLP	Multi-objective optimization model for the investment planning for the outline of heating and electricity networks. Several energy resources including various heating and power units and storage systems are taken into account into this model. A comparison between decentralized heating production units and centralized heating production with district heating networks is achieved to determine the most optimal one on a case-by-case analysis. The optimization problem is decomposed into three sub-problems to reduce the computational complexity. This enables to refine the accuracy of the model while studying large-scale case studies. The model is applied to a district in a medium-sized town in Germany in order to analyze different scenarios regarding the total costs and CO_2 emissions.
Fazlollahi (2015) [54]	Multi-objective Multi-period MINLP connected to a GIS	Multi-objective multi-period non-linear optimization model for the outline and the design of district heating networks including the design of the processes using integration techniques. The decision tool aims to help the decision makers to decide which kind of technologies (centralized or decentralized) are the most appropriate for the studied geographic area and where these technologies have to be located. The outline and the design of the network is based on a geographic information system.

continued ...

... continued

Authors	Methodology	Summary
Girardin (2012) [67]	Single-objective Single-period MILP connected to a GIS	Single-objective single-period MILP model connected to a GIS to integrate energy efficient conversion technologies (including heating networks) into urban energy planning processes. The purpose of this platform is to model with sufficient details the energy services requirements of a given geographic area in order to establish energy integration solutions into this area which are economically and environmentally interesting. The model looks for minimizing the total cost of the energy system while promoting the use of energy efficient conversion technologies and renewable energies. The model is applied to an urban district in Switzerland.
Haikarainen (2014) [63]	Single-objective Multi-period MILP	Model for optimizing the structure and operation of a district heating network from a set of alternatives for heating production and distribution. Heating and pipes technologies and locations as well as thermal storage solutions are included into the model as a set of decision variables. From these variables, the model can determine the optimal outline and sizing in terms of costs or greenhouse gases emissions. The model is applied to a small-scale case study aiming for the development of an urban area using a heating network.
Jebamalai (2019) [46]	Single-objective Single-period MILP connected to a GIS	Automated decision tool based on a geographic information system. The tool is developed as a plug-in to a GIS tool and includes optimized and automated network routing algorithms, including the main features for the outline of a district heating network dimensioning. A case study in the city of Nijmegen (Netherlands) is used as a case study to demonstrate the main features of the tools. This tool takes into account existing heating sources and heating demands to determine the optimal outline of the pipes.

continued ...

... continued

Authors	Methodology	Summary
Lambert (2016) [65]	Single-objective Multi-period MILP	Multi-stage stochastic mixed-integer linear programming formulation to determine the annual capital expenditure that maximises the net present value of a heating network project. The approach can simulate the optimal growth of a network from both a single heat source or separate islands of growth with a multi-stage phasing development of heating networks. The objective of phasing is to modulate capital expenses over the project lifetime to gradually develop a heat network to minimize investment risks. Contrary to the classical NPV approaches which treats the problem as if it is a now-or-never decision, this optimization formulation takes into account the possibility for decision-makers to gradually develop heating network projects. The optimization approach is applied to a hypothetical case study in the city of Marston Vale in the United Kingdom.
Mertz (2016) [50]	Single-objective Single-period MINLP	Model aiming to provide the optimal outline and sizing of a heating network while minimizing total costs of the system. This model tries to take into account as accurately as possible the physics of the network by putting into equation the heat and pressure losses from general energy conservation equations. The optimization of the network is based on nominal operating conditions and does not take into account the fluctuation of the heating demand over the year. The formulation leads to a mixed integer non-linear programming (MINLP) problem. One of the specific features of this model is the choice of the layout of the network, either in parallel or in cascade such that a consumer with hot temperature requirements can supply another consumer with lower temperature requirements.

continued ...

... continued

Authors	Methodology	Summary
Molyneaux (2010) [55]	Multi-objective Single-period MINLP	Model aiming to size a district heating network based on a combination of centralized and decentralized heat pumps combined with on-site cogeneration using a multi-objective non-linear formulation. Both objectives of the optimization problem are the minimization of the total costs of the system and the minimization of the pollutants emissions thanks to a *Clustering Pareto Evolutionary Algorithm* (CPEA). The model determines then a trade-off between the centralized units to install to feed the consumers using a heating network and decentralized heat pumps to feed locally the heating demand.
Omu (2013) [59]	Single-objective Multi-period MILP	Mixed Integer Linear Programming (MILP) model for the sizing of a distributed energy system combining electricity and heating demands of a set of commercial and residential buildings. The goal of the model relies on the selection and the sizing of the optimal heating and electricity sources providing synergies between electricity and heating demands. The objective of the optimization problem relies on the minimization of the capital and operating expenses. The model is used to analyze the economic and environmental impacts of distributed energy systems at the neighbourhood scale in comparison to conventional centralized energy generation systems.
Roland (2020) [51]	Single-objective Single-period MINLP	Mixed-integer non-linear single-period optimization model for computing the optimal expansion of an existing heating network to a defined number of new potential heating consumers. A detailed model takes into account thermal and hydraulic phenomena into the network thanks to the Euler momentum and thermal energy equation. The expansion decision is related to binary variables picking up new consumers to connect or not to an existing heating network. The model is applied to a case study with 15 streets and 10 heating consumers at 10 nodes of the graph of the network.

continued ...

... continued

Authors	Methodology	Summary
Samsatli (2018) [62]	Single-objective Multi-period MILP	Mixed-integer linear programming model for the design and operation of urban energy systems taking into account a large range of resources representing any energy or material involved in the production of heat and electricity. The model can be applied to urban energy systems problems at different temporal and spatial scales and is used for the design of an eco-town in England. The model relies on a diagram representation linking the set of resources and of available technologies to transform these resources into heat or electricity in an optimal way.
SigOpti (2019) [69]	Single-objective Single-period MILP connected to a GIS	Open-source decision support tool based on a single-period single-objective linear optimization model for helping cities and network operators to optimally size a new heating network into a geographic information system. The network outline is defined by the user of the software such that *SigOpti* can determine the cheapest solution based on a global cost analysis in terms of network sizing (pipe diameters and flow rates) as well as in terms of heating production selection and sizing (gas, biomass, geothermal energy, ...). From a predefined outline, the software can directly define the optimal sizing of the heating network and the heating production units into the geographic information system. This tool has been applied to a case study in Asnières Gennevilliers Les Courtilles (France).

continued ...

... continued

Authors	Methodology	Summary
Soderman (2006) [64]	Single-objective Multi-period MILP	Model for the optimization of the outline and the sizing of district energy systems. Electricity and heating production as well as their transport are taken into account. The problem is formulated as a mixed integer linear programming (MILP) problem where the objective is to minimize the total cost of the district energy system including the capital and operating expenses. The model is applied to a case study with a few streets determining the optimal outline of the network and the required size of the heating units to minimize total costs. Thermal storage units are included in the range of solutions to illustrate their benefits into heating networks.
Unternährer (2017) [68]	Single-objective Multi-period MILP connected to a GIS	Methodology to spatially assess the optimal integration of district heating networks in urban energy systems based on the minimization of the total costs of the system. An ILP approach is proposed for the spatial clustering of urban energy system models. For the spatial configurations of district heating networks into clusters, routing techniques are used. The routing forces the district heating pipelines to follow the road network. A MILP urban energy system model based on the clusters configuration and on the district heating network lengths is applied to economically evaluate the district heating integration in each cluster. The model considers non-spatially limited resources which can be used everywhere and spatially limited resources dedicated to a specific location (for example, waste heat from an industrial process). The quality of the method is assessed by comparing the obtained network configurations with existing district heating networks using an applied case study with the integration of geothermal energy in the city of Lausanne.

continued ...

... continued

Authors	Methodology	Summary
URBio (2017) [70]	Single-objective Multi-period MILP connected to a GIS	MILP model to identify optimal energy strategies and insights about the urban layout, distribution and size of buildings. The approach aims to achieve early-stage planning in specific areas defined in a geographic information system. The methodology generates building informations based on available data and constraints and generates district energy solutions from these informations and energy densities. The software helps to identify the most adequate energy system and the urban layout of the buildings even though the detailed outline of the energy system is not directly provided by this tool. The main goal of this tool is to achieve early-stage planning. The model has been applied to an existing project for the urban planning of a new township.
van der Heijde (2019) [57]	Multi-objective Multi-period MINLP	Python-based toolbox named *Modesto* which provides a full-year operational optimisation tool for possible heating network designs with varying sizes of heating systems. The optimization objectives are the minimization of the total cost of the network and of the share of primary energy import into the network. The total cost function includes non-linearities such as investment costs, which can vary with the size of the installed system such that the design optimisation algorithm is implemented as a genetic algorithm. This tool enables to provide an accurate sizing of the network modelling accurately physical phenomena into the network.

continued ...

... continued

Authors	Methodology	Summary
Weber (2011) [56]	Multi-objective Multi-period MINLP connected to a GIS	Model for the whole design of district energy systems from the information available for the studied area (available energy sources and energy demand profiles and their locations) with a thermo-economic modelling of the energy conversion technologies and the constraints on the network in order to minimize CO_2 emissions and total costs. This multi-objective formulation uses a decomposition strategy into two sub-problems. The first optimization sub-problem takes into account the energy conversion technologies whereas the second one optimizes the outline of the network. The method is validated on a real case study in Geneva (Switzerland).

1.4 Manuscript overview

The PhD manuscript is organised in six chapters whose main goals are summarised as follows:

- **Chapter 1 : Introduction**
  This chapter gives a brief overview of the energy sector focusing on the heating sector and the district heating network technology. An overview of the main issues related to the district heating sector and of some specific issues linked to the *EcoSystemPass* research project is presented. Based on the identified goals of this research project, a non-exhaustive review of previous existing works and methods related to the optimization of district heating networks is presented. Based on this review, a positioning of this thesis is established to fill in the main objectives of the research project while leaving the possibility to replicate the work done into this thesis to new heating network projects.

- **Chapter 2 : Presentation of the decision tool**
  This chapter aims to present the decision tool developed into this thesis and its main components including the connection to a geographic information system, the assessment of the hourly heating demands of the consumers and the optimization model implemented to provide the optimal outline and sizing for a new heating network project. The main contribution of this thesis concerns the optimization model which uses the heating demand profiles as inputs of the model and the visualization into a geographic information system as an output. This chapter also looks for highlighting some of the limitations of the decision tool due to some modelling assumptions.

- **Chapter 3 : Tests of the decision tool on a small-scale theoretical case study**
  The decision tool presented in Chapter 2 is applied to a theoretical small-scale case study in order to illustrate the main results that the decision tool may provide and the influence of some user-defined economic and physical parameters on the outline and the sizing of a heating network. This theoretical case study is considered as a reference case which could be used for a comparison with other optimization formulations. This decision tool also tries to use theoretical scenarios which can illustrate the benefits of the integration of some heating sources into a heating network. It also aims for showing the usefulness of the decision tool for new heating network projects starting from a blank sheet and to compare centralized and decentralized heating production scenarios.

- **Chapter 4 : Calibration of the optimization model from dynamic simulations**
  The optimal heating network defined from the theoretical case study in Chapter 3 is modelled using a dynamic approach to assess more accurately the heat losses. Different dynamic modelling approaches are compared such that the most adequate dynamic model developed under the *Dymola* platform is used. This dynamic modelling aims to highlight the limitations of

the optimization formulation and some assumptions related to this formulation. From these identified limitations, the optimization model is calibrated based on the results obtained with the dynamic simulations.

- **Chapter 5 : Application of the decision tool to a large-scale real case study**
  The decision tool is finally applied to the real case study linked to the *EcoSystemPass* research project for the development of a district heating network connected to a waste incinerator and feeding a set of buildings including offices, residential dwellings and a greenhouse. This chapter aims to illustrate the replicability of the optimization tool to any new heating network project from small-scale to large-scale case studies and to give some answers to the company *Coriance* in charge of the design and the building of the future heating network in the prescribed area.

- **Chapter 6 : Conclusions and perspectives**
  A discussion about the strengths and the weaknesses of the decision tool developed in this thesis is achieved. Improvements are proposed in order to provide some perspectives for future work into this research field.

Chapter 2

Presentation of the decision tool

"A bad plan is better than no plan."
—Chess adage

This chapter aims to describe the different main parts of the decision tool mentioned previously for providing an optimized scenario for a district heating network project focused on a specific area into a geographic information system. The decision tool retrieves information from a geographic information system listing all streets and dwellings into a prescribed geographic area. This geographic information system combined to a cadastral matrix of the area enables to determine the hourly heating demand of each dwelling constitutive of the studied neighbourhood from its annual heating consumption using an appropriate *Python* library (*demandlib*). A pre-processing stage with the selection of representative days out of the hourly heating consumption profile is then achieved to reduce the computation time of the decision tool. These representative heating consumption profiles combined with user-defined economic and urbanistic parameters are then used as inputs of the optimization model implemented in the *Julia* language. The decision tool provides then as outputs the main economic and design data with a layout of the network into the geographic information system.

This thesis focuses mainly on the preprocessing stage and the optimization model stage which are parts of the global decision tool. These stages require inputs data which are defined *a priori* by other research groups working on the *EcoSystemPass* project. These data are assumed as inputs of the preprocessing and optimization steps of the decision tool and can be refined or adapted from other available data sources if needed. The goal of this work is to provide a general optimization methodology which can be replicated to any new heating network optimization no matter the kind of inputs provided to the optimization tool. It is the responsibility of the user of the decision tool to provide enough accurately inputs data to ensure the validity of the outputs results. Based on these inputs, the visualization GIS-platform can provide the outputs of the optimization tool in an user-friendly way.

Regarding the pre-preprocessing and the optimization tool, some preliminary assumptions have been made to satisfy the requirements of the research project and are explained in the following of the manuscript:

- The optimization process is based on synthetic heating load profiles which

look for being as representative as possible of the real heating load profiles. Synthetic heating load profiles are used to speed up the optimization process, especially for large-scale instances with thousands of streets in a defined neighbourhood, in order to guarantee a solution to the user of the decision tool within a reasonible time lapse;

- Non linear physical phenomena are simplified into linear ones. The simplification also aims for reducing the computational time of the solved problem while guaranteeing a solution to the user of the tool. The tool being initially dedicated to industrial users and policy-makers, a choice of a simplified representation of physical phenomena to guarantee an user-friendly and replicable approach to any new heating network project is chosen;

- Urbanistic constraints rely on the available data sets for the studied area such that they are formulated in a general way but have to be fitted to any new specific area as a function of the available space into the ground for the pipes or the available space for the heating production and thermal storage units. The quality of the results provided by the optimization model are once again dependent on the quality of the urbanistic data provided by the user of the decision tool;

- Temperature levels are prescribed as inputs of the optimization model and assumed to be constant such that the optimization formulation is independent on the temperature levels into the network. This assumption also aims to simplify the formulation in order to solve large-scale problems in an easy and fast way. However, this assumption will be criticized in Chapter 4 because of the large temperature drop which can occur with a non-optimal operation of the network. The temperature levels are prescribed regarding nominal operating conditions in third generation heating networks to respectively 90 and 60°C for supply and return temperatures. Energy balances over the network are then computed as a function only of the power flows independently of the temperature levels. It can be noticed that the heat losses and pipe diameters linked to the power flows for prescribed temperature levels could be adapted to other temperature levels if needed;

- For the outline of the network, a tree-shaped unique primary circuit is considered without boosting heating units at some local places which would enable to operate at lower supply and return temperatures over the primary circuit. This assumption is made to simplify the optimization formulation and to fit with the main requirements of the project;

- All the potential heating technologies are considered on an even kneel such that they all produce water at 90°C to directly supply the heating network. Some heating production units being part of the set of available technologies like air-to-water heat pumps are therefore disadvantaged because of their low coefficients of performance for these ranges of operating temperatures. Even though this assumption can be criticized, it enables to simplify the problem formulation regarding the selection of the optimal heating source

and let the possibility to replicate the formulation to fourth generation heating networks;

- For thermal storage units, as discussed in Chapter 1, tank storage units are considered as the unique available thermal storage units for the heating network sizing. This assumption can be questionable due to the fact that these kinds of storages are not the most adequate for seasonal thermal storage but rather for daily thermal storage because of the bigger heat losses than with underground thermal storage solutions. This choice has been made to consider any storage size for various network sizes. Indeed, underground storages require a prior knowledge of the ground composition where a potential underground thermal storage unit could be installed. Moreover, these kinds of storages require a large space into the ground which is *a priori* unknown. Therefore, in order to keep the optimization formulation as replicable as possible to any kind of heating network project, only tank storage units are considered and are dependent on the available building surface to put a storage on it. Even though this choice disadvantages the seasonal thermal storage, the decision tool mainly aims to predefine an optimal outline for a heating network. After this pre-feasibility study, additional scenarios considering other types of storages can be studied *a posteriori*.

Based on these assumptions and the general description of the decision tool, the global architecture of the decision tool is illustrated in Figure 2.1 with the contributions of this thesis to the decision tool depicted in red. In the following, these 4 main components of the decision tool are described with a particular focus on the preprocessing and the optimization model.

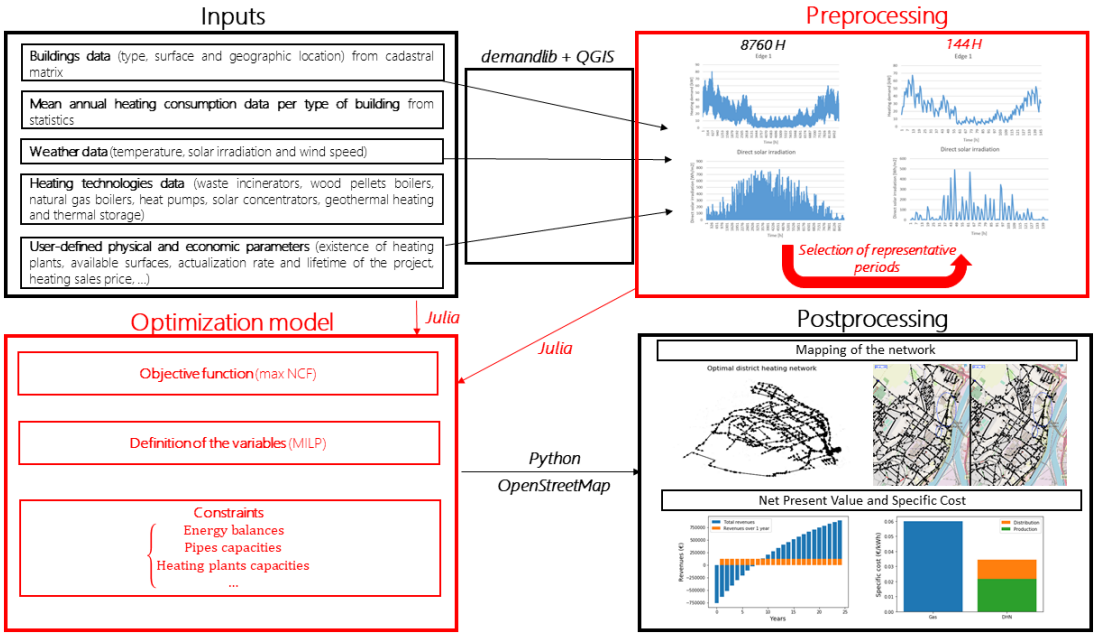

FIGURE 2.1: Methodology of the decision tool for the strategic planning of a district heating network project.

2.1 Inputs - Assessment of the heating demands

A geographic area can be represented from a geographic information system with databases related to different dwellings constitutive of the area. These databases include for each dwelling the living area, the number of floors, the kind of dwellings and their geographic location. Additionally, data about the annual space heating and domestic hot water demand and consumption [1] can be extrapolated from statistical data for each different category of dwellings. All these information can be used to compute synthetically hourly heating demands over a whole year for the considered dwellings.

2.1.1 Collection of annual heating demand data

A listing of all the features linked to the dwellings constitutive of the studied area into the geographic information system requires data collection from a cadastral matrix of this area. From this cadastral matrix, each dwelling can be categorized into a specific category of dwellings defined from statistical data grouping dwellings by their use and nature. These statistical data from the *Institut de Conseil et d'Etudes en Développement Durable (ICEDD)* [72] distinguish buildings from the residential and the tertiary sector. For the residential sector, 4 subcategories are defined and for the tertiary sector, 5 subcategories are defined. All these subcategories are summarized in Table 2.1.

TABLE 2.1: Categories of dwellings for the residential and tertiary sector.

Residential sector	**Tertiary sector**
Apartments	Shops
Terraced dwellings	Schools
Semi-detached dwellings	Culture, sports & other services
Detached dwellings	Health care
	Offices

In the cadastral matrix, some features of each dwelling including its category (cf. Table 2.1), its total area and its location can then be used for the computation of their annual heat demand. The total annual heat demand (including space heating and domestic hot water) of each subcategory a of dwellings is available in the most recent *ICEDD* available report [72] identifying the total consumption in Wallonia of each type of dwellings $\dot{Q}^a_{heat,tot}$ and the living surface S^a_l of the n_a dwellings of type a identified in Wallonia. The heat demand per unit surface of a dwelling of type a is thus defined by Eq. 2.1.

$$\dot{Q}^a_{heat,m^2}[\frac{kWh}{m^2.year}] = \frac{\dot{Q}^a_{heat,tot}}{\sum_{l=1}^{n_a} S^a_l} \tag{2.1}$$

where

[1] Heating demand characterizes the final energy demand while heating consumption is related to the primary energy used for the supply of the final energy demand. Demand and consumption are linked by the energy efficiency of the technology used for the heating supply.

$$S_l^a = S_{floor,l}^a \cdot (n_{floors} + \delta) \text{ with } \delta = \begin{cases} 0 & \text{if non habitable attic} \\ 1 & \text{if habitable attic} \end{cases} \tag{2.2}$$

For any dwelling l of type a constitutive of the studied area, its annual heat demand is finally determined by Eq. 2.3 where the total living area S_l^a is computed from the floor area $S_{floor,l}^a$ identified into the geographic information system. These annual heat demand values are then used to generate hourly heating demand profiles for each dwelling.

$$\dot{Q}_{heat,l}^a [\frac{kWh}{year}] = S_l^a \cdot \dot{Q}_{heat,m^2}^a \tag{2.3}$$

This approach used for characterizing the heat demand of each dwelling of the studied area has been used in the frame of the research project because of a lack of available data regarding the specific annual heating consumption of the considered dwellings. It can be noticed that this approach can be very limiting for the accuracy of the obtained results. Indeed, with this methodology, two dwellings of the same subcategory a and with the same living surface S_l^a get exactly the same annual heating consumption no matter their location and/or their behaviour as a heating consumer. This lack of data illustrates the importance to record real heating consumption data in open-source files for their easy use as inputs in energy optimization frameworks. Without these files, it is intricate to provide accurate results because of the lack of accuracy of the inputs data.

2.1.2 Generation of hourly heating demands profiles

The sizing of a district heating network generally requires an accurate knowledge of the hourly heating demands of the dwellings constitutive of the studied neighbourhood or city. The main difficulty related to the computation of these heating demands is generally due to the large amount of dwellings into a specific geographic area. Detailed physical models of dwellings have thus some limitations in terms of computational time for the modelling of the heating consumption of a large building stock. An alternative to the use of physical models for the computation of heating consumption is based on the use of synthetic heating load profiles and temperature forecasts taking into account the kinds of dwellings. Some open-source frameworks are already available to design these kinds of heating profiles. One of them, named *demandlib* [73], based on synthetic heating load profiles from the BDEW [74] is used in this research project. The decision tool retrieves the annual heating consumption of a dwelling $\dot{Q}_{heat,l}^a$ computed previously to create a new hourly heating demand profile using the *demandlib* library. Synthetic heating load profile is then described by a transfer function TF represented by Eq. 2.4. The reader can refer to [75] for more details about this generation of hourly heating demand profiles and its validation on an existing building stock in Germany.

$$TF(\theta_{geo,t}) = \frac{A}{1 + (\frac{B}{(\theta_{geo,t} - \theta_0)^C})} + D, \theta_0 = 40°C \tag{2.4}$$

where A, B, C and D are the parameters of the transfer function and are dependent on the kind of dwellings. θ_{geo} represents the geometric temperature defined by the following equation for a prescribed time period t:

$$\theta_{geo,t} = \frac{(T_t^{air,out} + \frac{1}{2}T_{t-1}^{air,out} + \frac{1}{4}T_{t-2}^{air,out} + \frac{1}{8}T_{t-3}^{air,out})}{(1 + \frac{1}{2} + \frac{1}{4} + \frac{1}{8})} \tag{2.5}$$

with $T_{t-3}^{air,out}$, $T_{t-2}^{air,out}$, $T_{t-1}^{air,out}$ and $T_t^{air,out}$ the respective outdoor temperatures from the time period t-3 to the time period t.

The heating consumption for a time period t can then be computed with the following equation based on the transfer function TF defined previously for any timestep t and any dwelling l of type a.

$$\dot{Q}_{heat,l,t}^{a} = TF(\theta_{geo,t}) \cdot F_{wd} \cdot KW \tag{2.6}$$

F_{wd} is a factor dependent on the day of the week and KW is a constant characterizing the consumer which is defined by the heating demand of this consumer and the transfer function:

$$KW_l = \frac{\sum_{t=1}^{N_{timesteps}} \dot{Q}_{heat,l,t}^{a}}{\sum_{t=1}^{N_{timesteps}} TF(\theta_{geo,t})} = \frac{\dot{Q}_{heat,l}^{a}}{\sum_{t=1}^{N_{timesteps}} TF(\theta_{geo,t})} \tag{2.7}$$

From the annual heating consumption of a dwelling l of type a during a year $\dot{Q}_{heat,l}^{a}$ and a weather file with all the hourly temperatures during a year for a characteristic year in Belgium, heating load profiles for each dwelling can then be directly computed. This generic solution provides in a fast way required hourly heating load profiles used as inputs of the optimization model. Even though this synthetic generation of heating loads does not take into account any physical parameter for the assessment of the heating demand, the previous validation of the methodology on existing building stocks in Germany enables to replicate the methodology to the Walloon building stock. The values of the parameters in Eqs. 2.4-2.7 are avalaible in [75]. However, the reader has to keep in mind that due to the fact that two buildings of the same type with the same living area are characterized by the same annual heating demand with this methodology, the generation of hourly heating loads will not take into account heating demand variations due to the human behaviour of the heating consumers. This factor is generally important to take into account into a heating network design because it can influence the aggregation effect presented in Section 1.2.2.

Moreover, this method considers as unique inputs the annual heating load demand and the category of dwellings. The type of insulation of the dwelling is not directly taken into account in the approach. It is indirectly considered with the annual heating load demand which is normally specific to each dwelling even though it is not the case in this study because of the lack of data for determining the annual heating demand of each dwelling. Therefore, inputs data provided for this research project are objectionable and other data should be provided to improve the quality of the inputs data.

2.2 Preprocessing - Selection of representative periods for heat demands

The complexity of the problem to solve is directly linked to the number of optimization variables. An optimization over a whole year with hourly timesteps can lead quickly to an exponential complexity leading to infeasibility for solving large-scale problems in a finite time. The large number of optimization variables defined with hourly heating consumption data can be decreased using representative periods to reduce the computation time of the decision tool. These representative periods have to be selected in order to represent as accurately as possible the heating demand profile over the whole year with a limited number of timesteps. Generally, these periods are chosen to fit as well as possible the heating load duration curve but don't include extreme periods with peak demands. The selection of representative days is already used in the electricity network optimization field and can also be applied to the heating sector. Different approaches exist and are used to represent as accurately as possible a real year with a synthetic representative year. The three main existing methods for this selection of representative periods are proposed as follows:

1. Simple heuristics choosing some representative days based on a specific rule. These methods rely on a simple selection of some days as representative days in order to cover a variety of different heating loads and weather conditions. An example of a simple heuristics method to choose some representative days is to select the days with respectively the minimum and maximum demand over the year and the days with the most widespread demand over the day [76]. The main problem with this kind of methods is that there is no robust criteria to determine the viability to pick up a specific day as a representative day [77].

2. Clustering algorithms used to cluster periods with similar energy demands using machine learning techniques. For each cluster determined by the algorithm, the cluster's center is chosen as a representative day for this cluster. All the days related to this cluster are then associated with this representative day. The goal of these algorithms is to define a prescribed number of clusters while minimizing the sum of the distances between the different components of the clusters and the cluster's centers. Two main categories of clustering algorithms can be identified in the literature: hierarchical and partitional clustering. Hierarchical clustering relies on the principle to merge smaller clusters in larger ones or to split larger clusters in smaller ones by producing a hierarchy of clusters. Compared to hierarchical clustering, partitional clustering aims to generate a large number of clusters and to evaluate them from some mathematical criteria. Even though partitional clustering is typically faster than hierarchical clustering, both methods are used in the energy sector to pick up representative periods [78]. The reader can refer to [79] for hierarchical clustering methods and [80–82] for partitional clustering methods applied to the selection of representative periods for energy optimization problems. These clustering

methods are by far the most employed in the literature thanks to their easy replicability to any set of data and to any new problem.

3. Optimization based on a user-defined predetermined optimization criterion. This method is more specific to energy datasets and aims to consider the datasets as a whole by approximating as well as possible the load duration curve resulting from these datasets using representative periods. This optimization approach is innovative compared to the previous ones and the only researches found in the literature following this approach are [77, 83]. [83] achieves a very comprehensive review of these methods defining comparison criteria between them to finally develop a novel optimization-based approach to select representative days.

Therefore, in the decision tool presented in this thesis, a procedure based on the optimization approach developed by [83] is readjusted to sort selected representative periods and to include peak demands in order to represent more accurately the chronology of the variable heating demand. The objective of the optimisation procedure consists in minimizing the deviation between the heating load duration curve of the full year period and its representation by the means of a selected number of representative days with assigned weights. The weights of each representative day are then used to scale the variable costs assessed into the optimization objective and to apply energy balances constraints on the thermal storages. The method developed by [83] has the disadvantage to select the best fitting time periods of the load duration curve without really representing peak demands and the dynamics of the system for its sizing. Indeed, for example, the sizing of the storage depends on the dynamics of the loading and unloading phases during the different time periods. [84] develops a sorting procedure for the different selected time periods. However, this new synthetic chronological representation of a year does not include peak demands which are important to consider for the sizing of heating sources and storages. Moreover, even with the selection of only a few representative days, the number of variables can increase exponentially with the number of selected representative days because each day is made up of 24 hours. In order to overcome this problem, a new procedure based on the selection approach developed by [83] is implemented as illustrated in Figure 2.2.

In this procedure, instead of selecting the best representative days over the whole year, a pre-processing is achieved to sort heating consumptions on a monthly basis. For each month, the day with the biggest hourly demand is directly chosen with a unitary weight $w_d = 1$ as a representative day and the optimization procedure developed by [83] is used to select the best $N_{repr,month}$ days for each month. Each representative day of a month is assigned with a weight w_d. For each month, $N_{repr,month}$+1 days are thus chosen to finally reshape a synthetic year with $12 \cdot (N_{repr,month} + 1)$ representative days. For a given hourly heating consumption profile, the procedure gives the results illustrated in Figure 2.3. In order to reduce even more the number of timesteps for the optimization process, a discretization of the representative days in $N_{repr,hours}$ bins for each representative day is achieved by using *KBinsDiscretizer* tool [85] in *Python*.

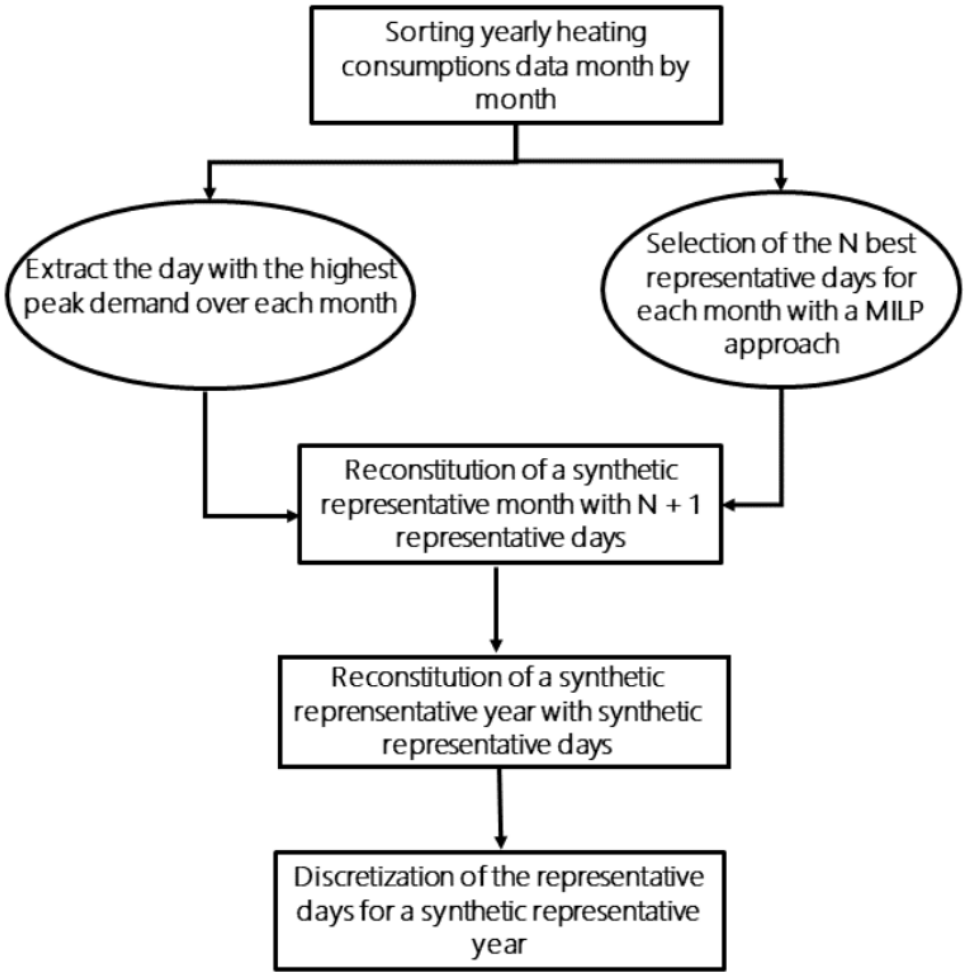

FIGURE 2.2: Readjusted methodology for the selection of representative time periods for a given year.

Each representative hour of a representative day is then assigned by a weight $w_t = \frac{24}{N_{repr,hours}}$. The discretization of a selected representative day is illustrated in Figure 2.3.

The selection of representative days enables to approximate the initial load duration curve with enough accuracy even though the new synthetic load duration curve slightly overestimates the initial load duration curve. It can also be noticed that the peak demand is a little bit underestimated with the computation of representative hours within a representative days. Nevertheless, with this synthetic year, the two main informations required for the design of a heating network are available:

- Representative days for approximating as well as possible the heating load duration curve and the total heating demand;
- Representative days for representing peak heating demand conditions in order to do not underestimate the total sizing of the heating network system.

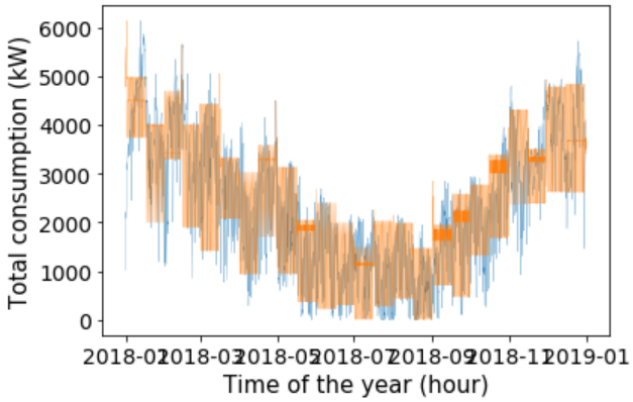

(a) Synthetic year with the selection days methodology.

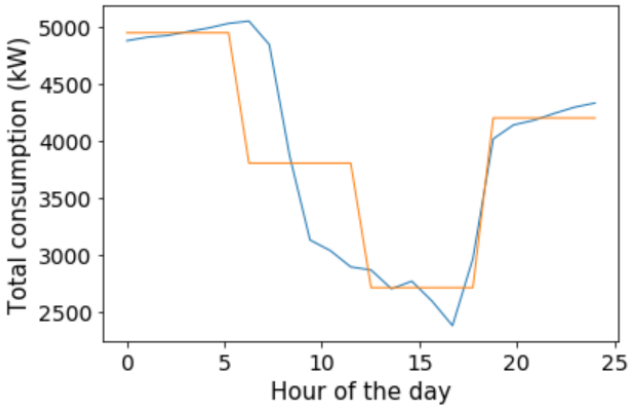

(b) Discretization of a selected representative day.

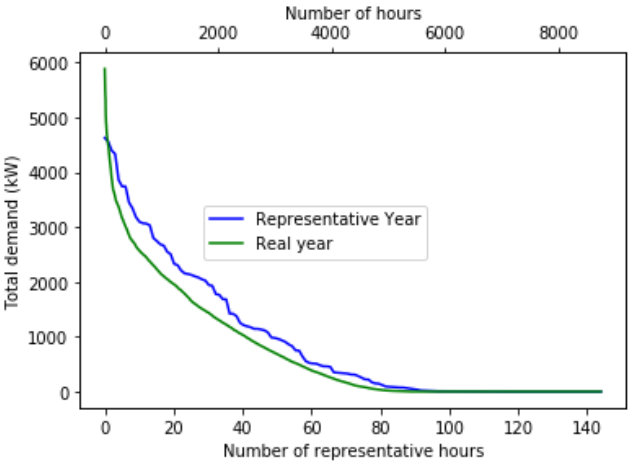

(c) Load duration curves for the synthetic year and the real year.

FIGURE 2.3: Selection of representative time periods.

2.3 Optimization model

2.3.1 Quick reminder on mathematical optimization

Mathematical optimization remains a powerful tool to provide optimal solutions to any problem by selecting the best set of values for prescribed variables in order to optimize (minimize or maximize) one or several functions named the objective functions. The set of potential values for each variable of the problem is defined by a discrete or continuous set of choices, named the feasible region. A mathematical modelling of the problem is then developed to describe as accurately as possible the problem by implementing some constraints related to the problem. The implementation of the mathematical modelling can be achieved using a mathematical programming language like *Julia*, *GAMS* or *Pyomo* for example. These languages enable to write down the problem in a way to tackle it using a license-free mathematical solver like *GLPK* or commercial solvers like *Cplex* or *Gurobi*.

Any mathematical optimization problem can be defined in a general form as follow:

$$\begin{aligned} \min_{\mathbf{x} \subset X} \quad & \mathbf{f}(\mathbf{x}) \\ \text{subject to} \quad & \mathbf{g}(\mathbf{x}) \leq 0 \\ & \mathbf{h}(\mathbf{x}) = 0 \end{aligned}$$

$\mathbf{x}$ represents all the variables of the optimization problem with their respective spaces of feasible solutions $\mathbf{X}$. $\mathbf{g}(\mathbf{x})$ includes all the inequalities constraints related to the optimization problem while $\mathbf{h}(\mathbf{x})$ takes into account all the equalities constraints. In an optimization problem, multiple objective functions $\mathbf{f}(\mathbf{x})$ can be defined simultaneously. Depending on the properties of the objective function and the constraints, different types of optimization can be distinguished and are summarized in three main categories in Table 2.2.

These three categories of optimization methods have both advantages and disadvantages such that the most suitable technique to the studied problem has to be taken into account. As explained in Chapter 1, the decision tool developed into this thesis is part of a research project to help decision-makers for the implementation of a new heating network project into a prescribed geographic area. The main goal is to develop a user-friendly decision tool which can be easily used by any decision-maker to provide a unique optimal solution for a heating network implementation from small-scale to large-scale case studies. Non-linear techniques, even though they enable a better representation of the studied problem, are therefore discarded for the implementation of the decision tool. Indeed, these non-linear methods do not guarantee a unique solution and can reach high computation times even for small-scale problems. Another feature expected for the decision tool is the possibility to easily adapt the mathematical formulation to any other energy system optimization by including additional constraints to the formulation. In this case, heuristics methods are also not convenient for the

required application because a small change in the general formulation of the problem could be difficult to implement with heuristics methods.

Table 2.2: Categories of optimization techniques.

Category	Advantages	Disadvantages
Linear programming	• Adapted to large-scale systems • Easy use of standard solvers (GLPK, Cplex, Gurobi) • A local optimal is globally optimal	• Limitations on the accurate representation of the problem
Non-linear programming	• Large possibilities for mathematical implementation • Accurate representation of the problem	• Poorly adapted to large-scale systems • No guarantee to find the optimal solution
Heuristics	• Total freedom for the mathematical implementation • Can fit well with large-scale systems	• Algorithms must be personalized for each problem • No guarantee to find the optimal solution

The framework of the decision tool is then based on a linear mathematical formulation of the problem which guarantees a unique optimal solution to the problem and can be adapted to large-scale problems. This linear formulation is implemented in the *Julia* language using the commercial solver *Gurobi* with an academic license to solve the optimization problem.

2.3.1.1 Linear optimization

Linear optimization relies on the fact that the objective function **f** as well as the set of inequality and equality constraints **g** and **h** are linear. The general

form of a linear formulation can be written in the following matrix form:

$$\begin{aligned} \min_{\mathbf{x} \subset X} \quad & \mathbf{c}^T \mathbf{x} \\ \text{subject to} \quad & \mathbf{A}\mathbf{x} \leq \mathbf{b} \\ & \mathbf{x} \geq 0 \end{aligned}$$

This canonical form allows to express the problem in a linear way to guarantee the convexity of the problem. A convex optimization problem formulation enables to provide a unique solution to the optimization by ensuring that this solution is the optimal one. This convexity enables to use iterative and search algorithms like the simplex algorithm to find the optimal solution. The simplex algorithm enables to find the optimal solution of an optimization problem with continuous variables by looking for the optimal solution from the space of possible solutions defined by a polygon of constraints. The optimal solution is located at one of the vertices of this polygon such that the simplex algorithm finds some feasible vertices solutions and then find directions in which objective improves and select one of these directions. As depicted in Figure 2.4 [86], the algorithm then iterates until no more improving direction is found.

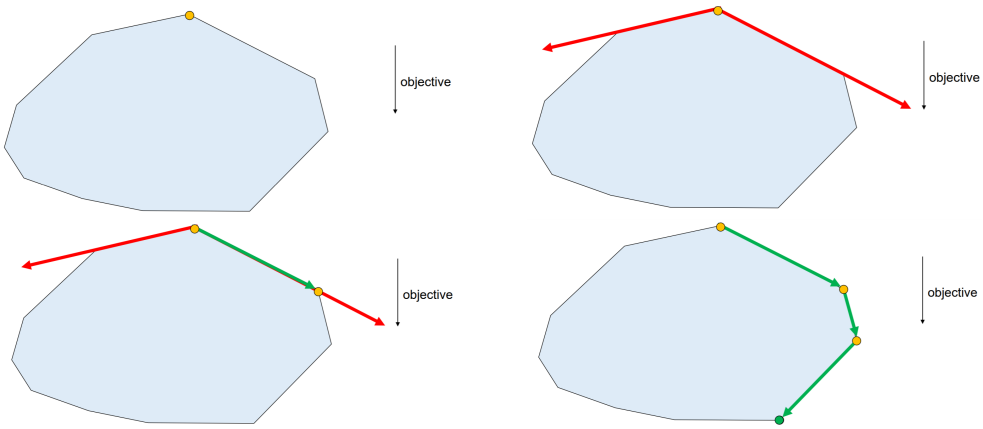

FIGURE 2.4: Simplex algorithm [86].

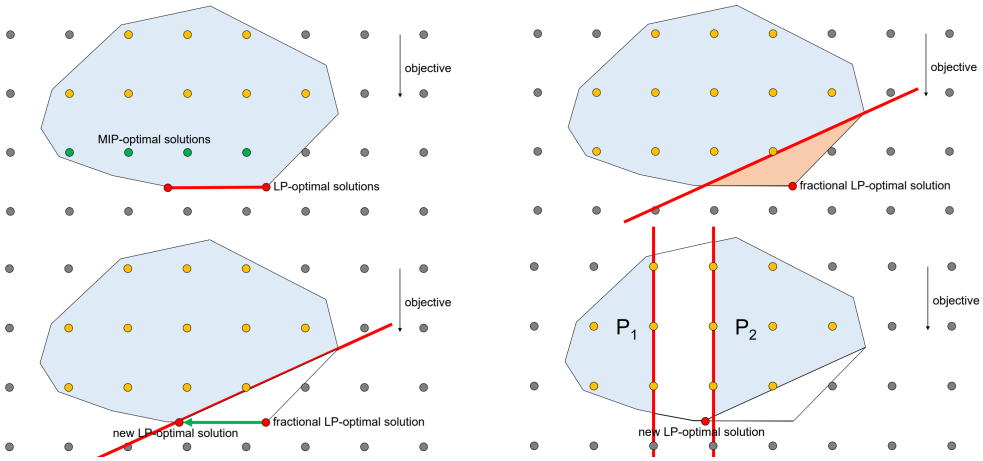

FIGURE 2.5: Branch-and-bound algorithm [86].

However, in this thesis, some of the decision variables of the problem are not continuous but discrete. These kinds of optimization problems are called mixed-integer linear problems. The solution from the simplex algorithm is thus not the final solution of the mixed-integer linear problems. In order to find the solution of this problem, as illustrated in Figure 2.5 [86], a branch-and-bound algorithm starting from the solution of the simplex algorithm can then be used to provide the optimal solution to the optimization problem including continuous and discrete variables.

The model developed in this thesis is based on a graph representation of any geographic area defined in a geographic information system such as edges e of the graph match with the streets of the studied area and their intersections are represented by the vertices v of the graph. A small neighbourhood with only a few streets which is used as a reference case in Chapter 3 is represented as in Figure 2.6. From this graph representation, a set of vertices and edges can be defined such that balance equations with some constraints are applied on the potential network to be built.

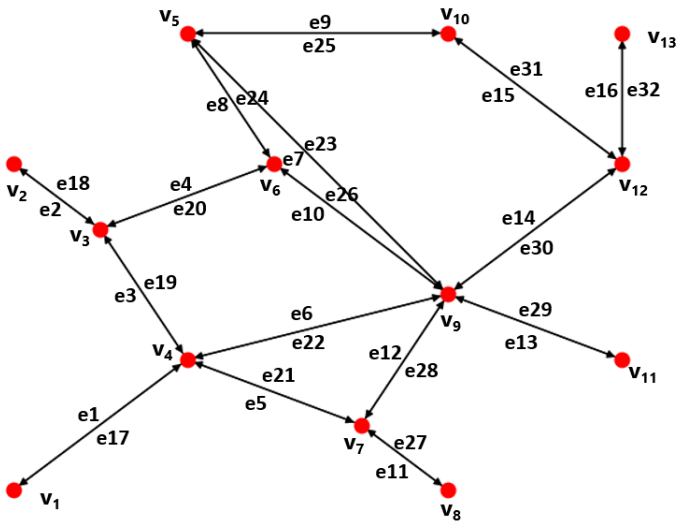

FIGURE 2.6: Graph representation of a neighbourhood of 16 streets with 13 intersections.

2.3.2 Sets

Defining V as the set of indices i of the vertices v_i of the graph, another subset $V_P \subset V$ containing the indices of the vertices v_i which are potential heating sources and thermal storages locations is defined. For each vertex $v_i \in V_P$, a set H_i listing all the available technologies m for heating production is defined. These sets of technologies include waste incinerators, wood pellets plants, gas boilers, heat pumps, solar collectors, geothermal plants and thermal storages. All these vertices have to be linked by edges e_j whose indices j are included into a set E and additional sets of edges N_i include all the indices j of the adjacent edges e_j

to a given node v_i. Finally, a time component has to be taken into account to determine a multi-period optimization problem by defining a set T made up of $N_{timesteps}$ of a duration of Δt hours including all the considered timesteps t for the optimization solving, a set D constitutive of all the representative days d and subsets $T_D \subset T$ containing timesteps t for a representative day d. The number of timesteps $N_{timesteps}$ is based on the number of selected days defined by the user of the decision tool such as the problem is defined by $12 \cdot (N_{repr,month} + 1) \cdot N_{repr,hours}$ timesteps.

2.3.3 Constraints

The solving of a linear optimization problem requires to define linear constraints delimiting the field of feasible solutions on which a branch-and-bound algorithm can be applied. These constraints are based on physical conservation laws but also on practical requirements defined by the user of the decision tool.

2.3.3.1 Energy balance at the vertices and the edges of the graph

Energy flows over potential supply pipes constitutive of the network have to satisfy heating requirements at each timestep including heat losses over the lengths of the pipes. Energy flows are fed by potential heating sources and/or thermal storages located at some vertices of the graph such that energy balances at the vertices and the edges of the graph have to be satisfied as illustrated in Figure 2.7.

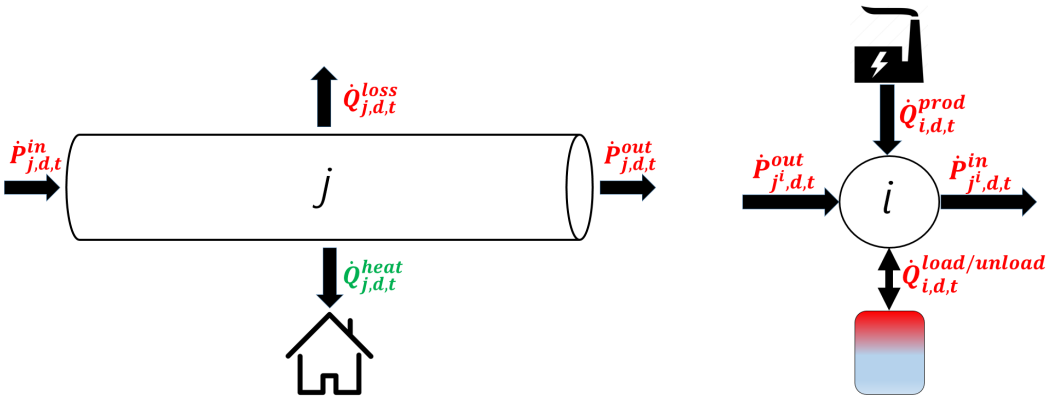

(a) Energy balance over an edge e_j of the network

(b) Energy balance over a node v_i of the network

FIGURE 2.7: Energy balances at the vertices and the edges of the graph

Based on this figure, an energy balance over each edge e_j and node v_i of the graph can be written as follows:

$$\begin{cases} \underline{\forall j \in E, \forall d \in D, \forall t \in T_D :} \dot{P}^{out}_{j,d,t} = \dot{P}^{in}_{j,d,t} - u_{j,d,t} \cdot p_j \cdot \dot{Q}^{heat}_{j,d,t} - \dot{Q}^{loss}_{j,d,t} & \text{(2.8a)} \\ \underline{\forall i \in V, \forall d \in D, \forall t \in T_D :} \sum_{j \in N_i} (\dot{P}^{in}_{j,d,t} - \dot{P}^{out}_{j,d,t}) = \dot{Q}^{prod}_{i,d,t} + \dot{Q}^{unload}_{i,d,t} - \dot{Q}^{load}_{i,d,t} & \text{(2.8b)} \end{cases}$$

where $\dot{P}_{j,d,t}^{in/out}$ are respectively the incoming and outcoming power flows into a pipe j characterized by a heating consumption $\dot{Q}_{j,d,t}^{heat}$ weighted by a connection rate p_j taking into account the ratio of consumers that would agree to be connected to the network. This ratio has a significant importance for urban energy planners because it impacts the total heating load over the potential streets to connect. A smaller heating load over a street due to the non connection of some heating consumers which do not want to be connected to a network project reduces the heating density of the project. A street which was assessed to be profitable to connect with a 100% connection could become non profitable to connect with a decrease of this connection rate. $\dot{Q}_{i,d,t}^{prod}$ represents the heating production at a node v_i and $\dot{Q}_{i,d,t}^{load/unload}$ are the loading and unloading power flows from a potential storage at this node. The binary variable $u_{j,d,t}$ is required to define if a pipe is used or not at a given timestep.

The heating production $\dot{Q}_{i,d,t}^{prod}$ for each node v_i of the network is related to the heating production $\dot{Q}_{i,m,d,t}$ of each technology m located at a given location v_i such that the following equality constraint can be defined:

$$\underline{\forall i \in V, \forall d \in D, \forall t \in T_D :} \dot{Q}_{i,d,t}^{prod} = \sum_{m \in H_i} \dot{Q}_{i,m,d,t} \tag{2.9}$$

This constraint ensures that the total heating production level at a node v_i at each timestep is equal to the sum of all the heating productions from different heating sources at this node v_i.

Heat losses $\dot{Q}_{j,d,t}^{loss}$ over an edge j

Thermal losses into the pipes are one of the main drawbacks of heating networks such that losses have to be taken into account to define the best way to build and size the network. A steady-state two-dimensional heat transfer model previously validated in the literature from experimental data [87] is used in this thesis to define an analytical formulation of these heat losses. Considering a supply and a return pipe with diameters D at a distance S from each other and buried into the ground with a temperature T^{gd} at a depth H (generally around 1 meter depth) as illustrated in Figure 2.8, a thermal equivalent resistance can be deduced taking into account all heat transfers taking place into the system. Unit heat losses $\dot{Q}^{,loss}$ can then be directly computed from the thermal equivalent circuit as defined in Eq. 2.10.

$$\dot{Q}^{,loss} = \frac{T^{w,in} - T^{gd}}{R'_{1pipe}} + \frac{T^{w,in} - T^{w,out}}{R'_{2pipes}} \tag{2.10}$$

The analytical formulation of R'_{1pipe} and R'_{2pipes} relies on the shape factors related to the heat transfer into a cylinder with a given insulation thickness and the heat transfer between 2 pipes buried into the ground.

For a cylinder as illustrated in Figure 2.9, the total thermal resistance R'_{1pipe} is defined by Eq. 2.11.

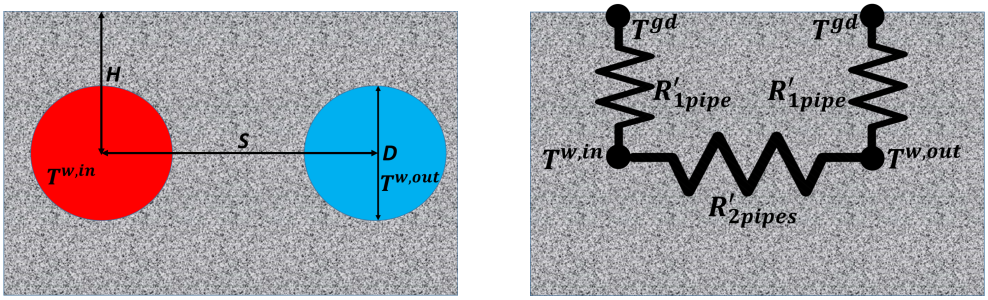

(a) Schematic representation of a two-pipes heating network

(b) Thermal circuit linked to this heating network

FIGURE 2.8: Physical representation of a 2-pipes distribution system.

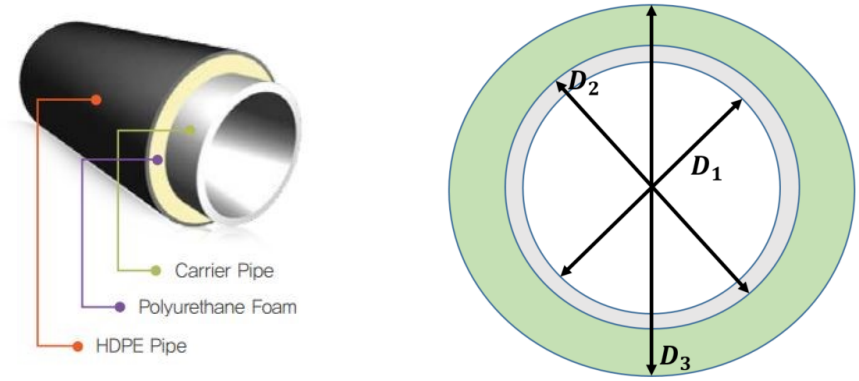

(a) Materials constitutive of the pipes

(b) Pipes diameters

FIGURE 2.9: Geometry of the pipes of a heating network.

$$R'_{1pipe} = \frac{1}{h_{in} \cdot \pi \cdot D_1} + \frac{ln(\frac{D_2}{D_1})}{2 \cdot \pi \cdot k_{steel}} + \frac{ln(\frac{D_3}{D_2})}{2 \cdot \pi \cdot k_{ins}} + \frac{ln(\frac{4H}{D_3})}{2 \cdot \pi \cdot k_{gd}} \tag{2.11}$$

where h_{in} is the internal convection coefficient and is dependent on the flow velocity related to the pipe diameter and k_{steel}, k_{ins} and k_{gd} are the thermal conductivities for the steel pipe and its insulation and the ground conductivity. The computation of the convection coefficient h_{in} is based on correlations for a turbulent flow into a pipe assuming a fully-developed turbulent flow into the pipes. The assumption of a turbulent flow relies on Reynolds numbers for the flow ranges into heating networks which are much higher than the critical Reynolds number of 2300 for a flow into a circular duct (cf. Figure 2.10).

It can be noticed from Figure 2.10 that the Reynolds numbers are computed for different values of the pipes diameters as a function of the considered range of power flows. An increase of the power flow implies an increase of the mass flow rate and of the flow velocity for a prescribed pipe diameter. Pipes diameters are generally chosen to limit pressure losses into the pipes to a maximum value linked to a nominal flow velocity into the pipes. Pressure losses ΔP for a fluid of

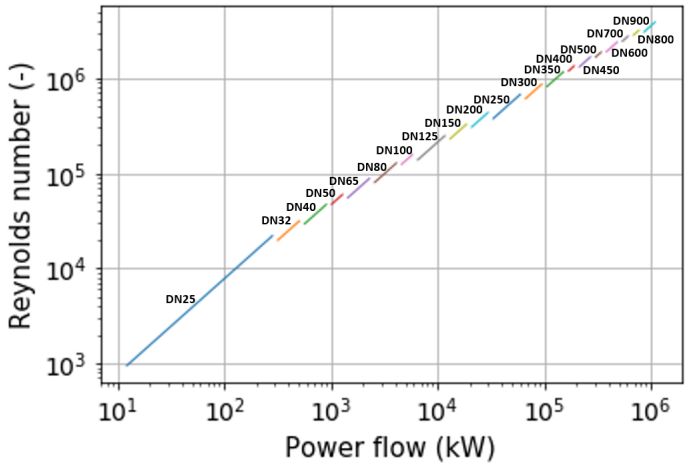

FIGURE 2.10: Reynolds number as a function of the power flow.

density ρ flowing with a velocity v into a pipe of length L and diameter D with a prescribed friction factor λ are defined by Eq. 2.12.

$$\Delta P = \frac{\lambda \cdot L}{D} \cdot \frac{\rho \cdot v^2}{2} \tag{2.12}$$

The mass flow rate $\dot{m}$ flowing into the pipe is directly proportional to the fluid velocity v and the cross-sectional area of the pipe as illustrated mathematically by Eq. 2.13.

$$\dot{m} = v \cdot \rho \cdot \frac{\pi \cdot D^2}{4} \tag{2.13}$$

Prescribing a fixed temperature difference ΔT_{sub} at the substations for the optimization of the network, the power flow $\dot{P}$ into a pipe is directly linked to the mass flow rate $\dot{m}$:

$$\dot{P} = \dot{m} \cdot c_{p,w} \cdot \Delta T_{sub} \tag{2.14}$$

The sizing of the pipes for nominal conditions enforces the limitation of the pressure losses to a nominal value ΔP_{nom} generally prescribed to 100 Pa/m related to a nominal power flow $\dot{P}^{nom}$ for each pipe. Combining Eqs. [2.12-2.14], an analytical expression linking this nominal power flow to the diameter of a pipe j of length L_j can be established as follows:

$$\dot{P}_j = c_{p,w} \cdot \Delta T_{sub} \cdot \sqrt{\frac{\Delta P_{nom} \pi^2 \rho}{8 \lambda L_j}} \cdot D_j^{\frac{5}{2}} \tag{2.15}$$

As mentioned in Section 1.2.3, diameters of the pipes provided by manufacturers have discrete values which would have to be included into the optimization variables for each edge of the graph for the sizing of the network. The problem would become highly complex to solve for large-scale cases because of the high number of additional discrete variables that would be introduced with the non-continuous values of the pipes. In order to limit the number of optimization variables and to use existing variables required

to constraint the system, the required diameter for a pipe is therefore linked to the nominal power flow into this pipe using Eq. 2.15. For each discrete value of a pipe diameter from manufacturer's datasheets, a nominal power flow $\dot{P}^{nom}$ can then be linked to the pipe diameter prescribing nominal pressure losses of 100 Pa/m. Each prescribed pipe diameter is then dedicated to a specific range of power flows limited by the allowable pressure losses into a pipe.

Having defined the power ranges dedicated to each pipe diameter, the internal convection coefficient can be computed from the Nusselt number given from correlations for a fully-developed turbulent flow into a pipe. The Colburn correlation (Eq. 2.16) is used in this thesis to determine the Nusselt number.

$$Nu_D = 0.023 \cdot Re_D^{4/5} \cdot Pr^{1/3} \tag{2.16}$$

with the following range of conditions which are generally fulfilled into heating networks:

$$\begin{cases} 0.6 \leq Pr \leq 160 \\ Re_D \geq 10000 \\ \frac{L}{D} \geq 10 \end{cases} .$$

By definition of the Nusselt number, the convection coefficient can finally be computed as follows:

$$Nu_D = \frac{h_{in} \cdot D}{k_f} \tag{2.17}$$

Considering the thermal resistance R'_{2pipes} between 2 pipes, it can be defined using the shape factor definition for this case by Eq. 2.18.

$$R'_{2pipes} = \frac{cosh(\frac{2 \cdot S^2}{D_3} - 1)}{2 \cdot \pi \cdot k_{gd}} \tag{2.18}$$

From standard values [33] for all the parameters presented in Eq. [2.10-2.18], a computation of the heat losses as a function of the power flows into the pipes with different ranges of diameters can then be determined and is illustrated in Figure 2.11. It can be observed that for the dedicated power flow ranges for each diameter, the heat losses per unit length are not really dependent on the power flow into the pipes but mainly on the pipes diameters. This is explained physically by the fact that within a given power range for a prescribed pipe diameter, the mass flow rate increase influences the temperature decrease profile over a unit length. The mass flow rate increase for a prescribed diameter increases the fluid velocity into the pipe decreasing then the temperature drop over a unit length of the pipe. The combined effects of an increasing mass flow rate and a decreasing temperature drop along the pipes make it possible to justify approximately constant heat losses for a prescribed diameter within a given power flow range. Heat losses defined by the variable $\dot{Q}^{loss}_{j,d,t}$ are then computed by linking the pipes diameters to their computed heat losses over their related power flow ranges as illustrated in Figure 2.12.

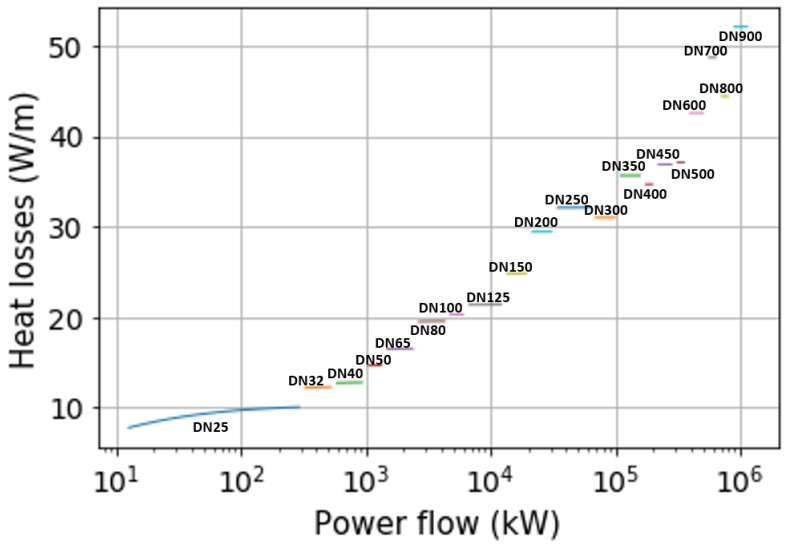

FIGURE 2.11: Heat losses into the pipes as a function of the power flows.

It can be observed from Figure 2.12 that heat losses are directly proportional to the pipes diameters such that they can be interpolated with a linear function. Using Eq. 2.15, these heat losses can also be expressed as a function of the power flows into a pipe.

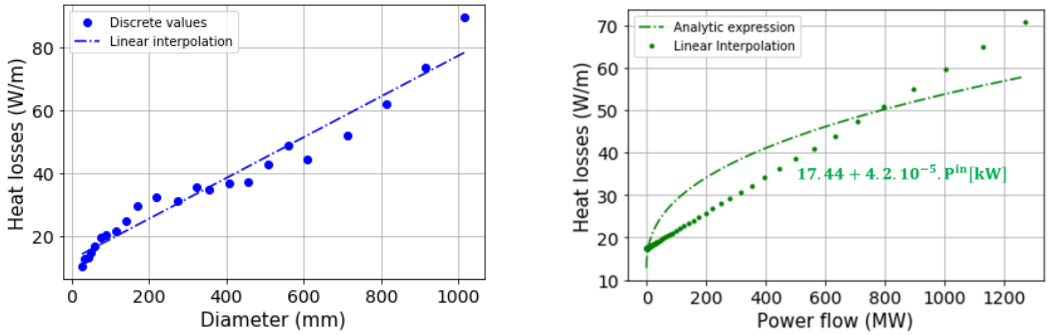

(a) Heat losses as a function of pipes diameters

(b) Heat losses as a function of maximum power flows

FIGURE 2.12: Characterization of the heat losses.

A linearization of the heat losses as a function of the power flows $\dot{P}^{in}_{j,d,t}$ into a pipe gives an analytical formulation of the variable $\dot{Q}^{loss}_{j,d,t}$ where the binary variable $u_{j,d,t}$ defines the use or not of a built pipe j at a timestep t:

$$\dot{Q}^{loss}_{j,d,t} = 0.001 \cdot L_j \cdot (4.2 \cdot 10^{-5} \cdot \dot{P}^{in}_{j,d,t} + 17.44 \cdot u_{j,d,t}) \tag{2.19}$$

Eq. 2.15 enables to link directly the power flow into a pipe to a function only dependent on the pipe diameter. However, this assumption is questionable because we consider with this formulation that the power flow $\dot{P}^{in}_{j,d,t}$ into a pipe j with a prescribed diameter D_j defined from nominal conditions will always be within the range of power flows dedicated to a given pipe diameter during the

whole operation of the network. In practise, this power flow is variable over the year such that the power flow into a pipe is not always included within the power range linked to a prescribed pipe diameter. As illustrated in Figure 2.13, smaller power flows for prescribed pipe diameters imply larger heat losses than the ones defined from nominal conditions. Accordingly, heat losses will always be underestimated with this formulation because of a linearization of the heat losses based on nominal operating conditions. Nevertheless, this assumption seemed to be required without knowing *a priori* the outline of the network such that the optimal pipes diameters are not known and have to be expressed as a function of the nominal power flows into the pipes. The influence of this assumption on the results of the optimization model will be tested later in Chapter 4 with dynamic simulations.

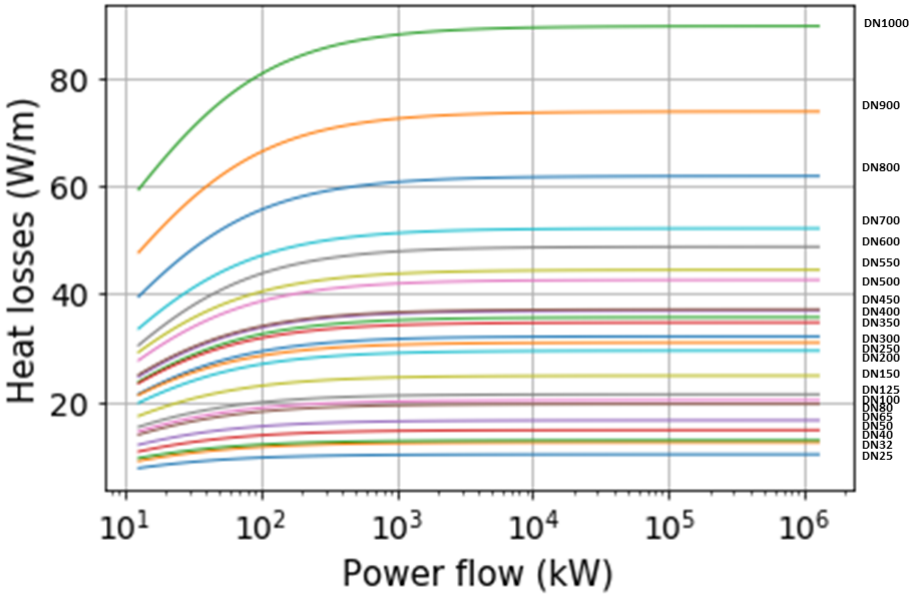

FIGURE 2.13: Heat losses for each pipe diameter over the whole range of power flows.

Considering Figure 2.12 which represents the heat losses as a non linear function of the power flows, a piecewise linear formulation of the function given by Eq. 2.15 can also be defined to compute more accurately the heat losses than with a linear function defined by Eq. 2.19. This piecewise formulation aims to fit as accurately as possible the heat losses function by defining linear functions over N_{ranges} discretized ranges of the power flows. An optimal choice of the bounds of these ranges can be achieved by using a *Python* module named *pwlf* [88]. In this thesis, 4 discretized ranges included between 0 and 1 GW with bounds defined respectively by $\dot{P}_0$, $\dot{P}_1$, $\dot{P}_2$, $\dot{P}_3$, and $\dot{P}_4$ are chosen to define a piecewise linear function over the whole range of considered power flows as illustrated in Figure 2.14.

Based on these 4 power ranges, a new set of decision variables for each edge and each timestep has to be defined to choose the piecewise linear function which has to be taken into account for the computation of the heat losses as a function

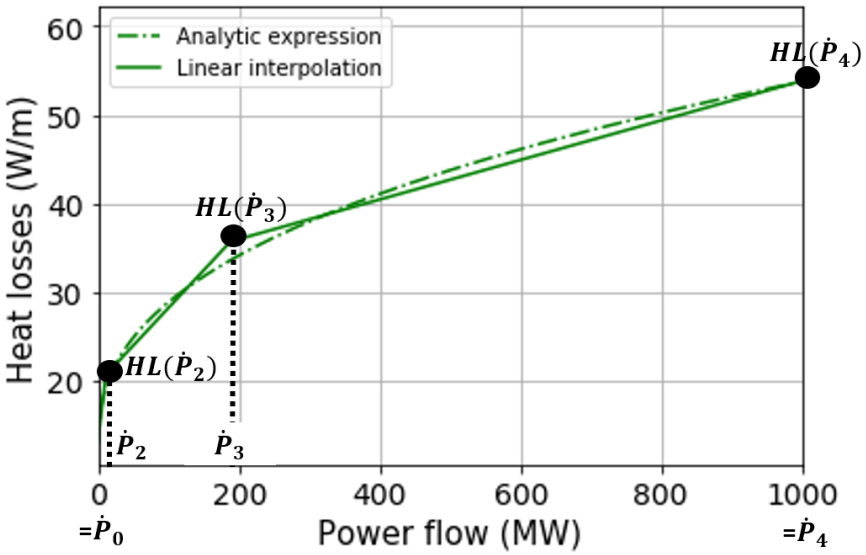

FIGURE 2.14: Picewise linear approximation of the heat losses as a function of their maximum power flows.

of the power flows into the pipes. For 4 ranges of values, 5 continuous variables $y^0_{j,d,t}, y^1_{j,d,t}, y^2_{j,d,t}, y^3_{j,d,t}$ and $y^4_{j,d,t} \in [0,1]$ are set with 4 binary variables $b^1_{j,d,t}, b^2_{j,d,t}, b^3_{j,d,t}$ and $b^4_{j,d,t} \in \{0,1\}$ to define the set of constraints 2.20. Eqs. 2.20a and 2.20b are used to link the value of the maximum power flow into an edge j with a linear combination of the bounds corresponding to the ranges of power flows used for the piecewise approximation of the heat losses function. Eqs. [2.20c-2.20h] are required to ensure that only one of the discretized power ranges is used to compute the heat losses. This piecewise linear formulation enables to increase the accuracy of the mathematical formulation even though it requires a definition of new variables for each edge of the network. These additional new variables can quickly increase the computational time for solving the problem, especially for large-scale case studies. A comparison between the purely linear and the piecewise formulations is achieved in Chapter 3 to illustrate the influence of the formulation on the computational time.

$$
\begin{cases}
\underline{\forall j \in E, \forall d \in D, \forall t \in T_D :} \dot{P}_{j,d,t} = \sum_{n=0}^{4} \dot{P}_n \cdot y^n_{j,d,t} & \text{(2.20a)} \\
\underline{\forall j \in E, \forall d \in D, \forall t \in T_D :} \sum_{n=0}^{4} y^n_{j,d,t} = 1 & \text{(2.20b)} \\
\underline{\forall j \in E, \forall d \in D, \forall t \in T_D :} y^0_{j,d,t} \leq b^1_{j,d,t} & \text{(2.20c)} \\
\underline{\forall j \in E, \forall d \in D, \forall t \in T_D :} y^1_{j,d,t} \leq b^1_{j,d,t} + b^2_{j,d,t} & \text{(2.20d)} \\
\underline{\forall j \in E, \forall d \in D, \forall t \in T_D :} y^2_{j,d,t} \leq b^2_{j,d,t} + b^3_{j,d,t} & \text{(2.20e)} \\
\underline{\forall j \in E, \forall d \in D, \forall t \in T_D :} y^3_{j,d,t} \leq b^3_{j,d,t} + b^4_{j,d,t} & \text{(2.20f)} \\
\underline{\forall j \in E, \forall d \in D, \forall t \in T_D :} y^4_{j,d,t} \leq b^4_{j,d,t} & \text{(2.20g)} \\
\underline{\forall j \in E, \forall d \in D, \forall t \in T_D :} \sum_{r=1}^{4} b^r_{j,d,t} = 1 & \text{(2.20h)}
\end{cases}
$$

With this set of constraints for each edge e_j constitutive of the potential network, the following piecewise linear heat losses function can be defined:

$$\dot{Q}^{loss}_{j,d,t} = \sum_{j \in E} 0.001 \cdot L_j \cdot [\dot{Q}^{loss}(\dot{P}_0) \cdot y^0_{j,d,t} + \dot{Q}^{loss}(\dot{P}_1) \cdot y^1_{j,d,t} + \dot{Q}^{loss}(\dot{P}_2) \cdot y^2_{j,d,t} + \dot{Q}^{loss}(\dot{P}_3) \cdot y^3_{j,d,t} + \dot{Q}^{loss}(\dot{P}_4) \cdot y^4_{j,d,t}] \quad (2.21)$$

where $\dot{Q}^{loss}(\dot{P}_0)$, $\dot{Q}^{loss}(\dot{P}_1)$, $\dot{Q}^{loss}(\dot{P}_2)$, $\dot{Q}^{loss}(\dot{P}_3)$ and $\dot{Q}^{loss}(\dot{P}_4)$ are the heat losses for the prescribed power flows chosen as bounds of the ranges of the piecewise linear function. The values of all these parameters are given in Appendix B.

Energy balance on the thermal storages

Thermal storages act as buffers to satisfy heating requirements that are not covered by heating production units at some time periods. These storages allow to shift the heating production from a time period to another and can have an influence on the sizing and the operating conditions of the network. Nevertheless, the integration of thermal storage solutions into optimization models involves more complex formulations, especially when using representative periods to define a new synthetic year with a reduced number of timesteps. The modelling of thermal storages requires to link time-dependent variables of any timestep to the previous one to compute the level of the storage at any moment. The selection of representative days reduces the total number of constraints and variables applied to the system compared to an optimization over a full real year but requires the definition of new sets of additional constraints and variables linking these representative days together. Time-series aggregation methods generally maintain chronology within each representative period but no chronology between periods is considered such that seasonal storage cannot be represented. To account for seasonal storage, a second time grid has to be introduced to describe the sequence of representative periods [89].

Indeed, the use of weighted representative days with a weight w_d assigned to each of these days in order to describe as accurately as possible the hourly heating demand over a year requires the definition of two kinds of periods which can be called respectively intra-periods and inter-periods based on [90] for thermal storage modelling. The intra-period timesteps are related to the cyclic operation within a representative day while the inter-period timesteps take into account operating changes due to the transition from one representative period to the next one. This general definition of intra and inter-periods is represented graphically in Figure 2.15 based on the selection of representative days illustrated in Section 2.2. This definition of two time grids enables to consider daily thermal storage but also thermal storage between two representative periods.

The selection of representative days assigned with weights w_d implies a discontinuity of the heating demand between 2 representative periods. The weight w_d

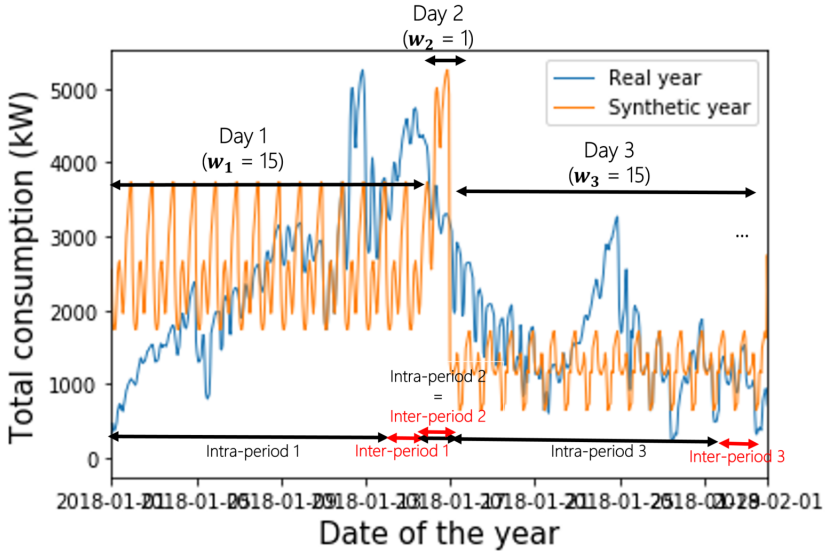

FIGURE 2.15: Definition of intra and inter-periods for the representation of the thermal storage units.

of a period defines the recurrence of this time period $w_d - 1$ times before switching to the next one during the w_dth recurrence of the period d. During this last recurrence of this time period, thermal storage loadings and unloadings can be different than during the previous recurrences of the period because the storage level at the end of this period does not have to be equal to the storage level at the beginning of this period. There is then a need to define two sets of constraints and variables related respectively to intra-periods and inter-periods. The first set of constraints and variables is related to the modelling of intra-period time layers as defined previously with Eqs. 2.8a and 2.8b for example. These constraints are applied within a single representative day considering a cyclic recurrence of the behaviour of the network for daily thermal storage assigned by the weight w_d related to the representative period. For thermal storage units into the optimization model, loading and unloading storage variables $\dot{Q}^{load}_{i,d,t}$ and $\dot{Q}^{unload}_{i,d,t}$ and a variable $\dot{Q}^{sto}_{i,d,t}$ assessing the level of the storage during these intra-periods are defined. This last variable enables to size the optimal thermal storage(s) for a given network. Assuming perfectly stratified storages and constant temperatures within the two laminate zones of water inside the storage tanks ($T^{w,in} = 90°C$ and $T^{w,out} = 60°C$), an energy balance over each timestep within an intra-period enables to link the stored heating energy to the loaded or unloaded heating power by the storage units. Prescribing that the storage level at the end of each recurrence of a representative day is equal to the storage level at the beginning of this day ($\dot{Q}^{sto}_{i,d,N_{reprhour}+1} = \dot{Q}^{sto}_{i,d,1}$), this energy balance is written as follows:

$$\underline{\forall i \in V_P, \forall d \in D, \forall t \in T_D :} \dot{Q}^{sto}_{i,d,t+1} - (1 - w_t \cdot \alpha^{loss}) \cdot \dot{Q}^{sto}_{i,d,t} - w_t \cdot \dot{Q}^{load}_{i,d,t} + w_t \cdot \dot{Q}^{unload}_{i,d,t} = 0 \quad (2.22)$$

where α^{loss} is a parameter quantifying hourly thermal storage losses.

However, this set of constraints and variables is not sufficient to describe the behaviour of the thermal storage units within inter-period time layers for seasonal thermal storage such that a second set of constraints and variables is defined to represent these inter-period behaviours. This requires the definition of new variables related to the previous ones and called respectively $\dot{Q}_{i,d,t}^{load,inter}$, $\dot{Q}_{i,d,t}^{unload,inter}$ and $\dot{Q}_{i,d,t}^{sto,inter}$ which are linked together using Eq. 2.23.

$$\underline{\forall i \in V_P, \forall d \in D, \forall t \in T_D}: \dot{Q}_{i,d,t+1}^{sto,inter} - (1 - w_t \cdot \alpha^{loss}) \cdot \dot{Q}_{i,d,t}^{sto,inter} - w_t \cdot \dot{Q}_{i,d,t}^{load,inter} + w_t \cdot \dot{Q}_{i,d,t}^{unload,inter} = 0 \quad (2.23)$$

An additional constraint has also to be defined to link intra-periods and inter-periods based on the same energy balance than the previous one:

$$\underline{\forall i \in V_P, \forall d \in D, \forall t \in T_D}: \dot{Q}_{i,d+1,1}^{sto} - (1 - w_t \cdot \alpha^{loss}) \cdot \dot{Q}_{i,d,N_{reprhour}}^{sto,inter} - w_t \cdot \dot{Q}_{i,d,N_{reprhour}}^{load,inter} + w_t \cdot \dot{Q}_{i,d,N_{reprhour}}^{unload,inter} = 0 \quad (2.24)$$

Finally, an initialization of the storage level $\dot{Q}_{i,1,1}^{sto}$ to 50% of the maximum potential storage capacity $\dot{Q}_{i,d,t}^{sto,max}$ which would be installed and prescribing that the initial and final storage levels at the end of the optimization period are equal ($\dot{Q}_{i,N_{reprday},N_{reprhour+1}}^{sto,inter} = \dot{Q}_{i,1,1}^{sto}$) enables to define a whole set of constraints related to thermal storage solutions. The definition of the additional variables related to inter-period time layers $\dot{Q}_{i,d,t}^{load,inter}$, $\dot{Q}_{i,d,t}^{unload,inter}$ and $\dot{Q}_{i,d,t}^{sto,inter}$ has also to be taken into account for the implementation of all the other constraints of the optimization model. For example, the set of constraints related to the energy balances over the edges and the nodes of the network has to be duplicated by adding energy balances during inter-periods such that two new constraints similar to Eqs. 2.8a and 2.8b are defined with Eqs. 2.25a and 2.25b. All the constraints which are defined in the following of this manuscript are written only for intra-period time layers even though an additional set of constraints related to inter-periods is also defined but not described for sake of simplicity.

$$\begin{cases} \underline{\forall j \in E, \forall d \in D, \forall t \in T_D}: \dot{P}_{j,d,t}^{out,inter} = \dot{P}_{j,d,t}^{in,inter} - u_{j,d,t}^{inter} \cdot p_j \cdot \dot{Q}_{j,d,t}^{heat} - \dot{Q}_{j,d,t}^{loss,inter} & (2.25a) \\ \underline{\forall i \in V, \forall d \in D, \forall t \in T_D}: \sum_{j \in N_i} (\dot{P}_{j,d,t}^{in,inter} - \dot{P}_{j,d,t}^{out,inter}) = \dot{Q}_{i,d,t}^{prod,inter} + \dot{Q}_{i,d,t}^{unload,inter} - \dot{Q}_{i,d,t}^{load,inter} & (2.25b) \end{cases}$$

This approach dividing the optimization formulation into intra- and inter-periods enables to simplify the problem and reduce the number of optimization variables by assuming cyclic behaviours within intra-periods of a representative day and a connection between two consecutive representative days with inter-periods. However, the reader can realize that with this formulation, seasonal

thermal storage is limited because of the cyclic behaviour of a thermal storage solution within a representative day. Indeed, thermal storages can be loaded or unloaded for the next inter-period only during the last recurrence of a representative day. This limits the loading and unloading power flows which could be supplied during the whole period of a representative day. However, this assumption has been made following the hypothesis of a tank storage unit as unique solution for thermal storage over the network. These kinds of storages are mainly dedicated to short-term storages because of their large heat losses compared to underground thermal storage solutions. For taking into account seasonal thermal storage potential, it is recommended to use the yearly heating load profiles instead of the synthetic ones. For small-scale instances, yearly heating demand profiles can be used to solve the optimization problem within a reasonable computational time.

Time-dependent heat losses of a water tank over time are computed considering transient conduction through the tank. An analytical formulation based on the lumped capacitance method making the assumption that the fluid temperature is spatially uniform at any moment during the transient process is used. Assuming an initial temperature $T^{w,in}$ into the tank, the temperature at a time t is given by:

$$T(t) = T^{sur} + (T^{w,in} - T^{sur}) \cdot exp(-\frac{t}{\tau}) \tag{2.26}$$

The thermal time constant τ is defined by the product of the thermal resistance R to convection heat transfer and the lumped thermal capacitance C of the water tank. A physical modelling based on Figure 2.16 can be used to define the thermal resistance R and the thermal capacitance C. This total thermal resistance $R^{eq,sto}$ is defined by Eq. 2.27a considering that the thermal storage is designed with $H = D$ in order to minimize heat losses by minimizing the ratio between the surface exchange of the storage and the storage volume.

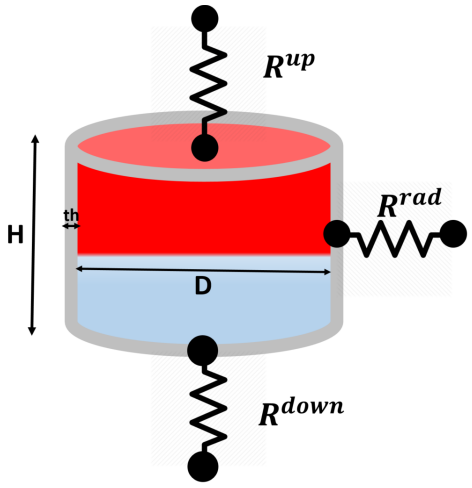

FIGURE 2.16: Thermal resistances linked to a thermal storage.

$$\begin{cases} R^{eq,sto} = R = \left(\frac{1}{R_{rad}} + \frac{1}{R_{up}} + \frac{1}{R_{down}}\right)^{-1} = \left(\frac{2\pi H k_{ins}}{ln(\frac{D+th}{D})} + \frac{\pi D^2 k_{ins}}{2 \cdot th}\right)^{-1} & (2.27a) \\ C = \rho_w \cdot c_{p,w} \cdot V_{sto} & (2.27b) \end{cases}$$

Considering that the sizing of the thermal storage is based on the available surface at a given location, a coefficient for hourly heat losses in nominal operating conditions can be defined as a function of the available surface A_{avail} at a potential heating location i. The sizing of the cylindrical thermal storage in order to minimize heat losses for a prescribed level of insulation thickness th (dependent on the diameter of the cylinder) can be achieved analytically by minimizing the total heat exchange surface A_{he} for a given available ground surface A_{avail}. This total heat exchange surface A_{he} is defined by Eq. 2.28.

$$A_{he} = \pi D H + 2\pi \frac{D^2}{4} = \pi D H + \pi \frac{D^2}{2} \quad (2.28)$$

Eq. 2.28 can be rewritten to highlight the value of the height H of the storage as a function of the diameter D and the exchange surface A_{he} of the storage.

$$H = \frac{A_{he} - \pi \frac{D^2}{2}}{\pi D} = \frac{A_{he}}{\pi D} - \frac{D}{2} \quad (2.29)$$

The diameter D is prescribed by the available surface A_{avail} at a given heating location k and the volume of the cylinder of height H can be linked to the available surface as follow.

$$\begin{cases} A_{avail} = \frac{\pi D^2}{4} & (2.30a) \\ V = \frac{\pi D^2}{4} \cdot H & (2.30b) \end{cases}$$

Inserting Eq. 2.29 into Eq. 2.30b, the storage volume takes the following analytical form.

$$V = \frac{\pi D^2}{4} \cdot \left(\frac{A_{he}}{\pi D} - \frac{D}{2}\right) = \frac{A_{he} D}{4} - \frac{\pi D^3}{8} \quad (2.31)$$

The optimal size of the storage volume V for a constant heat exchange surface A_{he} aims to minimize heat losses for an available building surface A_{avail}. Differentiating V according to D gives the analytical expressions in Eq. 2.32.

$$\begin{cases} \frac{\partial V}{\partial D} = \frac{A_{he}}{4} - \frac{3\pi D^2}{8} & (2.32a) \\ \frac{\partial^2 V}{\partial D^2} = -\frac{3\pi D}{4} < 0 \text{ for } D > 0 & (2.32b) \end{cases}$$

The second derivative being negative, the cancellation of the first derivative gives an analytical formulation of the diameter providing a maximum value of the volume:

$$\frac{\partial V}{\partial D} = 0 = \frac{A_{he}}{4} - \frac{3\pi D^2}{8} \tag{2.33}$$

Highlighting D from Eq. 2.33 and using Eq. 2.29 to determine the analytical expression of the height H of the storage, it can be observed that the height H and the diameter D of the storage have to be equal to maximize the storage volume for a constant heat exchange surface A_{he}.

$$\begin{cases} D = \sqrt{\dfrac{2A_{he}}{3\pi}} & \text{(2.34a)} \\ H = \sqrt{\dfrac{2A_{he}}{3\pi}} & \text{(2.34b)} \end{cases}$$

From these analytical expressions, the maximum installable storage volume for a given area A_{avail} can be expressed as follow:

$$V_{max,sto} = \pi\frac{D^3}{4} = A_{avail} \cdot D = \sqrt{\frac{4}{\pi}} \cdot A_{avail}^{\frac{3}{2}} \tag{2.35}$$

Considering operating temperatures $T^{w,in}$ and $T^{w,out}$ over the network with a temperature difference ΔT_{sub}, the maximum heating amount $Q^{max,sto,vol}$ which can be stored into a thermal storage per unit of volume can be linked to the storage volume with Eq. 2.28.

$$Q^{max,sto,vol} = \frac{Q^{max,sto}}{V_{max,sto}} = \rho_w \cdot c_{p,w} \cdot \Delta T_{sub} = \frac{1000 \cdot 4181 \cdot 30}{3600000} \approx 35\frac{kWh}{m^3} \tag{2.36}$$

Using Eq. 2.35 to link the storage volume to the available surface, the storage heating capacity can be directly linked to the available surface A_{avail} with Eq. 2.36 as illustrated in Figure 2.17. Based on this maximum thermal storage volume per unit of surface, the ratio of heat losses as a function of the available surface can be computed. Heat losses per unit of time period are put into equation using Eq. 2.37. Computing T(Δt) with Eq. 2.26, an analytical expression of a heat loss coefficient as a function of the available surface of the storage can be computed from Eq. 2.37 and is exhibited in Figure 2.17.

$$\dot{Q}^{loss,sto} = \frac{\rho_w \cdot V_{max,sto} \cdot c_{p,w} \cdot (T^{w,in} - T(\Delta t))}{3600000 \cdot Q^{max,sto,vol}} \tag{2.37}$$

Figure 2.17 illustrates the decrease of the heat losses coefficient for an increase of the available surface A_{avail}. This physical trend is explained by the decrease of the ratio between the heat exchange surface A_{he} of the storage and the storage volume implying a decrease of the heat losses per unit of stored heat. A linearization of the heat losses coefficient is achieved and given by Eq. 2.38.

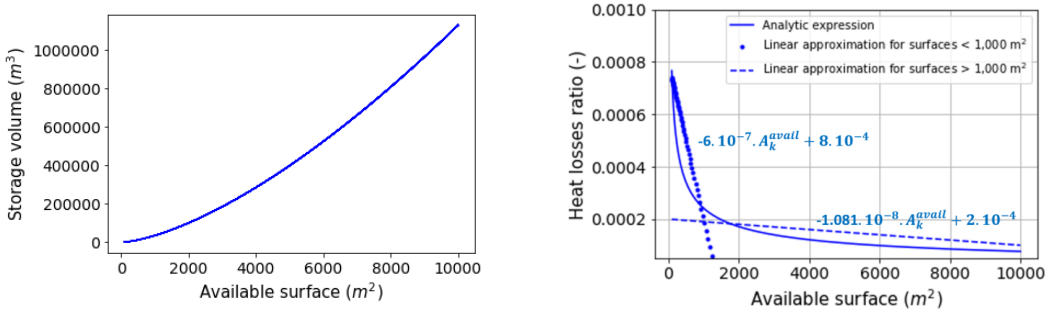

(a) Installable storage volume as a function of the available surface.

(b) Thermal storage losses as a function of the available surface

FIGURE 2.17: Characterization of the thermal storages.

$$\begin{cases} \underline{\text{For } A_{avail} \leq 1000m^2 :}\ \alpha^{loss} = -6 \cdot 10^{-7} \cdot A_{avail} + 8 \cdot 10^{-4} & \text{(2.38a)} \\ \underline{\text{For } A_{avail} > 1000m^2 :}\ \alpha^{loss} = -1.081 \cdot 10^{-8} \cdot A_{avail} + 2 \cdot 10^{-4} & \text{(2.38b)} \end{cases}$$

2.3.3.2 Maximum thermal capacity at the edges and vertices of the graph

Pipes diameters into the streets are generally limited by urbanistic constraints because of limited spaces into the ground due to the presence of other existing pipes like the gas and telecommunication pipes. Using Eq. 2.15 to compute the limited power flow $\dot{P}^{lim}$ for a maximum pipe diameter D^{lim} installable into the ground, a constraint about the maximum thermal power capacity for each pipe can be written as follows:

$$\begin{cases} \underline{\forall j \in E :}\ \dot{P}_j^{max} \leq x_j \cdot \dot{P}_j^{lim} & \text{(2.39a)} \\ \underline{\forall j \in E, \forall d \in D, \forall t \in T_D :}\ \dot{P}_{j,d,t}^{in} \leq \dot{P}_j^{max} & \text{(2.39b)} \end{cases}$$

This set of constraints defines at any timestep the power flow $\dot{P}_{j,d,t}^{in}$ into a pipe of the network while checking that the maximum thermal capacity $\dot{P}_j^{lim}$ into a street is not outreached. The binary variable x_j defines the building or not of a pipe j and the variable $\dot{P}_j^{lim}$ represents the maximum power flow into a pipe over all the timesteps of the optimization problem.

Heating power capacities are also limited by the size of the available existing heating plants and/or by the potential available surfaces for the implementation of new heating sources at a prescribed location v_i. The heating production $\dot{Q}_{i,m,d,t}$ at a location v_i with a technology m is constrained by the limited available heating capacity $\dot{Q}_{i,m}^{lim}$ of the plants at any timestep.

$$\begin{cases} \underline{\forall i \in V_P, \forall m \in H_i : \dot{Q}_{i,m}^{max} \leq \dot{Q}_{i,m}^{lim}} & \text{(2.40a)} \\ \underline{\forall i \in V_P, \forall m \in H_i, \forall d \in D, \forall t \in T_D :} \ \dot{Q}_{i,m,d,t} \leq CF_{d,t,m} \cdot \dot{Q}_{i,m}^{max} & \text{(2.40b)} \end{cases}$$

For new potential heating plants to install, their maximum thermal capacity $\dot{Q}_{i,m}^{lim}$ is computed from the required surface per unit of heating capacity A_m^{unit} (cf. Appendix C) for a given technology m. For an available surface A_i^{avail} at a specific potential heating location i, the limited heating capacity parameter $\dot{Q}_{i,m}^{lim}$ for each technology m is given by Eq. 2.41.

$$\dot{Q}_{i,m}^{lim} = \frac{A_i^{avail}}{A_m^{\text{unit}}} \tag{2.41}$$

Another parameter $CF_{d,t,m}$ taking into account the variability of the heating capacity over time has to be defined, especially for the solar heating production capacity. The intermittency of the solar irradiation is taken into account for the computation of the solar capacity production available with solar collectors with a prescribed inclination and orientation to determine the maximum installable capacity and the available capacity over each timestep over the year.

Capacity factor for solar heating

Based on solar radiation data over an horizontal surface collected from the database *Copernicus* [91] for a given year at a specific location of latitude ϕ and longitude ξ, the solar radiation for solar panels oriented with an angle γ to the south and an inclination i compared to the ground (cf. Figure 2.18) can be obtained from the solar radiation over an horizontal surface at the same location.

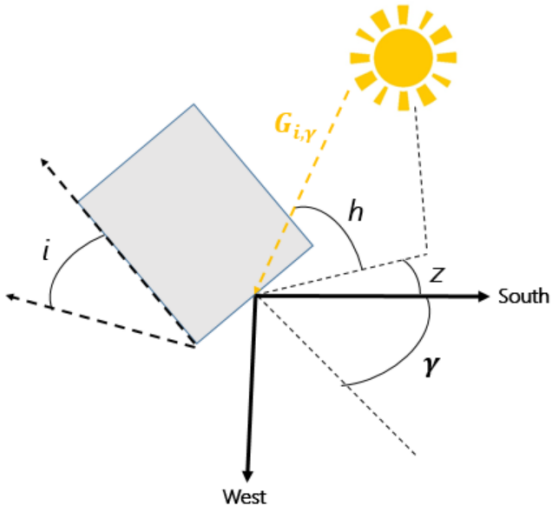

FIGURE 2.18: Solar radiation over a solar panel inclined with an angle i and an orientation γ.

The assessment of the potential heating capacity of concentrated solar panels relies on the direct solar radiation G_h [Wh/m^2] from *Copernicus* database computed for clear sky conditions and real conditions over a horizontal surface on the ground. The solar radiation $G_{i,\gamma}$ [Wh/m^2] over a surface of inclination i and orientation angle γ with south is then given by Eq. 2.42.

$$G_{i,\gamma} = \Big(\frac{sin(i) \cdot cos(z-\gamma)}{tan(h)} + cos(i)\Big) \cdot G_h \tag{2.42}$$

The choice of the optimal inclination angle i of the surface has to be chosen on a case-by-case basis as a function of the geographic location and is generally chosen equal to the latitude ϕ of this location [92]. Orientation and inclination of the surface are required to compute the solar radiation at any given time as well as a local coordinate system specific to a given location in order to link the sun location with the specific studied location. 2 additional local coordinates h and z are thus defined as represented in Figure 2.18. The angular height h represents the angle between the Sun and the horizontal plane tangent to the ground. The azimut z represents the angle between the meridian plane and the plane passing through the Sun. These two variables are computed by using the set of equations 2.43.

$$\begin{cases} h = arcsin\Big(cos(\delta) \cdot cos(\omega) \cdot cos(\phi) + sin(\delta) \cdot sin(\phi)\Big) \\ cos(z) = \frac{cos(\delta) \cdot cos(\omega) \cdot sin(\phi) - sin(\delta) \cdot cos(\phi)}{cos(h)} \\ z = \begin{cases} arcsin(\frac{cos(\delta) \cdot sin(\omega)}{cos(h)}) & \text{if } cos(z) \geq 0 \\ \pi - arcsin(\frac{cos(\delta) \cdot sin(\omega)}{cos(h)}) & \text{if } cos(z) < 0 \end{cases} \end{cases} . \tag{2.43}$$

ω and δ are based on an hourly coordinate system and are represented in Figure 2.19. The angle ω represents the solar time based on the position of the Sun in the sky and δ represents the angle between the Equator and the Sun-Earth direction.

$$\begin{cases} \omega = \dfrac{\text{hour} - 12}{24} \cdot 360 & \text{(2.44a)} \\ \delta = 23.45 \cdot sin\left(\dfrac{360}{365} \cdot (\text{day number} - 81)\right) & \text{(2.44b)} \end{cases}$$

In order to determine the maximum solar heating capacity installable at a given location of latitude ϕ and longitude ξ, the maximum solar radiation over the year $G_{i,\gamma}^{max}$ in clear sky conditions for a solar panel of inclination $i = \phi$ is computed. The required surface per kW_{th} installed is then directly computed by Eq. 2.45.

$$A_{solar}^{\text{unit}}[\frac{m^2}{kW_{th}}] = \frac{1}{G_{i,\gamma}^{max}} \tag{2.45}$$

This indirectly defines the maximum solar heating power installable $\dot{Q}_{i,solar}^{lim}$ at a specific location v_i with a prescribed surface using Eq. 2.41. To take into account the variability of solar radiation over the year, it is also necessary to define a capacity factor for each hour of the year. This capacity factor CF is

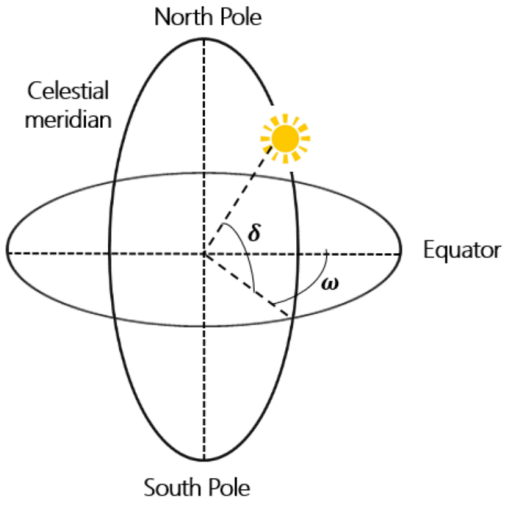

FIGURE 2.19: Solar time coordinate system.

a ratio defining the current available energy over a timestep compared to the installed capacity.

$$CF = \frac{\text{Available solar radiation during a timestep [kW]}}{\text{Installed capacity [kW]}} \tag{2.46}$$

Solar power plants are generally characterized by low ranges of capacity factors because of the intermittency of solar energy available only available during the days and without cloudy conditions. Computing solar radiation for the specific location of Liège in Belgium ($\phi = 50°38'01"$, $\xi = 5°34'02"$) oriented totally in the south direction ($\gamma = 0°$) with an inclination angle i equal to the latitude of the location ϕ, the following solar radiation data with respectively clear sky conditions and real conditions is figured out in Figure 2.20.

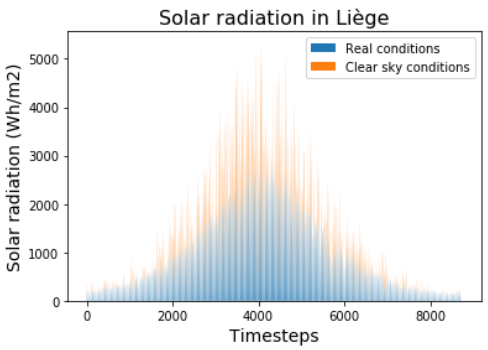

(a) Solar radiation in Liège.

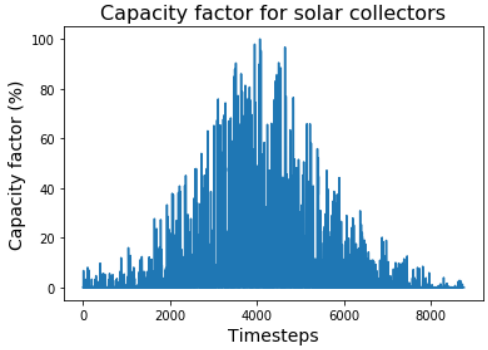

(b) Capacity factor in Liège.

FIGURE 2.20: Solar capacity in Liège.

It can be seen from Figure 2.20 that cloudy conditions can impact in a non-negligible way the solar potential during a given time period. Computing the capacity factor for a given year in Liège, this capacity factor related to solar technology is really low and has thus to be taken into account into the constraints

and the calculation of the maximum available heating capacity with solar heating at a given timestep.

2.3.3.3 Link between pipes over some edges of the graph

The last set of constraints is linked to the decision process to choose some pipes to be built or not into the network. Binary decision variables have to be linked as described in Eq. 2.47.

$$\begin{cases} \underline{\forall j \in E :} \; x_j \geq m_j^{build} & \text{(2.47a)} \\ \underline{\forall j \in E, \forall d \in D, \forall t \in T_D :} \; u_{j,d,t} \leq x_j & \text{(2.47b)} \\ \underline{\forall j \in E, \forall d \in D, \forall t \in T_D :} \; u_{j,d,t} + u_{j^*,d,t} \leq 1 & \text{(2.47c)} \end{cases}$$

Eq. 2.47a allows a degree of freedom about the decision to build some pipes. In the framework of political decisions linked to district heating projects, some consumers would have to be included to the district heating project. The mandatory feeding of some consumers by a heating network is expressed by a binary parameter m_j^{build} for each edge e_j which has a value of 1 if the building of a pipe is mandatory over an edge e_j and 0 otherwise. A binary variable x_j is defined to represent mathematically the decision process to build or not a pipe. This variable gets a value of 1 if a pipe is built and 0 otherwise. Eq. 2.47b links the building of a pipe to its use such that a pipe can not be used if it is not built. This constraint implies that the binary variable for using a pipe $u_{j,d,t}$ can get a value of 1 only if the binary decision variable for building a pipe x_j gets a value of 1. Eq. 2.47c links each edge e_j of the directed graph with its equivalent edge in the opposite direction e_{j^*}. This last equation satisfies the requirement of the use of a pipe in a unique direction at any timestep. This whole set of equations defines thus the optimization model used to compute the best scenario for the outline and the sizing of a potential heating network into a prescribed geographic area.

This optimization formulation can be applied to any new heating network project by defining a list of edges related to the streets of the studied neighbourhood from the geographic information system and by denoting their start and end nodes and their respective lengths into *Excel* inputs files. The formulation presented previously can then link together all the nodes and the edges of the graph representation of the neighbourhood to apply these constraints. These constraints aim for considering as accurately as possible the physical energy phenomena occurring into the system without knowing the outline of the network while keeping a simple optimization formulation by linearizing all non linear phenomena. These constraints also look for taking into account urbanistic constraints because these constraints impact in a non negligible way the outline of the network and therefore its sizing.

2.3.4 Objective function

The main goal of the optimization tool defined in this thesis consists in providing the network's outline with an optimal sizing of the heating technologies and thermal storages to maximize the net cash flow (NCF) over the lifetime N_{years} of a given district heating network project. The total cost of the project and its revenues have to be computed over the entire lifetime of the project taking into account that the value of money is fluctuating over time. Costs components can be divided into capital and operating expenditures (respectively CAPEX and OPEX) and combined to revenues to define the optimization function maximizing the net cash flow (NCF) of the project:

$$NCF = R_{\text{heat}} - (f_{CAPEX} \cdot C_{\text{CAPEX}} + f_{OPEX} \cdot C_{\text{OPEX}}) \tag{2.48}$$

where

$$\begin{cases} C_{CAPEX} = C_{\text{plants}} + C_{\text{pipes}} + C_{\text{sub}} + C_{\text{sto}} & \text{(2.49a)} \\ C_{OPEX} = C_{\text{prod}} + C_{\text{pump}} & \text{(2.49b)} \end{cases}$$

This objective function aims for maximizing the revenues from the point of view of stakeholders taking part to the funding of the heating network project. Indeed, in the frame of the *EcoSystemPass* project, the decision tool is dedicated for helping the industrial and political stakeholders to develop the best strategy for the implementation of a heating network project into a given geographic area. This formulation therefore only considers interesting heating consumers to connect to a network without including consumers which are assessed by the decision tool to be economically non profitable to connect. These consumers are then not considered into the energy planning solution for the optimal heating network project and will be fed by alternative heating sources. Accordingly, the total costs computed in the following only take into account costs related to the heating network project and not the total cost for providing heat to the whole studied neighbourhood.

Capital expenditures are defined to be accounted for only at the beginning of the investment period while operating expenditures are taken into account during the whole lifetime of the project. Actualization factors are defined to include the value of money over time by means of an actualization rate a. The value of the actualization rate depends on the borrowing rate available on the markets, the debt to equity ratio of the borrowing company and the expected return on equity expected by the stakeholders of the project. This rate is generally particularly favourable to the development of district heating because district heating networks' projects are considered as low risk assets and the current borrowing rates on the financial markets are low [93]. A general formula can be used to compute this actualization rate as follow:

$$a = \text{Borrowing rate X Debt ratio} + \text{Return on equity X Equity ratio} \tag{2.50}$$

Based on these actualization factors and considering that there is no energy price inflation, the actualization factors are defined by Eqs. 2.51a and 2.51b. The calculation of these actualization factors is based on the definition of the present

value of a cash flow over time. This value corresponds to the market price today (time 0) of a monetary unit available at a future date time t.

$$\begin{cases} f_{CAPEX} = (1+a)^{N_{years}} & \text{(2.51a)} \\ f_{OPEX} = \dfrac{1-(1+a)^{N_{years}}}{1-(1+a)} & \text{(2.51b)} \end{cases}$$

A cash flow (CF) after N_{years} has a current market price given by Eq. 2.52.

$$CF_{N_{years}} = CF_0 \cdot (1+a)^{N_{years}} \tag{2.52}$$

An application of this formula to all the capital and operating expenditures over the whole lifetime of the project is detailed in Table 2.3.

TABLE 2.3: CAPEX and OPEX over the lifetime of the project

Year	**CAPEX**	**OPEX**
0	C_{CAPEX}	C_{OPEX}
1	/	$C_{OPEX} \cdot (1+a)$
2	/	$C_{OPEX} \cdot (1+a) \cdot (1+a) = C_{OPEX} \cdot (1+a)^2$
3	/	$C_{OPEX} \cdot (1+a)^2 \cdot (1+a) = C_{OPEX} \cdot (1+a)^3$
...	/	...
$N_{years}-1$	/	$C_{OPEX} \cdot (1+a)^{N_{years}-1}$
N_{years}	/	$C_{OPEX} \cdot (1+a)^{N_{years}}$

Considering that the operating expenditures for each year are the terms of a geometric progression with a common ratio $(1+a)$, the sum of the $N_{years}+1$ terms of the geometric progression can be directly deduced from the definition of the sum of the terms of a geometric progression. CAPEX and OPEX values after N_{years} are then given by Eqs. 2.53a and 2.53b defining the actualization factors in Eqs. 2.51a and 2.51b:

$$\begin{cases} CAPEX_{N_{years}} = C_{CAPEX} \cdot (1+a)^{N_{years}} & \text{(2.53a)} \\ OPEX_{N_{years}} = \sum_{year=0}^{N_{years}} OPEX_{year} = C_{OPEX} \cdot \dfrac{1-(1+a)^{N_{years}}}{1-(1+a)} & \text{(2.53b)} \end{cases}$$

2.3.4.1 Capital expenditures (CAPEX)

Capital expenditures represent all the building costs related to the optimal outline and sizing of the network project for maximizing the net cash flow of the project. These costs are considered to be achieved at the beginning of the project (year 0) and are assessed based on current market prices.

Costs for the building of power plants

The building and operation of power plants depends on some parameters determining the kind of power plant and the capacity to install or to use if the heating

plant is already in operation. Based on data from [94] for different heating technologies summarized in Appendix C, a coefficient c_m^{build} [€/kW$_{th}$] for costs per unit of installed capacity for a technology m of the set H can be defined to compute a heating plant building cost function. This cost coefficient is equal to zero in the case of an already existing power plant. This cost coefficient is linked to the required maximum power capacity $\dot{Q}_{i,m}^{max}$ at the heating location i for the heating technology m which is a variable determined from the optimization model.

$$C_{\text{plants}} = \sum_{i \in V_P, m \in H_i} c_m^{build} \cdot \dot{Q}_{i,m}^{max} \tag{2.54}$$

Costs for pipes

For heating networks operating at temperature levels between 60 and 100°C, pipes are generally made up of steel surrounded by a polyethylene foam insulation. The costs of these pipes are dependent on their diameters and their location. The setting up of pipes in an urban area is more expensive than in a periurban or rural area. These costs are summarized in Appendix D and represented graphically in Figure 2.21.

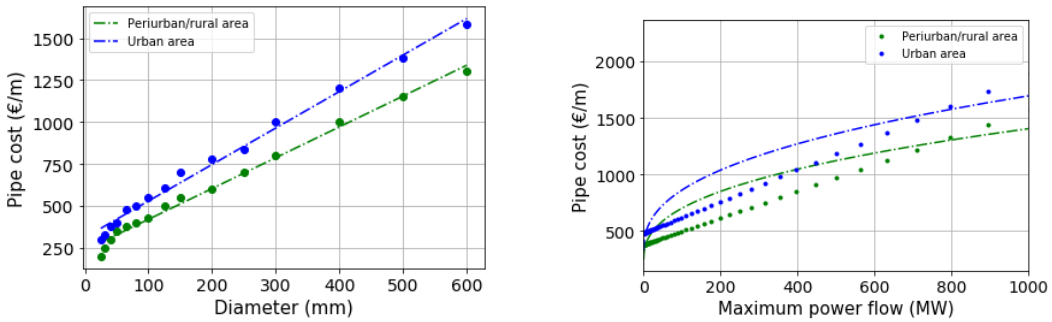

(a) Pipes costs as a function of their diameters

(b) Pipes costs as a function of their maximum power flows

FIGURE 2.21: Pipes costs from manufacturer's data

Interpolating the values of the pipes costs for diameters prescribed by manufacturers with the linear regression in Eqs. 2.55a and 2.55b and inserting Eq. 2.15 into Eqs. 2.55a and 2.55b, values of the pipe costs as a function of the maximum power flow into these pipes can be figured out.

$$\begin{cases} \text{For urban areas: } C_j^{inner}[€/m] = 2174.6 \cdot D_j^{pipe} + 312.45 \cdot x_j & \text{(2.55a)} \\ \text{For rural areas: } C_j^{outer}[€/m] = 1836.9 \cdot D_j^{pipe} + 236.78 \cdot x_j & \text{(2.55b)} \end{cases}$$

These values are linearized over a range of power flows P_j^{max} [kW] included until 1 GW giving the linear expression in Eqs. 2.56a and 2.56b for the pipes costs per unit length.

$$\begin{cases} \text{For urban areas: } C_j^{inner}[€/m] = 0.0014 \cdot P_j^{max} + 481.36 \cdot x_j & (2.56a) \\ \text{For rural areas: } C_j^{outer}[€/m] = 0.0012 \cdot P_j^{max} + 379.46 \cdot x_j & (2.56b) \end{cases}$$

The binary variable x_j is used to define a pipe cost function per meter of pipe only if the pipe is built. Otherwise, this cost becomes a zero cost. The definition of the pipe cost function relies on this linearization of the pipes costs per unit length and depends also on the length L_j of each edge of the potential network and of the location of the pipe in an urban or periurban/rural area defined respectively by both binary parameters l_j^{inner} and l_j^{outer}. These binary parameters have a value of 1 if the edge locates respectively in an urban or periurban/rural area and zero otherwise. The global pipe cost function is thus defined by Eq. 2.57.

$$C_{\text{pipes}} = \sum_{j \in E} (l_j^{inner} \cdot C_j^{inner} + l_j^{outer} \cdot C_j^{outer}) \cdot L_j \tag{2.57}$$

As put into equation in Section 2.3.3.1, the pipes costs which are a non linear function of the power flows into the pipes can be approximated by a piecewise linear function over the N_{ranges} power flow ranges defined previously. With this set of constraints for each edge j constitutive of the network, the following piecewise linear pipes cost function can be defined as in Eq. 2.58.

$$\begin{aligned} C_{\text{pipes}} = \sum_{j \in E} L_j \cdot \Big[& l_j^{inner} \Big(C^{inner}(\dot{P}_0) \cdot y_j^0 + C^{inner}(\dot{P}_1) \cdot y_j^1 + C^{inner}(\dot{P}_2) \cdot y_j^2 \\ & + C^{inner}(\dot{P}_3) \cdot y_j^3 + C^{inner}(\dot{P}_4) \cdot y_j^4 \Big) + l_j^{outer} \Big(C^{outer}(\dot{P}_0) \cdot y_j^0 + C^{outer}(\dot{P}_1) \cdot y_j^1 \\ & + C^{outer}(\dot{P}_2) \cdot y_j^2 + C^{outer}(\dot{P}_3) \cdot y_j^3 + C^{outer}(\dot{P}_4) \cdot y_j^4 \Big) \Big] \end{aligned} \tag{2.58}$$

where $C^{inner/outer}(P_0), C^{inner/outer}(P_1), C^{inner/outer}(P_2), C^{inner/outer}(P_3)$ and $C^{inner/outer}(P_4)$ are the pipes costs for the prescribed power flows chosen as bounds of the ranges of the piecewise linear function. The values of all these parameters are given in Appendix B.

Costs for substations

Considering that one substation is installed per built pipe, the sizing of these substations is based on the maximum heating demand $\dot{Q}_j^{max}$ over an edge and the percentage of connection p_j to this edge. Substations costs are directly proportional to their heating capacity (data for substations are available in Appendix E and represented in Figure 2.22) such that a linear expression of the substations cost per thermal unit installed is defined as in Eq. 2.59.

$$C_j^{sub}[€] = 17.905 \cdot p_j \cdot \dot{Q}_j^{max} + 24588 \tag{2.59}$$

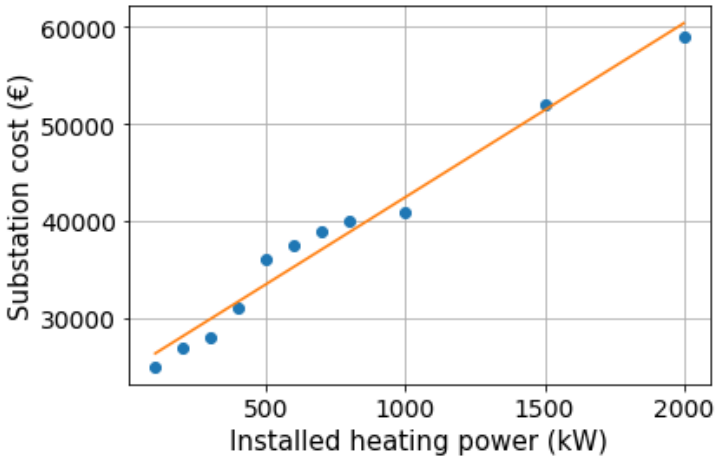

FIGURE 2.22: Substations costs.

This cost depends on a parameter of connection percentage p_j representing the ratio of inhabitants over an edge which agrees to be connected to a district heating network. This parameter is used to take into account that in real district heating projects, some inhabitants are opposed to the project and want to keep their current heating system at home. The global cost function for substations is then defined as in Eq. 2.60 taking into account which edges are connected to the network.

$$C_{\text{sub}} = \sum_{j \in E} x_j \cdot C_j^{sub} \tag{2.60}$$

Costs for thermal storages

Similarly to the definition of a cost function for the heating plants, the computation of the thermal storages costs are based on data from [94] defining a coefficient c_{sto}^{build} $[€/kWh_{th}]$ for costs per unit of installed storage.

$$C_{\text{sto}} = \sum_{i \in V_P} c_{sto}^{build} \cdot \dot{Q}_{i,sto}^{max} \tag{2.61}$$

2.3.4.2 Operating expenditures (OPEX)

Operating expenditures represent all the ongoing costs to operate the network in the best way based on the optimally sized components in order to maximize the net cash flow over the whole lifetime of the project. These costs are considered to be achieved continuously over the lifetime of the project and are neglecting any energy inflation assuming a constant energy price over the years.

Costs for heating production

Heating production costs have to be computed over each timestep of the optimization period taking into account the heating production level $\dot{Q}_{i,m,d,t}$ of each heating technology m at each heating location v_i. These production levels are linked to a time-dependent parameter $c_{i,m,d,t}^{prod}$ because the heating production cost

of some technologies like heat pumps are dependent on external time dependent factors like the electricity price and weather conditions affecting the value of the coefficient of performance of this technology. A generic formulation of the costs for heating production is given by Eq. 2.62.

$$C_{\text{prod}} = \sum_{d \in D} w_d \cdot \sum_{i \in V_P, m \in H_i, t \in T_D} w_t \cdot c^{prod}_{i,m,d,t} \cdot \dot{Q}_{i,m,d,t} \cdot \Delta t \tag{2.62}$$

These production costs can be found in Appendix C but can also be provided directly by the user of the decision tool. Indeed, a new heating technology can be defined at any vertex v_i of the graph with a prescribed heating capacity and a heating production cost which is variable over the year. This hand-crafted definition of a new heating technology enables the user of the decision tool to include all the potential available heating technologies specific to a heating network project into a prescribed geographic area like industrial waste heat additionally to the standard heating technologies defined in Appendix C. For the heating technologies included into the standard list of technologies predefined in the decision tool, data available in the literature [94] are used as inputs even though they can also be modified manually by the user of the decision tool if he gets other datasets.

For the air-to-water heat pump technology included into this standard list of heating technologies, the assessment of the parameter $c^{prod}_{i,HP,d,t}$ is dependent on the time such that a polynomial laws' model is used to assess the coefficient of performance of an air-to-water heat pump for a given level of temperature at the condenser of the heat pump prescribed by the operating temperature of the heating network and a prescribed hourly electricity price for a reference year. A polynomial laws' model for air-to-water heat pumps is considered into the set of available technologies because this model is generic and can be fitted to any new heating network project as a function of the supply temperature level of the heating network. In the frame of this research project considering third generation heating networks with a 90°C nominal supply temperature over the network, this temperature level limits the performance of the heat pumps such that this technology would not be suitable in practise. However, one of the goals related to the development of this optimization model remains its replicability to fourth generation heating networks by simply tuning the parameters of the polynomial laws presented herefater as a function of the temperature level of the network and the kind of air-to-water heat pump. Moreover, the decision tool looks for being generic such that the user of the decision tool can also supply its own performance curves for the heating technology as inputs of the optimization model for more accuracy.

Other types of heat pumps like geothermal heat pumps or water-to-water heat pumps could also be considered to reach higher performance levels using higher temperature heat sources. However, these kinds of heat pumps are dependent on the site where they would be installed such that they could not be installed on any available surface without an analysis of the adequate locations to put these types of technologies. They are therefore not considered into the standard list of predefined technologies in the decision

tool. Nevertheless, the user of the decision tool can indirectly consider these technologies by adding manually a new additional heating technology at a vertex v_i of the graph prescribing a variable heating production cost of this new technology dependent on the performances of the heat pump and the electricity price.

For the air-to-water heat pump, in addition to the influence of the part-load regime, the coefficient of performance also varies with the temperature of the heat source [95]. The modelling of the air-to-water heat pump technology is based on three polynomial laws developed by [96] in order to determine the coefficient of performance and the full heating load capacity as a function of the heating source temperature, the outlet temperature of the water and the part-load ratio for an air-to-water heat pump. Parameters for the polynomial laws are identified from manufacturers' data such that each heat pump has specific parameters values which are based on nominal conditions. These nominal conditions are prescribed for the sizing of the machine. In this thesis, a water set point temperature of 90°C and an air temperature based on weather data on an hourly basis are taken into account. In this case study, reference heat pumps chosen for the performance assessment are -7°C/65°C *Daikin Altherma* heat pumps whose polynomial coefficients have been identified by [97] (cf. Appendix F). The 3 polynomial laws mentioned above are represented by the following set of equations. The two first ones (*EIRFT* and *CAPFT*) provide the coefficient of performance and the heating capacity of the heat pumps at full load conditions as a function of the outdoor air temperature $T_{air,out}$ and the water outlet temperature at the condenser T_w. The last law (*EIRFPLR*) provides heat pumps performances at part-load regime.

$$\begin{cases} EIRFT = \dfrac{COP_n}{COP_{fl}} = C_0 + C_1 \cdot \Delta T + C_2 \cdot \Delta T^2 & \text{(2.63a)} \\ CAPFT = \dfrac{\dot{Q}_{fl}}{\dot{Q}_n} = D_0 + D_1 \cdot (T_{air,out} - T_{air,out,n}) + D_2 \cdot (T_w - T_{w,n}) & \text{(2.63b)} \\ EIRFPLR = \dfrac{\dot{W}_{pl}}{\dot{W}_{fl}} = K_1 + (K_2 - K_1) \cdot PLR + (1 - K_2) \cdot PLR & \text{(2.63c)} \end{cases}$$

where

$$\Delta T = \frac{T_{air,out}}{T_w} - \left(\frac{T_{air,out}}{T_w}\right)_n$$
$$PLR = \frac{\dot{Q}_{pl}}{\dot{Q}_{fl}}$$

Eq. 2.63a is used to determine the coefficient of performance at full load regime for a prescribed air temperature $T_{air,out}$ and a water set point temperature T_w. Eq. 2.63b aims to characterize the maximum available heating capacity of the heat pump compared to the nominal heating load capacity for the prescribed operating set points. Finally, a computation of the heat pump performance at part-load regime is achievable using Eq. 2.63c.

From this model, the coefficient of performance of this heat pump operating a whole year with an evaporator temperature fixed by the air outdoor temperature

has been extrapolated for a water outlet temperature of 90°C. The validity of this extrapolation can be questioned, especially for such high temperature levels generally limited to 80°C, such that it is always preferable that the user of the decision tool directly provides performance curves for heat pumps if they are available. Otherwise, this generic approach is used as a function of the supply temperature level $T_{w,su}$ over the network. Even if considering air-to-water heat pumps as a heating technology for a third generation heating network does not make a lot of sense from a thermodynamic point of view, this technology is included into the model to let the possibility to pick up these heat pumps as a heating source for future fourth generation heating network projects operating at lower temperatures.

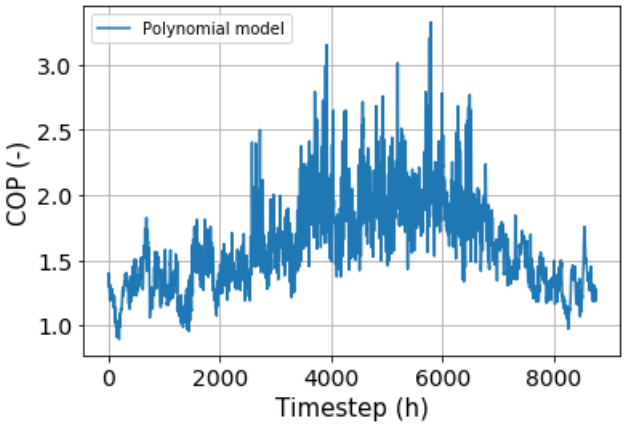

FIGURE 2.23: COP for heat pumps using a polynomial model for an air-to-water heat pump with water at 90°C.

From the COP curve illustrated in Figure 2.23, the annual hourly coefficient of performance can be linked to the annual hourly electricity price over a reference year such that a variable heating cost for the heat pump technology $c^{prod}_{i,HP,d,t}$ can then be computed for the optimization formulation using Eq. 2.64.

$$c^{\text{prod}}_{i,HP,d,t} = \frac{c^{elec}_{d,t}}{COP_{d,t}} \tag{2.64}$$

The heating cost to produce hot water at 90°C using an air-to-water heat pump is assessed to be included between 0 and 0.10 €/kWh. Even though this production cost is definitely underestimated because of the assumptions linked to the heat pump modelling, this heating source remains interesting to consider for the study of the research project. A solution to minimize the heating production costs could be to rely on the use of the electricity from the network during low-cost periods to produce heat with heat pumps and store this energy into thermal storages. This heat could be used instantly or later depending on the heating demand. As illustrated in Figure 2.24 for example, heating production costs with heat pumps are very variable on short-term and mid-term periods such that they could be integrated into district heating networks solutions to benefit from storage solutions. This will be illustrated in Chapter 3.

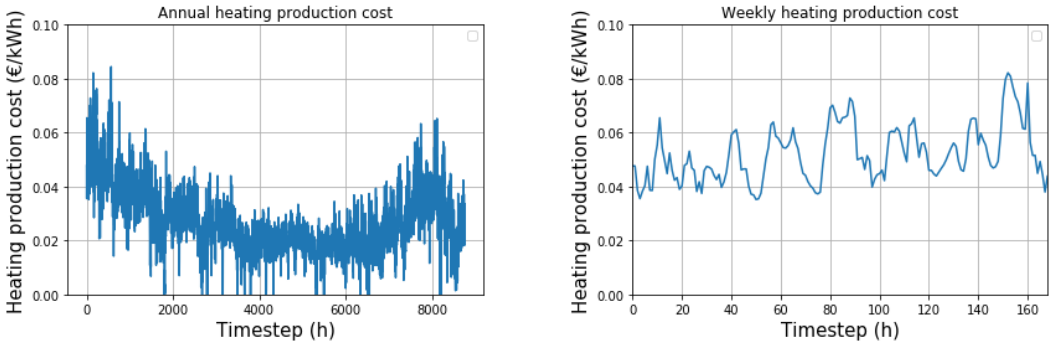

(a) Annual heating production cost (b) Weekly heating production cost

FIGURE 2.24: Heating production cost with a heat pump

Costs for pumping power

Water circulation over the network requires pumping power to satisfy the heating requirements at each timestep of the optimization problem. These pumps are fed by electricity such that the pumping power is dependent on the electricity price and the power flow into a pipe. The electrical consumption of a pump circulating a fluid with a mass flow rate $\dot{m}$ considering unit pressure losses ΔP into the pipe is given by Eq. 2.65.

$$\dot{W}_{elec} = \frac{\dot{m} \cdot \Delta P_{nom}}{\rho \cdot \eta_{pump}} \tag{2.65}$$

Considering nominal pressure losses $\Delta P_{nom} = 100$ Pa/m with a prescribed pump efficiency ($\eta_{pump} = 75\%$) and using Eq. 2.14 to determine the mass flow rate from the power flow, the electrical consumption over any edge j can be computed. Constant pressure losses and pump efficiencies are assumed because the outline of the network is not known before the optimization process while these two factors are dependent on the flow velocities and therefore the pipes diameters which are prescribed by the nominal power flows which are optimization variables of the problem.

The global pumping cost function including the pumping consumption over all the edges of the network is then defined as follows:

$$C_{\text{pump}} = \sum_{d \in D} w_d \cdot \sum_{j \in E, t \in T_D} w_t \cdot c^{elec}_{d,t} \cdot \dot{W}^{elec}_{j,d,t} \cdot \Delta t \tag{2.66}$$

2.3.4.3 Heating revenues

Revenues from heating sales are the main incomes useful to refund all the tackled expenses to build and operate the network. As explained in Section 1.2.2.1, contracts for heating sales can take various forms from one district heating project to another. However, pricing models are generally based on a market approach for private owners projects and on a cost approach for municipal owners projects [9] to define the total heating bill of the consumer. In this thesis, a pricing model based on market prices is used considering the gas market as

the main competitor for heating supply. This pricing model is used because one of the goals of this thesis is to highlight the economic benefits of district heating networks compared to conventional decentralized heating production units like gas. Therefore, a purely competitive pricing scheme is used as a comparison to show to policy-makers the potential interest of heating networks for a prescribed heating sales price. For sake of simplicity, a unique heating sales price r^{heat} is considered for all the consumers over the network even though it has been shown that the heating sales price is partially dependent on the heating demand of each consumer and also of the kind of consumers. The optimization formulation makes possible to define a specific heating sales price r_j^{heat} for each edge of the graph representation of the network if it is required for the project.

Total heating revenues are computed over the whole network based on potential heating consumptions $\dot{Q}_{j,d,t}^{heat}$ as defined in Eq. 2.67.

$$R_{\text{heat}} = N_{years} \cdot \sum_{d \in D} w_d \cdot \sum_{j \in E, t \in T_D} u_{j,d,t} \cdot w_t \cdot r^{heat} \cdot p_j \cdot \dot{Q}_{j,d,t}^{heat} \cdot \Delta t \tag{2.67}$$

Even though this objective function is used for the test cases in the next chapter, it has to be noticed that this function does not account for penalty costs if some streets connected to the optimal network are not supplied during some time periods of the year by the network. The optimization formulation is based on a stakeholder point of view which wants to operate its network in the most economically profitable way. However, in practise, penalty costs would disadvantage these kinds of scenarios such that a more accurate formulation of the objective function could include this penalty cost c^{pen} as follows:

$$R_{\text{heat}} = N_{years} \cdot \sum_{d \in D} w_d \cdot \sum_{j \in E, t \in T_D} \left[u_{j,d,t} \cdot r^{heat} - (x_j - u_{j,d,t}) \cdot c^{pen} \right] \cdot w_t \cdot p_j \cdot \dot{Q}_{j,d,t}^{heat} \cdot \Delta t \tag{2.68}$$

2.4 Outputs

This model formulation provides optimized scenarios for given inputs and user-defined economic and urbanistic parameters such that some key performance indicators (KPI) can be drawn out of the results. These KPIs are summarized in an *Excel* file containing all the main outputs required to assess the profitability of a heating network project.

2.4.1 Mapping into the Geographic Information System

The main output of the decision tool provides a map of the optimal heating network determined by the decision tool into the geographic information system. Geometric features including built heating sources and edges as well as pipes diameters are stored into *CSV* files after a post-processing of the results coming from the optimization model. These results are readjusted to be integrated into

the geographic information system to map the optimal heating network. This mapping relies on a *Python* script used to post-process all the useful pieces of information to give an overview of the heating network project to the stakeholders.

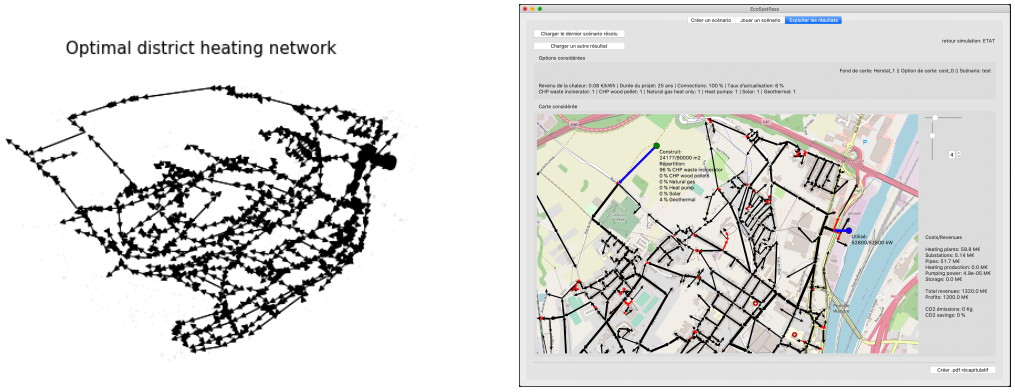

(a) Mapping with *Python*. (b) Mapping with *Open Street Map*.

FIGURE 2.25: Mapping into a Geographic Information System.

2.4.2 Specific cost

A profitable district heating project relies on the minimization of both the heating production costs and the heating distribution costs to remain competitive compared to other markets like the gas distribution companies. It is therefore important to assess and to split the production costs and the distribution costs related to heating network projects in order to figure out what are the economic benefits or losses linked to the distribution costs including heat losses over the network and pumping costs to feed the network.

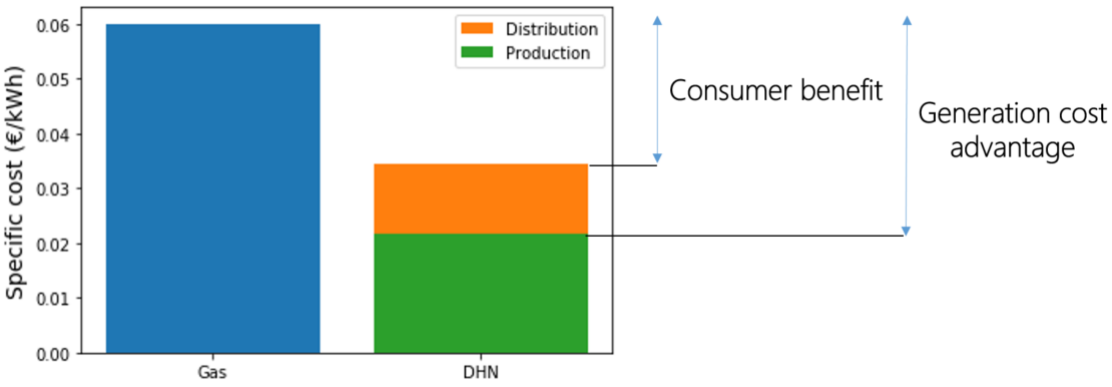

FIGURE 2.26: Comparison of the specific cost with a gas boiler or a heating network.

An illustration of these specific costs enables to compare the costs related to the two current main solutions for the heating sector and to highlight the potential consumer benefit with a connection to a heating network instead of the use of an individual gas boiler at home. This indicator aims for convincing heating consumers to switch from decentralized heating production technologies to centralized ones by showing the benefits of these centralized ways of production.

2.4.3 Net Present Value

Even though the environmental aspect is taken into account into heating networks projects, the economic profitability remains essential to ensure viability to investors to take part in the project. The profitability over the lifetime of the project is based on yearly assessments of all the incoming and outcoming payments related to the network. The incoming payments include the revenues from heating sales but also fees received for waste incineration for example [33] or subsidies provided by public institutions. The outcoming payments include the investment costs, the maintenance costs and the operation costs. Eq. 2.69 used for the assessment of the net present value (NPV) enables to quantify on a yearly basis the net present value of the project and to figure out the payback time period beyond which the project becomes economically profitable. R_y represents the net cash flow of the year y computed by substracting the outcoming cash flows from the incoming cash flows.

$$NPV = \sum_{y=1}^{N_{years}} \frac{R_y}{(1+a)^y} \tag{2.69}$$

A graphical illustration as depicted in Figure 2.27 enables decision-makers to assess the evolution of the yearly net cash flows over the years in order to analyze the return on investment period of the project.

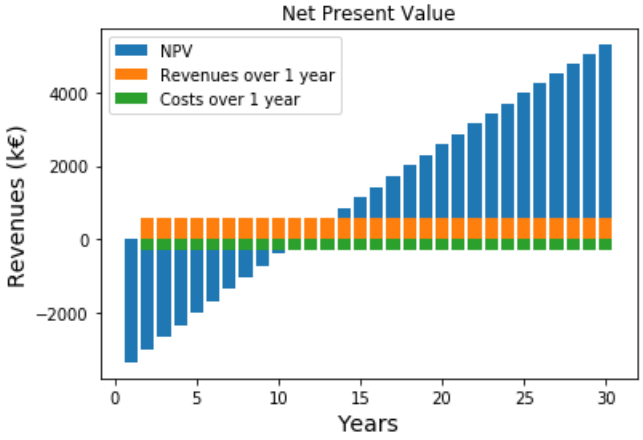

FIGURE 2.27: Net Present Value of a project over 30 years.

2.4.4 Savings of CO_2 emissions

Compared to decentralized heating production units, centralized heating production units included into heating networks can provide CO_2 emissions savings thanks to the use of low-carbon emissions heating sources. These CO_2 savings are assessed for a prescribed geographic area by comparing the emissions from a decentralized heating production scenario where the connected dwellings of the area are fed locally by gas boilers to a partially or totally centralized way of heating production with the building of the optimal heating network set up by the decision tool.

$$CO_2 \text{ savings} = \frac{CO_2^{gas} - CO_2^{DHN}}{CO_2^{gas}} \tag{2.70}$$

with

$$\begin{cases} CO_2^{DHN} = \sum_{i \in V_P, m \in H_i, d \in D, t \in T_D} CO_{2_m} \cdot \frac{\dot{Q}_{i,m,d,t}}{\eta_{i,m,d,t}} & \text{(2.71a)} \\ CO_2^{gas} = \sum_{j \in E, d \in D, t \in T_D} CO_{2_{gas}} \cdot u_{j,d,t} \cdot p_j \frac{\dot{Q}_{j,d,t}^{heat}}{\eta_{gas,d,t}} & \text{(2.71b)} \end{cases}$$

These 2 equations enable to link CO_2 emissions to the heating production and consumption for each street of the network while taking into account the efficiencies $\eta_{i,m,d,t}$ of the different heating technologies. These efficiency values can be provided by the user of the decision tool if they are available. Otherwise, by sake of simplicity, the decision tool prescribes standard values for the efficiency and the CO_2 emissions of the heating technologies which are summarized in Appendix C. It can be noticed that for the heat pump technology, the efficiency value is equal to the value of the coefficient of performance of the heat pump and CO_2 emissions are based on the average value of the CO_2 emissions linked to the electricity production in Belgium around 0.247 kg CO2/kWh [98]. This CO_2 factor can obviously be adapted to the kind of electricity production such that the user of the decision tool could consider for example a heat pump using green electricity with zero CO_2 emissions.

2.4.5 Repartition of the pipes diameters

The sizing of the pipes remains essential to limit the heat losses into the network. The location and the number of heating sources and thermal storages can provide different selections of the optimal pipes diameters over the network. Therefore, a plot of the diameters repartition with the number of pipes for each existing diameter is proposed into the decision tool.

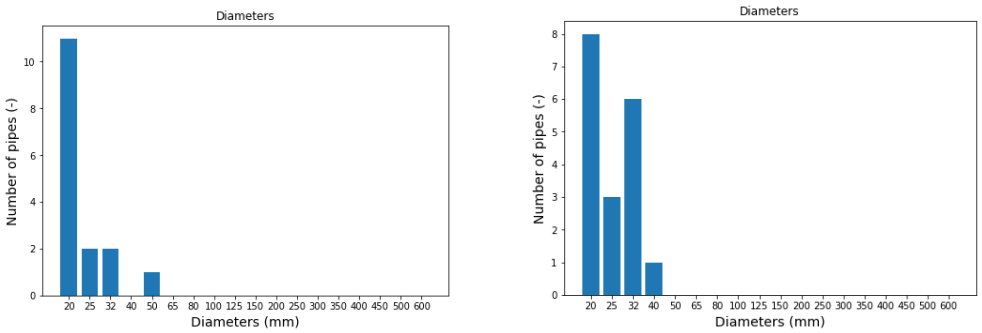

(a) Without thermal storage. (b) With thermal storage.

FIGURE 2.28: Repartition of the pipes diameters into the heating network.

2.5 Conclusion

This chapter introduces and describes the developed methodology to answer the issue related to the *EcoSystemPass* project while remaining generic for other heating network projects. This decision tool is based on inputs data which can be directly used to compute generic heat demand profiles for different kinds of dwellings with diversified heating consumption loads. However, this generation of heating demands being very generic, it is not recommended to use it as the main solution for inputs data if more accurate heating consumption data are available. Indeed, the user of the decision tool can also directly provide the heating consumption profiles as inputs of the decision tool.

From these heating demand profiles and other inputs parameters which can be defined by the users of the decision tool regarding the kind of heating network project they are working on, an optimization model for the outline and the sizing of a third generation heating network in any new geographic area is formulated. The assessment of the optimal outline of a heating network including the pipes to build and their diameters remains essential for an industry or a policy-maker which wants to study the profitability of a heating network into a prescribed geographic area and the limits of this network. However, not knowing the outline of the network before the optimization process makes difficult to assess accurately physical phenomena into the network. The definition of the optimal outline is also very time consuming for large-scale instances because of the large number of binary optimization variables for choosing the streets to connect or not to the network. Research works handling with the optimal outline of a heating network are generally limited in terms of sizing, especially for variable heating demand and storage solutions, but also in terms of problem sizes that can be solved. The methodology in this chapter aims for formulating an optimization model which can tackle these issues and fill in the general features mentioned in Section 1.3.1:

1. Applicability to small-scale cases with a neighbourhood of a few streets to large-scale problems including heating network projects into cities thanks to a linear formulation;

2. Simultaneous optimization of the outline, the sizing and the multi-period operation of the network including thermal storage solutions;

3. Link with a geographic information system for the replicability of the decision tool to any new heating network project.

However, to fill in these criteria, some hypotheses are made to simplify the formulation in this thesis such that this model can lack of reliability compared to other existing models. Nonetheless, the reader has to be aware that this decision tool looks for providing general insights about the potential economic and environmental benefits of a heating network solution into a geographic area before any feasibility study. The decision tool provides a pre-feasibility study which can be used as an input by other existing tools like *PowerDIS* [99] for example to refine the heating network solution given by the optimization tool. Accordingly, this decision tool has some limitations which are important to consider while

interpreting the results of the optimization model and proceeding on the different stages of a heating network design. A summary of the main assumptions of this optimization model is summarized as follows:

- Operating supply and return temperatures are prescribed to values of respectively 90°C and 60°C over the network with a constant temperature difference of 30°C at the substations. In practise, these temperatures are not constant during the network operation. Moreover, these temperatures are also used as operating set points for fitting the parameters linked to heat losses into the network. The values of the heat losses parameters have to be refitted for new operating temperatures. These reference operating temperatures have been chosen to satisfy the requirements of the research project considering third generation heating networks. However, lower operating temperatures adapted for fourth generation heating networks could be considered for future heating network projects;

- Heat losses are linearized as a function of the nominal power flows into the pipes. The assessment of the heat losses takes then into account the mass flow rate into the pipes regarding nominal operating conditions but does not estimate heat losses out of these nominal conditions. Control strategies can be applied to optimize the network operation by adapting the temperature levels over the network. However, into this optimization formulation, constant temperature levels are considered such that the network might operate far away from nominal conditions, especially during low heating demand periods;

- Some representative days are selected to reduce the number of optimization variables and the computational load of the problem. However, the formulation used to choose representative days enforces cyclic behaviour for a representative day assigned with a weight w_d such that seasonal thermal storage solutions are disadvantaged with this formulation for selecting representative days;

- Some heating production technologies like air-to-water heat pumps are considered for high temperature heating production in third generation heating networks even though they are generally not tailored for these temperature levels. Heat pump performances have been extrapolated for these high temperature levels in order to provide generic performance curves. It is recommended that the user of the decision tool provides available data specific for the project as inputs of the model if they are available.;

- Inputs parameters are prescribed by the users of the decision tool as deterministic values. However, strategic energy planning generally implies uncertainty because of the non-exact knowledge of the values of some parameters. Therefore, an optimization method taking into account inputs uncertainties and their uncertainty levels like in [100] could be developed. It is not considered into the optimization model presented in this chapter.

These assumptions enable to provide a solution for a pre feasibility study of the optimal outline and sizing of a network but limit the accuracy of the model

at some point. This model helps then to get an idea over the potential of the location of a heating network into a given geographic area but then requires the use of more specific models available in the literature for a sophistication of the results coming from this optimization tool. The main limitations of the decision tool will be illustrated in Chapter 4 by simulating the optimal network designed in Chapter 3 and by comparing the differences in terms of results between the optimization formulation and the dynamic simulations.

Chapter 3

Tests of the decision tool on a small-scale theoretical case study

"All intelligent thoughts have already been thought; what is necessary is only to try to think them again."

—Johann Wolfgang von Goethe

The decision tool described in Chapter 2 can be used on any case study from a small neighbourhood of a few streets to a large-scale case study including hundreds or thousands of streets. In order to highlight some of the features of the optimization model and to draw conclusions about results and trends to maximize the net cash flow out of a heating network project, a first theoretical case study with 16 streets and 3 potential heating sources is considered in this chapter. This theoretical case study looks for being used as a reference test case on which different optimization methods could be applied for comparison from the literature review.

3.1 Description of the case study

This first case study is based on the *Annex 60* proposal [101] and the district heating network case presented by [66]. The *Annex 60* proposal provides a set of standardized types of buildings with their geometric and physical properties. From these properties, a thermodynamic model can determine the heating demand profiles for each dwelling based on a yearly weather file. These standardized sets of buildings are used in this chapter such that heating load profiles can be reused by other research units if they want to test their optimization formulations on this reference case. Regarding the layout of the neighbourhood, it is inspired by [66] which uses a test case with a limited number of streets and nodes such that different kinds of optimization formulation with different levels of details can be applied using this test case. The reference case study presented in this chapter aims then for representing different scenarios of neighbourhoods from low heating consumptions eco-neighbourhoods to old neighbourhoods characterized by a large heating demand due to a building stock made up of dwellings with a poor thermal insulation.

TABLE 3.1: Main features of the dwellings constitutive of the case study

Type	Description
A	5-floor apartment blocks
D	Detached houses
G	Greenhouse
O	5-floor office buildings
S	Semi-detached houses
T	Terraced houses

(A) Types of dwellings

Class	Level of insulation
1	Well-insulated dwellings
2	Poorly insulated dwellings

(B) Levels of thermal insulation

As illustrated in Table 3.1, 6 types of dwellings and 2 types of thermal insulations are defined to generate heating demand profiles and the features of these dwellings are detailed in Appendix G. For the two levels of thermal insulation, the first one refers to the requirements of the European Performance of Buildings Directive (EPBD) in Belgium [102] and the second one represents typical buildings of the period 1946-1970 based on [103]. For these 2 types of thermal insulations, two different hypotheses are made. For new generation well-insulated dwellings of type 1, domestic hot water is considered to be provided by an independent heating system such that only space heating demand would be provided by the heating network. For poorly insulated dwellings of type 2, the total heating demand of each dwelling includes space heating and domestic hot water. These dwellings are constitutive of a small neighbourhood of 16 streets as represented in Figure 3.1. The locations of the nodes are given in Appendix I. 3 existing potential heating sources are defined at nodes v_1, v_2 and v_{13} whose technical and economic parameters are defined in the following section. These potential heating sources are considered to be already available [1] such that they have no capital expenses for their building.

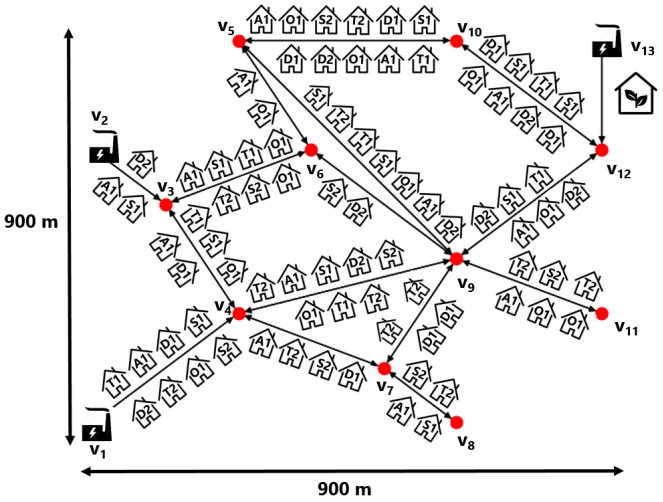

FIGURE 3.1: Case Study with 16 streets and 3 potential existing heating sources.

[1] They are for example residual waste heat from industrial processes.

Space heating and domestic hot water consumptions of these dwellings are then assessed from thermodynamic models described in the following using the *Modelica* modelling language to tackle the dynamic behaviour of these heating demands. For the greenhouse, the heating load profile is based on the open-source *Greenhouses Modelica* library for the simulation of greenhouse climate [104] implemented in the frame of the *EcoSystemPass* research project. The number of dwellings constitutive of each street is defined randomly for different test cases to represent various heating demand profiles having an influence on the outline and the sizing of the heating network. These scenarios are illustrated in the following section with a definition of all the parameters linked to this case study.

3.1.1 Definition of the scenarios

4 different scenarios with various heating demand profiles are considered in order to represent different cases which could occur in real conditions.

1. An eco-neighbourhood with only well-insulated residential dwellings (types A1, D1, S1 & T1);
2. An eco-neighbourhood with well-insulated residential and office dwellings (types A1, D1, S1, **O**1 & T1);
3. An eco-neighbourhood with well-insulated residential and office dwellings (types A1, D1, S1, O1 & T1) **and** a greenhouse between nodes v_{12} and v_{13};
4. A neighbourhood with well-insulated and poorly insulated residential and office dwellings (types A,D,S,O & T 1/**2**) and a greenhouse between nodes v_{12} and v_{13}.

These 4 scenarios have specific heating demands features which are illustrated in Figure 3.2 and a detail of the number of dwellings of each type constitutive of the network is given in Appendix H. In the first two scenarios, it can be observed that the heating demand during the summer is zero because of a building stock made up only of well-insulated dwellings of type 1 without demand for domestic hot water. In district heating networks, this could be non profitable because the network does not operate during a whole part of the year generating no incomes from heating sales. Moreover, with well-insulated dwellings, the total heating demand is lower than with poorly thermally insulated dwellings such that heating revenues are sometimes lower than required investment costs to feed all the consumers of the network. These scenarios can then be used as comparison case studies to assess the influence of the heating demand on the economic profitability of a potential heating network.

For Scenario 2, the apartments A_1 of Scenario 1 are replaced by offices O_1 whose daily heating consumption profile is shifted compared to apartments with the same physical and geometric features. This is due to the occupancy rate of the dwellings: for offices, the traditional occupancy rate occurs during working hours (8am to 8 pm) while for residential dwellings, it occurs between

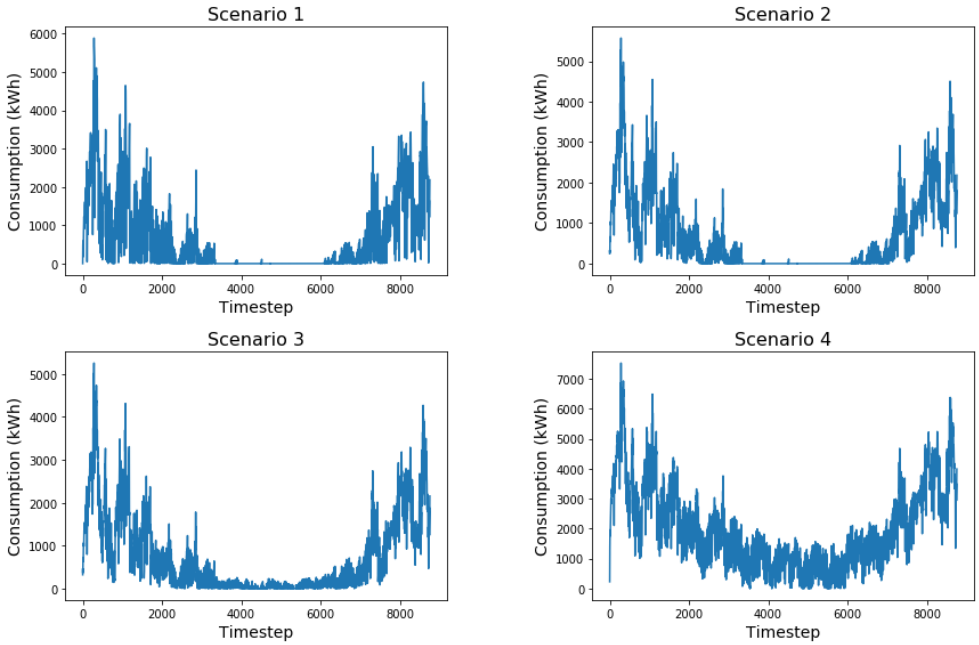

FIGURE 3.2: Yearly heating demands for the 4 different scenarios.

the rest of the day (8pm to 8 am). As represented in Figure 3.3, this heating demand shift ensures a more constant heating demand over the day which can be interesting for reducing the size of the heating plants to connect to a potential heating network. As explained in Section 1.2.2, the diversity of dwellings into the neighbourhood enables to promote the development of heating networks because of the more constant heating demand over the day due to this aggregation effect.

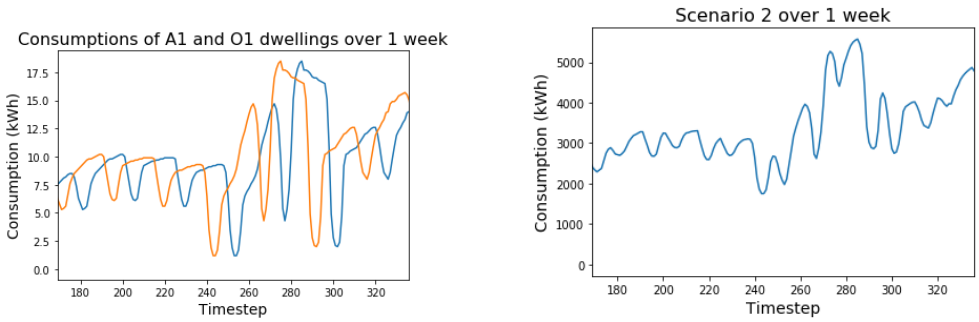

(a)

(b) Consumptions over 1 week for the Scenario 2 (8-15 January).

FIGURE 3.3: Consumptions over 1 week for the Scenario 2.

For Scenario 3, the greenhouse acting as a large consumer with an approximately constant non zero heating demand is added to the neighbourhood. The advantage for the implementation of a district heating network with these kinds of consumers is that there are incomes from heating sales all over the year thanks to this continuous non zero heating demand. It can be seen from Figure 3.4 that the heating demand over the year is never zero thanks to the greenhouse consumption. Finally, for the last case study, a neighbourhood mixing new and

old dwellings and a greenhouse between nodes v_{12} and v_{13} is considered. Old dwellings have a larger heating consumption because they are poorly-insulated and moreover, they have a non-zero heating demand all over the year because of the additional demand for domestic hot water. This non zero heating demand is due to the heating profiles of D2, S2 and T2 dwellings (cf. Figure 3.4).

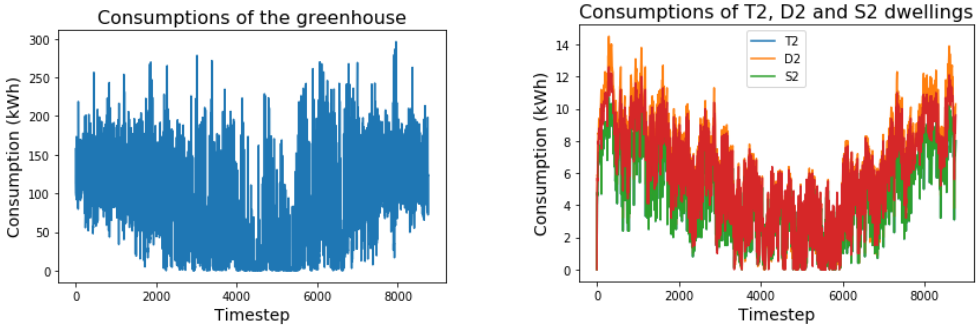

FIGURE 3.4: Consumptions of the greenhouse and the poorly thermally insulated dwellings.

For these 4 scenarios, the optimization model is used based on pre-defined economic and technical parameters. Firstly, the prospective heating plants are considered to have a sufficient capacity. The maximum heating demand out of the 4 case studies is around 7 MW_{th} such that 10 MW_{th} plants capacities are considered to ensure a sufficient heating capacity at each heating plant.

TABLE 3.2: Properties of the power plants

Heating source	**Maximum heating capacity (MW_{th})**	**Heating production cost (€/kWh_{th})**	**Specific CO_2 emissions (kg/kWh_{th})**
v1	10	0.03	0.150
v2	10	0.04	0.200
v13	10	0.05	0.250

3.1.2 Dwellings models

The physical models for the dwellings heating requirements have been developed for the *Annex 60* study [105]. These physical models are used instead of generic models presented in Section 2.1 for this theoretical case study in order to get replicable models that can be handled by other researchers if they want to test their models on this case study and bring a critical point of view on the models presented into this thesis. Moreover, the generic models have some limitations, as explained in Chapter 2, such that physical models enable to handle more accurately the dynamics of the heating demand of various kinds of dwellings.

For the modelling, dwellings are divided into different zones related to constant volumes of air supposed to be at a uniform temperature prescribed to a set point of 21°C. As illustrated in Figure 3.5, for example, detached (D) houses are divided into 5 different zones corresponding to specific parts of the house. The

first one is related to the kitchen and the living room and the second one to the office. The third one represents the hall and the storage. The two last zones correspond respectively to the three bedrooms and the bathroom. These zones are connected together through mass and energy conservation equations taking into account heat and mass exchanges between zones and with the outside to determine energy requirements for each dwelling.

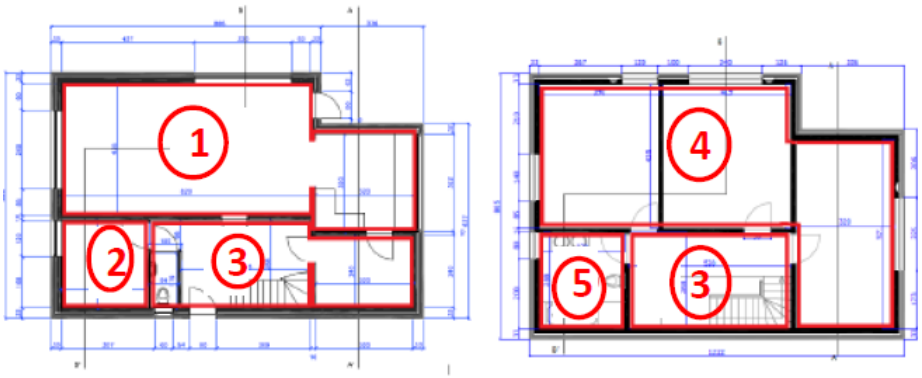

FIGURE 3.5: Division of the detached (D) dwellings into zones: first (left) and second (right) floors.

Heat transfers through walls and windows are computed using a network of thermal resistances R $[K/W]$ combined with lumped capacitances C $[J/K]$. The thermal resistance corresponds to the resistance to conduction heat transfer through the walls and the lumped capacitance is intended for representing the thermal inertia of the wall material. For windows, inertia effects are neglected which is represented by a strictly resistive branch for the heat transfer model. The resulting model is made up of the following set of differential equations:

$$\begin{cases} \dot{Q}_{in} = \dfrac{T_{wall} - T_{in}}{R_{in}} \\ \dot{Q}_{out} = \dfrac{T_{wall} - T_{out}}{R_{out}} \\ \dot{Q}_{out} - \dot{Q}_{in} = C_{wall} \cdot \dfrac{dT_{wall}}{dt} \end{cases} \tag{3.1}$$

In the above equations, T_{out} and T_{in} represent respectively the outdoor and indoor temperatures $[°C]$ and T_{wall} corresponds to the mean temperature of the wall $[°C]$. Conservation equations 3.2 are applied to connect the different zones together taking into account lighting, electrical appliances and building occupancy to build the complete model of a dwelling. These conservation equations represent a simplified approach to get an assessment of the heating demands of the dwellings. However, they do not consider some physical phenomena like solar gains. Even though this approach is simplified compared to a global modelling of a dwelling, this enables to handle with variable heating demands and dynamic phenomena while the generic models presented in Chapter 2 can not take these phenomena into account.

$$\begin{cases} \dfrac{d\dot{m}_{air}}{dt} = \dot{m}_{air,su} - \dot{m}_{air,ex} \\ \dfrac{dU}{dt} = \dot{Q}_{in} - \dot{Q}_{out} \\ \dot{Q}_{in} - \dot{Q}_{out} = \dot{Q}_{windows} + \dot{Q}_{walls} + \dot{Q}_{inf} + \dot{Q}_{int} + \dot{Q}_{vent} + \dot{Q}_{TU} \end{cases} \tag{3.2}$$

with $\dot{Q}_{windows}$ corresponding to the heat flow through windows, $\dot{Q}_{walls}$ to the heat flow through walls, $\dot{Q}_{inf}$ to the heat rate due to air infiltrations, $\dot{Q}_{int}$ to the heat rate due to internal gains (lighting, appliances and occupancy), $\dot{Q}_{vent}$ to the heat rate due to the ventilation in the dwellings and $\dot{Q}_{TU}$ represents the heat input from terminal units for heating or cooling. $\dot{m}_{air,su}$ and $\dot{m}_{air,ex}$ are respectively the supplied and extracted mass flow rates in each zone. U corresponds to the internal energy of the volume of air in each zone. Based on this set of equations, a thermodynamic model of the whole dwelling is implemented by considering heat flows between adjacent walls and with the floor and the ceiling. The heating consumption profile of each kind of dwellings is computed by using a dynamic model solving the set of equations presented above based on weather data for a reference year as boundary conditions. The total annual heating demands determined from this model are represented in Figure 3.6 for all the different sets of dwellings.

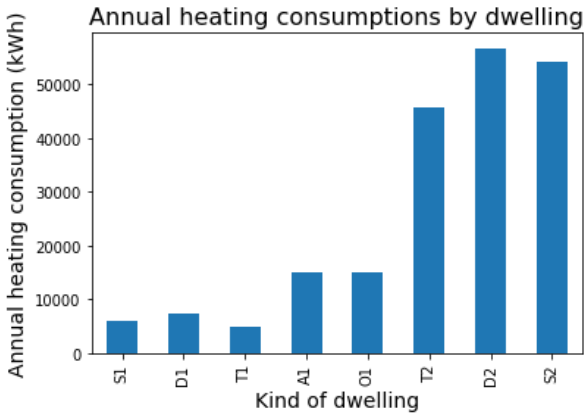

FIGURE 3.6: Total consumption over a reference year of the different dwellings.

It can readily be observed that well-insulated dwellings (type 1), with a level of insulation based on the directive 2010/31/EU, consume up to ten times less energy than the poorly insulated ones (type 2) with an average level of insulation corresponding to buildings insulation from 1946 to 1970 in Belgium. Obviously, a reduction of primary energy consumption related to the latter dwellings can be achieved by a deep retrofit towards low energy buildings [106]. However, such a retrofit is not always possible in real-life applications as this requires long-term inhabitants relocations and difficult permitting procedures. Inversely, the implementation of a district heating network is another way to reduce primary energy consumption through the use of highly efficient centralized heating production without the recourse to deep renovation processes. The

resulting reduction in fuel consumption would be profitable from an economic and environmental point of view with a decrease of both cost of heating and CO_2 emissions. Moreover, it can be observed that even for the same level of insulation, heating demands are variable from one dwelling type to another. A dynamic simulation model is able to catch the high variability of the heating demands in order to assess the global performance of the system and its related costs.

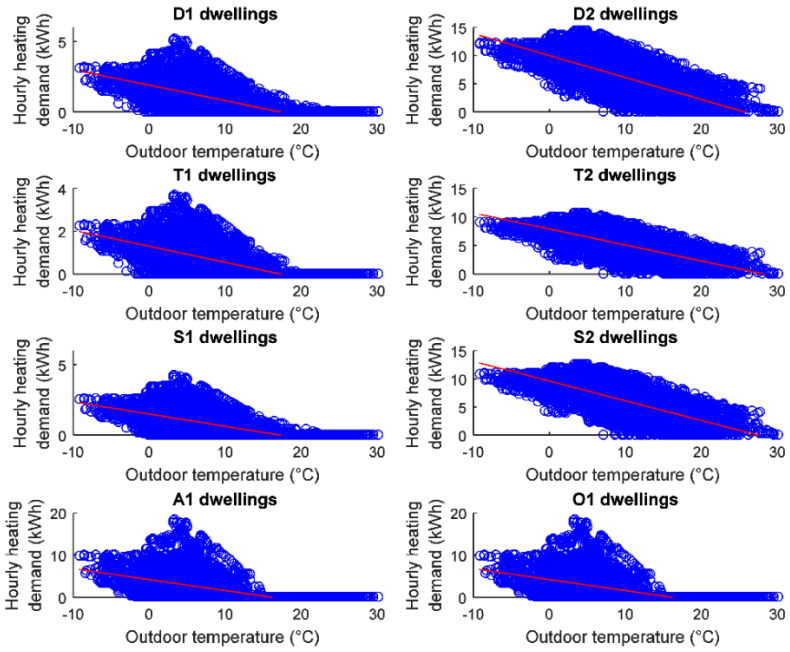

FIGURE 3.7: Dwellings heating load profiles as a function of the outdoor temperature.

Figure 3.7 depicts the heating consumption (including domestic hot water for dwellings of type 2) on an hourly basis over a reference year as a function of the outdoor temperature. The blue circles represent the consumption calculated by the dynamic model taking into account the thermal inertia while the red lines represent the steady-state consumption. For all the dwelling types, the dynamic solution exhibits a large scattering around the steady-state solution: for the same outdoor temperature, the predicted dynamic heat load can be twice or three times larger than the steady-state solution which claims for the use of dynamic models for the assesment of heating demands. A simple interpolated heating curve using only the outdoor temperature as input is not representative of the dynamic effects occurring in the dwellings. An accurate estimation of the heating demand depends upon the previous states of the system and requires a dynamic or state-space modelling.

As already previously illustrated in Figure 3.6, it can also be observed that hourly heating demands are logically higher for poorly insulated (type 2) dwellings than for well-insulated dwellings (type 1). Even though heating demand profiles follow a similar trend as a function of the type of dwellings, it can be seen that

the energy consumption is dependent on the type of dwellings. This physical modelling approach enables thus to distinguish heating consumption profiles as a function of the kind of dwellings and their thermal insulation. However, the reader has to keep in mind that this approach remains simplified and can be questionable but is simply used to get a possibility to handle with diversified variable heating demands for the optimization theoretical case study.

3.2 Influence of the heating demand of the neighbourhood

The reference scenario is based on three existing potential heating sources with a sufficient heating capacity to feed the whole heating demand of the network and a heating sales price r_{heat} based on a market approach comparing with alternative competitors prices. For the heating sector, the main competitors are the gas companies such that the heating sales price with a heating network are based on the mean gas price illustrated in Figure 3.8 [107]. The average gas price in the European Union is around 0.07 €/kWh and is chosen as a standard market price on which the heating network sector must be competitive.

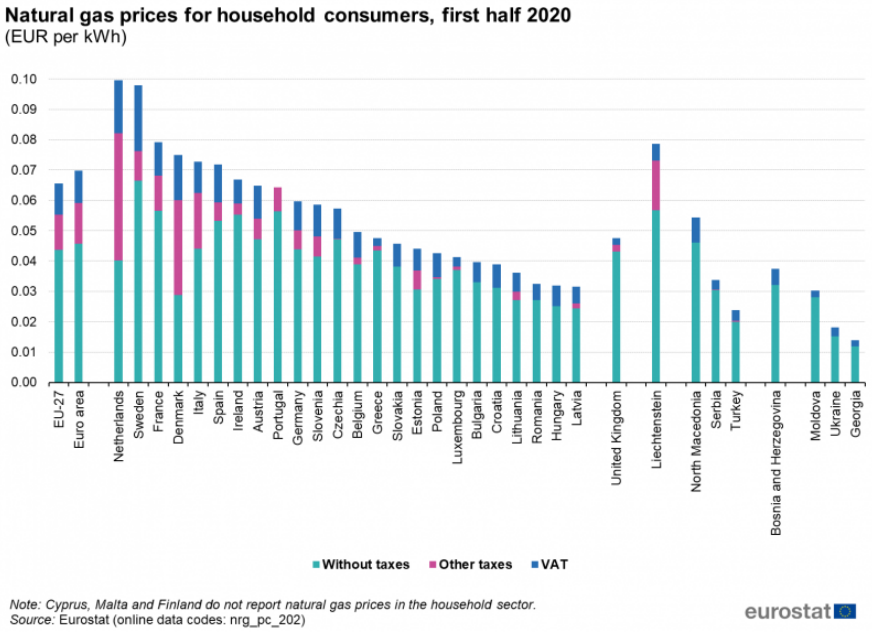

FIGURE 3.8: Gas prices in the European Union [107].

The model related to this reference scenario contains 35,111 variables and is solved using the Gurobi solver with an optimality gap of 0.1%. The computations are executed in 25 seconds on a computer with an Intel® Core™ i7-8650U processor with 8 threads at 1.90 GHz and 16GB RAM. Considering a project lifetime of 30 years with an actualization rate of 1% and assuming that all the potentials consumers over a given street would be connected to the network if a pipe is built into this street ($p_j = 1$), results regarding the outline of the heating

network for the 4 scenarios are illustrated in Figure 3.9. For a heating sales price of $0.07€/kWh$, the optimal heating network connects all the streets of the neighbourhood using the heating source with the cheapest heating production cost at node v_1. This optimal heating network enables CO_2 emissions savings of 24.24% in the 4 scenarios compared to a decentralized heating production with gas boilers in each house of the network.

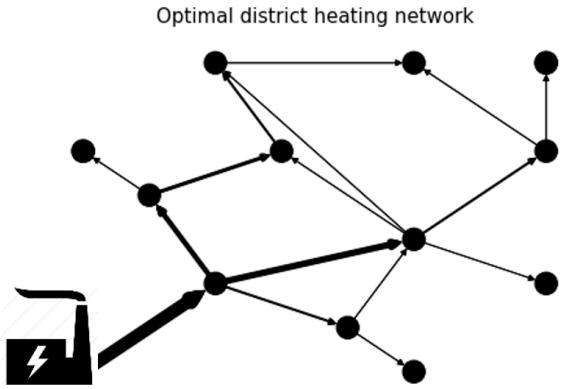

FIGURE 3.9: Outline of the heating network for the 4 scenarios.

TABLE 3.3: Comparison of the 4 initial scenarios.

	Scenario 1	**Scenario 2**	**Scenario 3**	**Scenario 4**
Yearly heating demand (GWh_{th})	6.252	6.252	6.533	17.925
Maximum heating demand (MWh_{th})	5.887	5.571	5.253	7.528
Used heating capacity (MW_{th})	5.958	5.644	5.324	7.599
CAPEX (M€)	3.358	3.350	3.346	3.632
OPEX (M€)	6.856	6.856	7.180	19.357
Revenues (M€)	13.093	13.093	13.684	37.631
Profits (M€)	2.879	2.887	3.157	14.642
Return On Investment period ROI (years)	12	12	12	4

These 4 scenarios can be compared from different criteria that are summarized in Table 3.3. The first comparison to achieve concerns Scenario 1 and Scenario 2 whose main difference into the building stock relies on the substitution of apartment blocks by offices. These offices have the same shifted heating consumption than the apartments. This shifting of a part of the heating demand (as illustrated in Figure 3.3) enables to reduce the used heating capacity of the heating source at node v_1 by 314 kW_{th} and also the initial investment costs linked to the pipes and substations by 8 000 €.

Thanks to a better repartition of the heating demand during the whole day between residential and non-residential dwellings, the maximum power flow into each pipe is decreased implying a reduction of the required pipe diameters. As illustrated in Figure 3.10, one of the pipes with a diameter of 65mm in Scenario 1 is substituted by a pipe with a diameter of 50mm in Scenario 2 thanks to the lower power flows into the network. These lower power flows are obtained thanks to a shift of a part of the heating demand from apartment blocks to offices. Pipes with smaller diameters have a lower cost per unit length such that the capital expenditures including the pipe costs are slightly lower in Scenario 2 than in Scenario 1. This decrease of the capital expenditures is also linked to the reduced sizing of the substations because of the decreasing maximum heating demand over each edge. Substations costs related to a specific edge being proportional to the maximum heating demand over this edge implies that the costs related to substations slightly decrease in Scenario 2. The total amount of heating production remains the same for both scenarios such that operating expenditures and revenues are identical in both cases. A decrease of the maximum heating demand with the shifting of a part of the total heating demand of the network enables then to increase total profits generated out of the network project.

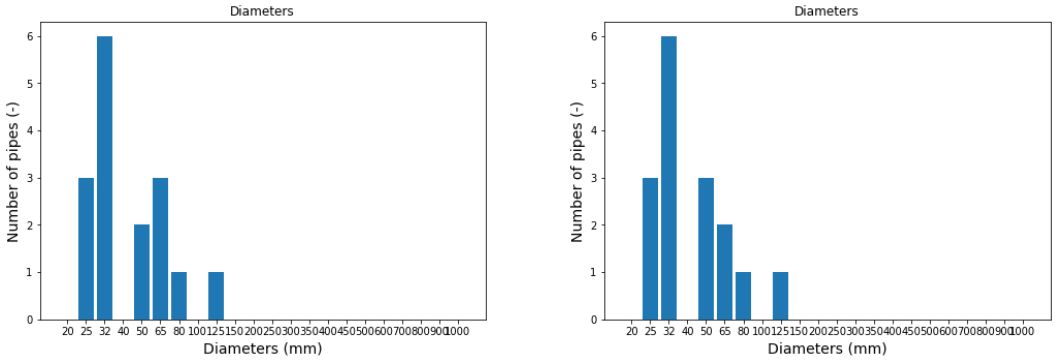

(a) Pipes diameters with Scenario 1.

(b) Pipes diameters with Scenario 2.

FIGURE 3.10: Pipes diameters for the 2 first scenarios.

As illustrated in Figure 3.2, the substitution of the dwelling stock by a greenhouse at the edge $v_{12}v_{13}$ from Scenario 2 to Scenario 3 changes the heating demand profile of the whole network with a non zero heating demand all along the year thanks to the greenhouse heating demand profile. It also reduces the hourly maximum heating demand of the whole neighbourhood of 318 kWh_{th} from Scenario 2 to Scenario 3. On the other hand, the yearly total heating demand increases of 281 MWh_{th} in Scenario 3 compared to Scenario 2 thanks to the introduction of the greenhouse into the neighbourhood. This increase of the total yearly heating demand implies an increase of the operating expenses but also of the heating sales revenues. The increase of the heating sales revenues being greater than the increase of the operating costs enables to raise the profits coming from the optimized heating network project.

It can be noticed that the capital expenses have slightly decreased from Scenario 2 to Scenario 3 thanks to the reduction of the pipe diameters as from Scenario 1 to Scenario 2. It can be observed from Figure 3.11 that some of the pipes

with a diameter of 32mm in Scenario 2 are replaced by pipes with a diameter of 25mm and one of the pipes with a diameter of 65mm in Scenario 2 is replaced by a pipe with a diameter of 50mm. Finally, the bigger pipe with a diameter of 125mm is replaced by a pipe with a diameter of 100mm. The reduction of the pipe diameters contributes to the decrease of the capital expenses and indirectly to the increase of the profits linked to the heating network project.

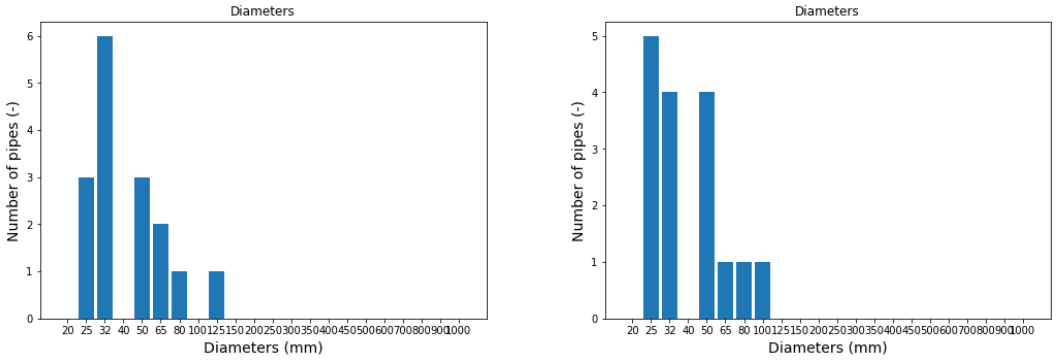

(a) Pipes diameters with Scenario 2.

(b) Pipes diameters with Scenario 3.

FIGURE 3.11: Pipes diameters for Scenarios 2 and 3.

Finally, substituting a part of the well-insulated dwellings from the three first scenarios by poorly insulated dwellings get the bigger impact on the outline and the sizing of the network. As illustrated in Figure 3.2, poorly insulated dwellings get heating demand profiles defining a large non zero heating demand all over the year and a quite larger heating demand compared to well-insulated dwellings. This large increase of the yearly heating demand compared to Scenario 3 impacts the operating expenditures to produce heat but also the revenues generated from heating sales. As in Scenario 3, the increase of heating sales revenues being larger than the increase of operating expenditures implies a larger profit over the investment period of the heating network of the project. It can also be noticed from Figure 3.12 that the increase of the heating demands obviously influences the increase of the capital expenditures due to the requirement of larger pipes (and substations) to feed the streets of the network.

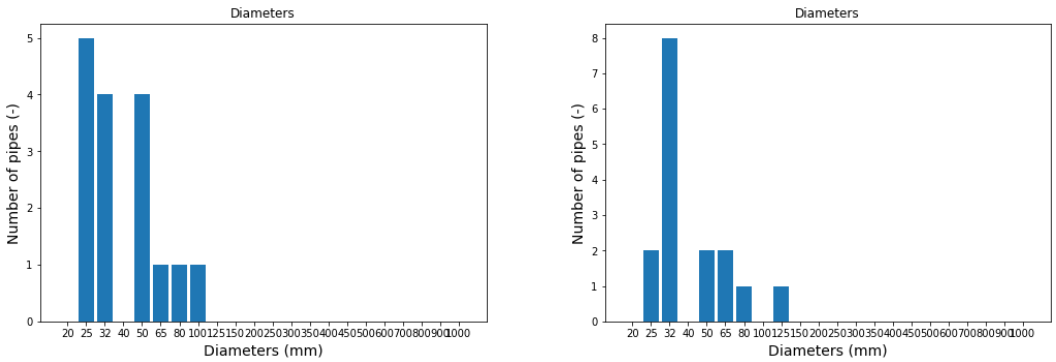

(a) Pipes diameters with Scenario 3.

(b) Pipes diameters with Scenario 4.

FIGURE 3.12: Pipes diameters for Scenarios 3 and 4.

However, this increase of the capital expenses is not really significant despite the large increase of the heating demand because only pipes and substations costs are involved in the capital expenses for this scenario. Indeed, the 3 potential heating sources are assumed to be already available (like residual waste heating sources could be) such that there are no additional costs linked to the use of available extra heating capacity from these heating sources. This scenario obviously remains theoretical such that in practise, the use of available extra heating capacity could get an impact on the heating production cost for example. However, in this theoretical case, this factor is not included into the sensitivity analysis.

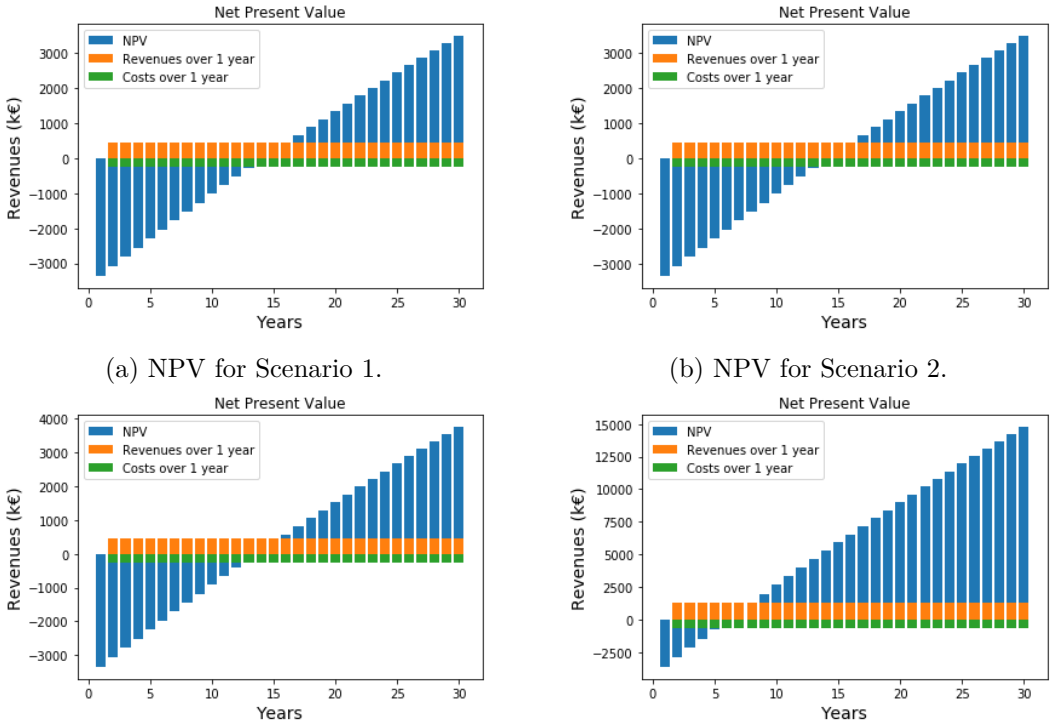

(a) NPV for Scenario 1.

(b) NPV for Scenario 2.

(c) NPV for Scenario 3.

(d) NPV for Scenario 4.

FIGURE 3.13: Net Present Value of the project for the 4 scenarios.

Comparing these 4 scenarios on their net present value over the investment period defined for the project, economic conclusions can also be drawn. An analysis of the variation of the return on investment period from the net present value can be achieved to show the influence of the heating demand profile on the profitability of a new heating network project. From Figure 3.13, it can be observed that for the first three scenarios defining eco-neighbourhoods with different heating demand profiles, there are no significant effect on the return on investment period. The shifting of a part of the total heating demand from residential dwellings to offices and the introduction of consumers with a non zero heating demand have a positive influence on the profits generated from the heating network. However, due to the small increase of profits generated with these solutions because of their relatively small heating consumption compared to poorly thermally insulated dwellings, heating networks remain profitable but have a period of return on investment around 12 years. The reduction of

the period of return on investment can be achieved with neighbourhoods made up of old dwellings whose heating consumption ensures large revenues for the stakeholders of the heating network. Indeed, for Scenario 4, the period of return on investment is only of 4 years which is quite lower than the period of return on investment for the first three scenarios.

This first study shows the importance of consistency of an energy policy for reducing the total primary energy consumption and its related greenhouse gases emissions in a specific geographic area. A deep retrofit of existing dwellings or the creation of new eco-neighbourhoods to get a stock of well-insulated dwellings obviously remains essential to decrease the total primary energy consumption of a neighbourhood and indirectly its total amount of CO_2 emissions. However, in cases of existing neighbourhoods made up of old dwellings and available waste heating sources with no capital expenses related to their buildings, the implementation of a heating network project using low-carbon heating technologies could be a temporary alternative solution to the refurbishment of dwellings for CO_2 savings. An analysis of the Net Present Value for heating networks with different heating demand profiles has shown the influence of the heating demand profile on the return on investment period of the project. Heating network projects relying on consumers with large and diversified heating demands are more profitable than heating networks into eco-neighbourhoods characterized by low and uniform heating demands.

Even though this first analysis tends for promoting third generation heating networks into neighbourhoods with poorly insulated dwellings, it is important to understand that this network solution remains a short-term solution for the heating sector partial decarbonization in a fast way to reach climate targets within the next few years. This is not sufficient for decreasing our CO_2 emissions in a global way such that the refurbishment of old dwellings into new well-insulated dwellings is also required to reach mid-term emissions targets. However, this refurbishment has to be achieved by the owners of the dwellings and is not always considered as a priority in a short-term period. Public fundings for technologies which can be installed in a short-term period can then be a temporary solution waiting for a refurbishment of the old dwellings. Moreover, even if a refurbishment stage is achieved after the implementation of a heating network project, the network remains viable and can even be extended for new dwellings in the surroundings which would be not yet connected to the network. The investment into a heating network may then be seen as a long-term solution which can be adapted from new heating demand profiles due to refurbishments.

In this section, the heating demand profile was studied as a first influence parameter on the design of the network prescribing all other user-defined parameters to fixed values. A parametric analysis of the influence of these different parameters can also be achieved to highlight the main design parameters to take into account in any new heating network project. Based on the real case study of the development of a heating network connecting a waste incinerator to a greenhouse and other dwellings, Scenario 3 is considered in the following sections.

3.3 Influence of the heating sales price r_{heat}

The heating sales price also influences the outline and the sizing of the prospective heating network such that it is important to set up a price which is fair and attractive for consumers in order to ensure a maximum connection rate to the network while remaining economically profitable. The main case study considered in the previous section relies on a heating sales price of 0.07€/kWh based on the mean gas price in the European Union. This heating sales price remains competitive but does not ensure attractiveness for heating consumers which are used with their current heating production means. The heating sales price is then considered as an input parameter of the decision tool and can be used for a sensitivity analysis on the outline and the sizing of the network. This heating sales price is generally estimated from market surveys asking people the price they are ready to pay for connecting to a heating network. The decision tool developed in this thesis can then study the influence of a reduction of the heating sales price on the heating network project for a prescribed neighbourhood. Considering a heating sales price decreasing from 0.07€/kWh to 0.04€/kWh for Scenario 3, economic results for the project lifetime of 30 years are drawn out in Table 3.4.

TABLE 3.4: Economic comparison of Senario 3 with a decrease of the heating sales price from 0.07€/kWh to 0.04€/kWh.

	r_{heat} = **0.07 €/kWh**	r_{heat} = **0.06 €/kWh**	r_{heat} = **0.05 €/kWh**	r_{heat} = **0.04 €/kWh**
Used heating capacity (MW_{th})	5.324	4.510	2.894	/
CAPEX (M€)	3.346	2.537	1.806	/
OPEX (M€)	7.180	6.037	4.118	/
Revenues (M€)	13.684	10.286	6.104	/
Profits (M€)	3.157	1.712	0.179	/
Return On Investment period ROI (years)	12	15	22	/

It can be observed that a decrease of the heating sales price significantly impacts the profits generated from the heating network project. Moreover, the main interesting result related to the decrease of the sales price stands in the outline of the optimized network. As illustrated in Figure 3.14, the decrease of the sales price implies a reduction of the number of connected streets to the built network. The streets remaining connected are the streets which are assessed to be economically profitable by the optimization model. These economically interesting streets are the streets with a large heating demand to ensure sufficient heating revenues compared to investment and operating costs. For example, the connection of the street between nodes v_{12} and v_{13} with a greenhouse as a heating consumer enables to offset the investment costs related to pipes and substations and the operating expenses for the heating production. Indeed, the network links the heating source at node v_1 to the street $v_{12}v_{13}$ despite the

additional heat losses and pumping power costs related to the heat transport through the network while some closer streets to the heating source are no longer connected. The decision tool aims for identifying these interesting consumers for a heating network project from an economic profitability point of view.

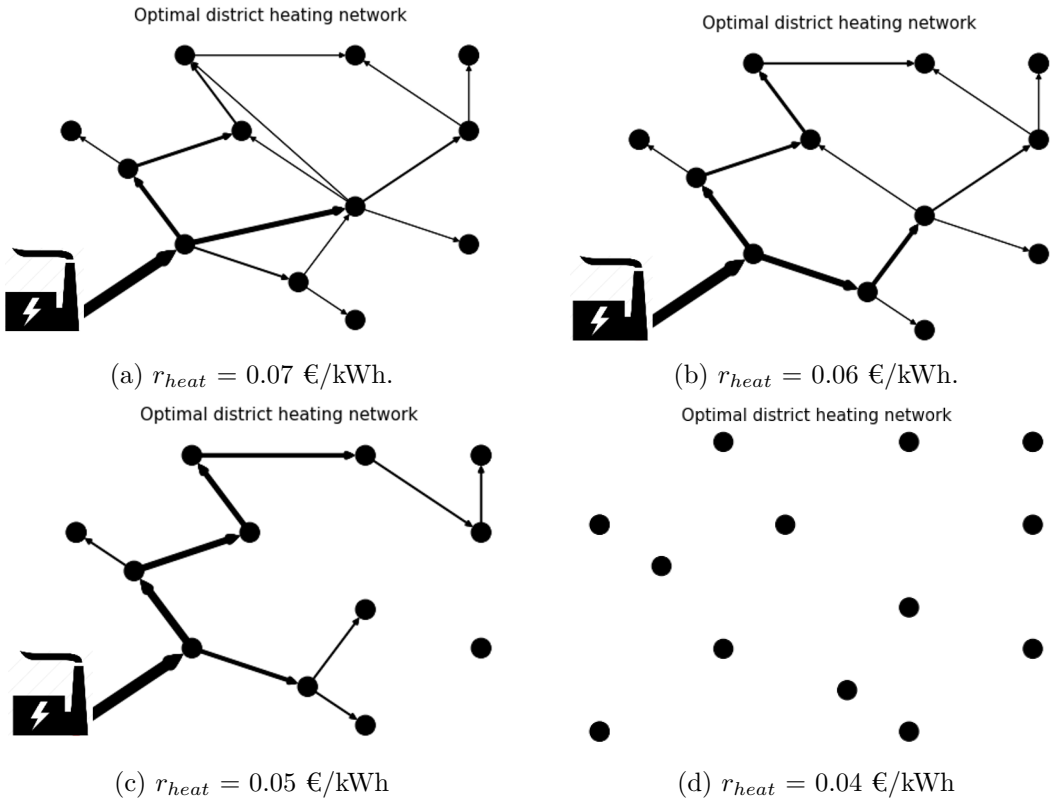

(a) $r_{heat} = 0.07$ €/kWh. (b) $r_{heat} = 0.06$ €/kWh.

(c) $r_{heat} = 0.05$ €/kWh (d) $r_{heat} = 0.04$ €/kWh

FIGURE 3.14: Outline of the heating network project with a decrease of the heating sales price from 0.07€/kWh to 0.04€/kWh.

This economic profitability can also be illustrated with the net present value of the heating network project and its return on investment period. This period increases with a reduction of the heating sales price until a critical sales price under which the period of return on investment becomes larger than the project lifetime. The heating network project becomes no more profitable such that no pipes are built. Figure 3.15 shows that for a competitive heating sales price of 0.07€/kWh, a return on investment period around 12 years is assessed and remains acceptable for the development of a heating network project. A decrease of the heating sales price reduces the number of streets connected while also extending the return on investment period to 15 years for a heating sales price of 0.06€/kWh and more than 22 years for a heating sales price of 0.05€/kWh. This highlights the importance to choose adequately the heating sales price to satisfy heating consumers with a sufficiently competitive heating price and to guarantee to the potential stakeholders of the project a sufficiently short return on investment period. This heating sales price given as an input parameter by the user of the decision tool can be assessed by market surveys dedicated to the

potential future customers of the network.

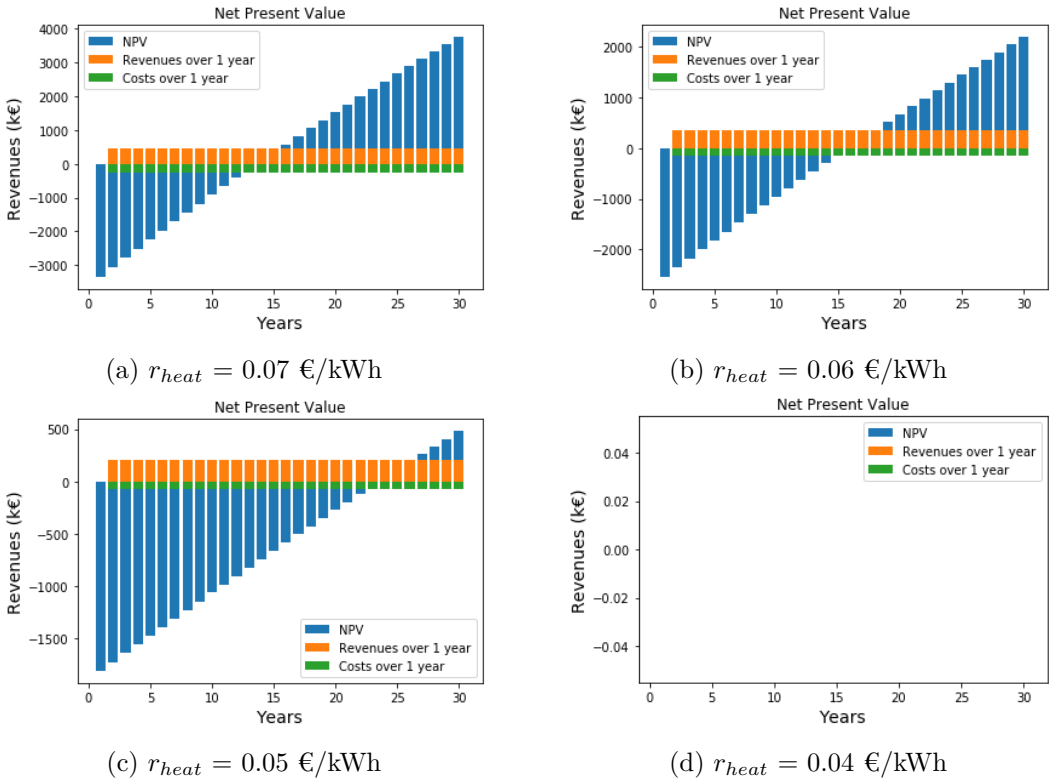

(a) $r_{heat} = 0.07$ €/kWh

(b) $r_{heat} = 0.06$ €/kWh

(c) $r_{heat} = 0.05$ €/kWh

(d) $r_{heat} = 0.04$ €/kWh

FIGURE 3.15: Net Present Value of the heating network project with a decrease of the heating sales price.

As previously explained in Section 2.3.3.1, the connection rate p_j of heating consumers to an edge j of the network is indirectly linked to the heating sales price proposed to the consumers. Indeed, consumers can arbitrarily choose to be connected or not to a new heating network passing through their street. One of the main criteria decision relies on the proposed heating sales price which is assessed to be sufficiently competitive for the consumer to connect to the network or not. In the next section, the influence of this connection rate parameter is studied to show its consequences on the outline and the sizing of the network project.

3.4 Influence of the connection rate p_j

As for the study of the influence of the heating sales price, a gradual reduction of the connection rate is achieved for the assessment of the optimal outline and sizing with different values of this parameter. The reduction of the connection rate parameter decreases the amount of sold heat to the consumers implying a decrease of the total revenues useful to refund the initial capital expenses for building the network. This connection rate can be estimated for each street independently based on a market study among heating consumers even though this connection rate remains generally a partial unknown during the design of the

network. In this thesis, an identical connection rate for each edge j of the graph is considered.

TABLE 3.5: Economic comparison of Scenario 3 with a decrease of the connection rate from 100% to 40%.

	p_j = **100%**	p_j = **80%**	p_j = **60%**	p_j = **40%**
Used heating capacity (MW_{th})	5.324	3.519	2.364	/
CAPEX (M€)	3.346	2.708	2.462	/
OPEX (M€)	7.180	5.072	3.430	/
Revenues (M€)	13.684	9.598	6.400	/
Profits (M€)	3.157	1.817	0.507	/
Return On Investment period ROI (years)	12	15	18	/

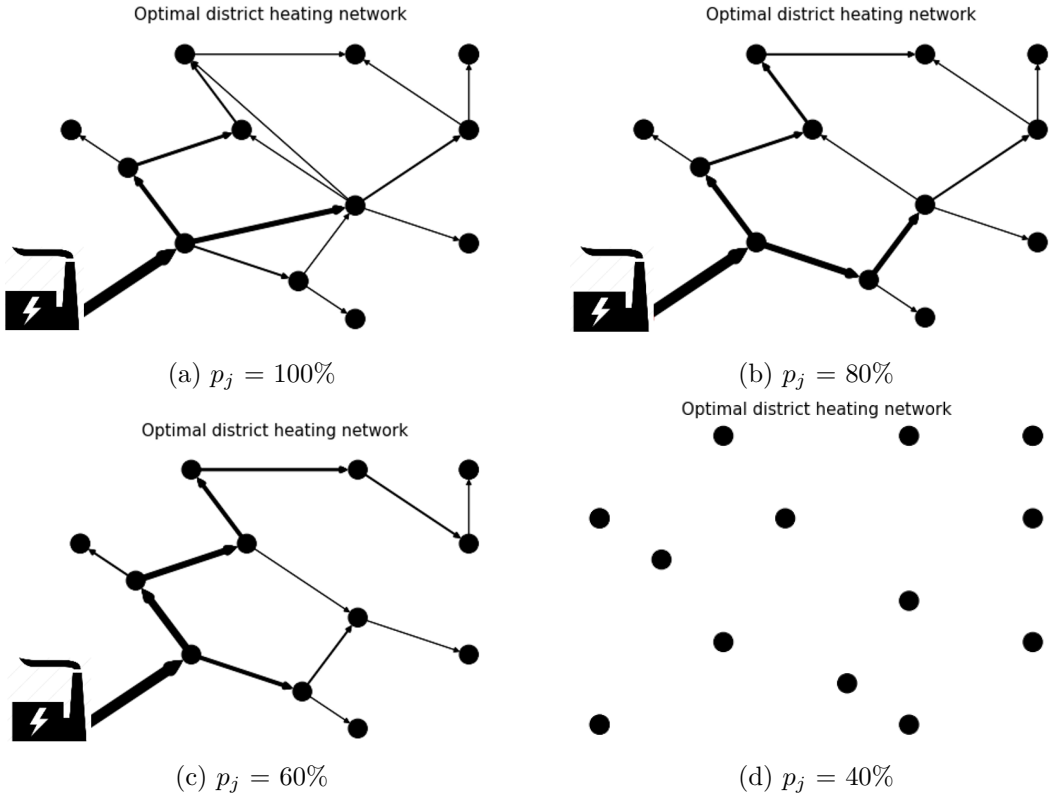

(a) $p_j = 100\%$ (b) $p_j = 80\%$

(c) $p_j = 60\%$ (d) $p_j = 40\%$

FIGURE 3.16: Outline of the heating network project with a decrease of the connection rate.

As illustrated in Figure 3.16, the optimization model determines the interesting streets to connect for a prescribed connection rate. It can be noticed that some streets fed by the network and requiring large diameters for a prescribed connection rate are no longer connected with a small change of a parameter like the connection rate. Observing the street linking node v_4 and v_9, this street represents a main pipe of the network with $p_j = 100\%$

because it feeds a large part of the whole network. However, a decrease of this connection rate from 100% to 80% modifies the outline of the network such that this street is no longer chosen to be part of the network. Streets v_4v_3 and v_4v_7 are thus chosen alternatively as main lines to feed the rest of the network.

The decision tool is thus able to assess for each street the economic profitability due to the generation of revenues compared to the capital and operating expenses required to feed the street. This trend can also be observed with a decrease of the heating sales price (cf. Figure 3.14). This is justified by the fact that the heating consumption density of the street v_4v_9 is lower than for streets v_4v_3 and v_4v_7 implying more capital expenses for a prescribed heating amount.

As for the heating sales price, the decrease of the connection rate impacts the return on investment period increasing from 12 years to 18 years (cf. Figure 3.17) . This parameter gets a lower influence than the heating sales price on the increase of this return on investment period even if it has to be taken into account during a pre-study of the economic profitability not to underestimate this period of return on investment.

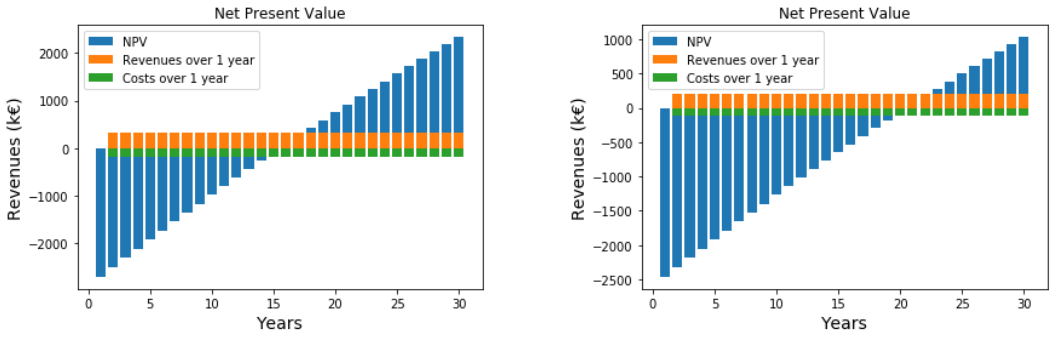

(a) $p_j = 80\%$ (b) $p_j = 60\%$

FIGURE 3.17: Net Present Value of the heating network project for Scenario 3 with a decrease of the connection rate.

The heating sales price and the connection rate are two parameters getting a direct impact on the revenues generated from heating sales. Other parameters, like the actualization rate, get rather an influence on the expenditures linked to the network. An increase of the actualization rate leads to higher interests to pay to the stakeholders of the heating network project.

3.5 Influence of the actualization rate a

As explained in Section 2.3.4, the actualization rate aims for taking into account the value of money over time and is dependent on the borrowing rates of the market and the return on equity expected by the stakeholders of the project. Stakeholders can come from various backgrounds in district heating networks projects such that investments forms from one district heating project to another can be very different. Financial organisations or individuals can

invest in this type of project by ensuring a given return on investment in the medium or long term while helping to finance the initial expenditures of these projects. This return on investment is indirectly defined by the actualization rate.

TABLE 3.6: Economic comparison with for different actualization rates.

	$a = \mathbf{1}\%$	$a = \mathbf{1.5}\%$	$a = \mathbf{2}\%$	$a = \mathbf{2.5}\%$
Used heating capacity (MW_{th})	5.324	4.384	3.733	/
CAPEX (M€)	3.346	3.168	3.370	/
OPEX (M€)	7.180	6.766	6.440	/
Revenues (M€)	13.684	12.001	10.600	/
Profits (M€)	3.157	2.066	0.790	/
Return On Investment period ROI (years)	12	13	15	/

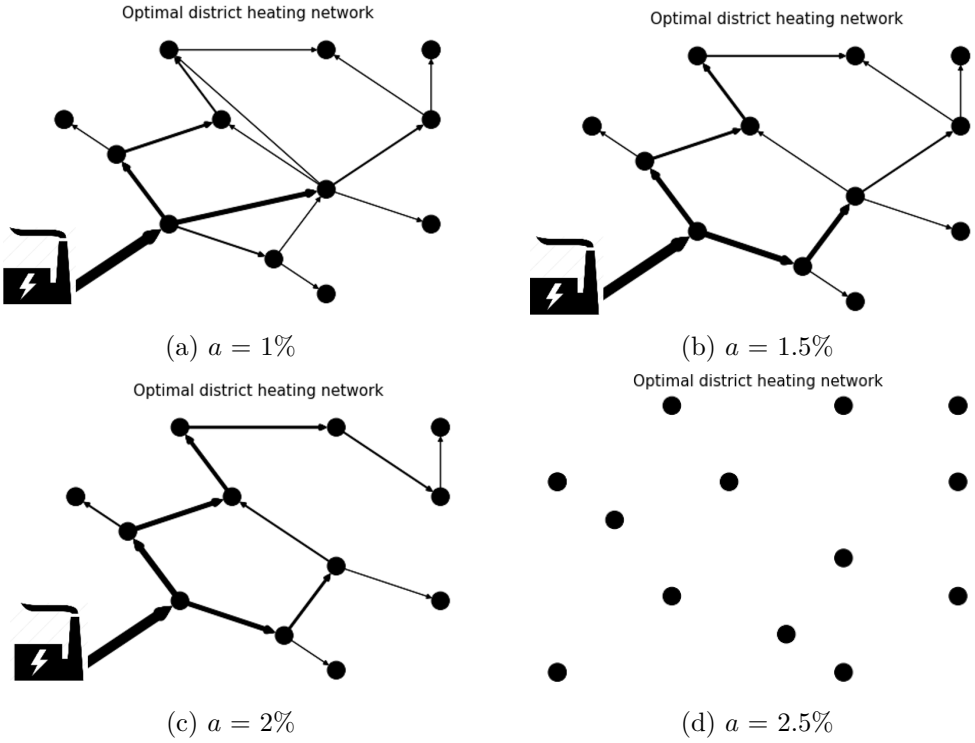

(a) $a = 1\%$ (b) $a = 1.5\%$

(c) $a = 2\%$ (d) $a = 2.5\%$

FIGURE 3.18: Outline of the network for different actualization rates.

An increase by steps of 0.5% of the actualization rate leads to a decrease of the profits until a critical value of $a = 2.5\%$ of the actualization rate above which it is no longer profitable to build a heating network for the studied scenario. Figure 3.18 illustrates this trend by highlighting the decrease of the number of streets connected with a small increase of the actualization rate until the critical value of 2.5% for which the heating network project is no more profitable. The significant influence of the actualization rate on the economic profitability of the

project can also be illustrated with Table 3.7. A small increase of the actualization rate gives a small increase of the period of return on investment from 12 to 15 years until a 2.5% critical value of the actualization rate for which there is no optimal heating network solution to build for the prescribed neighbourhood.

Regarding the slight increase of the period of return on investment with a small increase of the actualization rate, this sudden economic unprofitability switching from an actualization rate of 2% to 2.5% could seem surprising without getting any intermediate optimal heating network solution. Actually, as illustrated in Figure 3.19, the exponential increase of the actualization factors f_{CAPEX} and f_{OPEX} involves a quick fluctuation of the net present value of a heating network project. A small increase of the actualization rate can lead to a non profitable heating network project. With a zero actualization rate, the CAPEX and OPEX actualization factors are respectively equal to 1 and the project lifetime N_{years} (30 years). However, an increase of the actualization rate can result to quite larger investment costs getting an impact on the outline and the sizing of the network. It is thus important to define as accurately as possible this actualization rate by a detailed business plan listing all the investors linked to the project and to compute their expected return on equity or the borrowing rate at which they are lending money. Fundings forms (public or private) used for financing the network can play a key role in the value of the actualization rate and therefore on the profitability of a heating network project.

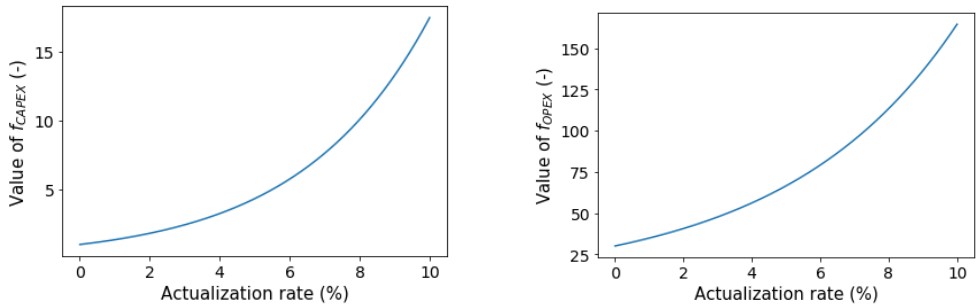

(a) CAPEX actualization factor.

(b) OPEX actualization factor.

FIGURE 3.19: CAPEX and OPEX actualization factors.

3.6 Influence of the limited pipe diameters into the streets

The building of heating networks requires the installation of pipes into the ground such that the installation of these pipes can be constrained in some streets where the space is limited because of the existing gas and telecommunication pipes into the ground. This constraint limiting the diameter of a pipe into a network can be linked to the maximum power flow allowed into a pipe as explained in Section 2.3.3.1. Setting up an additional constraint prescribing no space into the ground of the street on edges e_6 and e_{22} (cf. Figure 2.6) linking nodes v_4 and v_9 (i.e., $\dot{P}_6^{lim} = 0$ and $\dot{P}_{22}^{lim} = 0$), the optimization model can provide a new optimal

solution for Scenario 3. Even though this constraint is considered in a theoretical way in this scenario, this constraint can be defined in practise for each street based on available data from underground maps. However, these kinds of data are generally missing for heating network projects because of the poor mapping of the underground.

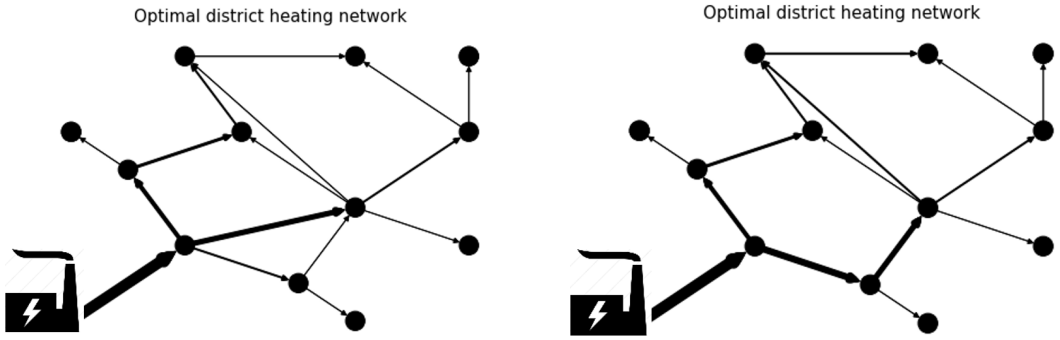

(a) Without limited diameters (b) With limited diameters

FIGURE 3.20: Outline of the heating network project with a zero diameter constraint at edges e_6 and e_{22}.

This optimal solution changes the outline of the network by not building a pipe between the nodes v_4 and v_9. The water flows through the edges linking nodes v_4-v_3 and v_4-v_7. The non-building of the pipe between v_4 and v_9 which was profitable to build in the reference scenario implies a decrease of the profits generated from the network and also a decrease of the total used heating capacity. Capital expenditures are also lower with this constraint because of the pipe and this related substation between nodes v_4 and v_9 are not built. However, the savings of capital and operating expenses being lower than the losses of heating sales revenues implies a lower total net cash flow with this constraint on the limitation of pipes diameters.

TABLE 3.7: Economic comparison of Scenario 3 with a limitation on the pipes diameters linking nodes v_4 and v_9.

	Without limited diameters on e_6 and e_{22}	**With limited diameters on e_6 and e_{22}**
Used heating capacity (MW_{th})	5.324	4.869
CAPEX (M€)	3.346	3.102
OPEX (M€)	7.180	6.824
Revenues (M€)	13.684	13.022
Profits (M€)	3.157	3.095

3.7 Influence of the limited thermal capacities at the heating power plants

The previous case studies consider available heating sources with a sufficient capacity to feed the whole neighbourhood. However, the capacity of available heating sources is generally limited such that the use of a unique heating source is not always sufficient to satisfy the whole heating demand. The decision tool presented in this thesis also aims to select the optimal heating sources and capacities to use or install to maximize the net cash flow of the project. Considering from Scenario 3 a decrease of the heating capacities of the 3 available existing power plants from 10 MW_{th} to 2.5 MW_{th} (less than the maximum heating demand over the neighbourhood which is of 5.253 MWh_{th}), the assessment of the potential optimal network leads to a new outline and sizing of the network.

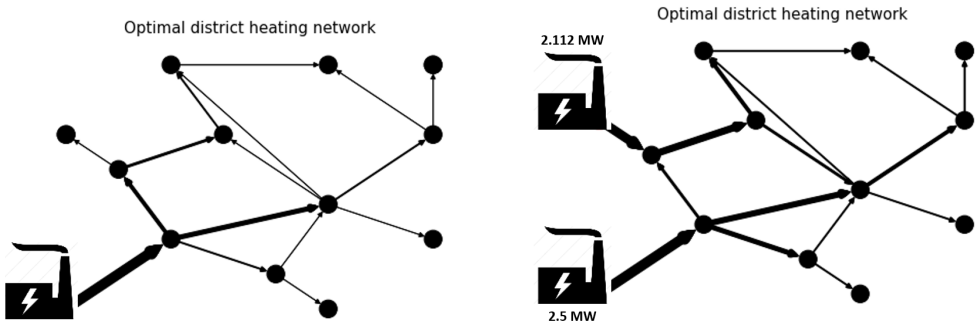

(a) Without limited thermal capacity (b) With limited thermal capacity

FIGURE 3.21: Outline of the heating network project with a limitation on the heating capacity.

The limitation on the heating capacity at node v_1 requires the use of an additional heating source and new pipes to link this heating source to the network. The second available cheapest heating source is located at node v_2 and is used to satisfy the required additional heating demand to feed the whole network. It can be noticed that the maximum heating demand (5.253 MWh_{th}) would require the use of the 3 heating plants to feed the whole demand of the network due to the limitation of the capacity of each plant to 2.5 MW_{th}. However, regarding the heating consumption profile of the Scenario 3 (cf. Figure 3.2), this maximum heating demand occurs only one hour over the whole year. Therefore, the supply of this peak demand would require the building of a new pipe connecting the heating source at node v_{13} to the rest of the network only for the heating sales over one hour of the year. The building of this potential pipe is assessed to be non profitable to recover the additional capital expenses linked to the building of this potential pipe by selling heat only for this peak demand period.

Regarding the total expenses, the operating costs increase with the use of a second heating source more expensive than the first one. Capital expenses also slightly increase because of the use of larger pipe diameters related to the use of two heating sources at two different locations of the network. The use

TABLE 3.8: Economic comparison with a limitation on heating capacity of 2.5 MW_{th} at each power plant.

	Without limitation on heating capacity	**With limitation on heating capacity**
Used heating capacity (MW_{th})	5.324	$\begin{cases} 2.500 \text{ @ node } v_1 \\ 2.112 \text{ @ node } v_2 \end{cases}$
CAPEX (M€)	3.346	3.378
OPEX (M€)	7.180	7.411
Revenues (M€)	13.684	13.651
Profits (M€)	3.157	2.860

of multiple heating sources influences the direction of the pipes and the choice of their diameters to build the network because of the different repartition of the power flows into it. As observed in Figure 3.21, for the scenario with limited heating capacities at the heating plants, the 2 pipes linking edges v_2v_3 and v_6v_9 get their direction reversed due to the use of the additional heating source at node v_2. Moreover, the pipes near the second heating plant get bigger diameters because of the larger power flows passing through the pipes near this second heating plant. Indeed, it can be seen from Figure 3.22 that two pipes with a diameter of 25mm have been replaced by two bigger pipes with respective diameters of 50mm and 80mm due to the larger heating power flows passing through theses pipes.

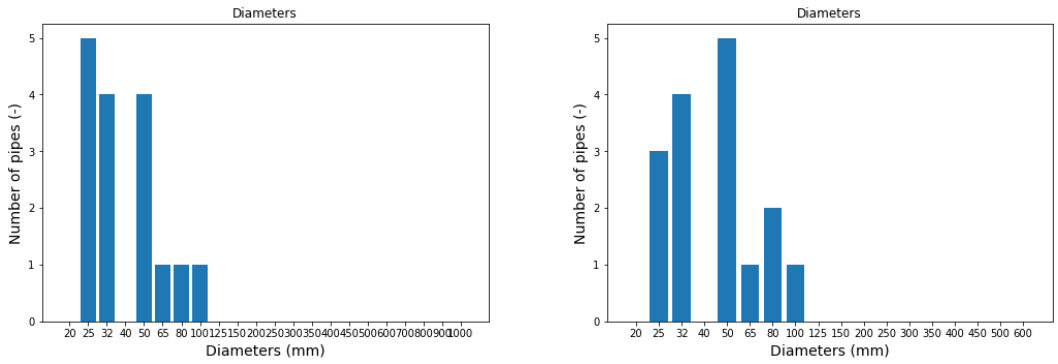

(a) Without limited thermal capacity (b) With limited thermal capacity

FIGURE 3.22: Repartition of the diameters with a limitation on the heating capacity.

This scenario illustrates that the decision tool always tries to select the most adequate available heating sources for minimizing the heating production costs and their related costs (heat losses and pumping power costs). In this scenario, it is shown that the 2 most remote heating production units are used because they are the cheapest available heating sources. The optimization model could have chosen the closest heating production unit to the biggest heating consumer of the network (the greenhouse) to minimize heat losses and required pumping power. However, this solution is not assessed as the optimal one because these two factors implying additional costs remain cheaper than the use of the most expensive available heating source.

3.8 Influence of the selection of the representative days on the optimal solution and the computation time

The optimization model used in the previous sections is based on hourly heating demand profiles in order to represent as accurately as possible the real behaviour of the system. However, the use of a big number of timesteps can quickly lead to a large amount of optimization variables leading to a complex optimization problem to solve. For the optimization of energy systems, as explained in Section 2.2, a pre-processing is generally applied to heating consumption data to decrease the number of timesteps of the optimization problem. In this section, a comparison of the solutions given by an optimization based on the whole heating demand dataset and on a reduced dataset based on the optimal selection of representative periods is achieved in order to show the usefulness to select representative periods for optimization processes.

TABLE 3.9: Comparison of the model with 8760H and 144H.

	With 8760H	**With 144H**
Installed heating capacity (MW_{th})	5.324	5.200
CAPEX (M€)	3.346	3.340
OPEX (M€)	7.180	7.106
Revenues (M€)	13.684	13.497
Profits (M€)	3.157	3.051
Computation time	34 511 s ≈ 9.5h	91s ≈ 1 min 30
Number of variables	2 128 799	35 111

Choosing a tolerance criteria of 0.01% between the primal and the dual bound of the branch-and-bound algorithm, the running of the 2 optimization problems based on the reference Scenario 3 with respectively 8760 timesteps and 144 timesteps gives the results shown in Table 3.9. These results are rather similar in both cases even though the peak heating demand is a little bit underestimated with the selection of representative periods. Moreover, the reduction of the number of timesteps by a factor 60 leads to a reduction of the computation time by a factor of 380 such that the reduction of the number of timesteps can clearly speed up the optimization process without lacking of accuracy about the optimal solution. Indeed, comparing profits generated in both cases from Table 3.9, the relative error between the optimization with a real year and a representative year is assessed to be around only 3.5%. This small relative error is fair compared to the computation time savings achieved using a representative year for the optimization process. For the following scenarios integrating thermal storage solutions and alternative heating sources, an optimization model with a reduced number of timesteps is then used to reach an optimal solution in a feasible time.

3.9 Integration of thermal storages solutions

Previous test cases are based on existing heating sources with constant heating production costs defined by zero capital expenses. The building of new additional heating sources or thermal storage solutions has not been considered. The use of a thermal storage to eventually shift the heating production from one period to another can be useful in some heating network projects in order to reduce global expenses and increase the economic profitability of the project. Therefore, new case studies adding potential thermal storages to build are achieved in this section by defining an available building surface of 1 000 m^2 for a new thermal storage or heating plant next to the three heating sources at nodes v_1, v_2 and v_{13}.

Including the potential of thermal storage solutions into the Scenario 3 defined in Section 3.2, the optimization model provides the same solution than for the initial case study. The integration of thermal storages into the network is then assessed to be non profitable for this case study. The building of a new storage and the required pipes to connect the storage to the network are indeed additional costs which have to be counterbalanced by a decrease of the initial capital and operating expenses to be profitable. The zero capital expenses linked to the existing heating plants and the constant heating production costs of these plants imply that thermal storages do not provide economic benefits compared to the additional costs related to these solutions for this case study. The available heating capacity is sufficient and free of capital expenses such that there are no requirements to adapt the total installed capacity. Moreover, the shifting of the heating production from one period to another is not justified in this case because the heating production cost is constant all over the year. Therefore, this thesis provides a non-exhaustive list of situations for which thermal storage solutions could bring economic benefits to the network. Four main goals of storage solutions into heating networks are identified as follows:

1. Increase the total available heating capacity over the network from the limited heating capacity of the prescribed available heating sources. Without thermal storages, the total heating capacity over the network is limited by the maximum heating capacity of the heating sources which can be insufficient to feed the whole heating demand of the network during peak periods. On the other hand, due to the large fluctuation of the heating demand over the year, there are some time periods during which the heating capacity is under-exploited because of low heating demands compared to the available heating capacity. During these periods, the loading of a thermal storage could be useful to use this under-exploited thermal capacity to shift the heating production for next periods when the heating demand becomes bigger.

2. Adapt the heating production planning to minimize the production costs by shifting a part of the heating production from one period to another. In the case of heat pumps, for example, the heating production costs are very variable from one period to another because of its reliance on the electricity

price and the weather conditions influencing the coefficient of performance of the heat pump. Thermal storages can be economically interesting for scenarios based on heating plants with variable production costs. With these scenarios, these thermal storages can be filled in during periods with low heating production costs and emptied during periods with larger heating production costs. These thermal storages are appropriate with intermittent energy sources whose heating production costs are generally variable.

3. Adjust the heating production as a function of the available heating capacity. With intermittent energy sources like solar energy, the heating capacity can be variable from one period to another such that capacity factors have to take into account this availability of the installed heating capacity. For scenarios with a variable limited heating capacity like solar collectors for example, thermal storages can be filled in during periods with large capacity factors enabling to produce a large amount of heat from solar collectors and emptied during periods with a limitation on the heating capacity such that there is not enough heating capacity during this period to supply the heating demand only with the solar collectors.

4. Undersize the heating capacity of new heating plants to build in order to reduce the initial investments costs by adding thermal storages at some locations into the network. The inclusion of thermal storages enables to build heating plants with smaller capacities while remaining able to feed the heating demand all over the year thanks to an adequate regulation between the heating production sources and the thermal storages. The heating production sources can then produce heat more constantly over the year with larger heating production amounts during low heating demand periods such that a part of the heating production is stored into thermal storages. Conversely, during high heating demand periods, the part of the heating demand which can not be satisfied by the insufficient heating plant capacity can then be fed by the thermal storage.

These four situations are considered from a theoretical point of view in the following by studying new test cases taking into account these limitations on the outline and the sizing of a new heating network project without or with thermal storage solutions. The following sections aim for highlighting the benefits of thermal storages into some specific cases and to illustrate the utility of the decision tool presented in Chapter 2 to provide an optimal solution taking into account the variation of the heating demand. These test cases are artificially created to depict for each of them the utility of the decision tool developed in this thesis. All these scenarios could be mixed up in a unique scenario considering all the heating technologies mentioned in the following. However, this unique scenario would be more difficult for understanding the results obtained from the decision tool. Theoretical case studies in the following therefore aim for depicting the contribution of the decision tool to study the integration of thermal storage solutions into a network for different scenarios.

3.9.1 Limitation on the heating capacity

Existing heating sources are useful for district heating networks because they do not require capital expenses for the building of new plants such that some money savings can be achieved into the heating project increasing the profitability of the project. The main problem with existing heating sources is that they have not been sized to satisfy the whole heating demand of a heating network. Therefore, some streets could be considered as non-profitable to connect to a heating network because of this limited available heating capacity. The building of thermal storages could then increase the number of streets which could be connected to a new network.

Considering two new test cases starting from the optimal solution found for the initial scenario in Section 3.7 with a prospective heating source only at node v_1, the benefits of the use of a thermal storage can be drawn out in the following. For the first new test case, the maximum heating capacity of the heating source at node v_1 is decreased from 10 MW_{th} to 2.5 MW_{th} and an additional building surface of 1 000 m^2 is considered as available at this node to build a potential storage next to the heating source. A comparison of both scenarios without and with storage gives the results illustrated in Table 3.10 and Figure 3.23.

TABLE 3.10: Comparison for a limited heating capacity of 2.5 MW_{th}.

	Without storage	**With storage**
Used or installed heating capacity (MW_{th} or MWh_{th})	2.500	2.500 of heating capacity @ node v_1 17.712 of thermal storage @ node v_1
CAPEX (M€)	2.969	3.431
OPEX (M€)	6.452	7.062
Revenues (M€)	12.279	13.400
Profits (M€)	2.858	2.907

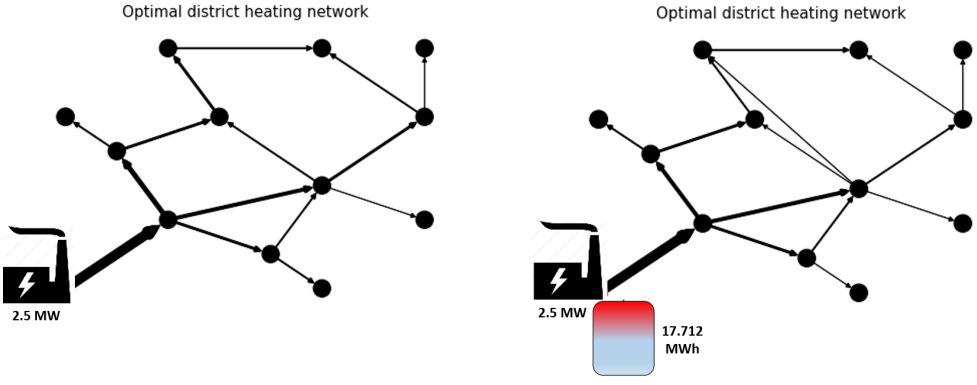

(a) Outline without limited thermal capacity

(b) Outline with limited thermal capacity

FIGURE 3.23: Influence of the thermal storage on the outline of the heating network project with a limitation on the heating capacity of 2.5 MW_{th}

The additional available surface of 1 000 m^2 at node v_1 prescribing a maximum thermal capacity of 175MWh_{th} for the storage leads to the use of a part of this surface for the building of a storage with a thermal capacity of 17.712 MWh_{th}. The building of this new thermal storage leads to an increase of 462,000 € of the capital expenses due to the building of the storage and the additional required pipes to connect it to the network. The operating costs also increase due to the additional heating production to load the storage during periods of low heating demand although the increase of these costs are offset by the additional revenues from heating sales. The total increase of revenues being slightly bigger than the increase of the costs due to the use of an additional thermal storage, the optimal solution includes then a thermal storage to raise more profits from the heating network project.

Comparing the outlines of the network without and with thermal storage, it can be noticed from Figure 3.23 that without thermal storage, the street linking nodes v_5 and v_9 is not connected to the network. The inclusion of a thermal storage solution enables to connect this street and to increase heating sales revenues. The increase of revenues being slightly bigger than the increase of additional costs, the building of a thermal storage generates an additional profit of 49 000 €. The benefits of the building of a new thermal storage can be shown comparing the loading and unloading phases of the storage with the variation of the heating demand.

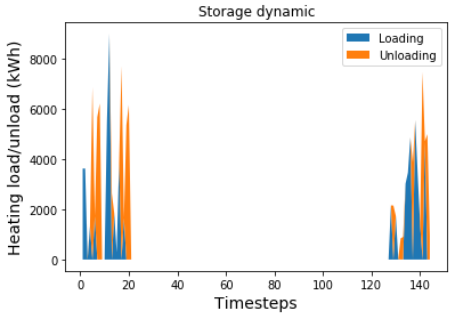

(a) Loading and unloading of the storage during the whole year

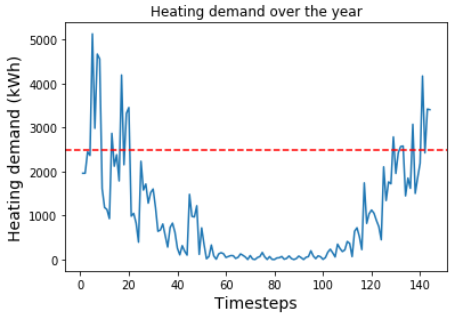

(b) Heating demand over the whole year

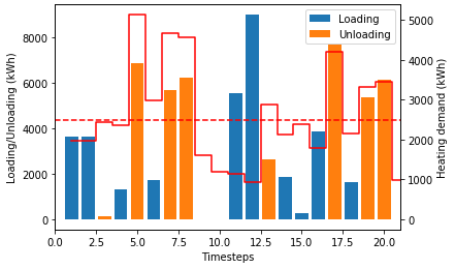

(c) Loading and unloading of the storage during the beginning of the year

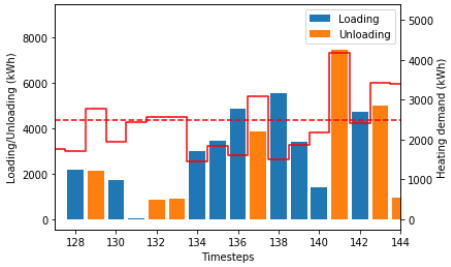

(d) Loading and unloading of the storage during the end of the year

FIGURE 3.24: Loading and unloading of the thermal storage compared to the heating demand of the network with a limited capacity of 2.5 MW_{th}.

It can be observed from Figure 3.24 that the loading and unloading of the storage are carried out only at the beginning and the end of the year

during periods with higher heating demands than the available heating capacity. Looking more into details about the dynamics of the storage during these 2 periods, it can be illustrated that the unloading phases of the storage always operate during periods of higher heating demands compared to the available capacity of the heating source. The dynamics of the storage follows the level of the heating demand over the network in order to be able to supply at each period of the year as much as heat as possible while remaining economically interesting.

A second test case with a lower maximum heating capacity at node v_1 is defined to analyze the influence of the maximum heating capacity on the sizing of the heating network and the thermal storage units. The maximum heating capacity of the heating source at node v_1 is decreased from 2.5 MW_{th} to 1.25 MW_{th} while always considering an additional building surface of 1 000 m^2 at this node. New results obtained for this scenario are drawn out in Table 3.11 and the outline of the new network is exhibited in Figure 3.25 for both cases.

TABLE 3.11: Economic comparison for a limited heating capacity of 1.25 MW_{th}.

	Without storage	**With storage**
Used or installed heating capacity (MW_{th} or MWh_{th})	1.250	1.250 of heating capacity @ node v_1 4.688 of thermal storage @ node v_1
CAPEX (M€)	1.848	1.922
OPEX (M€)	4.159	4.276
Revenues (M€)	7.938	8.166
Profits (M€)	1.931	1.968

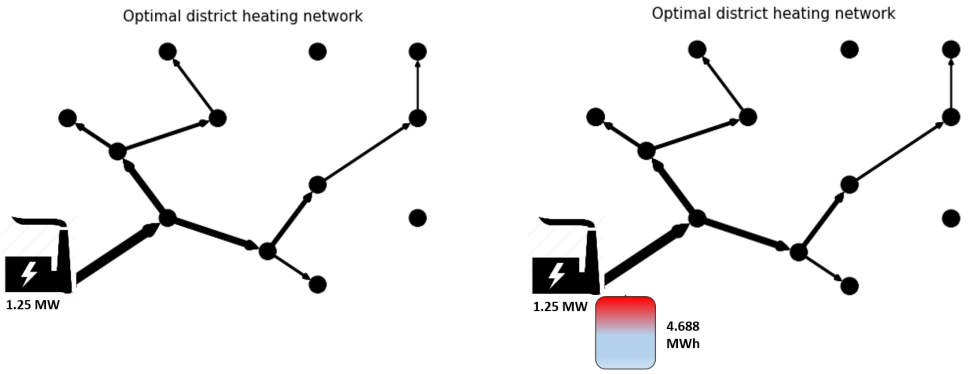

(a) Outline without limited thermal capacity

(b) Outline with limited thermal capacity

FIGURE 3.25: Influence of the thermal storage on the outline of the heating network project with a limitation on the heating capacity of 1.25 MW_{th}.

The decrease of the maximum heating capacity has a significant influence on the outline whether a thermal storage solution is used or not. Indeed, the thermal storage solution can slightly increase the heating production and indirectly the

revenues from the additional heating sales. However, this thermal storage implies additional costs which reduces the margin made on profits. The optimization model is useful to find a trade-off between the thermal storage capacity to install and the additional costs that are linked to this storage in order to design the optimal heating network. As for the previous case study, the capital and operating costs increase with the use of an additional storage but are counterbalanced by the increase of revenues thanks to the additional heating sales. It results in a profit gain around 37,000 € compared to the solution without storage.

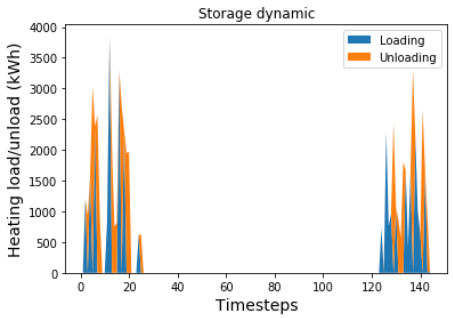

(a) Loading and unloading of the storage during the whole year

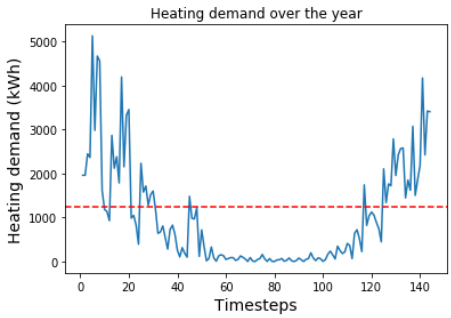

(b) Heating demand over the whole year

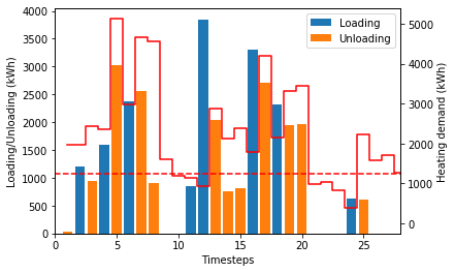

(c) Loading and unloading of the storage during the beginning of the year

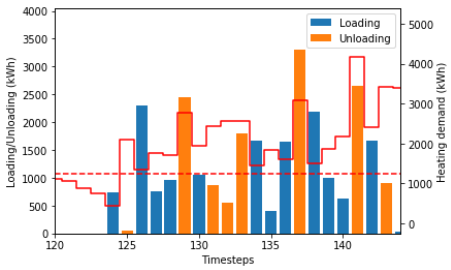

(d) Loading and unloading of the storage during the end of the year

FIGURE 3.26: Loading and unloading of the thermal storage compared to the heating demand of the network with a limted capacity of 1.25 MW_{th}.

The dynamics of the storage follows the same trend than for the previous case with loading phases of the storage during periods of low heating demands while the storage is unloaded during periods of high heating demand. It can be noticed from Figure 3.26 that the storage is loaded during some periods even though the heating demand is higher than the installed available heating capacity. This is justified by the fact that the limited heating capacity can not provide the whole heating demand over some streets of the network during some time periods. The optimal strategy consists then to load the storage during these periods of insufficient capacity without feeding some streets of the network to be able to supply the whole heating demand over the streets during the next periods.

It is important to notice that even though the optimization formulation presented in Chapter 2 allows to determine which pipes have to be built for a heating network project, it does not imply that built pipes will be used at any timestep if it is assessed to be non profitable by the decision tool. Feeding some streets

during some time periods is assessed to be non profitable with thermal storages because it is more profitable to load the thermal storage if the heating capacity is insufficient to feed the whole network and to use the total heating capacity (including thermal storages) during the next time periods to provide heat to the whole network. In these test cases, the penalty cost c^{pen} for not providing heat to heating consumers has not been taken into account such that it can be profitable to do not feed a street during some time periods. However, as explained and formulated in Section 2.3.4.3, this additional penalty cost can be easily accounted for in the formulation if it is required.

3.9.2 Variable heating production costs using heat pumps

Previous scenarios consider heating sources with a constant heating production cost without any available surface for the building of a new heating source or a thermal storage. The introduction of new heating sources with variable heating production costs over the year, like heat pumps for example, can significantly affect the outline and the sizing of the heating network. Heat pumps use electricity from the network which has a variable cost over the year and the heating production cost with a heat pump is also dependent on its variable coefficient of performance linked to weather conditions. The benefits of thermal storage units to produce and store heat when heating production costs are low can be assessed with the optimization formulation addressed in this thesis.

Considering now that the heating source at node v_1 is replaced by existing heat pumps with a limited capacity of 10 MW_{th} and by a potential thermal storage with a limited storage capacity of 175 MWh_{th} (based on an available surface A_{avail} of 1 000 m^2), new optimal solutions can be computed for this scenario. Considering a case without and with thermal storage using only an existing heat pump and a prospective thermal storage at node v_1, the optimal outline and sizing defined by the decision tool is given in Figure 3.27.

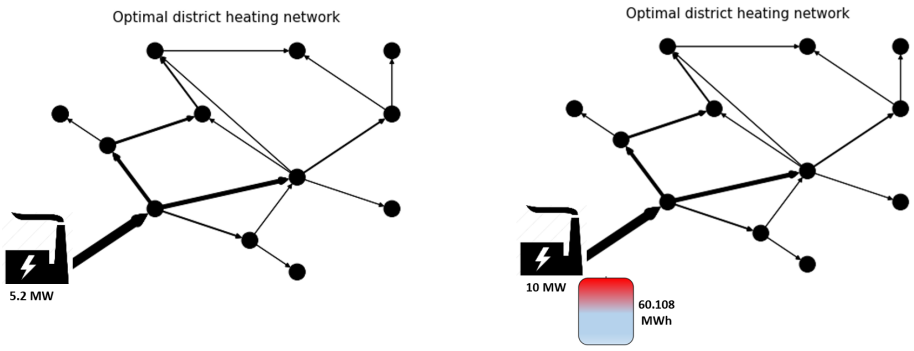

(a) Without storage (b) With storage

FIGURE 3.27: Outline of the heating network project for a scenario with a heat pump capacity of 10 MW_{th}.

The use of an additional storage increases the used heating capacity of the heat pumps in order to load the storage during economically interesting periods.

TABLE 3.12: Economic comparison with 10 MW_{th} heat pumps and a thermal storage.

	Heat pumps without storage	**Heat pumps with storage**
Used or installed heating capacity (MW_{th} or MWh_{th})	5.200	$\begin{cases} 10 \text{ of heat pumps @ node } v_1 \\ 60.108 \text{ of thermal storage @ node } v_1 \end{cases}$
CAPEX (M€)	3.340	3.490
OPEX (M€)	7.744	6.249
Revenues (M€)	13.497	13.497
Profits (M€)	2.413	3.758

Because of the zero capital expenses linked to existing heat pumps, the used heating capacity is only limited by the maximum available heating capacity. For the solution including a thermal storage, the maximum capacity of heat pumps is then used to produce as much heat as possible during low heating production costs periods. Even though the building of the new storage implies additional capital expenses, these expenses are counter-balanced by a large reduction of the operating expenses thanks to the use of heat pumps during periods of low heating production costs while the thermal storage is unloaded during periods of higher heating production costs.

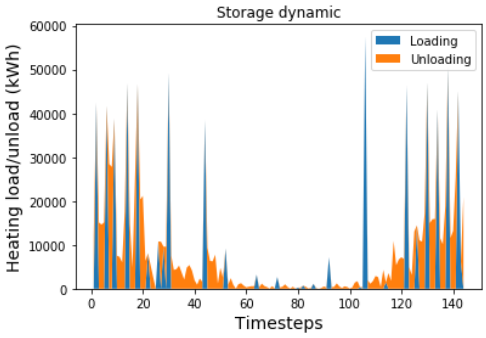

(a) Loading/Unloading of the storage

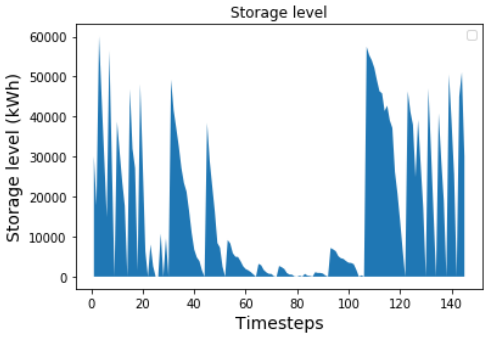

(b) Energy level of the storage

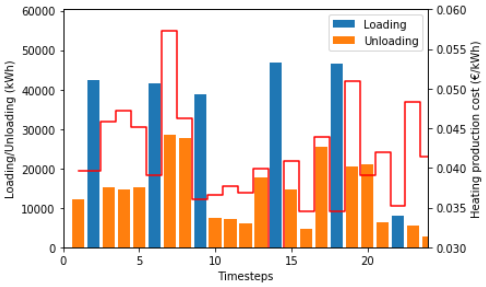

(c) Loading/Unloading of the storage during the beginning of the year

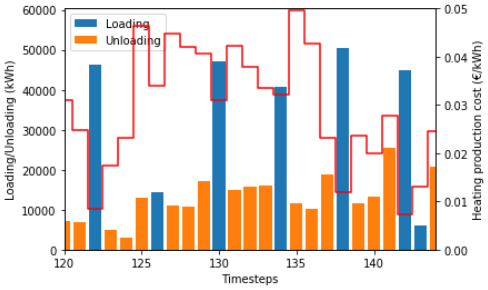

(d) Loading/Unloading of the storage during the end of the year

FIGURE 3.28: Link between the levels of the thermal storage and the heating production costs.

The optimal operating strategy to minimize these production costs can be observed by analyzing the loading and unloading behaviours of the thermal storage. Figure 3.28 clearly shows that during some periods of the day characterized by low production costs, the storage is loaded thanks to the heating production with heat pumps. As it can be observed for two time periods at the beginning and the end of the year, the storage loading is mainly based on periods with low heating production costs and the thermal storage is unloaded during periods with larger heating production costs. This allows to reduce global heating production costs by shifting the heating production from periods with high costs to periods with lower costs by storing the surplus of heating production. Thanks to this strategy of heating production, the optimal heating network can benefit from the advantages of heating production technologies with variable heating production costs.

The previous case considers a limited thermal capacity of the heat pumps of 10 MW_{th} while a larger heating capacity could increase the part of the heating production that could be stored during periods of low heating production costs. Increasing this thermal capacity from 10MW_{th} to 50 MW_{th}, more profits are generated using a larger thermal storage capacity than previously as illustrated in Table 3.13. It can be observed that only a part of the total available heating capacity (16.377 MW_{th} out of 50 MW_{th}) is used in this case.

TABLE 3.13: Economic comparison with a maximum heat pump capacity of 50 MW_{th}.

	Heat pumps without storage	**Heat pumps with storage**
Used or installed heating capacity (MW_{th} or MWh_{th})	5.200	16.377 of heat pumps @ node v_1 83.293 of thermal storage @ node v_1
CAPEX (M€)	3.340	3.522
OPEX (M€)	7.744	6.206
Revenues (M€)	13.497	13.497
Profits (M€)	2.413	3.769

Capital expenses linked to this new heating network design are slightly higher because of the building of a bigger thermal storage with a thermal capacity of 83.293 MWh_{th} compared to the previous case with a thermal storage capacity of 60.108 MWh_{th}. The increase of these capital expenses around 32,000 € is also linked to the use of larger pipe diameters because of the increasing power flows required to load and unload the thermal storage characterized by a larger thermal capacity. However, the sizing of a larger thermal storage enables to reduce the global operating costs by around 43,000 € thanks to the additional shifting of a part of the heating production from periods with higher heating production costs to periods with lower heating production costs. In the case of a limited capacity of 10 MW_{th} heat pumps, this heating capacity is insufficient to load optimally a potential storage during periods of low heating production costs. The increase of the available heating capacity of the heat pumps to 50 MW_{th} enables to achieve a

better shift of the heating production costs by using a heating capacity of 16.377 MW_{th} and by reducing the operating costs. The optimization tool is then able to determine the optimal size of the thermal storage to optimize its loading strategy.

Therefore, the introduction of heat pumps as heating sources into new heating network projects may be profitable if they are combined with thermal storages. They could be used to promote the integration of intermittent renewable energies using the surplus of electricity to produce heat stored through heating networks. Based on the electricity price and the features of the heat pumps, the optimization model developed in this thesis can also be used as a decision tool to study the integration of these heating technologies into new heating network projects.

3.9.3 Limitation on the heating availability with solar collectors

Heating technologies considered in the previous sections are featured by a constant available heating capacity such that the maximum installed heating capacity is available all over the year. With intermittent energy sources like solar energy for example, the variable availability of the heating source can significantly influence the heating supply and indirectly the outline and the sizing of the network. Thermal solar collectors for heating production are characterized by large required surfaces for the collectors such that the available heating power is defined from available surfaces in this section. For a detailed calculation of the maximum available heating power from an available surface, the reader can refer to Section 2.3.3.2.

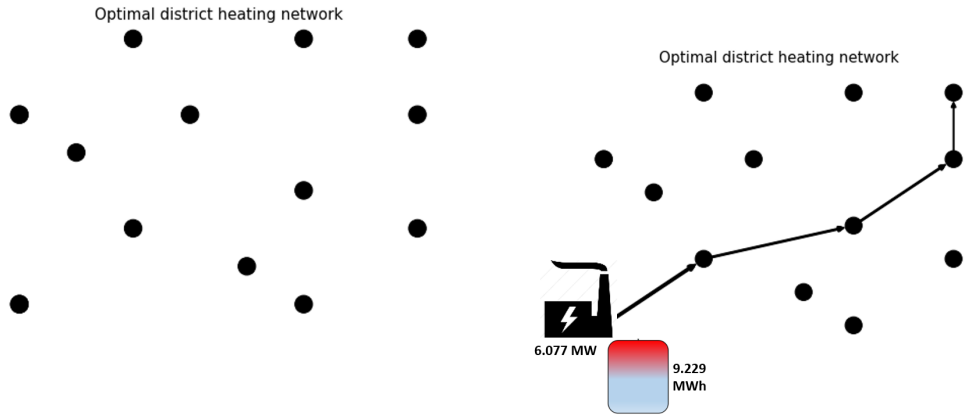

(a) Outline of the network with solar collectors of 10 000 m^2

(b) Outline of the network with solar collectors of 10 000 m^2 and a thermal storage

FIGURE 3.29: Outline of a heating network with solar collectors and a thermal storage.

Considering firstly an available surface of 10,000 m^2 at node v_1 defining a maximum thermal capacity around 6 MW_{th}, the influence of the use of an additional thermal storage at node v_1 can be shown in Figure 3.29. The use of thermal solar collectors as a heating source requires the use of a thermal storage

to store heat during periods of low heating availability. Even with the integration of an additional thermal storage, the heating network project only feeds the most economically profitable streets. For example, the street between nodes v_{12} and v_{13} characterized by an important heating consumer which is the greenhouse is fed by the network even though this street is far from the heating source. Indeed, the greenhouse acts as an important consumer, especially during the summer with a non zero heating demand, enabling to consume the significant heating production during the summer due to a large solar irradiation.

TABLE 3.14: Economic comparison with solar collectors and thermal storage.

	Solar collectors without storage	**Solar collectors with storage**
Used or installed heating capacity (MW_{th} or MWh_{th})	/	6.077 of solar collectors @ node v_1 9.229 of thermal storage @ node v_1
CAPEX (M€)	/	1.006
OPEX (M€)	/	0.363
Revenues (M€)	/	2.007
Profits (M€)	/	0.638

Assuming an existing infrastructure for the solar collectors, the capital expenses only include the required costs for the building of pipes and substations. These costs are combined with operating expenses for the heating production with solar collectors which are very low such that the main constraint for solar heating remains on the available heating capacity during each period of the year. From Table 3.14, it can be observed that capital and operating expenses are indeed very low compared to other previous case studies. Moreover, the maximum available thermal capacity of 6.077 MW_{th} is used to supply as much as possible heat to the consumers of the network. Consumers with the more interesting heating demand profile are then selected based on the available heating capacity.

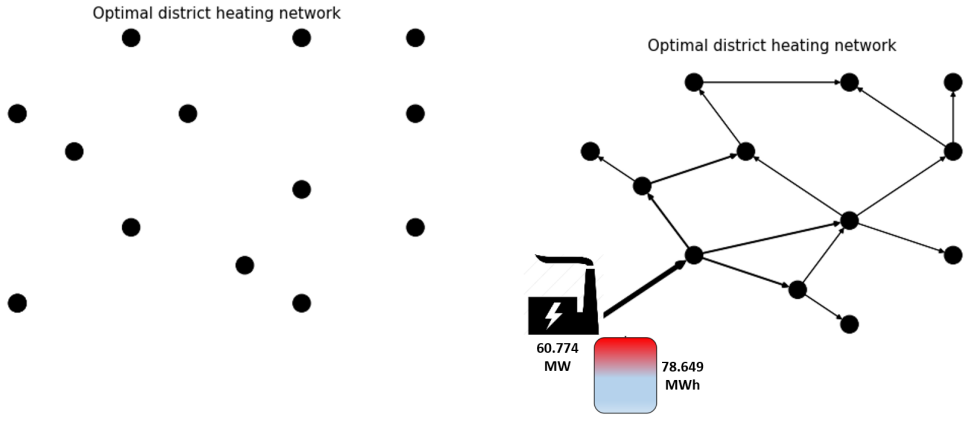

(a) Outline with solar collectors of 100 000 m^2

(b) Outline with solar collectors of 100 000 m^2 and a thermal storage

FIGURE 3.30: Outline with solar collectors of 100 000 m^2.

An increase of the heating capacity for solar collectors can be studied by considering a larger available surface from 10 000 m^2 to 100 000 m^2 characterized by a maximum available heating capacity around 60 MW_{th} for solar radiation in Liège. The increase of the available surface enables to connect more consumers to the network thanks to a bigger heating capacity available all over the year despite the intermittency of the solar energy. A case without and with a thermal storage solution is depicted in Figure 3.30 to highlight the need of a thermal storage for the development of heating network projects with thermal solar collectors.

TABLE 3.15: Economic comparison with solar collectors of 100 000 m^2.

	Solar without storage	**Solar with storage**
Used or installed heating capacity (MW_{th} or MWh_{th})	/	60.774 of solar collectors @ node v_1 78.649 of thermal storage @ node v_1
CAPEX (M€)	/	3.179
OPEX (M€)	/	1.568
Revenues (M€)	/	8.704
Profits (M€)	/	3.957

The storage dynamics related to 10 000 m^2 solar collectors is illustrated in Figure 3.31. The main trends related to the thermal storage are that the storage is generally loaded during periods with a high capacity factor and unloaded during periods with lower capacity factors in order to supply as much heat as possible all over the year considering the fluctuation of the available heating capacity. Indeed, focusing on a shorter period of time at the beginning of the year, the storage loading only occurs during periods with a sufficiently high capacity factor while the storage is unloaded when there is no more available solar energy (i.e. the capacity factor is zero).

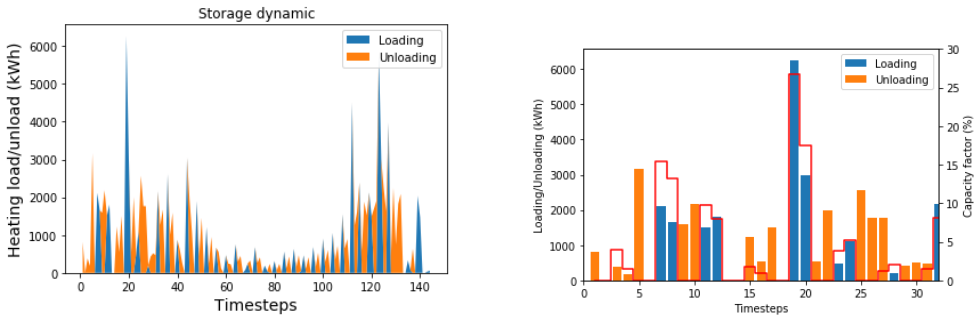

(a) Storage dynamics for 10 000 m^2

(b) Storage dynamics for 10 000 m^2 at the beginning of the year

FIGURE 3.31: Storage dynamics with 10 000 m^2 solar collectors and a thermal storage.

Thermal solar collectors combined with a thermal storage can be put in place only for large available surfaces ensuring a sufficient heating capacity to feed the network and the thermal storage. In this section and the previous ones, the

heating technologies are supposed to be already available such that there are no additional costs linked to the building of these plants. However, in practise, there is generally a need to build these plants implying additional costs. For example, for solar collectors, these building costs are significant (cf. Appendix C) penalizing this technology for a heating network project starting from scratch. In the next section, a new case starting from the initial one but adding these building costs is considered in order to assess their impact on the outline and the sizing of a heating network.

3.9.4 CAPEX of the heating sources

Including the components of the building costs into the optimization model, a parametric study showing the impact of the capital expenses for the building of heating plants can be achieved in the following. Restarting from the initial reference scenario and considering capital expenses of respectively 600 €/kW and 1 000 €/kW for the building of the heating technologies, the new outlines defined for these 2 cases are drawn out without and with storage solutions in Figure 3.32.

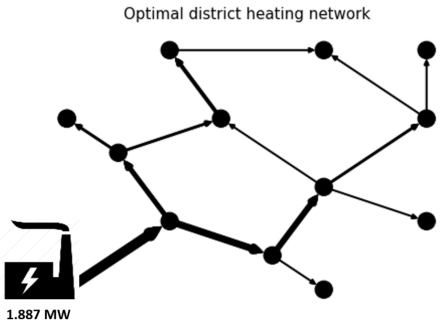

(a) CAPEX = 600 € without storage

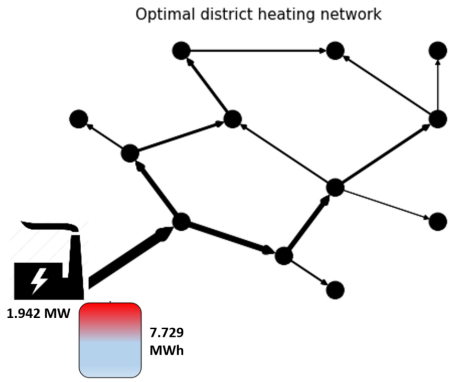

(b) CAPEX = 600 € with storage

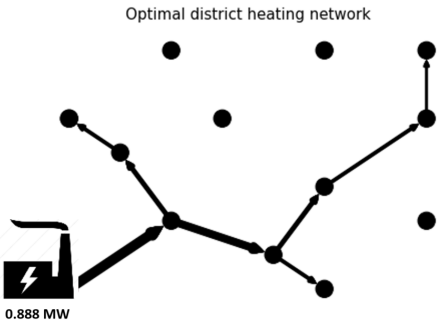

(c) CAPEX = 1 000 € without storage

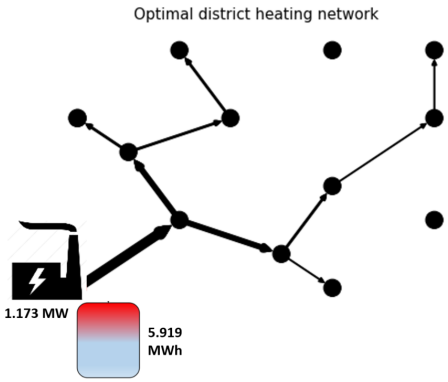

(d) CAPEX = 1 000 € with storage

FIGURE 3.32: Outline of the heating network with different CAPEX for the heating sources.

The capital expenses of the heating plants are a key component to take into account to maximize the profits generated from the heating network project. Indeed, an increase of the capital costs linked to the buildings of the

heating plants leads to a decrease of the number of streets connected to remain economically optimally profitable. On the other hand, the addition of a thermal storage solution into the network slightly increases the profits made up from the heating network project as illustrated in Table 3.16 and 3.17. However, it does not affect significantly the outline of the network.

It can be noticed that the increase of the building costs obviously leads to a decrease of the installed capacity because it becomes no longer profitable to add more kW of heating capacity at some point. The optimization formulation is useful to assess the optimal trade off between the heating capacity to put in place and the number of streets to connect to the network in order to maximize the net cash flow of the heating network project.

TABLE 3.16: Economic comparison with CAPEX = 600 €/kW.

	Without storage	**With storage**
Installed heating capacity (MW_{th})	1.887	1.942 of heating plant @ node v_1 7.729 of thermal storage @ node v_1
CAPEX (M€)	4.251	4.374
OPEX (M€)	5.848	6.098
Revenues (M€)	11.133	11.617
Profits (M€)	1.035	1.145

TABLE 3.17: Economic comparison with CAPEX = 1 000 €/kW.

	Without storage	**With storage**
Installed heating capacity (MW_{th})	0.888	1.173 of heating plant @ node v_1 5.919 of thermal storage @ node v_1
CAPEX (M€)	2.670	3.505
OPEX (M€)	3.248	4.184
Revenues (M€)	6.196	7.988
Profits (M€)	0.278	0.299

As for the test cases with a limited thermal capacity at the heating plants (cf. Section 3.9.1), the storage is mainly used during periods of high heating demands to cover the additional heating demand that can not be covered by the installed heating capacity. A more significant part of the total heating demand can then be supplied by the heating source combined with a thermal storage by loading it optimally based on the optimally sized capacity assessed by the optimization tool.

3.9.5 Location of the thermal storage

The thermal storage plays a key role in the design of district heating networks acting as a buffer for shifting a part of the heating production in an optimal way. An optimal operation of the storage enables to reduce the operating

costs or to increase the total heating capacity available for the supply of the network. However, the connection of the storage to the network generally implies additional costs for building the required pipes to feed the network from the storage. Therefore, the location of the thermal storage is also a part of the decision process for the optimal outline and design of a new heating network project.

The influence of the location of the thermal storage on the outline and the sizing of the network can be illustrated by restarting from the example in Section 3.9.2 using heat pumps at node v_1 with an additional thermal storage at this node. Considering that there is no more space to put this additional storage at node v_1, it can be considered that a potential storage could be put in place at node v_{13} near the greenhouse of the studied neighbourhood. The optimization model is processed in order to compare the case with a thermal storage at node v_1 and a thermal storage at node v_{13}.

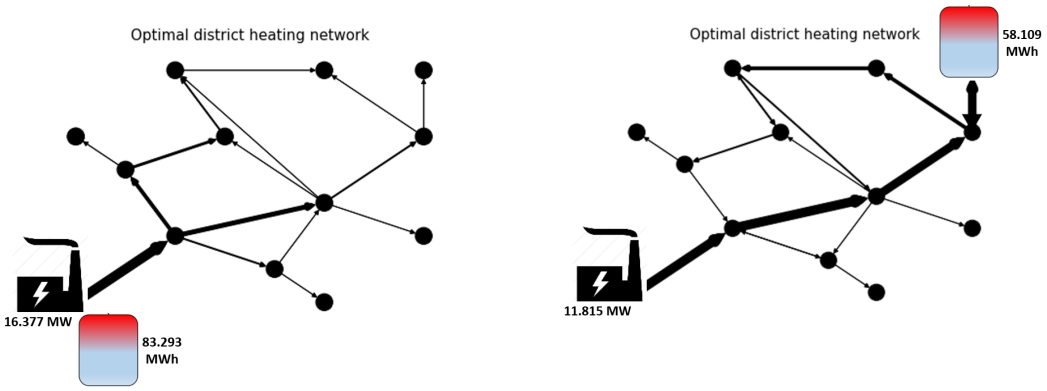

(a) With storage at node v_1 (b) With storage at node v_{13}

FIGURE 3.33: Outline of the heating network project for a scenario with a heat pump and thermal storage at node v_1 or v_{13}.

TABLE 3.18: Comparison with thermal storage at node v_1 or v_{13}.

	Heat pumps with storage @ node v_1	**Heat pumps with storage @ node v_{13}**
Used or installed heating capacity (MW_{th} or MWh_{th})	16.377 of heat pumps 83.293 of thermal storage	11.815 of heat pumps 58.109 of thermal storage
CAPEX (M€)	3.522	3.681
OPEX (M€)	6.206	6.315
Revenues (M€)	13.497	13.497
Profits (M€)	3.758	3.501

The outline of the network, depicted in Figure 3.33, is modified due to the integration of the thermal storage at another place. Indeed, it can be observed that 2 new pipes are built in order to guarantee a connection of the heating

consumers to both heating sources that are the heat pumps and the thermal storage. New pipes between respectively nodes v_{13} and v_{12} and v_5 and v_6 are built to ensure a bidirectional flow between these edges.

The building of these new pipes gets an impact on the capital expenses with additional costs for the building of these pipes. It can be observed from Table 3.18 that these capital expenses have slightly increased of 159,000 € as well as the operating costs have increased of 109,000 €. The raise of the operating costs is due to the additional heating production during loading phases of the storage. The heating production needs to be carried out from the heating source at node v_1 to the thermal storage at node v_{13} implying additional heat losses and pumping power. These additional costs justify the smaller sizing of the heat pumps and the thermal storage.

For a case where the thermal storage is not close to the heating source, an optimal operation of the network promotes the use of the heat pump instead of loading the thermal storage during some time periods with low heating production costs. The optimization model enables to assess the best trade-off between loading the thermal storage while counterbalancing additional losses or producing heat using heat pumps with slightly higher heating production costs. The location of the thermal storage is therefore ideal when it is close to the main heating source of the network because it reduces the operating losses as well as the initial additional investment costs to build new pipes to guarantee a bidirectional flow into some edges of the network.

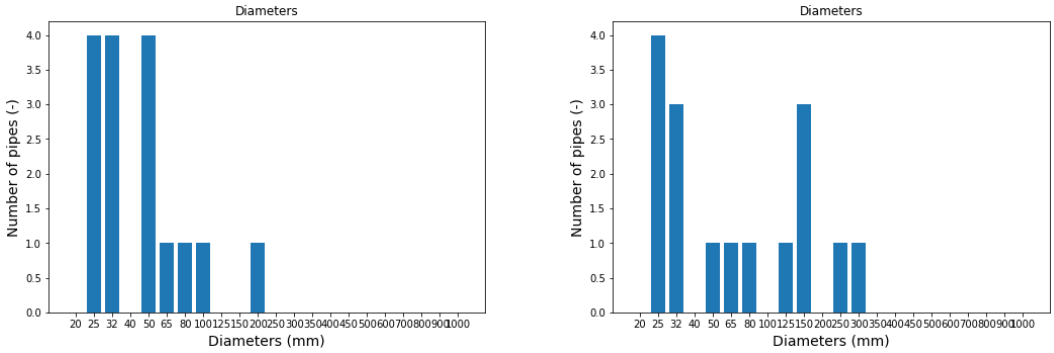

(a) With storage at node v_1 (b) With storage at node v_{13}

FIGURE 3.34: Repartition of the diameters for a scenario with a heat pump and thermal storage at node v_1 or v_{13}.

The influence on the outline and the sizing of the network can also be figured out by representing the repartition of the diameters into the network as illustrated in Figure 3.34. With the inclusion of a storage at the opposite of the heating source, the required diameters close to the heating source and the thermal storage have to be bigger. Indeed, during unloading periods of the storage where the storage is mainly used, larger power flows occur near the thermal storage such that the pipe diameters have to be sized for these nominal operating conditions. Therefore, it can be observed from Figure 3.34 that bigger pipes diameters are used with a thermal storage at node v_{13} because of the

additional bigger pipes required close to the thermal storage.

In practise, the location of the thermal storage is determined as a function of the available surface at different locations. One of the goals of the optimization formulation presented in this thesis relies on the design of any new prospective heating network project from a blank sheet by finding the best synergies between the available heating sources/surfaces and the heating consumers to determine the most economically profitable solution to build a heating network. This final feature is presented in the following section.

3.10 Outline and sizing of a heating network from a blank sheet

The decision tool developed in this thesis has been used to determine the optimal heating network from existing heating sources or prescribed alternative heating sources from a given building surface. The optimization model can also determine from a blank sheet which available surface could be used to build a heating source feeding optimally the studied area with a heating network. Generally, a new heating network project starts without any available heating source which could be used to supply the network. In these new district heating network projects, the main goal is then to identify which area could be economically profitable to connect and which zones could be used to install a new heating production unit which would supply the network. These zones are defined by a prescribed surface limiting the available heating capacity to install on this surface.

The decision tool can be used to select and size the optimal heating production units and their locations minimizing the capital and operating expenses of a heating network project while maximizing revenues from the building of this network. This computation is really difficult to achieve because of the wide range of possibilities for building a new heating network project. In this section, the decision tool is therefore used to define the optimal network for a heating network project starting from scratch.

Considering 3 available surfaces of 1000 m^2 at nodes v_1, v_2 and v_{13} with the possibility to select from a set of heating technologies described in Section 2.3.4.1 (except gas boiler units because we want to decarbonize the heating production mix with alternative heating sources), the optimal outline and sizing of a potential economically profitable heating network can be drawn out from the optimization process and data available in Appendix B.

All the results related to two scenarios including or not prospective thermal storage solutions are summarized in Table 3.19 and an outline for both cases is provided in Figure 3.35. The integration of a thermal storage modifies the outline of the network thanks to the storage capacity enabling to increase the heating supply during high heating demand periods.

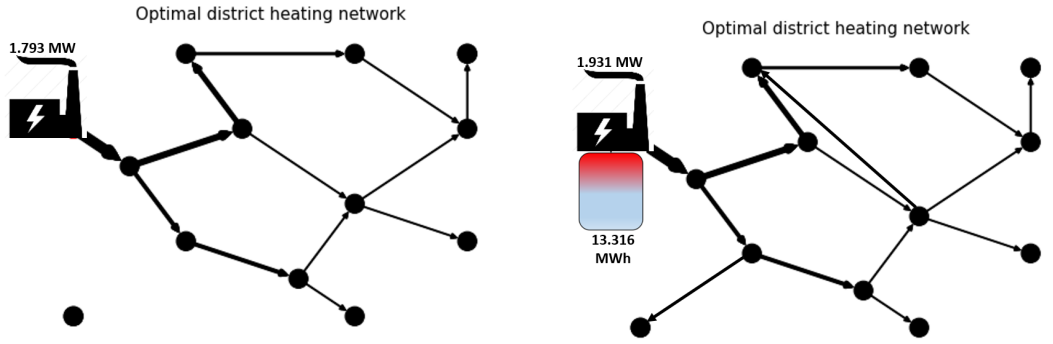

(a) Optimal outline without storage prospectives for 1 000 m^2

(b) Optimal outline with storage prospectives for 1 000 m^2

FIGURE 3.35: Optimal outline for a new heating network starting from a "blank sheet".

TABLE 3.19: Economic comparison of Scenario 3 starting from scratch.

	Without storage potential	**With storage potential**
Installed heating capacity (MW_{th} or MWh_{th})	@ node v_2 { 0.496 of waste incinerator; 1.135 of wood pellets; 0.162 of heat pumps }	@ node v_2 { 0.560 of waste incinerator; 1.188 of wood pellets; 0.183 of heat pumps; 13.316 of thermal storage }
CAPEX (M€)	5.261	5.779
OPEX (M€)	3.726	4.060
Revenues (M€)	10.577	11.670
Profits (M€)	1.590	1.831
CO_2 **savings (%)**	50.94	55.58

Two of the streets constitutive of the neighbourhood were assessed to be non profitable if there were no thermal storage solutions. The integration of a thermal storage solution enables to cover a more significant part of the total heating demand such that all the streets are connected to the network with a thermal storage. Regarding Table 3.19, the additional thermal storage leads to additional capital expenses for the building of the thermal storage and the new additional built pipes compared to the scenario without thermal storage. However, these additional capital expenses are counterbalanced by an increase of the heating sales revenues generated thanks to an additional heating production capacity from the thermal storage.

It can also be noticed from Table 3.19 that without thermal storage, the maximum installed capacity is insufficient to cover the whole heating demand all over the year. The optimization model determines the optimal thermal capacity

to install as well as the optimal selection of the streets to connect to the network in order to maximize the net cash flow from this network. Regarding the thermal capacities installed for the case without storage solutions, it can be noticed that the optimization formulation determines a trade off between heating technologies characterized by small capital expenses but large heating production costs and heating technologies with a small heating production cost but larger initial capital costs. The sizing of these different heating technologies remains theoretical and wants to illustrate general trends for the sizing of heating production units into a heating network. Indeed, for example, a heating plant like a waste incinerator will not be custom-sized based on the total heating demand of the network but is sized from the total amount of waste to manage. This will be illustrated in Chapter 5 with an existing waste incinerator retrofitted for its connection to a heating network. From these theoretical considerations, the optimal building strategy for a heating network consists then of:

1. Building a heating source characterized by relatively small heating production costs. This heating plant is assigned as the main heating source to provide the base heating load. The capital expenses linked to this technology being bigger, the heating capacity of the base load plant is limited to a certain amount which is assessed as the optimal base load heating capacity to install.

2. Building an additional heating source characterized by slightly bigger heating production costs but smaller capital costs. This heating source is assigned as a heating source to stand for the main heating source during periods with a higher heating demand.

3. Building a back-up heating source with a variable production cost that can be used during periods of low heating production costs or periods of peak demand.

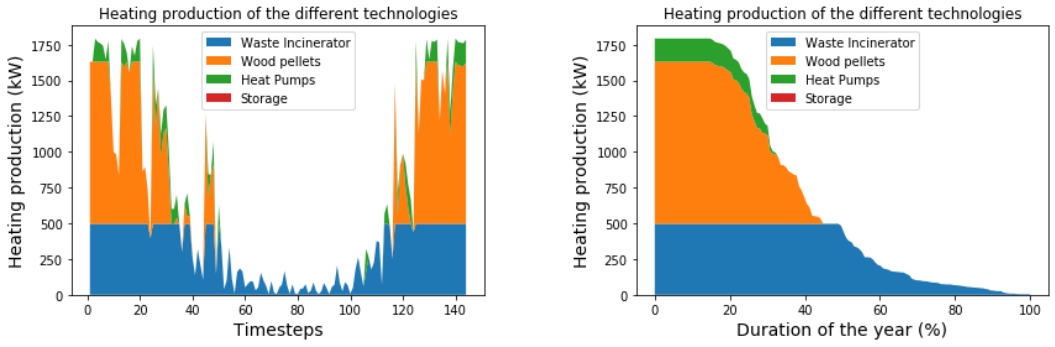

(a) Heating production of the different heating technologies for 1 000 m^2

(b) Load duration curve of the heating production for 1 000 m^2

FIGURE 3.36: Dynamics of the heating production for an available surface of 1 000 m^2 without thermal storage.

This repartition of the heating production can be shown by analyzing the outputs of the decision tool given for the scenario defined in this section. Figure

3.36 shows that the waste incinerator is used all over the year to guarantee a base load heating production. The wood pellets heating plant then serves as an additional heating unit to provide heat for higher heating demands. Finally, the heat pumps are used during periods of peak demands.

The heating production levels can be related to the installed power of the different heating technologies units in Table 3.19. Indeed, it can be observed that the decision tool prescribes a waste incinerator capacity around 500 kW_{th} which is operating all over the year with an additional wood pellets heating unit with a heating capacity around 1 100 kW_{th} operating around 45% of the year. Finally, heat pumps are considered as an optimal back-up heating technology operating around 30% of the year to ensure peak heating production with a heating capacity around 150 kW_{th}.

It can also be observed from Table 3.19 that adding a thermal storage at node v_2 makes profitable to build additional thermal capacity of the 3 different heating plants in order to load the storage during periods characterized by low production costs or by low heating demands. As illustrated in Figure 3.37, the thermal storages are used during periods of high heating demands and are fed by the additional installed capacity compared to the case without storage. This additional capacity enables to guarantee a bigger total available heating capacity leading to the connection of more streets to the network. It also enables to integrate more easily heat pumps with a heating production which can be stored during periods of low heating production costs. In terms of CO_2 savings, the use of thermal storages also enables to decrease the CO_2 emissions thanks to the use of alternative heating sources like these heat pumps.

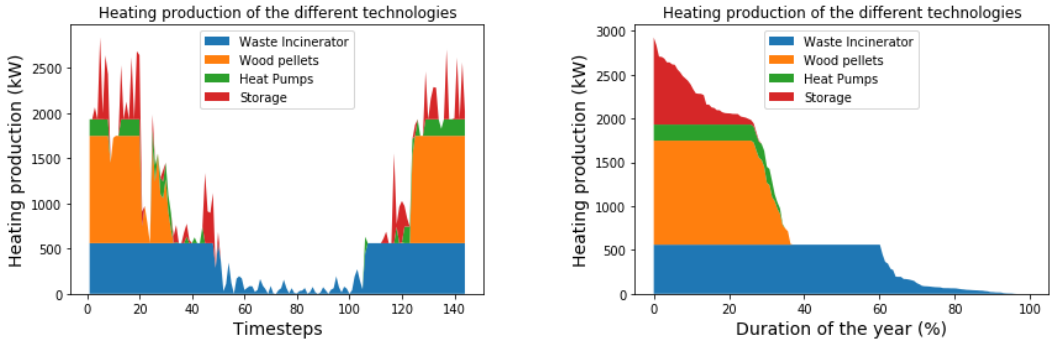

(a) Heating production of the different heating technologies for 1 000 m^2

(b) Load duration curve of the heating production for 1 000 m^2

FIGURE 3.37: Dynamics of the heating production for an available surface of 1 000 m^2 with thermal storage.

This theoretical case study starting from a "blank sheet" shows that the decision tool can optimally select the best locations to install heating production technologies and which technologies to pick up and build in an optimal way. However, this case has some limitations because capital costs are considered as a purely linear function of the installed capacity for the building costs. These costs are actually dependent on the power range on which they are considered

such that the costs per unit of installed thermal capacity generally decrease with an increase of the total installed power. These non linear costs would imply a non-linear optimization formulation in the objective function such that a piecewise linear formulation would also have been required to tackle this issue and keep a linear formulation. This has not been considered in this thesis.

Moreover, for a real case study, some heating production units like waste incinerators are not sized with the main goal to cover the heating needs of a neighbourhood. Despite the automatically decision process of the optimization model, the selection of these kinds of heating sources has therefore to be discussed from the results of the model and can be constrained in some cases.

3.11 Comparison of a centralized and a decentralized heating production scenario

This last scenario starting from a blank sheet can be used to be compared to a totally decentralized heating production scenario where gas boilers units would be installed in each dwelling constitutive of the neighbourhood. Compared to the previous scenario, in this new scenario, all the streets are constrained to be connected to the heating network and the heating network mandatorily supplies the whole heating demand of the neighbourhood. From these constraints, the optimization model enables to determine and size the optimal heating sources mix.

For the decentralized heating production scenario, considering a gas boiler cost of 4000€ per unit for individual buildings, 16,000€ per unit for apartments and offices [108] and 18,000€ per unit for the greenhouse (60€/kW) [109], a total capital cost for gas boilers of 4.902 M€ is computed based on the total number of dwellings into the neighbourhood:

Table 3.20: Capital expenses for gas boilers.

Type of dwellings	**Number of dwellings**	**Total heating capacity to install (kW)**	**Cost of a gas boiler (€)**	**Total cost (€)**
S1	182	910	4000	728,000
D1	161	805	4000	644,000
T1	250	1000	4000	1,000,000
A1	0	0	16,000	0
O1	157	3140	16,000	2,512,000
Greenhouse	1	300	18,000	18,000
TOTAL	800	6155		4,902,000

For the heating production costs with individual gas boilers considering a 30 years project lifetime, they can also be computed in a simple way considering a gas price of 0.07€/kWh and knowing the annual heating consumption of each kind of dwelling:

TABLE 3.21: Operating expenses for gas boilers.

Type of dwellings	**Number of dwellings**	**Annual heating consumption per dwelling (kWh)**	**Total heating production cost over 30 years (M€)**
S1	182	5952	2.275
D1	161	7278	2.461
T1	250	4956	2.602
A1	0	14,913	0
O1	157	14,944	4.927
Greenhouse	1	691,242	1.452
TOTAL			13.717

For the centralized heating scenario using a heating network, as illustrated in Figure 3.38, the same heating mix than in the previous scenario is used except that bigger heating sources capacities are installed to cover the whole heating demand of the neighbourhood. All the economics outputs from the optimization model are also provided in Table 3.22 for a 30 years project lifetime and compared to the decentralized heating production scenario.

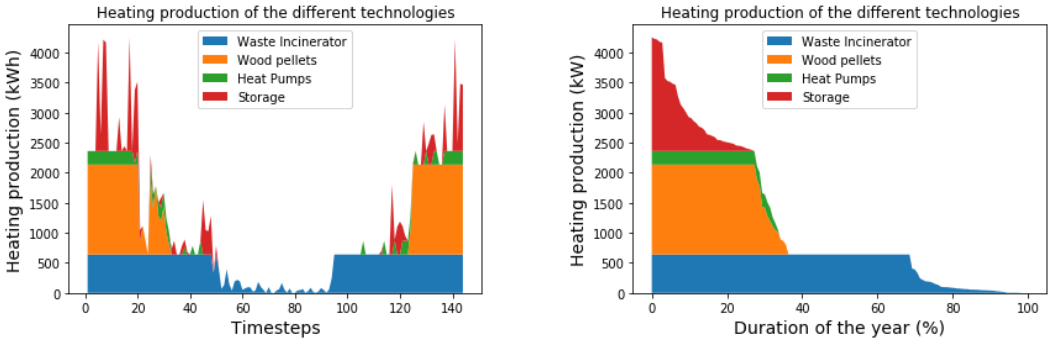

(a) Heating production of the different heating technologies for 1 000 m^2 with thermal storage

(b) Load duration curve of the heating production for 1 000 m^2

FIGURE 3.38: Load Duration Curve for the different heating production technologies.

TABLE 3.22: Comparison of the costs and CO_2 emissions with a centralized and decentralized heating production scenario for a 30 years lifetime project.

	Heating network	**Gas boilers**
CAPEX (M€)	10.299	4.902
OPEX (M€)	4.781	13.717
Total costs (M€)	15.080	18.619
CO2 savings (%)	56.68	/

The reader can quickly understand that the capital expenses linked to the building of a heating network are really higher than the costs for implementing

gas boilers in each dwelling. Even if these capital expenses are large, costs savings achieved with heating networks by using heating production units with lower production costs than the gas costs are significant over the lifetime of the project. For the heating consumer, it is interesting to be connected to a network because he pays the same heating price than using a gas boiler without paying any heating production unit installation. Therefore, a heating network technology is thus very interesting compared to a gas boiler into its house while reducing its CO_2 emissions. However, for the stakeholders of the funding of the network, prescribing a heating sales price equivalent to the gas market price might be uncompetitive. Indeed, it can be observed from Figure 3.39 that the payback period to cover the capital and operating expenses is larger than 30 years because of the mandatory constraint to connect all the streets to the network and to supply the whole heating demand over the year. The payback period of this heating network project would be around 38 years. Therefore, it becomes questionable to implement a heating network technology for the whole neighbourhood because of the long-term payback period of the project. Therefore, the heating network operator should provide heat at a larger cost than 0.07€/kWh if he wants to remain economically profitable over the 30 years project lifetime. However, even though it is not profitable over 30 years, the project lifetime of a heating network is generally higher than 30 years such that it could still be profitable if larger lifetimes are assumed.

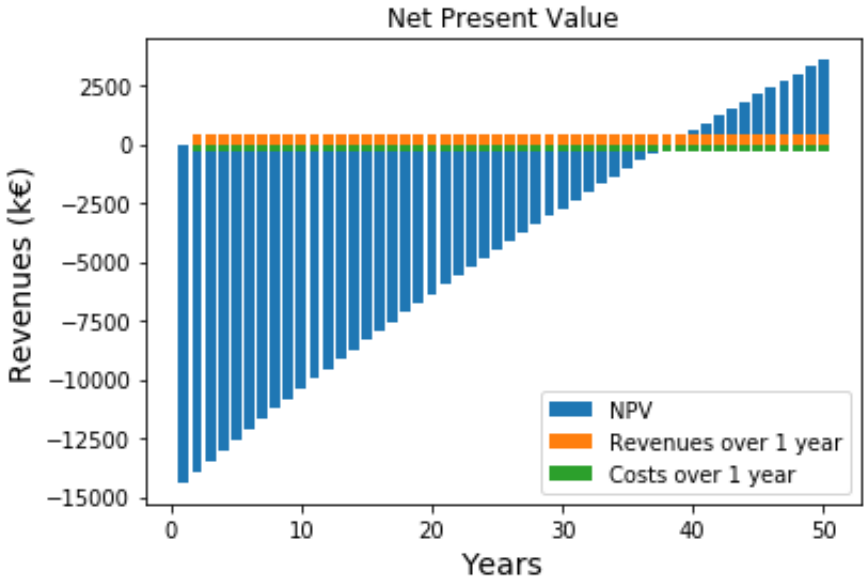

FIGURE 3.39: Evolution of the Net Present Value of the project over 50 years.

Despite this long return on investment period, CO_2 savings achieved with a centralized heating production scenario and a heating network are significant and are assessed to be around 56.68% (cf. Table 3.22) compared to a decentralized heating scenario with gas boilers units in each dwelling. This scenario shows that even if heating networks are not profitable on a short-term period, they can provide long-term benefits by reducing the total heating production costs

for the consumer while guaranteeing CO_2 savings thanks to the use of partially decarbonized heating sources. In these kinds of cases with new heating network projects designed from a blank sheet, it is therefore important to get a long-term vision from a network operator point of view. Another key factor which could promote the heating network concerns the allocation of public subsidies. Indeed, these subsidies could help for financing capital expenses of heating networks while guaranteeing an environmentally-friendly solution with an economic benefit for the heating consumers.

3.12 Comparison of the linear and piecewise linear optimization formulations

In order to guarantee a quick computation time and numerical convergence, a purely mixed-integer linear formulation has been used for all the previous cases. The linearization of some functions like the pipes costs and the heat losses linked to these pipes can lead to underestimations of the real costs and heat losses related to the heating network. As described in Section 2.3.3.1, a purely linearized formulation underestimates the real values of these variables such that a piecewise linearization would be more appropriate to increase the accuracy of the solution. The problem of the piecewise formulation relies on the significant increase of the number of decision variables of the optimization problem which could lead to larger computation times. Therefore, a comparison of the purely linear and the piecewise linear formulations is achieved.

The use of a piecewise linear formulation on the test case described in Section 3.8 slightly changes the results obtained from the optimization model. Even though the outline of the network remains the same for both formulations, the piecewise formulation leads to a different sizing of the used heating capacity and of the diameters of the pipes. As illustrated in Figure 3.40, it can be observed that with the piecewise formulation, the decision tool defines smaller diameters as optimal diameters for the pipes due to a smaller used heating capacity and the larger pipes costs for a given power flow linked to the piecewise linear formulation.

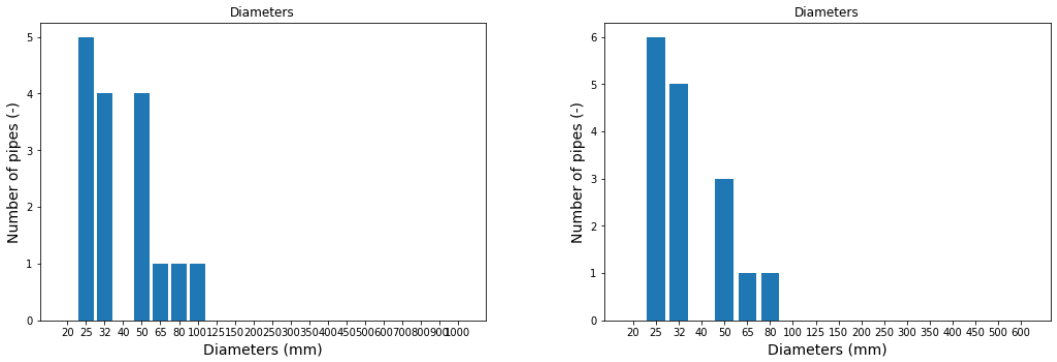

(a) Purely linear formulation (b) Piecewise formulation

FIGURE 3.40: Pipes diameters for both formulations.

Table 3.23 illustrates this use of a smaller heating capacity with a piecewise formulation in order to decrease the pipes diameters into the network. This implies a very small decrease of the revenues generated from the heating sales because the heating plant can not feed the heating demand all over the year. This decrease of heating revenues illustrated in Table 3.23 is relatively small compared to the total revenues.

TABLE 3.23: Comparison of the model with a purely linear and piecewise linear formulation for 144H.

	Purely linear	**Piecewise linear**
Used heating capacity (MW_{th})	5.200	3.780
CAPEX (M€)	3.340	3.592
OPEX (M€)	7.106	7.073
Revenues (M€)	13.497330	13.497080
Profits (M€)	3.051	2.832
Computation time	91s = 1 min 31s	1 217s = 20 min 17s
Number of variables	35 111	84 359

As illustrated in Figure 3.41, an installed heating capacity of 3.780 MW_{th} enables to feed the heating demand of the whole network during 99% of the year while decreasing the largest sized pipe diameter due to the lower maximum heating demand over the year. The use of the piecewise linear formulation can therefore provide a better trade-off between the maximum heating capacity to install or use and the related pipes diameters to install thanks to a better assessment of the pipes costs.

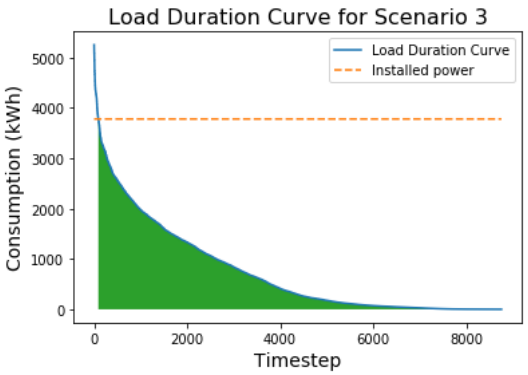

FIGURE 3.41: Load Duration Curve of the studied neighbourhood.

However, the number of variables with the piecewise formulation significantly increases for this case study characterized by a small number of edges. Defining 5 continuous variables $y^{0,1,2,3,4}$ and 4 discrete variables $b^{0,1,2,3}$ per edge j for each timestep t leads to the definition of 49 248 additional variables [2] here. There are indeed 38 edges constitutive of the network including 16 edges connecting all

[2] $(5+4) \cdot 38 \cdot 144 = 49248$ new variables

the nodes of the graph with 3 additional edges linking the heating sources to the nodes and their 19 reverse edges. There are then indeed 84 359 - 35 111 = 49 248 additional variables defined into the optimization formulation. This large increase of the number of variables leads to a significantly higher computation time which is non negligible in cases with large neighbourhoods made up of thousands of streets. For the application of the decision tool to large case studies like the one in Chapter 5, the purely linear formulation has been used to guarantee a trade-off between a sufficient accuracy and a feasible computation time. Indeed, it has been tried to apply the piecewise linear formulation to the large-scale case study in Chapter 5 without any success.

3.13 Conclusion

This chapter aims for highlighting the main features of the optimization model presented in the previous chapter. Small theoretical case studies used in this chapter show that a heating network project can be designed from existing heating sources or from a blank sheet starting from available building surfaces for different scenarios whose parameters are defined by the user of the decision tool. This general approach can give a pre-design of the outline and the sizing of any heating network even though this decision tool is not sufficient to entirely optimize a heating network project. Indeed, some assumptions about heat and pressure losses have been made into the model to keep it as a linear formulation while in practise, these assumptions are not verified due to dynamic physical phenomena occurring into the network. In order to bring a critical point of view about the optimization model developed into this thesis and to show its main weaknesses, a dynamic modelling method is used in the next chapter to check the validity of some assumptions of the optimisation model and to calibrate the parameters of the optimization model based on this dynamic modelling.

Some simplifications have also been applied to the model for its use with large-scale case studies like the one in Chapter 5. The selection of representative days for reducing the number of optimization variables and the choice of a purely linear formulation to avoid an increase of the number of binary variables into the problem are questionable because it has been shown in this chapter that these simplifications impact the value of the solution provided by the optimization model. The reader has to be aware that these simplifications are achieved for the applicability of the tool to large-scale case studies. Even if these simplifications are responsible for quantitative errors because of some approximations, it has been illustrated that these simplifications are not responsible for large qualitative errors such that they can help the user of the tool to take good pre-design decisions in a feasible computational time. As already mentioned in Section 2.5, other existing decision tools can then be used to refine the accuracy of the solution for the sizing of the heating network based on the outline defined by the optimization tool.

Chapter 4

Calibration of the optimization model from dynamic simulations

"The good Lord is in the detail"

—Gustave Flaubert

The optimization tool presented in Chapter 2 and exhibited in Chapter 3 enables to size a new heating network project from a blank sheet or from existing available heating sources by maximizing the net cash flow taking into account some physical constraints linked to the network. However, the linearization of some physical equations for the optimization formulation can lead to inaccurate solutions compared to the real physical behaviour of the heating network. The use of a dynamic model for the modelling of the theoretical heating network presented in Chapter 3 is achieved in order to provide a critical analysis of the linear formulation simplifying some physical phenomena that can occur into the network. Dynamic simulations based on operating conditions prescribed by the optimization formulation are then used to calibrate the parameters of the linear formulation and check if the new results obtained with this calibration are consistent or not.

This chapter mainly aims for criticizing some assumptions made in Chapter 2 and for providing a quantitative analysis of the numerical errors linked to the approximation of the heat losses into the optimization model. Indeed, it has been illustrated in Chapter 2 that heat losses have been linearized as a function only of the power flows in nominal operating conditions. This assumption enables to formulate linearly the problem as a unique function of the power flows into the pipes. Nevertheless, this simplification might lead to an underestimation of the real heat losses into the system such that dynamic simulations are used to show the impact of this assumption on the results. The following dynamic model is then involved into a calibration of the parameters defined in Chapter 2 to try to take into account more accurately about these physical phenomena in the optimization formulation.

4.1 Description of the dynamic model

The implementation of an optimization model for the outline and the sizing of a heating network taking into account heat losses is not sufficient for accurately taking into account these heat losses for the real design of a network. An optimization model enables to identify the main trends to follow in order to minimize the capital expenses while maximizing heating revenues but does not determine the optimal operating conditions for the network to gain some more savings regarding the additional heating production to counter-balance heat losses. Once the outline and the sizing of the network is achieved, dynamic models can be used to define optimal control strategies for costs and energy savings. Several control strategies are studied in the literature based on a dynamic modelling of the network [110–114]. These techniques provide adapted regulations for optimal operating temperatures over the network and are based on a more detailed dynamic optimization of the system than the optimization framework provided in this thesis. However, in this chapter, these optimal regulation models are not used because they are not the core of this thesis. The main goal of this chapter is to provide a critical insight on the optimization framework used in Chapter 3 based on a simple dynamic model to assess more accurately the physics of the system.

A dynamic model enables to assess the distribution of the mass flow rates among all of the pipes while taking into account inertia effects. Consequently, transportation delays of the heat waves from the heating sources to the substations are estimated according to the pipe lengths. These physical phenomena can be handled through the use of dedicated dynamic simulation softwares. In this thesis, the software *Dymola* based on the object-oriented language *Modelica* is used. Different existing components from available libraries based on the *IBPSA* project like *Buildings* [115] in *Dymola* are used to model the whole heating network. These models are useful to handle more accurately the behaviour of the heating network taking into account the inertia effects. An accurate modelling of these effects enables to provide a critical analysis of the optimization model previously presented and to try to increase the accuracy of the assessment of the heat losses for prescribed operating conditions in the decision tool. Based on the studied test cases in this thesis for third generation heating networks, supply and return temperatures $T^{w,in}$ and $T^{w,out}$ of respectively 90°C and 60°C are considered for the calibration of the parameters of the optimization model from dynamic simulations. Other operating temperatures could of course been considered for new applications in the future while fitting the parameters of the optimization model from the heat transfer model presented in Section 2.3.3.1 and calibrating these parameters using dynamic simulations from this chapter.

4.1.1 Piping model

The piping model is the key part of the whole system as it represents the link between the several heating consumers and the heating production units. Two main numerical models exist in the literature for the dynamic modelling of a flow into a pipe: the finite volume model (FVM) and the plug flow model (PFM).

4.1.1.1 Finite Volume Model

Generally, numerical methods used to model thermo-hydraulic flows in pipes are Finite Volume Methods [116]. As shown in Figure 4.1, they consist in dividing the pipe along its longitudinal axis in a discrete number of cells such that thermodynamic properties are computed, as depicted in Figure 4.1, based on an upwind scheme. h_i and $\dot{m}_i$ represent the enthalpy and the mass flow rate in a cell i, T_i and P_i stand respectively for the temperature and pressure in these cells. In each cell, one-dimensional Euler equations are applied, namely the mass, momentum and energy conservation equations assuming an incompressible fluid with a constant density ρ. The upwind scheme enables to determine the enthalpy at the inlet of a new cell i based on the enthalpy at the outlet of the previous cell: $h_i^{su} = h_{i-1}^{ex}$.

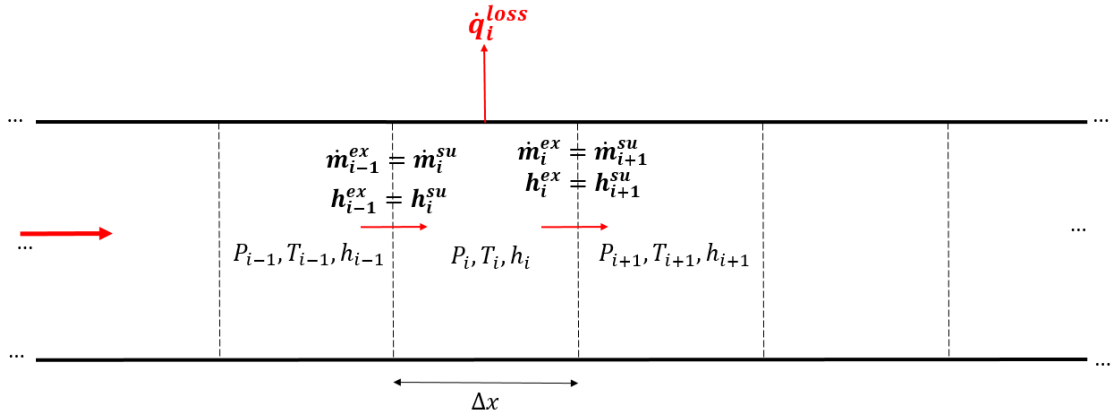

FIGURE 4.1: Finite Volume Method.

Conservation of mass

For any control volume defined by a cell of the discretization, the mass conservation can be represented by the following general equation:

$$\frac{\partial \rho}{\partial t} + \boldsymbol{\nabla} \cdot (\rho \boldsymbol{v}) = 0 \tag{4.1}$$

Simplifying the problem to a one-dimensional flow in the x-direction considering a radially uniform velocity flow v into the pipe, the conservation of mass can be written as:

$$\frac{\partial \rho}{\partial t} + \frac{\partial (\rho \cdot v)}{\partial x} = 0 \tag{4.2}$$

Considering a constant cross-section pipe area ($A_S = Cst$) and an incompressible fluid ($\rho = Cst$), this differential equation can be rewritten in its simplest form for the finite volume method:

$$\dot{m}^{ex} - \dot{m}^{su} = 0 \text{ where } \dot{m} = \rho \cdot A_S \cdot v \tag{4.3}$$

Conservation of momentum

The general unidimensional form of the equation related to the momentum conservation is represented as below:

$$\frac{\partial(\rho \cdot v)}{\partial t} + \frac{\partial(\rho \cdot v^2 + P)}{\partial x} = \beta_{gravity} + \beta_{friction} \tag{4.4}$$

with

$$\begin{cases} \beta_{gravity} = \rho \cdot g \cdot \frac{\partial z}{\partial x} \\ \beta_{friction} = \beta_{friction,reg} + \beta_{friction,sing} \end{cases} .$$

For the friction terms in the momentum conservation equation, the singular term $\beta_{friction,sing}$ is related to complex equations due to local singular variations of pressure related to a section pipe variation. Considering a constant cross-section area into a pipe, this term can be deleted from the general momentum conservation equation such that regular friction $\beta_{friction,reg}$ is only taken into account. For an incompressible fluid and making the assumption [1] that there is no elevation between the inlet and the outlet of the pipe ($\frac{\partial z}{\partial x} = 0$), the 1D momentum equation can then be simplified as follow:

$$P_i^{su} - P_i^{ex} = \beta_{friction,reg} \tag{4.5}$$

Conservation of energy

The last 1D Euler equation with regard to the conservation of energy takes the following form:

$$\frac{\partial(\rho \cdot e)}{\partial t} + \frac{\partial((\rho \cdot e + P) \cdot v)}{\partial x} = v \cdot \beta_{gravity} + \beta_{convection} \tag{4.6}$$

with

$$\begin{cases} e = h + \frac{1}{2} \cdot v^2 \\ \beta_{convection} = \dot{q}^{loss} \end{cases} .$$

Considering an incompressible fluid and applying the previous equation for mass conservation (cf. Eq. 4.2), a simplification of the energy equation could be obtained as in [117]:

$$\dot{q}^{loss} = \rho \cdot V \cdot \frac{\partial h}{\partial t} \tag{4.7}$$

These 3 simplified conservation equations can be solved numerically using the finite volume method for the modelling of the flow of an incompressible one-dimensional flow into a pipe. Assuming an incompressible fluid, fluid properties calculations are simplified with the finite volume method to reduce the computation time. In order to keep the computational time in acceptable bounds, the

[1] This assumption is made to simplify the conservation equation even though it is not always the case in a real heating network.

cell size Δx as well as the integration timestep Δt have to be kept sufficiently large which can lead to numerical diffusivity. For computational fluid dynamics problems, a dimensionless number, the Courant number (Co), is defined:

$$Co = \frac{v \cdot \Delta t}{\Delta x} \tag{4.8}$$

To avoid numerical diffusivity, this number must be as close as possible to unity (while remaining lower than one). Large numerical diffusivity appears with low Courant numbers. These aspects are detailed in [118] where the interested reader can refer to for more information. The influence of this Courant number on the numeric solution is also indirectly illustrated in the following while comparing this method with the Plug Flow Method.

4.1.1.2 Plug Flow Model

The Plug Flow method is an alternative approach where thermodynamic properties are calculated only at both ends of the pipe. A time delay function determines the residence time of an amount of fluid within the pipe in order to assess heat losses. This method can be characterized as a Lagrangian approach regarding the motion of a fluid particle as a function of the time and initial flow conditions. The resulting model gives an analytic expression of the pipe outlet temperature from conservation equations.

As illustrated in Figure 4.2, the Plug Flow Method considers an amount of flow entering the pipe at a given time t_0 and outcoming after $t_0 + \Delta t$ seconds. An amount of fluid entering at a temperature T_3 for example is flowing into the pipe of length L during Δt seconds. Based on this representation, a time delay function taking into account this timestep Δt can be defined. This method enables to compute fluid properties only at the inlet and the outlet of the pipe reducing significantly the number of calculations to perform and indirectly the computation time. Moreover, this method enables to avoid numerical diffusivity which can be a problem for the dynamic modelling of heating networks.

Time delay function

The time delay is computed from the one-dimensional wave equation enabling to compute properties of each fluid segment in spatial and time coordinates:

$$\frac{\partial z(y,t)}{\partial t} + v(t) \cdot \frac{\partial z(y,t)}{\partial y} = 0 \tag{4.9}$$

with $z(y,t)$ representing the transported quantity as a function of the normalized spatial coordinate y and $v(t)$ the normalized velocity of the fluid in the pipes. A more detailed explanation of the time delay model can be found in [119]. This wave equation is useful for analyzing the dynamic behaviour of the network and to consider the heating network itself as a heating storage system using the dynamics phenomena occuring into the system since it does not involve any additional investment cost compared to thermal storage tanks [120].

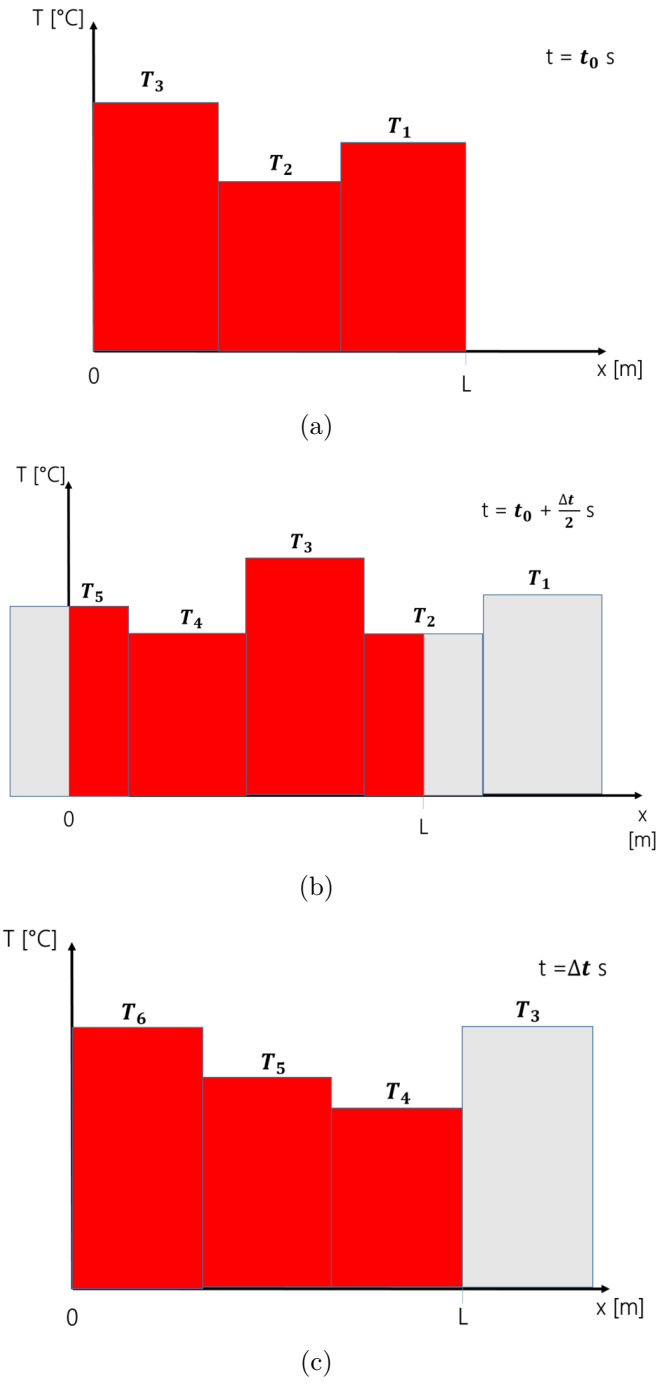

FIGURE 4.2: Principle of the Plug Flow Method.

Heat losses calculation

The aforementioned plug flow method implemented in the *IBPSA* library [121] in *Dymola* is based on a combination of the energy and continuity equation. Neglecting axial diffusion and dynamic effects due to pressure losses and pipe frictions, the conservation equation can be written as follow:

$$\frac{\partial(\rho c_V AT)}{\partial t} + \frac{\partial(\rho c_V AvT)}{\partial t} = -\dot{q}_{loss} \text{ with } \dot{q}_{loss} = \frac{T(t) - T_{sur}}{R} \tag{4.10}$$

A corresponds to the total circumferential area of the pipe, v is the velocity of the fluid in the pipe and $\dot{q}_{loss}$ represents heat losses along the pipe in W/m assuming a constant thermal resistance R between the pipe and its surroundings. Considering a constant surroundings temperature T_{sur} prescribed by the ground temperature for the case of buried pipes into a heating network and setting a constant heat capacity per unit length $C_V = \rho c_V A$, Eq. 4.10 can be integrated spatially on a non-zero infinitesimal step δx:

$$C_V \cdot \frac{dT(t)}{dt} \cdot \delta x = -\frac{T(t) - T_{sur}}{R} \cdot \delta x \tag{4.11}$$

Integrating this ordinary differential equation on the time delay Δt computed from Eq. 4.9, the analytical expression of the pipe outlet temperature can be written:

$$T_{out} = T_{sur} + (T_{in} - T_{sur}) \cdot e^{-\frac{\Delta t}{R \cdot C_V}} \tag{4.12}$$

From Eq. 4.12, it can be seen that the outlet temperature is only dependent on the inlet temperature, the surroundings temperature and the time delay. Thermodynamic properties at intermediate locations inside the pipe are thus not necessary in this case. Thermal inertia of the pipe is included in the model by an addition of thermal capacities to this plug flow model.

4.1.1.3 Comparison of the finite volume and plug flow method

Before simulating the test case presented in Chapter 3, a simple test case is used to compare both methods. It simply consists in studying a 1 km long pipe with a step increase of temperature of 10°C at the inlet of the pipe. Due to the significant length of the pipe and the relatively slow prescribed velocity of the fluid ($\approx$ 1m/s) in the pipe in order to avoid important pressure drops, delay effects can appear in the pipe due to the propagation time of the heat wave due to these slow velocities.

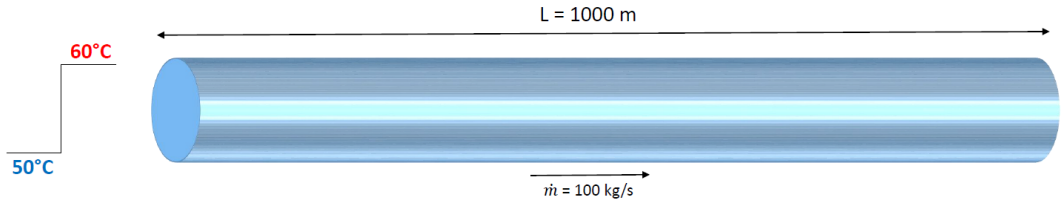

FIGURE 4.3: Case study: 1km long pipe with an increase of temperature of 10°C at the inlet.

Firstly, the use of a finite volume model from the *ThermoCycle* library in *Dymola* with different discretization steps (10, 100 cells or 200 cells) shows the influence of the discretization scale on numerical diffusivity effects.

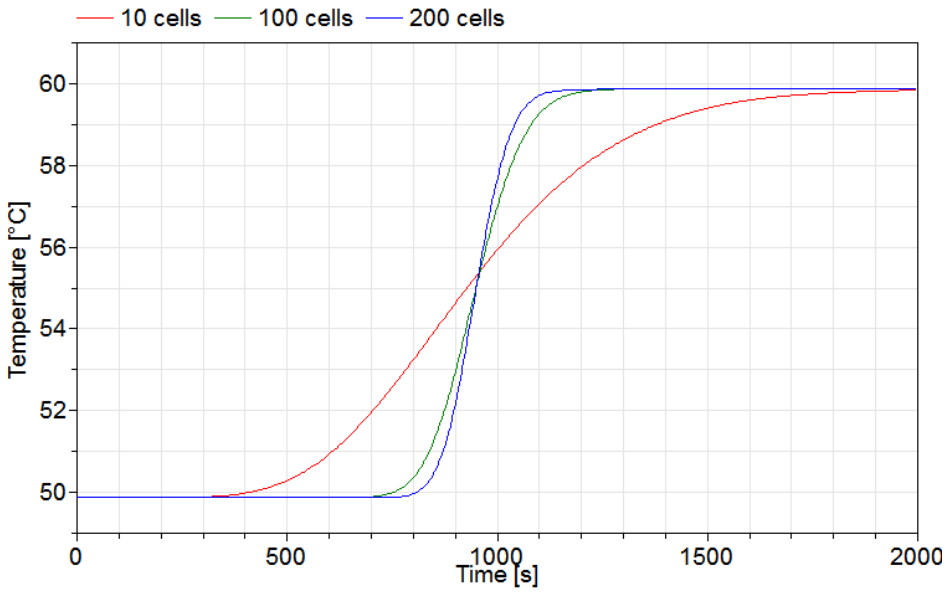

FIGURE 4.4: Evolution of the temperature with a finite volume model in *Dymola* for different discretization scales.

As can be observed in Figure 4.4, the increasing number of cells enables to decrease the numerical diffusivity of the problem approximating more accurately the exact solution of the problem. However, the increase of the number of cells requires a more significant computation time. Compared to the finite volume model commonly used in the modelling of thermal systems, the use of a plug flow model for the computation of the temperatures at the inlet and outlet of the pipes enables to avoid any numerical diffusivity in the numerical solution (cf. Figure 4.5). Therefore, from a numerical point of view, it is more interesting to use this approach for the computation of the temperatures into the system.

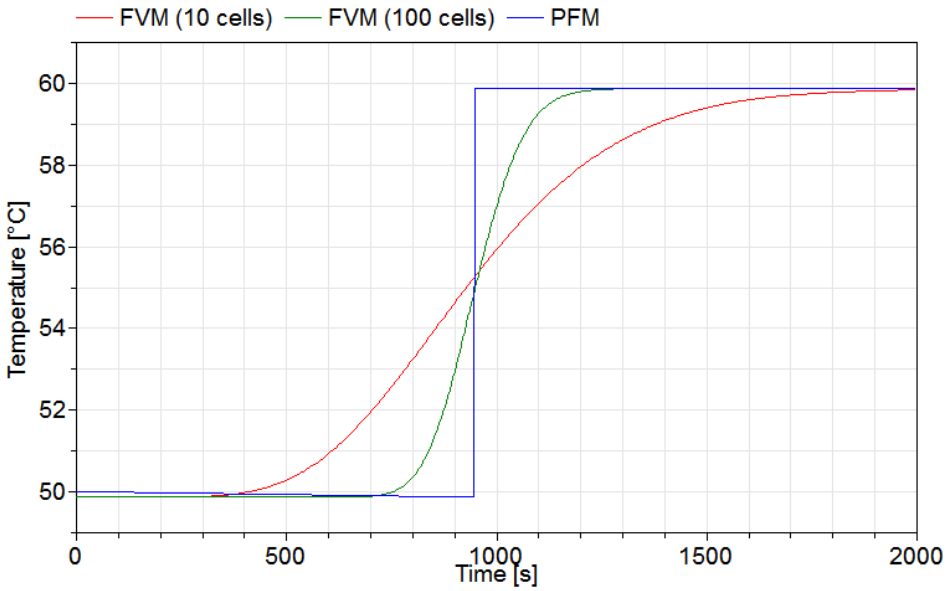

FIGURE 4.5: Evolution of the temperature with a PFM in Dymola.

As shown in the previous section, the plug flow model gives more accurate results than the finite volume model. Comparing in Table 4.1 the finite volume method with 100 cells and the plug flow model with regard to the computation time, it can be observed that in addition to provide a better solution, the plug flow method is faster than the finite volume method. This computation speed is mainly due to the computation of the temperatures at only two points (the inlet and the outlet of the pipe) compared to the finite volume method which requires the computation of thermodynamic state variables in each discretized cell of the pipe.

TABLE 4.1: Computational performance with Finite Volume Model (FVM) and Plug Flow Model (PFM).

Dymola FVM [s]	1.49
Dymola PFM [s]	0.19

Consequently, following this analysis, the plug flow model in *Dymola* seems to be the best solution to consider for the modelling of district heating systems. There are two models using the plug flow method in the *IBPSA* library from *Dymola*:

- An adiabatic model that does not take into account heat losses in the pipes due to a temperature difference between the fluid in the pipes and the outdoor temperature;
- A pipe core model taking into account heat losses in the pipes;

Models including heat losses are used for the modelling of the network in this chapter in order to compare heat losses computed from the optimization model and the dynamic model. A graphical representation of this type of pipe in *Dymola* is proposed in Figure 4.6.

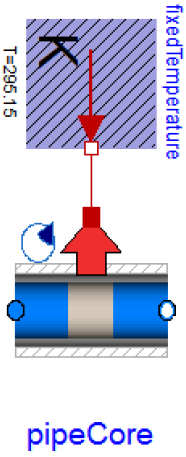

FIGURE 4.6: Model of pipes with heat losses in *Dymola*.

4.1.2 Heating source model

For the heating source, an ideal heating source sets prescribed temperatures and pressure levels as a function of the total heating demand over the network. Heating temperatures are prescribed as inputs of the model such that the model enforces the outlet temperature of the heating source being equal to the operating set point temperature $T^{w,in}$ (= 90°C) of the network prescribed for third generation heating networks. A detailed view of the component is proposed in Figure 4.7.

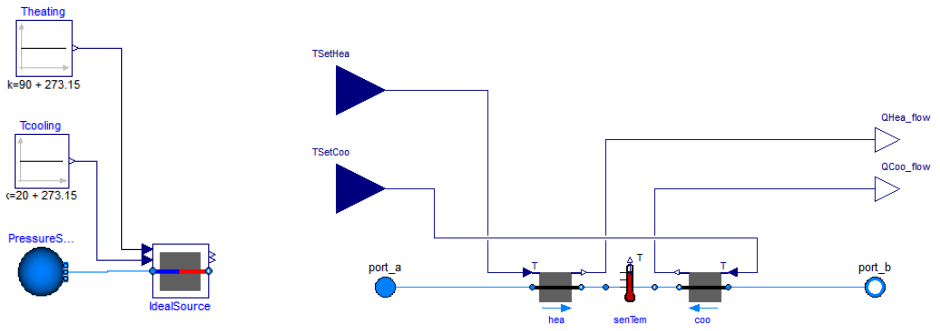

(a) (b)

FIGURE 4.7: Model for the heating source.

Prescribing a set point temperature at the inlet of the network and knowing the total mass flow rate $\dot{m}_{tot}$ over the network (prescribed by the mass flow rates flowing through the substations with a prescribed temperature difference ΔT_{sub} = 30 °C as in the optimization model in Chapter 2), the required heating production to feed the whole network can be computed as in Eq. 4.13.

$$\dot{Q}_{tot} = \dot{m}_{tot} \cdot c_{p,w} \cdot (T^{w,in} - T^{w,out}) \tag{4.13}$$

with $T^{w,in} = 90°C$ and $T^{w,out}$ is prescribed by the temperature difference ΔT_{sub} at the substations.

4.1.3 Substation model

For the modelling of the substations feeding the heating consumers all over the network, a simple model developed in the *Buildings* library is used. This model gets as an input a time table identifying hourly heating demands for each substation $\dot{Q}^{heat}$ and the temperature difference at the primary side of the substation is prescribed. Mass flow rates into the substations can then be directly computed as described in Eq. 4.14 considering a constant heat exchanger efficiency. In practise, this efficiency is dependent on the operating conditions. However, for the simulations, a constant efficiency is assumed as in the optimization model. The substation model simply computes a mass flow rate from a prescribed temperature difference ΔT_{sub} at the substation and the total heating demand linked to the substation $\dot{Q}_{sub}$.

$$\dot{m}_{sub} = \frac{\dot{Q}_{sub}}{c_{p,w} \cdot \Delta T_{sub}} \tag{4.14}$$

4.2 Dynamic simulations of the theoretical case study

The optimization tool presented in this thesis has been applied to the theoretical case studied in Chapter 3 in order to optimize the sizing of the heating sources and the pipes as well as the outline of the network. The optimal heating network resulting from the optimization process can now be modelled with the dynamic model described in the previous section in order to take into account real physical phenomena into the network. Results relying on dynamic simulations are useful to check the consistency of the main assumptions linked to the optimization model. The optimized heating network in Scenario 3 of the theoretical case study in Section 3.2 based on a 90-60°C temperature regime is illustrated in Figure 4.8.

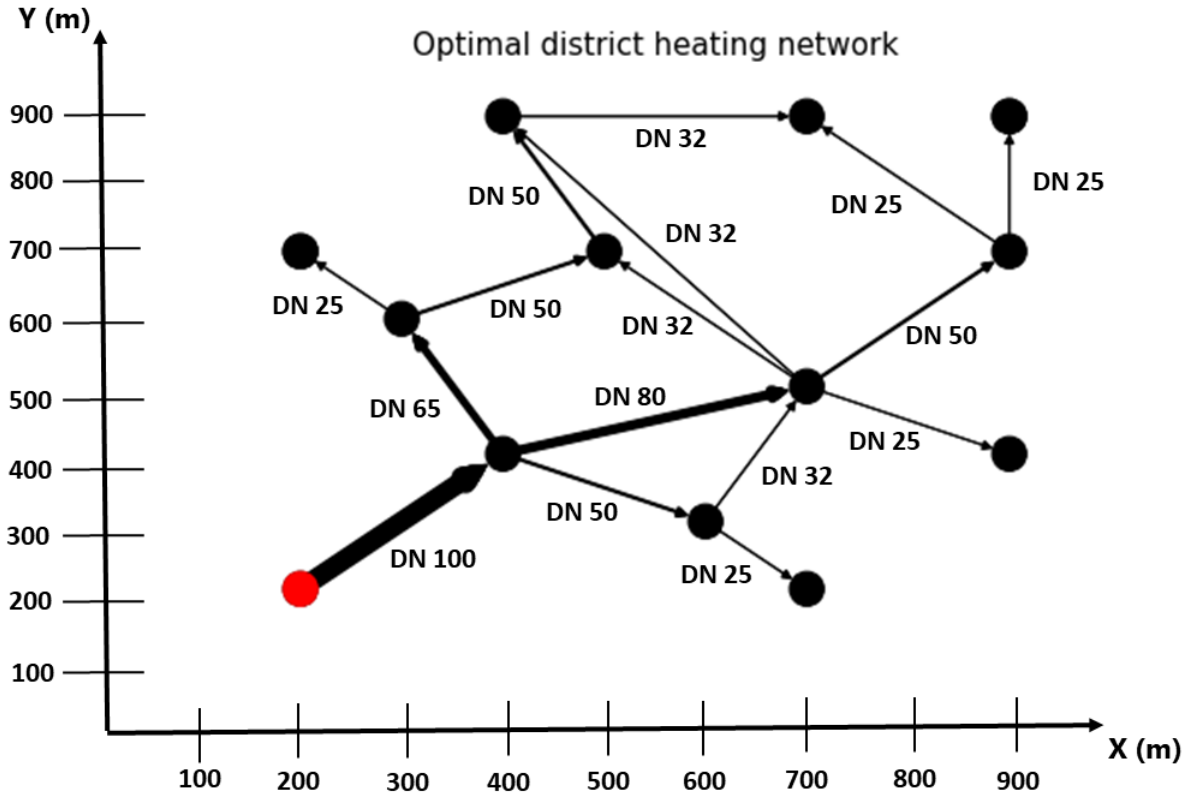

FIGURE 4.8: Map of the optimal network sized by the decision tool.

This heating network can be modelled using *Dymola* prescribing all the features of the network like the pipe diameters as well as the temperature operating set points from the optimization formulation in Chapter 2. The *Dymola* model depicted in Figure 4.9 can then be used to study the behaviour of the network over the whole year. Prescribing the hourly heating demands computed in Chapter 3, the use of the dynamic model can provide the value of the main operating features of the network including heat losses.

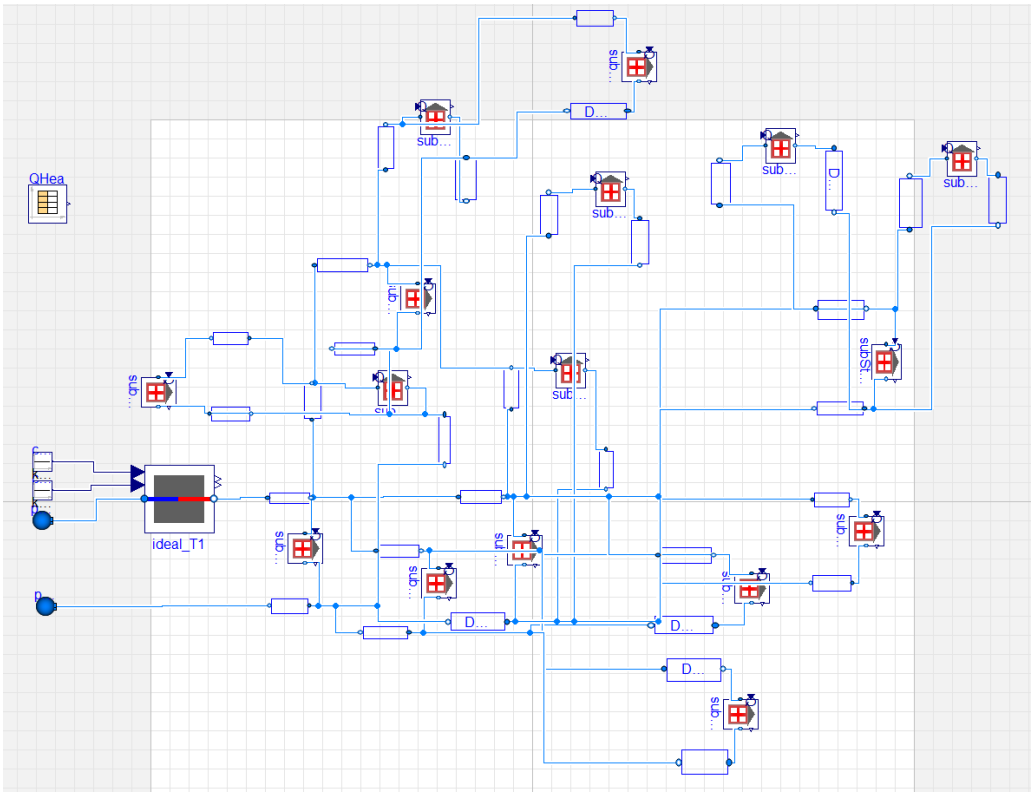

FIGURE 4.9: Dynamic model of the optimal network sized by the decision tool.

4.2.1 Heat losses for a 90-60°C operating network

The optimized network has been sized considering a 90-60°C nominal operating regime. Based on this operating regime with a constant temperature difference at the substations, the dynamic model can be used to assess the heat losses throughout the year. Figure 4.10 exhibits the heat losses computed with the optimization model and with the dynamic model.

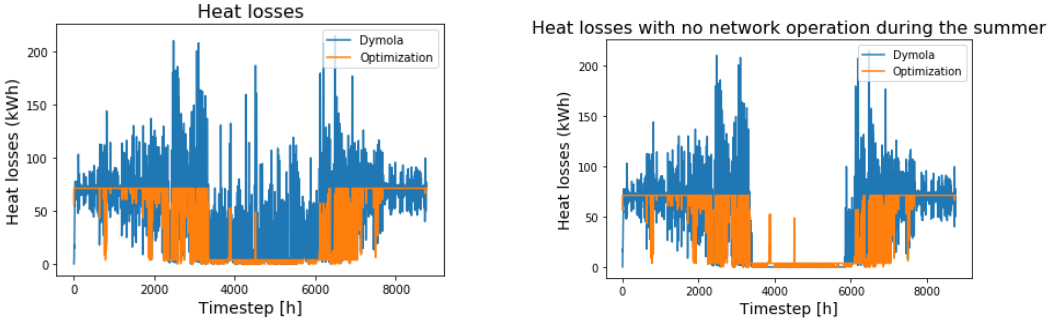

(a) Normal operation.

(b) Without operation during the summer.

FIGURE 4.10: Comparison of the heat losses with the optimization model and the dynamic simulations.

It can be observed that with the optimization model, heat losses are assessed to be more or less constant over the year except during very low heating demand

periods (in the summer for example) for which they are equal to zero because of the non operation of the network during too low heating demand periods. This approximately constant heat losses profile is due to the linearization of the heat losses as a function only of the power flows into the pipes. As can be observed in Figures 2.11 and 2.12, heat losses are dependent on the range of power flows into the pipes. For the studied case in this chapter, global power flows are included between 0 and 5 MW_{th} such that heat losses vary very little within this power range using the linear formulation presented in Chapter 2. However, as explained in this chapter, this formulation takes into account nominal operating conditions using a generic formula dependent only on the power flows. For operating conditions out of the nominal conditions, small power flows are supplied into large pipe diameters such that heat losses computed with the dynamic model are larger than the ones computed with the optimization model.

For a prescribed temperature difference at the substations, heat losses with the dynamic model compared to the optimization model are significant during the summer characterized by periods of very low heating demands. These non-zero very low heating demands lead to very low mass flow rates into the pipes of the network. Pipes diameters of the network being sized for nominal operating conditions, the velocities into the pipes during these low heating demand periods are significantly low. The time residence of the fluid into the pipe then increases leading to a large temperature decrease into the pipe as represented mathematically by Eq. 4.12. In a well-regulated heating network, the temperature difference at the substations is not constant because the network operator looks for optimally operating the network prescribing the most adequate temperature levels in order to minimize heat losses. Indeed, the optimal operation of the network requires to guarantee an optimal mass flow rate into the pipes by decreasing the prescribed temperature difference at the substations during periods of lower heating demands. However, it is not the goal of this thesis: other scientific works mentioned previously focus on this research topic. A constant temperature difference is prescribed in the dynamic model used in this chapter to compare fairly the optimization model and the dynamic simulations. In order to take into account these heat losses as consistently as possible compared to real operating conditions and based on the optimal operation determined by the decision tool, a scenario without network operation during too low heating demand periods (especially during the summer) due to too large heat losses is considered to fairly compare heat losses with the optimization tool and the dynamic model. Table 4.2 compares heat losses with the optimization model and the dynamic simulations.

TABLE 4.2: Comparison of the heat losses with the optimization model and the dynamic simulations.

	Optimization model	**Dynamic simulations**	**Dynamic simulations with no summer operation**
Heat losses (GWh)	0.355	0.856	0.776
Heat losses ratio (%)	5.43	13.10	11.88

As previously explained, heat losses are underestimated with the optimization model because of the assumption to operate the network in nominal conditions all over the year even with a constant temperature difference at the substations. However, even if these heat losses are underestimated, a heat losses ratio around 5% seems acceptable for a heating network. However, heat losses ratios around 10-15% are generally observed in real third generation district heating network projects [122]. Moreover, as shown in Table 4.2, a heat loss ratio of the same order of magnitude has been computed with dynamic simulations. In order to take into account this underestimation of the heat losses in the optimization model, a calibration factor increasing the heat losses variable $\dot{Q}^{loss}_{j,d,t}$ is used to show the influence of the assessment of the heat losses in the optimization model on the outline and the sizing of the heating network.

4.2.1.1 Calibration on the parameters for the assessment of the heat losses

To fit as well as possible the heat losses computed with the dynamic model with no network operation during the summer, a scale factor based on the heat losses computed for both cases is used to fit the value of the global heat losses over the year of the optimization model with the value of the heat losses with dynamic simulations. Based on values from Table 4.2, a scale factor is applied to the value of the variable $\dot{Q}^{loss}_{j,d,t}$ in Eq. 2.19. This scale factor is computed as follows:

$$\text{Scale factor [-]} = \frac{\begin{array}{c}\text{Heat losses with dynamic simulations} \\ \text{with no summer operations [GWh]}\end{array}}{\text{Heat losses with the optimization model [GWh]}} = 2.19$$

Based on this scale factor, a comparison of the initial scenario and the new one with a scale factor applied to the heat losses variable $\dot{Q}^{loss}_{j,d,t}$ is then provided hereafter.

TABLE 4.3: Comparison of the results with the initial and the calibrated optimization model.

	Initial optimization	**Calibrated optimization**
Used heating capacity (MW_{th})	5.324	5.409
CAPEX (M€)	3.346	3.346
OPEX (M€)	7.180	7.518
Revenues (M€)	13.684	13.603
Profits (M€)	3.157	2.739

From Table 4.3, it can be observed that the calibration of the heat losses in the optimization model implies a slight increase of the total used heating capacity with an additional thermal capacity of 85 kW to counterbalance the additional heat losses. These additional heat losses require larger heating production levels including these additional heat losses into the total heating production. Total

operating expenses over the 30 year project lifetime then increase by 339,000 € due to additional heating production costs to counterbalance these additional heat losses. However, due to the fact that this increase of the heating production is relatively small compared to the total heating production, there are no consequences on the outline of the network (cf. Figure 4.11). Indeed, the outline remains the same than for the initial scenario such that capital expenses also remain identical to capital expenses of the initial scenario. However, because of the larger heat losses, the optimization model sometimes chooses to do no more operate the network compared to the initial scenario because it assesses the operation as non profitable due to too small heating demands over the network. This implies a reduction of the total revenues of 81,000€ related to the heating sales to the consumers as shown in Table 4.3.

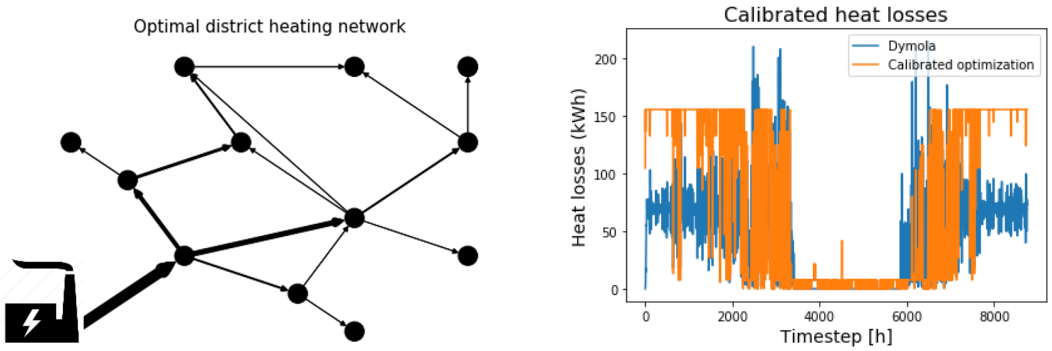

(a) Outline with the calibrated optimization model.

(b) New heat losses with the calibrated optimization model.

FIGURE 4.11: Results with the calibrated optimization model.

Figure 4.11 also illustrates the new heat losses computed from the optimization model compared to the total heat losses computed over the whole year with previous dynamic simulations. The calibration of the heat losses using a scale factor enables to reoptimize the network such that the new optimal heating network and the related heat losses can fit more accurately with heat losses computed with dynamic simulations. As illustrated in Table 4.4, a simple dynamic model based on the operating conditions prescribed by the optimization formulation can therefore be useful to guarantee a more accurate solution by updating the parameters linked to the heat losses for any new heating network project.

TABLE 4.4: Comparison of the heat losses with the calibrated optimization model and the dynamic simulations.

	Calibrated optimization model	**Dynamic simulations with no summer operation**
Heat losses (GWh)	0.718	0.776
Heat losses ratio (%)	10.99	11.88

Indeed, from a dynamic model using the optimal outline and sizing of the first optimization run as an input, the output of this dynamic model

could provide a scale factor used for updating the computation of the heat losses in the optimization model. A feedback looping until reaching convergence between the heat losses computed from the optimization model and with the dynamic simulations could also be useful for this calibration. This was not the core of this thesis but can be seen as a future perspective of this work.

Even though this calibration enables to increase the accuracy of the assessment of the heat losses over the network, prescribing temperature levels over the network in order to optimize the outline and the sizing of the network as a unique function of the power flows into the pipes of the network might imply some limitations about guaranteeing thermal comfort for any consumer connected to the network. Temperature decreases over heating networks may sometimes do not guarantee a sufficient temperature level for the consumers at the end of the network. These temperature evolutions into a heating network are illustrated in the following section to point out the limitations when considering constant temperature levels over the network.

4.2.1.2 Temperature profiles over the network

The optimization tool relies on the assumption of a constant temperature difference at the substations all along the year without any temperature decrease at some points of the network such that a 90-60°C operating regime is prescribed for a third generation heating network. In practise, this assumption is not verified because a temperature decrease is observed along the network. Considering firstly the temperature profile along the main line of the network for nominal conditions, Figure 4.12 illustrates the temperature gradient into the network for nominal conditions.

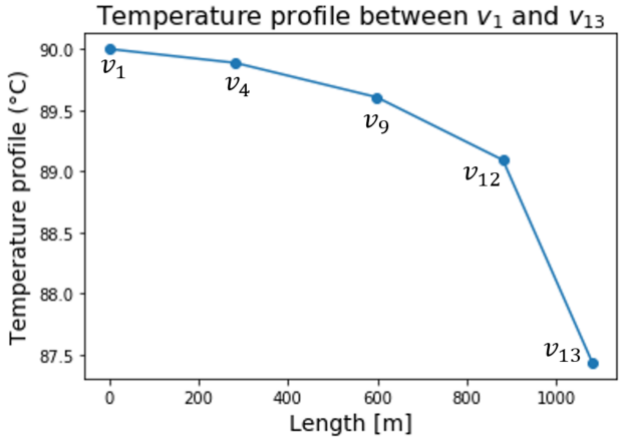

FIGURE 4.12: Temperature decrease along the network for nominal conditions.

The temperature decrease is assessed around 2°C per kilometer of pipe for nominal operating conditions. This temperature decrease is relatively low even if it could get a significant impact for a large-scale heating network spanning over tens of kilometers. Moreover, the temperature decrease can really be affected during periods of low heating demands as previously explained.

As observed in Figure 4.13, the temperature profile throughout the year is totally different during a period of high heating demand compared to a period of low heating demand for a prescribed temperature difference at the substations.

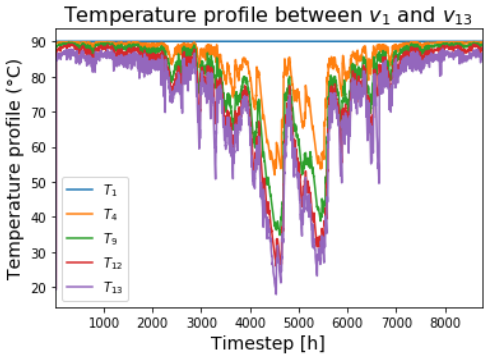

(a) Temperature between node v_1 and v_{13}

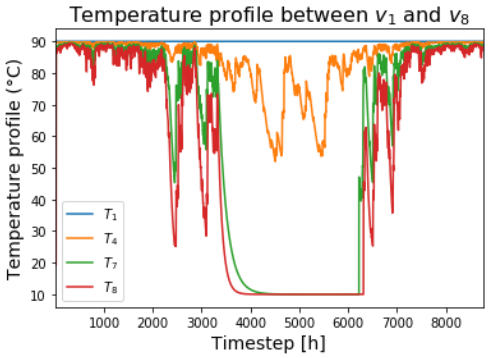

(b) Temperature between node v_1 and v_8

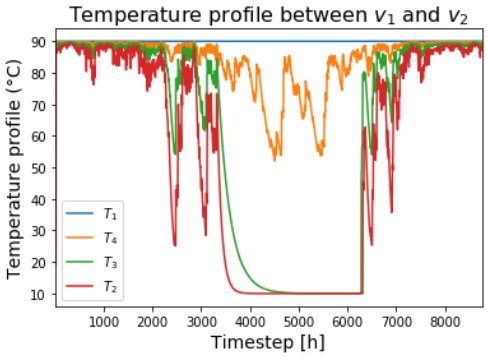

(c) Temperature between node v_1 and v_2

FIGURE 4.13: Temperature profile along different branches of the network.

Two main observations can be drawn out from Figure 4.13. The first one is that the temperature decrease is really significant during periods characterized by a low heating demand for a prescribed temperature difference at the substations such that assuming heat losses as linearly proportional to the heat flow into a pipe does not represent the real physics of the system. The second one is that this temperature decrease can mainly be observed in network pipes with a nearly zero heating demand during a part of the year as observed in edges v_7v_8 and v_3v_2. In these edges, the heating demand is really close to zero such that the residence time of the fluid into the pipe is sufficiently high for a decrease of the temperature from a supply water temperature of 90°C to the surroundings temperature of 10°C. As explained previously, during these periods of low heating demands, it is thus required that the operator reduces the prescribed temperature difference at the substations in an optimal way to avoid a too important temperature decrease over the network or that the operator does not operate the network because of the too low heating demands.

The decision tool presented in this thesis has thus some limitations for the modelling of physical phenomena like the heat losses into the network. One of the goals of the decision tool relies on the robustness of an optimization

process applied to a heating network for large-scale case studies such that a linear formulation has been chosen to guarantee a unique optimal solution for any new case study. However, this linearization leads to some assumptions and approximations which neglect some physical phenomena into the optimized designed network.

The use of the decision tool has thus to be complemented by the use of a dynamic model, as the one presented in this chapter, to analyze the main physical trends linked to the pre-designed strategy defined by the decision tool. The dynamic model can then be a powerful tool to calibrate the optimization model in order to assess in a more consistent way heat losses over the network.

4.3 Conclusion

The decision tool presented in this thesis relies on an optimization model which has been linearized to guarantee robustness and convergence for any case study from small-scale instances like in Chapter 3 to large-scale instances like in Chapter 5. This linearization leads to some approximations which can provide trends to estimate the profitability of a heating network into a given area. However, the optimization model can not determine accurately the heat losses which are linked to the mass flow rates into the network in a non-linear way. This chapter highlights this weakness of the presented optimization methodology by providing a complementary dynamic model to the optimization tool to illustrate more accurately the physics of the system.

A literature review has been performed to identify simple dynamic models which could be used for modelling the heating network based on operating conditions prescribed by the optimization model. After selecting the optimal dynamic model to handle with physical phenomena, a comparison of the results obtained with the optimization model and the dynamic model shows that as expected, the optimization model underestimates the total heat losses. Even though the assessment of the heat losses with the optimization model seems to provide an acceptable heat losses ratio around 5%, a calibration on the heat losses variable is achieved in the optimization model.

This calibration enables to fit the assessed heat losses in the optimization model with the heat losses computed from the optimization model. This calibration could be considered in a generic retroactive looping using dynamic simulations to update heat losses in the optimization formulation until reaching convergence between both models. This is not implemented in this thesis but is considered as a perspective for further works.

Chapter 5

Application of the decision tool to a large-scale real case study

"The scientist is not a person who gives the right answers, he's one who asks the right questions."

—Claude Levi-Strauss

One of the goals of the decision tool presented in Chapter 1 relies on the applicability of this tool to any new case study from small-scale to large-scale applications. More specifically, as a reminder, the initial purpose of the tool is based on its applicability to a large-scale neighbourhood of the township of Herstal (Liège, Belgium) for helping the industrial company (*Coriance*) to design of a third generation heating network based on different inputs parameters defined by the company. As illustrated in the previous chapters, in the frame of the *EcoSystemPass* research project, this thesis aims for developing a generic optimization tool which can be applied to third generation heating networks and easily replicated to fourth generation heating networks for future projects. From pre-defined inputs data given by other research groups working on this research project, the decision tool can then optimize different scenarios for implementing the future Herstal heating network from prescribed constraints.

Chapter 3 illustrated the main application fields of the decision tool on a theoretical case study showing the influence of some economic and urbanistic parameters on the outline and the sizing of heating networks. Before applying this decision tool to the real case for which this tool is dedicated, some limitations of the decision tool have been highlighted in Chapter 4. It has been shown that the user of the decision tool has to be careful about the consistency of the results provided by the optimization model because of the limitations on the accuracy of the results linked to some hypotheses into the optimization formulation. However, this decision tool can be used for a pre-feasibility study for providing the first trends to follow for implementing a heating network into a specific geographic area. This last chapter finally aims for showing that the model fills in one of the main features mentioned in Section 1.3.1: its applicability to large-scale cases like the one studied for the initial research project linked to this thesis. In order to help the decision-makers of the heating network project for implementing a third generation network based on the main parameters they want to study, a quick

overview of the influence of these parameters on the outline and the sizing of the network is provided into this chapter.

5.1 Introduction

Herstal is a municipality in the province of Liège in Belgium. It has an area of 23.5 km^2 and has 38,355 inhabitants, i.e. a density of 1629.2 inhabitants per km^2 [123]. This municipality is characterized by a waste incinerator in charge of the waste treatment of the city district of Liège. This incinerator manages waste from 72 municipalities such that an average of 1 000 tons of waste are burnt every day into the waste incinerator. This combustion process is used to generate 180 tons/h of steam at 400°C which is used to produce electricity using a turbine with a nominal electric power of 35 MW_{el}. Annually, 320,000 tons of waste enable to produce 240 GWh_{el} equivalent to the electricity consumption of 54,000 households [124]. Currently, the energy recovery of incinerated waste is carried out exclusively as electricity. The opportunity to recover a part of the residual energy for the feeding of a heating network has been recently studied. This heating network would aim to connect dwellings around the waste incinerator as well as a future greenhouse dedicated to the production of pharmaceutical molecules. The heating network project wants to promote the access to cheap and decarbonized heat to the several end consumers located in the area: schools, hospitals, public buildings, nursing homes and residential dwellings.

5.2 Case Study

The studied case considers a geographic area of 3 km^2 around the waste incinerator with a potential connection of a future greenhouse at a given location close to the incinerator and another available surface of 250 000 m^2 for the building of new prospective dwellings and/or heating sources. A graph representation of the studied area and its heating source is given in Figure 5.1. The area is made up of 1780 streets with a representative graph related to this area of 3560 edges and 1296 nodes.

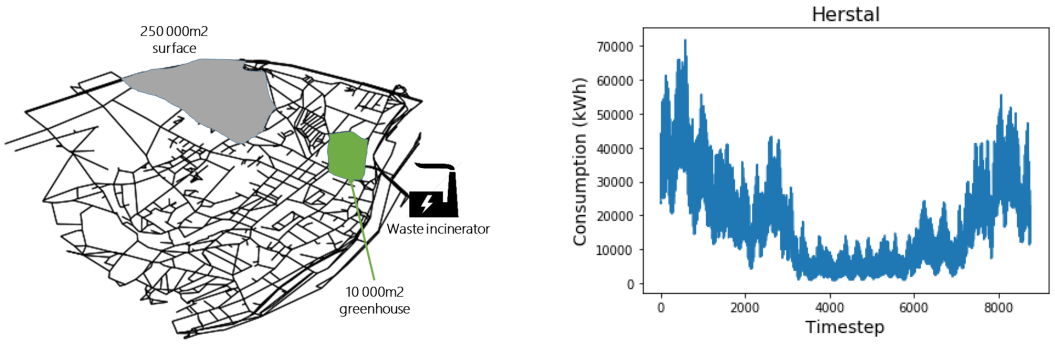

(a) Graph representation of the area

(b) Heating consumption of the area

FIGURE 5.1: Representation of the case study of Herstal.

At the initial stage, the district heating project relies only on the use of the waste incinerator to feed the neighbourhood made up of dwellings of different kinds but also of a future greenhouse of 10,000 m2 which could be built in the following years. The initial project is based on this unique heating source with a prescribed constant heating production cost of 0.03€/kWh. The waste incinerator is going to be upgraded into a combined heat and power plant. For this case study, using a representative year with 144 timesteps, the model contains 2,808,510 variables and is solved using the Gurobi solver with an optimality gap of 5% in order to limit the computation time of the problem due to the large number of variables. The computations are executed in 4,465 seconds on a calculation server with 48 Intel® Xeon® E7 v4 2.20 GHz processors with a total RAM of 126GB.

5.2.1 Influence of the heating sales price on the network

The decision tool enables to provide a support to the stakeholders for heating network projects defining inputs parameters specific to each studied area and based on the market conditions.

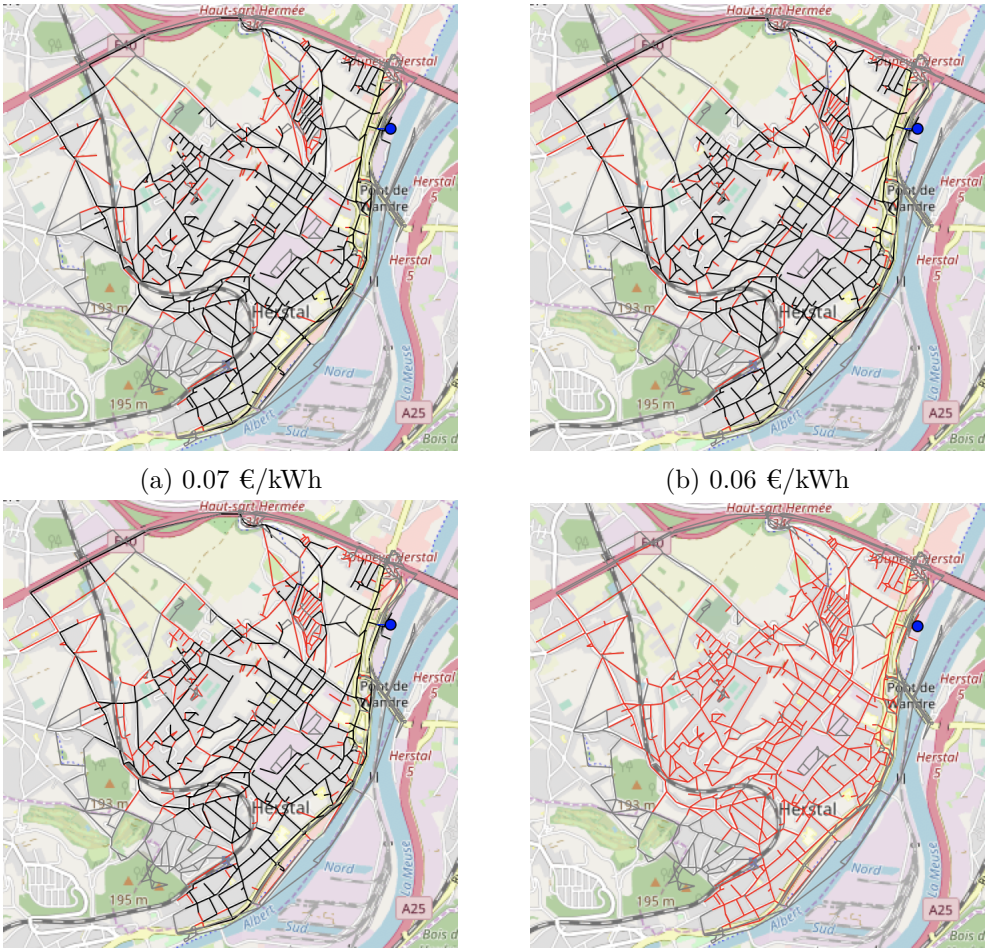

(a) 0.07 €/kWh (b) 0.06 €/kWh

(c) 0.05 €/kWh (d) 0.04 €/kWh

FIGURE 5.2: Outline of the network for different heating sales prices.

As previously in Chapter 3, the initial scenario considers a market price equivalent to the current gas price on the market. However, this status quo market

price is not necessarily a sufficient condition for heat consumers to change their heating production supply from a gas network to a heating network. The influence of the heating sales price on the profitability of the heating network is thus analyzed in this section. A parametric study decreasing the heating sales price from 0.07€/kWh to 0.04€/kWh enables to show the influence of the heating sales price on the outline of the heating network as represented in Figure 5.2. It can be observed that for a heating sales price of 0.07 €/kWh, most streets (806 out of 866 streets), depicted in black, are connected to the network while some others, depicted in red, are not integrated into the heating network because they are assessed to be non-economically profitable to connect.

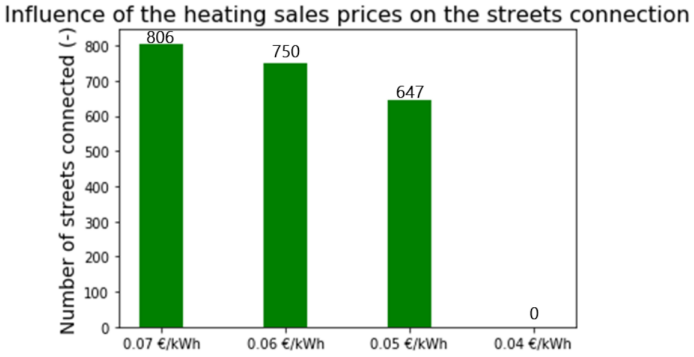

FIGURE 5.3: Number of connected streets for different heating sales prices.

As illustrated in Figures 5.2 and 5.3, the decrease of the heating sales price reduces the number of connected streets to the network for remaining economically profitable. Some streets which were attractive consumers to connect are no longer profitable because their heating consumption does not ensure a sufficient return on investment compared to the initial investment costs required to connect these streets to the network. The optimization tool also enables to determine a trade-off of the critical heating sales price below which it is no longer profitable to build a heating network because of the too high capital and operating expenses compared to the heating sales revenues. The decrease of the heating sales price obviously increases the period of return on investment linked to the network project.

As illustrated in Figure 5.4, despite the smaller capital expenses due to a decreasing number of connected streets to the network, the heating sales revenues from the network are smaller with a decreasing heating sales price. Therefore, the expenses linked to the network are recovered after a longer period of time such that the period of return on investment is directly linked to this heating sales price. Indeed, a decrease of the heating sales price from 0.07€/kWh to 0.05€/kWh leads to an increase of the period of return on investment from 10 years to 17 years. The assessment of the optimal heating sales price enabling to guarantee a maximum connection rate to the network is thus an important step before the outline and sizing of any new heating network project. The submission of market surveys to the potential heating consumers of a new heating network project remains essential to ensure consistency between the optimization model and the market reality.

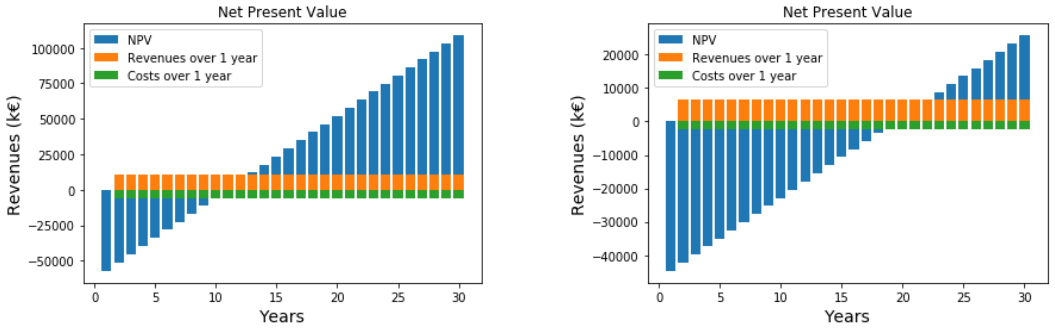

(a) 0.07 €/kWh (b) 0.05 €/kWh

FIGURE 5.4: Influence on the net present value of the project for a heating sales price of (a) 0.07€/kWh (b) 0.05€/kWh.

5.2.2 Influence of the connection rate on the network

As for the study of the influence of the heating sales price on the network, a parametric analysis concerning the connection rate into a street can be achieved in the following. There is no obligation for a heating consumer to connect to a heating network even if the street is fed by a pipe of the network. For the stakeholders of a future network project, it is thus important to assess the heating load specific to each street of the network in order to design as consistently as possible the network. As depicted in Figure 5.6 and 5.6, a decrease of this connection rate from 100% to 40% has a similar effect than the decrease of the heating sales price by reducing the number of streets connected to the network.

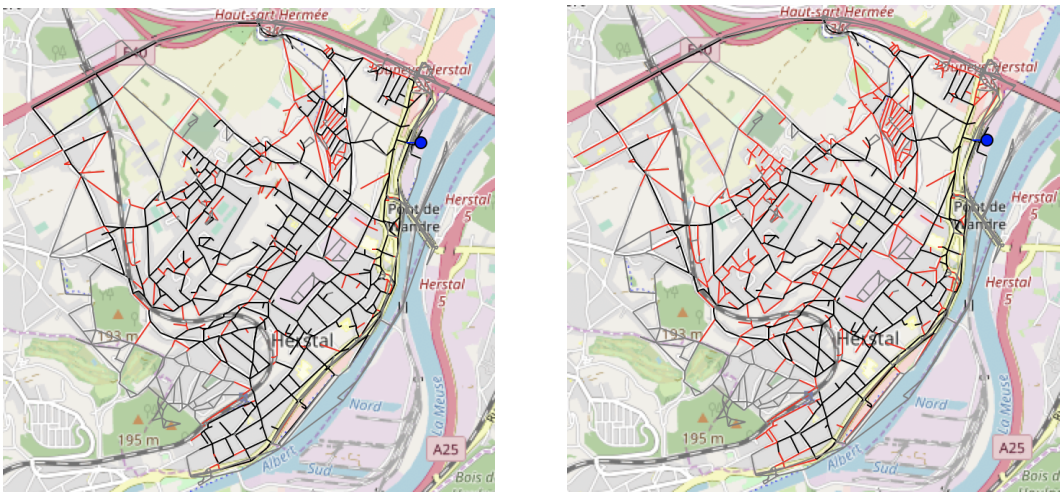

(a) 80% (b) 40%

FIGURE 5.5: Outline of the network for different connection rates.

The decrease of the connection rate obviously decreases the number of connected streets until a break-even point around 20% of connection rate below which it is no longer profitable to build a heating network. Once again, it is therefore important to assess as accurately as possible through market surveys the consumer interest in connecting to a heating network.

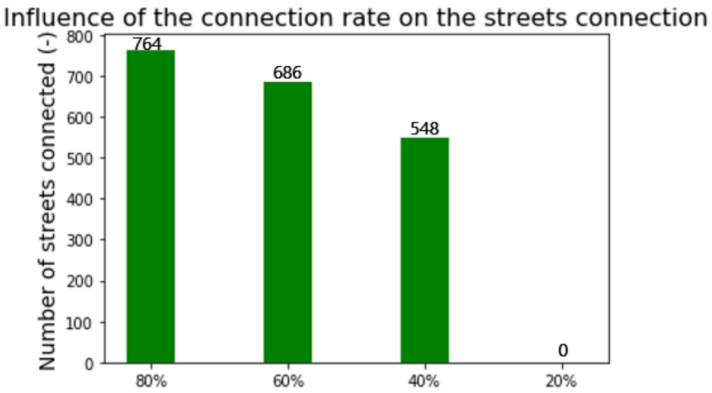

FIGURE 5.6: Number of streets connected to the network for a connection rate from 80% to 20%.

5.2.3 Influence of the greenhouse as a new heating consumer on the network

One of the goals of the research project also relies on the assessment of the profitability to integrate a greenhouse into the studied neighbourhood. This decision tool looks for evaluating the interest for building the greenhouse and to connect this greenhouse to the future heating network project. This scenario then consists in studying the influence of the integration of a 10,000 m^2 greenhouse on the outline and the sizing of an economically optimal heating network. As highlighted in Chapter 3, the greenhouse could be an interesting consumer to integrate into a network thanks to its little fluctuating heating consumption all over the year and especially non zero heating demand during the summer. The optimization formulation presented in this thesis has thus been used to determine the design of the optimal heating network that could be built into the studied area. Results regarding the influence on the sizing of the network for the integration of a greenhouse are summarized in Table 5.1.

TABLE 5.1: Influence of the greenhouse on the economic outputs

	Without a greenhouse	**With a greenhouse**
Used heating capacity (MW_{th})	62.817	62.946
CAPEX (M€)	57.102	57.140
OPEX (M€)	145.930	146.562
Revenues (M€)	315.618	317.054
Profits (M€)	112.586	113.352

The connection of the greenhouse to the network slightly increases the capital and operating expenses linked respectively to the building of a new pipe and substation to connect the greenhouse to the network while increasing the total heating production to supply the additional heating demand of the greenhouse. However, the integration of a greenhouse into the studied area enables to have an additional heating consumer increasing the heating revenues more significantly than the increase of the capital and operating expenses. An influence of the

increase of the size of the greenhouse on the outline and sizing of the network can also be studied. Two additional test cases considering a greenhouse of respectively 50 000 m^2 and 100 000 m^2 are studied for eventually resizing the greenhouse compared to the initial project.

TABLE 5.2: Influence of the size of the greenhouse on the economic outputs

	10 000 m^2	**50 000** m^2	**100 000** m^2
Used heating capacity (MW_{th})	62.946	63.462	64.105
CAPEX (M€)	57.140	57.216	57.237
OPEX (M€)	146.562	149.081	152.204
Revenues (M€)	317.054	322.796	329.973
Profits (M€)	113.352	116.498	120.532

An increase of the size of a consumer like the greenhouse does not influence the outline of the network. 806 streets remain connected to the network while the used heating capacity slightly increases to feed the additional heating demand due to a bigger greenhouse. Revenues from heating sales are again larger than additional expenses for bigger pipes and substations. Therefore, as illustrated in Table 5.2, the profits made up from the new optimal heating network are increasing. The heating demand profile of the consumers influences the required heating capacity and the revenues generated from the heating network. The available building surface of 250 000 m^2 could then be considered as a potential site for the building of new dwellings which would be new heating consumers which could be economically profitable or not to connect to a heating network.

5.2.4 Integration of new heating consumers on the available building surface

The available building surface of 250 000 m^2 could be dedicated for the building of a new neighbourhood. Property investors for the development and implementation of new real estate projects study the heating solutions that can be provided to the new dwellings constitutive of the neighbourhood. One of the solutions could be either to connect the neighbourhood to an existing heating network or a new one thanks to a centralized way of heating production or to feed each dwelling individually with a decentralized heating technology. The decision tool developed all along this thesis can be used to determine which option is the most economically profitable one.

The influence of the building of a new neighbourhood on an existing available building surface can be studied using the decision tool. Considering the 3 first theoretical case studies defined in Section 3.2, these scenarios are considered for the building of a new neighbourhood into the prescribed geographic area. An analysis comparing the integration of these 3 potential future neighbourhoods into the heating network is performed to assess the economic and environmental potential to restore the available building area into a new neighbourhood. The outline of the new heating network is given in Figure 5.7 with the new connected

neighbourhood encircled in green and a summary of the main economic and environmental values is shown in Table 5.3.

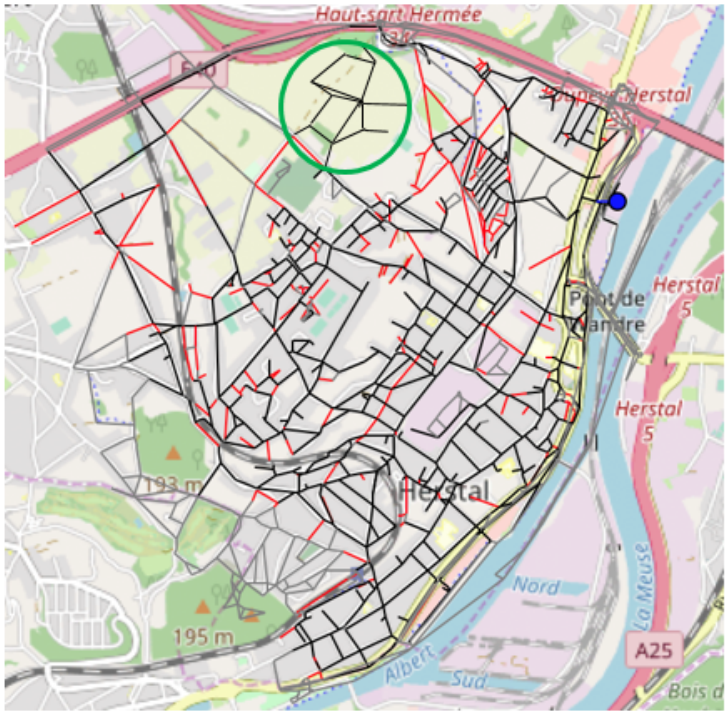

FIGURE 5.7: Optimal network with the inclusion of a new neighourhood.

The outline of the network remains the same except that the 16 additional streets of the new neighbourhood are connected to the heating network project because they are assessed to be economically profitable. Regarding the capital expenses, they slightly increase due to the building of 16 additional pipes and substations. For the operating expenses, they are increasing from one scenario to another because of the larger total heating demand while in parallel, the revenues are increasing due to the larger amount of sold heat to the new consumers. The increase of revenues being larger than the increase of capital and operating expenses, the profits generated from these new scenarios increase as expected.

TABLE 5.3: Influence of the integration of a new neighbourhood.

	Scenario 1	**Scenario 2**	**Scenario 3**
Used heating capacity (MW_{th})	64.334	64.252	64.105
CAPEX (M€)	59.020	59.012	59.008
OPEX (M€)	154.272	154.510	154.842
Revenues (M€)	333.885	334.315	335.103
Profits (M€)	120.593	120.793	121.253

5.3 Influence of the combined heat and power plant on the heating network

For the previous case studies, retrofitted combined heat and power plants were considered as providing mainly heat with electricity as a by-product. However, combined heat and power plants are generally designed for electricity production such that heat is considered as a by-product. The heating capacity of the waste incinerator could therefore be limited by the operation of the combined heat and power plant for the electricity production. Initially, the waste incinerator was designed to produce only electricity from waste incineration exhaust gases. Considering the diagram of the combined heat and power plant linked to the waste incinerator, illustrated in Figure 5.8, a part of the steam used to generate electricity can be tapped to be used as a heating source for the feeding of the heating network.

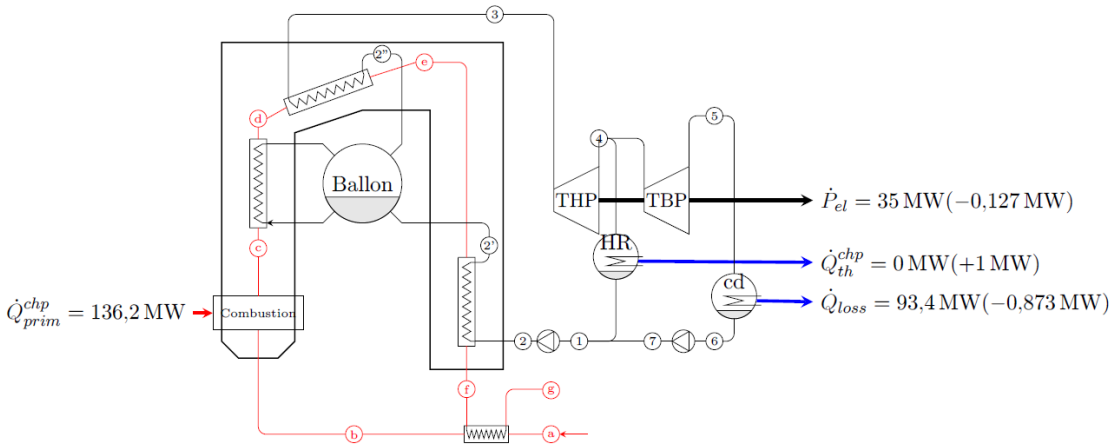

FIGURE 5.8: Diagram of the combined heat and power plant of Intradel (Herstal, Belgium).

Based on an internal report in the frame of the *EcoSystemPass* project, the following available data were provided. The available primary power at the plant is assessed to be of 136.2 MW and can be splitted for producing both heat and electricity. With the current configuration, the plant is initially sized to produce only electricity with a nominal power of $35\mathrm{MW}_{el}$ rejecting a thermal amount of energy of $93.4\mathrm{MW}_{th}$. This thermal energy is at a very low temperature (35°C) such that this heat can not be directly supplied in a district heating network without the use of heat pumps to raise the temperature levels. Another solution which is considered by the future network operator *Coriance* relies on the use of a part of the steam from the turbines for heating production instead of electricity production. This steam extraction between high and low pressure turbines enables to produce heat at 120°C which might be used for a heating network. However, this part of tapped steam to produce heat is not used to produce electricity. For a kWh of heat produced, $0.127\ \mathrm{kWh}_{el}$ are not produced at the turbines. This electricity should have been sold over the electricity network on the day-ahead market. In order to take into account this loss of revenues from the electricity sales, a new computation of the heating revenues can then be defined as follows:

$$R_{\text{heat}} = N_{years} \sum_{d \in D} w_d \cdot \sum_{e \in E, t \in T_D} u_{j,d,t} \cdot w_t \cdot p_j \cdot (r^{heat} - 0.127 c_{d,t}^{elec}) \dot{Q}_{j,d,t}^{heat} \cdot \Delta t \quad (5.1)$$

This new objective function quantifying the net revenues coming from the heating production with the existing cogeneration plant enables to take into account the loss of revenues from the electricity sales by producing heat. A new test case taking into account this electricity sale is then presented in this section to study the optimal layout linked to a cogeneration plant for a real case. Results related to this new case study are summarized in Table 5.4.

It can be seen that revenue losses from electricity sales due to heat production slightly impact the outline and the sizing of the heating network. Indeed, taking into account money losses from electricity sales, the optimal heating network is marginally undersized compared to the initial case such that less streets are connected to the network and profits are decreasing compared to the case with electricity as a by-product. The optimal strategy for a combined heat and power plant aims for maximizing the total revenues from both the heating and the electricity sales. Therefore, some streets with a small heating demand are no longer connected to the network because it is more profitable to produce electricity than additional heat for supplying these streets.

Table 5.4: Influence of the greenhouse on the economic outputs

	Electricity as a by-product	**Heat as a by-product**
Used heating capacity (MW_{th})	62.946	60.569
CAPEX (M€)	57.140	55.560
OPEX (M€)	146.562	143.529
Revenues (M€)	317.054	285.707
Profits (M€)	113.352	86.618
Connected streets (-)	806	776

These results show the importance to take into account the configuration of the existing combined heat and power plants as heating sources for their integration into heating networks. Combined heat and power plants operators try to maximize the total revenues from electricity and heating production such that they are not always interested to sell heat instead of electricity. The outline and the sizing of a heating network can therefore be significantly impacted by the operation of the combined heat and power plant. In order to accurately assess the profitability of a heating network connected to a combined heat and power plant, some dynamic models could be useful to predict the dynamics of the system and optimize the revenues from both heating and electricity sales.

5.4 Conclusion

At the conclusion of this chapter, it has been shown that the methodology developed all along this thesis can be applied to large-scale optimization problems. This feature of the optimization model was one of the main features expected at the beginning of this thesis (cf. Section 1.3.1): the solving of large case studies for the implementation of heating networks at a city scale. Even though this model still presents some limitations which will be reminded in the following chapter, one of the main objectives of this thesis is therefore achieved.

This thesis is part of the *EcoSystemPass* research project which looks for implementing a third generation heating network into a specific geographic area. These first results are optimistic regarding the implementation of a heating network based on an industrial waste heat source and the integration of a greenhouse in the urban landscape. This first large-scale case study could be the opportunity to promote the development of heating networks in other areas in Wallonia. New heating network projects would be the opportunity to continue to develop and enhance the decision tool presented in this thesis by testing it on new case studies. Indeed, the lack of heating network projects in Belgium limits the range of application of the decision tool for the moment and the possibility to add new features to this tool based on the requirements of the stakeholders of the network. This decision tool could for example be adapted for fourth generation heating network projects.

This thesis also relies on provided data whose the consistency can be questionable. Indeed, some inputs data are provided by other research or industrial groups without a sufficient level of details for the required application. There are therefore some limitations about the accuracy of the results independently of the validity of the methodology proposed in this thesis. New contributions for a more accurate assessment of energy demands of the building stocks in Wallonia could be really useful for these kinds of urban planning. Open-source data regarding urbanistic constraints like the available space into the groud are also generally missing while they are of significant importance for heating network projects. This data pre-processing is a part of global energy planning frameworks and therefore deserves a particular focus for future heating network projects in Wallonia.

Chapter 6

Conclusions and perspectives

"What we know is a drop, what we don't know is an ocean."

—Isaac NEWTON

The contribution of this thesis with the new decision tool described in the previous chapters aims for bridging the gap from existing tools which either consider a prescribed topology to optimize the sizing of the heating sources, thermal storages and pipe diameters/temperatures based on the yearly heating load profile or optimize the topology and the sizing of the heating sources and pipe diameters but for operating conditions without thermal storage solutions. Compared to some existing models, this new methodology also targets large ranges of problem sizes from small-scale to large-scale case studies (up to thousands of connected streets) while guarantying numerical robustness and providing solutions in a feasible computational time. A summary of the applied methodology as well as its main outcomes and issues is proposed here below.

Chapter 2 : Presentation of the decision tool

The core of this thesis was to provide a new decision tool for the optimal outline and sizing of heating networks thanks to an optimization method intended to draft efficient systems using heating consumption profiles into a prescribed geographic area. Such tools were already referred to in the scientific literature yet they were often restricted to limit the computational load. The main strengths of this new decision tool can be summarized as follows:

- A mixed-integer linear programming (MILP) model applicable from small-scale to large-scale case studies. The linearity of the model ensures a unique solution and guarantees robustness. All the constraints and objective functions have been linearized in order to solve the optimization problem in an easy way using standard solvers like *Cplex* or *Gurobi*. This linearization of the physics of the system enables to reduce the complexity of the problem for the application of the optimization formulation to large-scale case studies.

- A model combining both the optimization of the outline and the sizing of the network to map and size any new heating network project from a blank sheet. The simultaneous optimization of the outline and the sizing of a heating network requires high computational times such that it

is generally not applicable to large-scale heating networks. To the best of the author's knowledge, this thesis presents the first decision tool including thermal storage solutions able to optimize the outline and the sizing of large-scale heating networks.

- A model which can be connected to a geographic information system and applicable to any new geographic area with potential consumers to connect to a network. This model can then handle urbanistic constraints and be applied to real case studies taking into account the topology of the studied area. This replicability feature enables to propose a methodology that can be used in a general way without the need to change the methodology for a new optimization study.

The decision tool obtained through these specifications was then directly applicable to a range of case studies, from the small-scale to the large-scale, taking into account several different user-defined parameters significant in the optimization of heating networks.

Chapter 3 : Tests of the decision tool on a small-scale theoretical case study

Following the development of the methodology, a small-scale theoretical case study based on existing heating consumption profiles computed from physical models has been considered. This small-scale case study aimed for highlighting the main features of the optimization model and to give some trends about the influence of some parameters on the outline and the sizing of heating networks. The main outcomes provided by the optimization model are:

- Heating consumption levels of the dwellings have an influence on the profitability of a heating network such that consumers with a high heating demand are interesting to connect to a network because heating sales corresponding to these consumers enable to counterbalance the required capital and operating expenses to build the network. Poorly insulated dwellings are therefore interesting consumers to connect to a heating network. Even though a reduction of primary energy consumption related to the poorly insulated dwellings could be achieved by a deep retrofit towards low energy buildings, such a retrofit is not always possible in real-life applications as this requires long-term inhabitants relocations and difficult permitting procedures. Inversely, the implementation of a district heating network is another way to reduce partially primary energy consumption through the use of highly efficient centralized heat production units without the recourse to deep renovation processes. Additionally to these poorly insulated dwellings, heating consumers characterized by a constant large heating demand like greenhouses for instance are such consumers which are useful to integrate into heating networks. Heating networks can therefore be a temporary solution to quickly tackle the problem of decarbonization of the heating sector by substituting decentralized gas boilers by a centralized heating production using partially decarbonized heating sources.

- Heating consumption profiles of the dwellings also get an impact on the profitability of a heating network. Even if two kinds of dwellings are characterized by the same level of heating demand, the repartition of the heating demand over the day can influence the operation of the network and indirectly its outline. The integration of offices with residential dwellings implies a smaller sizing of the network due to a reduction of the total peak demand over this network.

- Centralized heating production using heating networks seems to be competitive compared to decentralized heating production using gas boilers. A heating sales price based on an average gas price of 0.07 €/kWh in the European Union implies that the building of a heating network is economically profitable while using available alternative heating sources like waste incinerators for example. Moreover, heating networks are also environmentally interesting because they generally enable to decrease CO_2 emissions compared to decentralized heating production with gas boilers.

- The heating sales price and the connection rate of consumers into a street are two main parameters which have to be accurately assessed through market surveys for the optimal outline and sizing of heating networks. The number of connected streets depends on these two parameters such that if they are not accurately assessed, the heating network project could become economically non-profitable.

- The funding mechanism used for implementing a new heating network project can lead to a non profitable project with increasing actualization rates. Heating networks have to be funded based on low actualization rates generally coming from public-private partnerships.

- Thermal storage solutions into heating networks can provide additional economic and environmental benefits by integrating new heating sources characterized by variable heating production costs like heat pumps or by a variable capacity factor for technologies like solar collectors.

- Compared to other existing models in the literature, the optimization model in this thesis provides the optimal locations of the heating technologies in order to maximize the net cash flow from the network. Any new heating network can then be defined starting from a blank sheet in an optimal way by using available heating sources and surfaces for the building of new production plants.

- The accuracy level of the optimization formulation gets a large influence on the computation time for solving the problem such that a trade off has been defined between the accuracy and the speed for solving. For speeding up the optimization solving, a reduced number of timesteps using a representative year as well as a purely linear formulation are used to save computation time and to guarantee a solution to the optimization problem in a feasible time for the kind of targeted problems.

These main results provided by the optimization formulation presented in this thesis highlight the benefits of heating networks compared to current existing heating technologies. The decision tool of this thesis aims then to provide a support to investors and public authorities on any new case study taking into account the opportunity to build a heating network into a specific geographic area.

Chapter 4 : Calibration of the optimization model from dynamic simulations

This chapter is intended for looking at the methodology developed and applied in the two previous chapters with a critical view. This methodology was developed in order to solve a large range of heating networks optimization problems such that some conservative assumptions have been made to simplify the problem. A dynamic modelling of the optimized heating network has shown that these assumptions are not sufficient to assess accurately the real operating costs related to the network:

- In the optimization model, for a prescribed temperature difference at the substations, heat losses are assessed to be directly proportional to the power flows for nominal operating conditions into the pipes. However, a dynamic modelling shows that these heat losses are high during low heating demand periods characterized by lower power flows being out of nominal operating conditions. The assumption of a prescribed heat loss for a given power flow is therefore questionable even though it was useful to simplify the linear formulation of the optimization problem without knowing the pipes diameters of the network in advance.

- Without a regulation strategy adapted to the heating network, there are some losses which are significant and could be avoided. Constant prescribed supply and return temperatures over the network are therefore not at all optimal even though they are once again useful for a simplification of the problem formulation. Temperature levels are also important to consider because of the temperature decrease into the pipes such that the thermal comfort of the heating consumers could not be guaranteed. This is not the goal of this thesis to guarantee the thermal comfort to the user but dynamic models can be useful to tackle this issue.

- Heat losses around 5% are computed with the optimization model. Even though this value is acceptable compared to orders of magnitude related to heat losses in real applications, the dynamic model has shown that these heat losses get a value rather around 10-13% for the studied case. The dynamic model can then be used for a calibration of the parameters linked to the assessment of the heat losses in the optimization model. However, the calibration does not impact the optimization solution from a qualitative point of view. It mainly changes the quantitative values of the different economic outputs of the heating network project.

From these results, it is recommended to use the decision tool as a first pre-optimization of a heating network project while a dynamic model from the literature has to be used to take into account more accurately the heat losses into the optimization model by an adequate calibration.

Chapter 5 : Application of the decision tool to a large-scale real case study

The initial contribution of this thesis was to optimize the outline and the sizing of large-scale heating networks from a geographic information system in a reasonable computation time. In the frame of a research project, a real case study of a new heating network based on an existing heating source has therefore been considered and optimized following the initial considerations of this thesis and the expectations of the industrial stakeholders in charge of the design of the heating network. Even though this optimization formulation presents some weaknesses which will be discussed, it provides the main useful outputs which were expected for the research project.

Perspectives

As previously highlighted, there are some limitations with the work presented in this thesis. Even though answering the initial questions, the goal of a thesis is also to identify the novel issues which could be interesting to consider. The main problems identified at the end of this thesis are the followings:

- Heat losses were considered as dependent only on the power flows into the pipes for prescribed temperature differences at the substations. This simplification enabled to linearize the problem in a simple way such that heat losses are independent of the flow velocities and the diameters of the pipes. These 2 variables are indirectly defined by the power flows into the network. However, this assumption does not take into account out of range operating regimes for which heat losses are significantly underestimated. The optimization formulation could therefore be adapted to fit more accurately the real heat losses occurring into the network. The main problem relies in the difficulty to assess simultaneously the heat losses without knowing the diameters of the pipes. Two additional optimization variables, the fluid velocity and the pipe diameter, should have been defined leading to a non linear formulation more difficult to apply to large-scale problems while guaranteeing reasonable computation times. A possible solution considered into this thesis relies on the use of a dynamic model for calibrating parameters linked to the heat losses into the optimization model. A feedback looping between the optimization model and dynamic simulations would enable to refine the accuracy of the solution provided by the decision tool.

- Operating temperature levels are prescribed in the presented formulation such that they are not defined as optimization variables of the problem. However, it has been discussed that the temperature levels also have an impact on the heating network operation such that they have to be optimally

set up during the operation of the heating network. These temperature levels could therefore be additional variables to include into the optimization formulation or could be optimized afterwards with other existing optimization tools dedicated for the optimal design of temperatures and velocities into the network.

- The selection of a prescribed number of representative days is used as a way to reduce the computation load for large-scale case studies. This selection procedure is based on the existing literature for the selection of representative periods for the optimization of electricity networks. This procedure has simply been customized for the optimization of heating networks by prescribing a fixed number of 36 days per year with 3 days per month. However, there is no sensitivity study performed about the influence of the number of selected days on the computation time and the solution accuracy. The development of a new customized procedure could be useful to reduce one step further the computation time without lacking of accuracy by decreasing the total number of selected days.

- The selection of representative periods of time with given weights being assigned to each of these periods prescribes cyclic behaviours over a same representative period. This cyclic behaviour tends for promoting daily storage instead of seasonal storage because there are only possibilities to change the storage behaviour during inter-periods with the formulation presented in this thesis. Indeed, the loading and unloading of the thermal storages can be achieved on a daily basis with the present formulation such that the storage level at the end of the day is equal to the storage level at the beginning of the day. However, with this formulation, a progressive loading or unloading of the storage based on the limited available heating capacity is not possible because the storage level between the beginning and the end of the day can only vary during inter-periods linking two representative days. A new procedure to define a representative year while enabling the opportunity of seasonal thermal storage could therefore be interesting to study. It can be noticed that this seasonal storage has been assumed to be not essential for the optimization formulation because it is generally limited by high heat losses during long time periods such that seasonal storage is assessed to be non profitable with thermal storage tanks into this thesis.

- A decrease of the computation time is also achieved by using a purely linear formulation of the constraints and the objective function. However, this thesis has also shown that a piecewise linear formulation can be applied to the problem to increase the fitting of the constraints and the objective function with the physics of the system by defining additional variables approximating in a piecewise way these functions. However, this formulation requires the definition of new binary variables slowing down the optimization computation time. A parametric study could be performed to assess the optimal number of piecewise functions which could be defined to increase the accuracy of the optimization without lacking of computation speed.

- Several kinds of energy sources have been considered with the main finality to produce heat which can be used for the supply of a heating network. However, different energy carriers could be considered including Power-to-X (P2X) technologies like Carnot batteries or fuel cells for an integration of new renewable energies into heating networks. These technologies could be integrated into the optimization formulation by taking into account their efficiencies and the available resources based on any new heating network project. This integration of P2X technologies would also requires an optimization of a prospective electricity grid connecting the different consumers included into the network. New constraints should therefore been defined to include the electricity grid into the network optimization.

- The optimization formulation is based on third generation district heating networks because this formulation was developed in the frame of a research project dedicated to the implementation of a heating network of this generation. However, this formulation could be easily replicated to fourth generation heating networks by adapting the temperature levels over the network and the related parameters to this new generation of networks. Indeed, one of the features of the decision tool presented into this thesis is that it has been implemented in a generic way in order to ensure its replicability to other case studies and to integrate a large set of heating sources. For example, air-to-water heat pumps are considered in the initial formulation presented in this thesis even though this technology does not seem to be viable in practise for third generation heating networks because of its very low coefficient of performance due to a high temperature level. Even if in this thesis, coefficients of performance have been extrapolated for temperature ranges around 90°C to enable the integration of heat pumps solutions into third generation heating networks, the use of fourth generation heating networks would allow the integration of heat pumps in an easier way because of lower operating temperature levels.

- The problem formulation does not divide the problem into sub-problems which could be solved using code parallelization in order to save computation time and provide a solution in a quicker way. This parallelization of the problem could be another way to save additional computation time for large-scale case studies.

- The decision tool presented in this thesis considers prescribed parameters pre-defined by the user of the decision tool. These parameters are supposed to get a constant value over the lifetime of the project. This can be criticized due to the variability of some parameters like the heating production costs for example. A stochastic approach regarding the estimation of the values of some parameters could be used in this decision tool to include an uncertainty feature about the values of some parameters.

- This decision tool looks for helping urban energy planners and industrials to optimize the outline and the sizing of a heating network over the project lifetime. However, a single-stage planning is considered in this thesis such that initial capital expenses which have to be spent at the beginning of the

project by the investors can be really huge. This can slow down the development of heating networks compared to other heating technologies with lower initial investment costs. A multi-stage planning approach could solve this issue by providing the progressive deployment of a heating network project by starting to connect the most interesting streets at the beginning of the project. The building of the whole network could then be achieved gradually over the years to spread the investment costs over the project lifetime.

All these issues highlight some important questions which could be interesting to solve for perspective researches. These questions leave the door open to new formulations of the problem using linear or non-linear techniques in order to satisfy the expected requirements for a heating network optimization while keeping an acceptable trade-off between computation time and accuracy. As mentioned at the beginning of this chapter, this thesis could be ended up by this quote: *"What we know is a drop, what we don't know is an ocean." Isaac Newton.*

Appendix A

Optimization variables

Table A.1: Continuous and discrete variables of the problem.

Continuous	Discrete
$\dot{P}^{in}_{j,d,t} \in \mathbb{R}^+_0$: Incoming power flow during timestep d,t in edge j [kW]	$x_j \in \{0,1\}$: Building or not of a pipe on edge j
$\dot{P}^{out}_{j,d,t} \in \mathbb{R}^+_0$: Outcoming power flow during timestep d,t in edge j [kW]	$u_{j,d,t} \in \{0,1\}$: Use or not of the potential pipe on edge j during timestep d,t
$\dot{P}^{max}_{j} \in \mathbb{R}^+_0$: Maximum incoming power flow in edge j over all the timesteps [kW]	
$\dot{Q}^{prod}_{i,d,t} \in \mathbb{R}^+_0$: Power production during timestep d,t at vertex i [kW]	
$\dot{Q}_{i,m,d,t} \in \mathbb{R}^+_0$: Power production during timestep d,t at heating location i with heating technology m [kW or kWh]	
$\dot{Q}^{max}_{i,m} \in \mathbb{R}^+_0$: Maximum power production during all the timesteps at heating location i with heating technology m [kW or kWh]	
$\dot{Q}^{sto}_{i,d,t} \in \mathbb{R}^+_0$: Energy stored into the potential thermal storage during timestep d,t at vertex i [kWh]	
$\dot{Q}^{load}_{i,d,t} \in \mathbb{R}^+_0$: Incoming power flow during timestep d,t into the potential thermal storage at vertex i [kW]	
$\dot{Q}^{unload}_{i,d,t} \in \mathbb{R}^+_0$: Outcoming power flow during timestep d,t into the potential thermal storage at vertex i [kW]	

Appendix B

Parameters of the pieceiwse linearization

Table B.1: Parameters of the piecewise linearization of the pipes costs and heat losses

Bounds of the power ranges	**Power value [kW]**	**Pipe cost value [€/m]**	**Heat losses value [W/m]**
P_0	0	0	0
P_1	12.2654	327.63 for inner pipe 249.61 for outer pipe	13.63
P_2	9866.75	558.88 for inner pipe 445.05 for outer pipe	19.71
P_3	181183	1062.44 for inner pipe 870.28 for outer pipe	31.49
P_4	10^6	1736.3 for inner pipe 1462.1 for outer pipe	53.82

Appendix C

Data for heating technologies in district heating networks

TABLE C.1: Heating technologies data [4, 98, 109].

	Waste incinerator	**Biomass**	**Natural gas**	**Air-to-water compression heat pumps**	**Solar**	**Geothermal**	**Thermal storage**
Fixed costs (€/kW$_{th}$)	1780	450-730	60	860-1400	200	2710	1
Heating production costs (€/kWh$_{th}$)	0.01	0.03	0.07	f(COP)	≈ 0	≈ 0	≈ 0
Required surface area per unit of heat produced (m^2/kW$_{th}$)	0.2-0.5	0.05-0.2	0.005	0.6-1	0.2	5	0.005
CO2 emissions per unit of fuel (kg CO2/kWh)	0.149	0.030	0.202	0.247[a]	≈ 0	≈ 0	≈ 0

[a] An average CO_2 emission factor based on the Belgian electricity mix [98]

Appendix D

Data for pipes

TABLE D.1: Pipes costs as a function of their diameters

DN (mm)	Outer city (€/m)	Inner city (€/m)
20	/	/
25	200	300
32	250	330
40	300	380
50	350	400
65	380	480
80	400	500
100	430	550
125	500	610
150	550	700
200	600	780
250	700	840
300	800	1000
350	/	/
400	1000	1200
450	/	/
500	1150	1380
600	1300	1500

Appendix E

Substations costs

Table E.1: Substations costs

Space Heating Substation	
Power kW	**Cost/ Substation €**
100	25,000
200	27,000
300	28,000
400	31,000
500	36,000
600	37,500
700	39,000
800	40,000
1000	41,000
1500	52,000
2000	59,000

Appendix F

Parameters of the heat pumps

TABLE F.1: Heat pump parameters for a Daikin Altherma heat pump

Parameters	**Value**
B_0 (-)	0.949
B_1 (-)	-8.05
B_2 (-)	111.09
D_0 (-)	0.968
D_1 (-)	0.0226
D_2 (-)	-0.0063
K_1 (-)	0
K_2 (-)	0.67
COP_n (-)	3.9505
$\dot{Q}_n$ (kW)	5

Appendix G

Features of the dwellings of the case study

TABLE G.1: Features of the dwellings constitutive of the case study

	Detached dwellings (D)	Semi-Detached dwellings (S)	Terraced dwellings (T)	Apartment blocks (A)	Office buildings (O)
Usable floor area $[m^2]$	102.7	100.9	107.5	107.5	107.5
Total floor area $[m^2]$	185.5	187.8	161.0	161.0	161.0
Heat loss area $[m^2]$	371.1	305.1	219.1	104.6	104.6
Air volume $[m^3]$	451.5	455.1	446.5	435.9	435.9

Appendix H

Repartition of the dwellings over the different scenarios of the theoretical case study

Table H.1: Repartition of the dwellings for Scenario 1.

	v1v4	v2v3	v3v4	v3v6	v4v7	v4v9	v5v9	v5v6	v5v10	v6v9	v7v8	v7v9	v9v11	v9v12	v10v12	v12v13	TOTAL
S1	21	17	5	24	17	17	2	7	2	12	12	8	16	5	17	9	191
D1	8	3	22	7	9	13	18	9	1	3	15	15	9	21	8	0	161
T1	19	13	21	12	16	18	13	13	25	23	15	14	21	17	10	25	275
A1	1	17	2	7	8	2	17	21	22	13	8	13	4	7	15	16	173
O1	0	0	0	0	0	0	0	0	0	0	0	0	0	0	0	0	0
Greenhouse	0	0	0	0	0	0	0	0	0	0	0	0	0	0	0	0	0
T2	0	0	0	0	0	0	0	0	0	0	0	0	0	0	0	0	0
D2	0	0	0	0	0	0	0	0	0	0	0	0	0	0	0	0	0
S2	0	0	0	0	0	0	0	0	0	0	0	0	0	0	0	0	0
TOTAL	49	50	50	50	50	50	50	50	50	51	50	50	50	50	50	50	800

Table H.2: Repartition of the dwellings for Scenario 2.

	v1v4	v2v3	v3v4	v3v6	v4v7	v4v9	v5v9	v5v6	v5v10	v6v9	v7v8	v7v9	v9v11	v9v12	v10v12	v12v13	TOTAL
S1	21	17	5	24	17	17	2	7	2	12	12	8	16	5	17	9	173
D1	8	3	22	7	9	13	18	9	1	3	15	15	9	21	8	0	161
T1	19	13	21	12	16	18	13	13	25	23	15	14	21	17	10	25	274
A1	0	0	0	0	0	0	0	0	0	0	0	0	0	0	0	0	0
O1	1	17	2	7	8	2	17	21	22	13	8	13	4	7	15	16	173
Greenhouse	0	0	0	0	0	0	0	0	0	0	0	0	0	0	0	0	0
T2	0	0	0	0	0	0	0	0	0	0	0	0	0	0	0	0	0
D2	0	0	0	0	0	0	0	0	0	0	0	0	0	0	0	0	0
S2	0	0	0	0	0	0	0	0	0	0	0	0	0	0	0	0	0
TOTAL	49	50	50	50	50	50	50	50	50	51	50	50	50	50	50	50	800

Table H.3: Repartition of the dwellings for Scenario 3.

	v1v4	v2v3	v3v4	v3v6	v4v7	v4v9	v5v9	v5v6	v5v10	v6v9	v7v8	v7v9	v9v11	v9v12	v10v12	v12v13	TOTAL
S1	21	17	5	24	17	17	2	7	2	12	12	8	16	5	17	0	182
D1	8	3	22	7	9	13	18	9	1	3	15	15	9	21	8	0	161
T1	19	13	21	12	16	18	13	13	25	23	15	14	21	17	10	0	250
A1	0	0	0	0	0	0	0	0	0	0	0	0	0	0	0	0	0
O1	1	17	2	7	8	2	17	21	22	13	8	13	4	7	15	0	157
Greenhouse	0	0	0	0	0	0	0	0	0	0	0	0	0	0	0	1	1
T2	0	0	0	0	0	0	0	0	0	0	0	0	0	0	0	0	0
D2	0	0	0	0	0	0	0	0	0	0	0	0	0	0	0	0	0
S2	0	0	0	0	0	0	0	0	0	0	0	0	0	0	0	0	0
TOTAL	49	50	50	50	50	50	50	50	50	51	50	50	50	50	50	1	751

Table H.4: Repartition of the dwellings for Scenario 4.

	v1v4	v2v3	v3v4	v3v6	v4v7	v4v9	v5v9	v5v6	v5v10	v6v9	v7v8	v7v9	v9v11	v9v12	v10v12	v12v13	TOTAL
S1	7	6	5	6	8	8	7	1	4	7	7	4	9	9	6	0	94
D1	5	2	1	6	1	7	4	9	3	4	5	1	6	1	2	0	57
T1	1	0	6	6	4	1	7	1	2	2	5	10	7	1	9	0	62
A1	5	7	4	10	8	8	3	9	11	6	6	8	1	4	9	0	99
O1	2	7	6	3	9	5	8	9	7	6	7	3	5	8	7	0	93
Greenhouse	0	0	0	0	0	0	0	0	0	0	0	0	0	0	0	1	1
T2	8	5	10	13	8	1	4	7	4	3	7	7	7	11	1	0	96
D2	6	6	4	1	5	10	5	8	6	7	5	2	4	7	6	0	82
S2	6	8	10	3	6	6	4	4	2	6	2	8	2	2	6	0	75
TOTAL	40	41	46	48	49	46	42	48	39	41	44	43	41	43	46	1	658

Appendix I

Coordinates of the nodes of the test case

TABLE I.1: Coordinates of the nodes of the theoretical case study in Chapter 3.

Nodes	X (m)	Y (m)
v1	200	200
v2	200	700
v3	300	600
v4	400	400
v5	400	900
v6	500	700
v7	600	300
v8	700	200
v9	700	500
v10	700	900
v11	900	400
v12	900	700
v13	900	900

Bibliography

[1] Hannah Ritchie. *Sector by sector: where do global greenhouse gas emissions come from?* Accessed: 2021-01-07. URL: https://ourworldindata.org/ghg-emissions-by-sector.

[2] Susana Paardekooper. "Heat Roadmap Belgium Quantifying the Impact of Low-carbon". In: (2018).

[3] European Commission. "An EU Strategy on Heating and Cooling". In: *Journal of Chemical Information and Modeling* 53.9 (2016), pp. 1689–1699. ISSN: 1098-6596. arXiv: arXiv:1011.1669v3.

[4] *Les chaudières gaz sont-elles compatibles avec la lutte contre le changement climatique?* Accessed: 2021-01-07. URL: http://www.carbone4.com/analyse-chaudieres-gaz-climat/.

[5] Population Division United Nations, Department of Economic and Social Affairs. "The World 's Cities in 2018". In: *The World's Cities in 2018 - Data Booklet (ST/ESA/ SER.A/417)* (2018), p. 34.

[6] EDORA. "BELGIUM National renewable energy action plan". In: (2010), pp. 1–95. URL: https://www.wasewind.be/frontend/files/userfiles/files/REPAP2020Belgium{_}Final.pdf.

[7] Nevin Cohen, Paul Robbins, and Michael Quinn Dudley. "District Energy". In: *Green Cities: An A-to-Z Guide* (2012). DOI: 10.4135/9781412973816.n47.

[8] D. Connolly, H. Lund, B. V. Mathiesen, S. Werner, B. Möller, U. Persson, T. Boermans, D. Trier, P. A. Østergaard, and S. Nielsen. "Heat roadmap Europe: Combining district heating with heat savings to decarbonise the EU energy system". In: *Energy Policy* 65 (2014), pp. 475–489. ISSN: 03014215. DOI: 10.1016/j.enpol.2013.10.035. URL: http://dx.doi.org/10.1016/j.enpol.2013.10.035.

[9] Sven Werner. "International review of district heating and cooling". In: *Energy* 137 (2017), pp. 617 –631. ISSN: 0360-5442. DOI: https://doi.org/10.1016/j.energy.2017.04.045. URL: http://www.sciencedirect.com/science/article/pii/S036054421730614X.

[10] Henrik Lund, Poul Alberg Østergaard, Miguel Chang, Sven Werner, Svend Svendsen, Peter Sorknæs, Jan Eric Thorsen, Frede Hvelplund, Bent Ole Gram Mortensen, Brian Vad Mathiesen, Carsten Bojesen, Neven Duic, Xiliang Zhang, and Bernd Möller. "The status of 4th generation district heating: Research and results". In: *Energy* 164 (2018), pp. 147–159. ISSN: 03605442. DOI: 10.1016/j.energy.2018.08.206.

[11] Sven Werner and Norela Constantinescu. "EcoHeatCool WP1: The European heat market". In: *Work package deliverable of Ecohaetcool EU project* (2006), pp. 58–62. URL: http://www.euroheat.org/Files/Filer/ecoheatcool/documents/Ecoheatcool{_}WP1{_}Web.pdf.

[12] Henrik Lund, Sven Werner, Robin Wiltshire, Svend Svendsen, Jan Eric Thorsen, Frede Hvelplund, and Brian Vad Mathiesen. "4th Generation District Heating (4GDH): Integrating smart thermal grids into future sustainable energy systems". In: *Energy* 68 (2014), pp. 1 –11. ISSN: 0360-5442. DOI: https://doi.org/10.1016/j.energy.2014.02.089. URL: http://www.sciencedirect.com/science/article/pii/S0360544214002369.

[13] International Renewable and Energy Agency. "Thermal Energy Storage Technology Brief E17". In: January (2013).

[14] IRENA. *Electricity storage and renewables: Costs and markets to 2030*. October. 2017, p. 132. ISBN: 978-92-9260-038-9. URL: http://irena.org/publications/2017/Oct/Electricity-storage-and-renewables-costs-and-markets{\%}0Ahttps://www.irena.org/-/media/Files/IRENA/Agency/Publication/2017/Oct/IRENA{_}Electricity{_}Storage{_}Costs{_}2017.pdf.

[15] Henrik Lund, Neven Duic, Poul Alberg Østergaard, and Brian Vad Mathiesen. "Smart energy systems and 4th generation district heating". In: *Energy* 110.2016 (2016), pp. 1–4. ISSN: 03605442. DOI: 10.1016/j.energy.2016.07.105.

[16] M. Galindo Fernández, C. Roger-Lacan, U. Gährs, and V. Aumaitre. *Efficient district heating and cooling markets in the EU: Case studies analysis, replicable key success factors and potential policy implications*. December. 2016. ISBN: 9789279650482. DOI: 10.2760/371045. URL: https://ec.europa.eu/jrc.

[17] Henrik Lund, Poul Alberg Østergaard, Tore Bach Nielsen, Sven Werner, Jan Eric Thorsen, Oddgeir Gudmundsson, Ahmad Arabkoohsar, and Brian Vad Mathiesen. "Perspectives on fourth and fifth generation district heating". In: *Energy* 227 (2021), p. 120520. ISSN: 0360-5442. DOI: https://doi.org/10.1016/j.energy.2021.120520. URL: https://www.sciencedirect.com/science/article/pii/S0360544221007696.

[18] Simone Buffa, Marco Cozzini, Matteo D'Antoni, Marco Baratieri, and Roberto Fedrizzi. "5th generation district heating and cooling systems: A review of existing cases in Europe". In: *Renewable and Sustainable Energy Reviews* 104 (2019), pp. 504–522. ISSN: 1364-0321. DOI: https://doi.org/10.1016/j.rser.2018.12.059. URL: https://www.sciencedirect.com/science/article/pii/S1364032118308608.

[19] International Energy Agency. "District Heating. IEA-ETSAP Techonology Brief E16". In: *ETSAP - Energy Technology Systems Analysis Programme* January (2013), p. 7.

[20] Eurostat. *Combined Heat and Power (CHP) data 2005-2017*. https://ec.europa.eu/eurostat/web/energy/data. Accessed: 2020-04-17. 2018.

[21] Karin Ericsson and Sven Werner. "The introduction and expansion of biomass use in Swedish district heating systems". In: *Biomass and Bioenergy* 94 (2016), pp. 57 –65. ISSN: 0961-9534. DOI: https://doi.org/10.1016/j.biombioe.2016.08.011. URL: http://www.sciencedirect.com/science/article/pii/S0961953416302793.

[22] P. Dumas and L. Angelino. "GeoDH: Promote Geothermal District Heating Systems in Europe". In: *Technika Poszukiwań Geologicznych* R. 54, nr 2 (2015), pp. 1–6.

[23] Annamaria Nador Mfgi. "A Geothermal DH map Output description : Methodology :" in: September (2013).

[24] Carlo Winterscheid and Thomas Schmidt. "Dronninglund District Heating Monitaring Data Evaluation for the Years 2015-2017". In: (2017), p. 27.

[25] Nicolas Perez-Mora, Federico Bava, Martin Andersen, Chris Bales, Gunnar Lennermo, Christian Nielsen, Simon Furbo, and Víctor Martínez-Moll. "Solar district heating and cooling: A review". In: *International Journal of Energy Research* 42.4 (2018), pp. 1419–1441. ISSN: 1099114X. DOI: 10.1002/er.3888.

[26] Francesco Calise, Francesco Liberato Cappiello, Massimo Dentice d'Accadia, Fontina Petrakopoulou, and Maria Vicidomini. "A solar-driven 5th generation district heating and cooling network with ground-source heat pumps: a thermo-economic analysis". In: *Sustainable Cities and Society* (2021), p. 103438. ISSN: 2210-6707. DOI: https://doi.org/10.1016/j.scs.2021.103438. URL: https://www.sciencedirect.com/science/article/pii/S2210670721007113.

[27] Kristina Lygnerud, Jonas Ottosson, Johan Kensby, and Linnea Johansson. "Business models combining heat pumps and district heating in buildings generate cost and emission savings". In: *Energy* 234 (2021), p. 121202. ISSN: 0360-5442. DOI: https://doi.org/10.1016/j.energy.2021.121202. URL: https://www.sciencedirect.com/science/article/pii/S036054422101450X.

[28] Gonzalo Quirosa, Miguel Torres, and Ricardo Chacartegui. "Analysis of the integration of photovoltaic excess into a 5th generation district heating and cooling system for network energy storage". In: *Energy* 239 (2022), p. 122202. ISSN: 0360-5442. DOI: https://doi.org/10.1016/j.energy.2021.122202. URL: https://www.sciencedirect.com/science/article/pii/S0360544221024506.

[29] Joana Neves and Brian Vad. *Heat Roadmap Europe : Potentials for Large-Scale Heat Pumps in District Heating*. 2018, pp. 1–35. ISBN: 9788791404962.

[30] Mikko Wahlroos, Matti Pärssinen, Jukka Manner, and Sanna Syri. "Utilizing data center waste heat in district heating – Impacts on energy efficiency and prospects for low-temperature district heating networks". In: *Energy* 140 (2017), pp. 1228–1238. ISSN: 0360-5442. DOI: https://doi.org/10.1016/j.energy.2017.08.078. URL: https://www.sciencedirect.com/science/article/pii/S0360544217314548.

[31] Alexandre Bertrand, Alberto Mian, Ivan Kantor, Riad Aggoune, and François Maréchal. "Regional waste heat valorisation: A mixed integer linear programming method for energy service companies". In: *Energy* 167 (2019), pp. 454–468. ISSN: 0360-5442. DOI: https://doi.org/10.1016/j.energy.2018.10.152. URL: https://www.sciencedirect.com/science/article/pii/S0360544218321492.

[32] Inger-Lise Svensson, Johanna Jönsson, Thore Berntsson, and Bahram Moshfegh. "Excess heat from kraft pulp mills: Trade-offs between internal and external use in the case of Sweden—Part 1: Methodology". In: *Energy Policy* 36.11 (2008). Transition towards Sustainable Energy Systems, pp. 4178–4185. ISSN: 0301-4215. DOI: https://doi.org/10.1016/j.enpol.2008.07.017. URL: https://www.sciencedirect.com/science/article/pii/S0301421508003637.

[33] S. Frederiksen and S. Werner. *District Heating and Cooling*. Studentlitteratur AB, 2013. ISBN: 9789144085302. URL: https://books.google.be/books?id=vH5zngEACAAJ.

[34] *Municipal waste statistics*. URL: https://ec.europa.eu/eurostat/statistics-explained/index.php/Municipal_waste_statistics#Municipal_waste_treatment.

[35] Elisa Guelpa and Vittorio Verda. "Demand response and other demand side management techniques for district heating: A review". In: *Energy* 219 (2021), p. 119440. ISSN: 0360-5442. DOI: https://doi.org/10.1016/j.energy.2020.119440. URL: https://www.sciencedirect.com/science/article/pii/S0360544220325470.

[36] H. Gadd and S. Werner. "18 - Thermal energy storage systems for district heating and cooling". In: *Advances in Thermal Energy Storage Systems*. Ed. by Luisa F. Cabeza. Woodhead Publishing Series in Energy. Woodhead Publishing, 2015, pp. 467–478. ISBN: 978-1-78242-088-0. DOI: https://doi.org/10.1533/9781782420965.4.467. URL: https://www.sciencedirect.com/science/article/pii/B9781782420880500183.

[37] Hafiz Haq, Petri Välisuo, Lucio Mesquita, Lauri Kumpulainen, and Seppo Niemi. "An application of seasonal borehole thermal energy system in Finland". In: *Cleaner Engineering and Technology* 2 (2021), p. 100048. ISSN: 2666-7908. DOI: https://doi.org/10.1016/j.clet.2021.100048. URL: https://www.sciencedirect.com/science/article/pii/S2666790821000082.

[38] A. Réveillère, V. Hamm, H. Lesueur, E. Cordier, and P. Goblet. "Geothermal contribution to the energy mix of a heating network when using Aquifer Thermal Energy Storage: Modeling and application to the Paris basin". In: *Geothermics* 47 (2013), pp. 69–79. ISSN: 0375-6505. DOI: https://doi.org/10.1016/j.geothermics.2013.02.005. URL: https://www.sciencedirect.com/science/article/pii/S0375650513000163.

[39] Elisa Guelpa and Ludovica Marincioni. "Demand side management in district heating systems by innovative control". In: *Energy* 188 (2019), p. 116037. ISSN: 0360-5442. DOI: https://doi.org/10.1016/j.energy.2019.116037. URL: https://www.sciencedirect.com/science/article/pii/S0360544219317311.

[40] International Energy Agency. "Technology Annex". In: *Energy Storage Technology Roadmap* March (2014), pp. 1–31.

[41] Thomas Schmidt, Thomas Pauschinger, Per Alex Sørensen, Aart Snijders, Reda Djebbar, Raymond Boulter, and Jeff Thornton. "Design Aspects for Large-scale Pit and Aquifer Thermal Energy Storage for District Heating and Cooling". In: *Energy Procedia* 149 (2018). 16th International Symposium on District Heating and Cooling, DHC2018, 9–12 September 2018, Hamburg, Germany, pp. 585–594. ISSN: 1876-6102. DOI: https://doi.org/10.1016/j.egypro.2018.08.223. URL: https://www.sciencedirect.com/science/article/pii/S1876610218305198.

[42] Oddgeir Gudmundsson, Jan Eric Thorsen, and Marek Brand. "Building solutions for low temperature heat supply". In: *REHVA Journal* October (2016).

[43] ACHRNEWS. *Heat Metering Makes Centralized Hydronic Heat a Viable Option*. https://www.achrnews.com/articles/141568-heat-metering-makes-centralized-hydronic-heat-a-viable-option. Accessed: 2020-05-12. 2019.

[44] O. Larsson. "Pricing models in district heating". In: 2011.

[45] Cerema. *Prix de la chaleur et facturation*. http://reseaux-chaleur.cerema.fr/prix-de-la-chaleur-et-facturation. Accessed: 2020-05-13. 2014.

[46] Joseph Maria Jebamalai, Kurt Marlein, Jelle Laverge, Lieven Vandevelde, and Martijn van den Broek. "An automated GIS-based planning and design tool for district heating: Scenarios for a Dutch city". In: *Energy* 183 (2019), pp. 487–496. ISSN: 03605442. DOI: 10.1016/j.energy.2019.06.111.

[47] D. Andrews, A. Riekkola, E. Tzimas, Serpa J., J. Carlsson, N. Pardo-Garcia, and I. Papaioannou. *Background Report on EU-27 District Heating and Cooling Potentials, Barriers, Best Practice and Measures of Promotion*. https://setis.ec.europa.eu/system/files/1.DHCpotentials.pdf. Accessed: 2020-04-19. 2012.

[48] *Coriance district heating and cooling networks*. Accessed: 2021-10-21. URL: https://www.groupe-coriance.fr/.

[49] Matthildi Apostolou. "Méthodologie pour la conception optimisée des réseaux de chaleur et de froid urbains intégrés Matthildi Apostolou To cite this version : HAL Id : tel-02274400 de l ' Université de recherche Paris Sciences et Lettres Préparée à MINES ParisTech Méthodologie". In: (2019).

[50] T. Mertz, S. Serra, A. Henon, and J. M. Reneaume. "A MINLP optimization of the configuration and the design of a district heating network: Study case on an existing site". In: *Energy Procedia* 116.July (2017), pp. 236–248. ISSN: 18766102. DOI: 10.1016/j.egypro.2017.05.071.

[51] Marius Roland and Martin Schmidt. "Mixed-integer nonlinear optimization for district heating network expansion Gemischt-ganzzahlige nichtlineare Optimierung für den Ausbau von Fernwärmenetzen". In: *At-Automatisierungstechnik* 68.12 (2020), pp. 985–1000. ISSN: 2196677X. DOI: 10.1515/auto-2020-0063.

[52] Maarten Blommaert, Y. Wack, and M. Baelmans. "An adjoint optimization approach for the topological design of large-scale district heating networks based on nonlinear models". In: *Applied Energy* 280.October (2020), p. 116025. ISSN: 03062619. DOI: 10.1016/j.apenergy.2020.116025. arXiv: 2008.08328. URL: https://doi.org/10.1016/j.apenergy.2020.116025.

[53] Tobias Falke, Stefan Krengel, Ann Kathrin Meinerzhagen, and Armin Schnettler. "Multi-objective optimization and simulation model for the design of distributed energy systems". In: *Applied Energy* 184 (2016), pp. 1508–1516. ISSN: 03062619. DOI: 10.1016/j.apenergy.2016.03.044.

[54] Samira Fazlollahi, Gwenaelle Becker, Araz Ashouri, and François Maréchal. "Multi-objective, multi-period optimization of district energy systems: IV - A case study". In: *Energy* 84 (2015), pp. 365–381. ISSN: 03605442. DOI: 10.1016/j.energy.2015.03.003.

[55] A. Molyneaux, G. Leyland, and D. Favrat. "Environomic multi-objective optimisation of a district heating network considering centralized and decentralized heat pumps". In: *Energy* 35.2 (2010), pp. 751–758. ISSN: 03605442. DOI: 10.1016/j.energy.2009.09.028. URL: http://dx.doi.org/10.1016/j.energy.2009.09.028.

[56] C. Weber and N. Shah. "Optimisation based design of a district energy system for an eco-town in the United Kingdom". In: *Energy* 36.2 (2011), pp. 1292–1308. ISSN: 03605442. DOI: 10.1016/j.energy.2010.11.014. URL: http://dx.doi.org/10.1016/j.energy.2010.11.014.

[57] Bram van der Heijde, Annelies Vandermeulen, Robbe Salenbien, and Lieve Helsen. "Integrated optimal design and control of fourth generation district heating networks with thermal energy storage". In: *Energies* 12.14 (2019). ISSN: 19961073. DOI: 10.3390/en12142766.

[58] Alexandre Bertrand, Alberto Mian, Ivan Kantor, Riad Aggoune, and François Maréchal. "Regional waste heat valorisation: A mixed integer linear programming method for energy service companies". In: *Energy* 167 (2019), pp. 454–468. ISSN: 03605442. DOI: 10.1016/j.energy.2018.10.152.

[59] Akomeno Omu, Ruchi Choudhary, and Adam Boies. "Distributed energy resource system optimisation using mixed integer linear programming". In: *Energy Policy* 61 (2013), pp. 249–266. ISSN: 03014215. DOI: 10.1016/j.enpol.2013.05.009. URL: http://dx.doi.org/10.1016/j.enpol.2013.05.009.

[60] Chiara Bordin, Angelo Gordini, and Daniele Vigo. *An optimization approach for district heating strategic network design*. 2016. DOI: 10.1016/j.ejor.2015.12.049.

[61] Joseph Maria Jebamalai, Kurt Marlein, and Jelle Laverge. "Influence of centralized and distributed thermal energy storage on district heating network design". In: *Energy* 202 (2020), p. 117689. ISSN: 0360-5442. DOI: https://doi.org/10.1016/j.energy.2020.117689. URL: http://www.sciencedirect.com/science/article/pii/S0360544220307969.

[62] Sheila Samsatli and Nouri J. Samsatli. "A general mixed integer linear programming model for the design and operation of integrated urban energy systems". In: *Journal of Cleaner Production* 191 (2018), pp. 458–479. ISSN: 09596526. DOI: 10.1016/j.jclepro.2018.04.198.

[63] Carl Haikarainen, Frank Pettersson, and Henrik Saxén. "A model for structural and operational optimization of distributed energy systems". In: *Applied Thermal Engineering* 70.1 (2014), pp. 211–218. ISSN: 13594311. DOI: 10.1016/j.applthermaleng.2014.04.049. URL: http://dx.doi.org/10.1016/j.applthermaleng.2014.04.049.

[64] Jarmo Söderman and Frank Pettersson. "Structural and operational optimisation of distributed energy systems". In: *Applied Thermal Engineering* 26.13 (2006), pp. 1400–1408. ISSN: 13594311. DOI: 10.1016/j.applthermaleng.2005.05.034.

[65] International Journal, Sustainable Energy Planning, and Management Vol. "Optimal Phasing of District Heating Network Investments Using Multistage Stochastic Programming". In: 09 (2016), pp. 57–74.

[66] Johannes Dorfner and Thomas Hamacher. "Large-scale district heating network optimization". In: *IEEE Transactions on Smart Grid* 5.4 (2014), pp. 1884–1891. ISSN: 19493053. DOI: 10.1109/TSG.2013.2295856.

[67] Luc Girardin. "A GIS-based Methodology for the Evaluation of Integrated Energy Systems in Urban Area". In: 2012.

[68] Jérémy Michel Pierre Unternährer, Stefano Moret, Stéphane Joost, and François Maréchal. "Spatial clustering for district heating integration in urban energy systems: Application to geothermal energy". In: *Applied Energy* 190 (2017), pp. 749–763.

[69] *SigOpti - L'outil open-source d'aide à la décision pour les réseaux de chaleur urbain*. Accessed: 2021-10-21. URL: https://github.com/sigopti/plugin-installer.

[70] Sébastien Cajot, Nils Schüler, Markus Peter, Jessen Page, Andreas Koch, and François Maréchal. "Establishing links for the planning of sustainable districts". In: 2016.

[71] Matthildi Apostolou, Sami Ghazouani, Solène Le Bourdiec, Cong Toan Tran, and Assaad Zoughaib. "District heating network design considering fluctuations in the demand and thermal storage means". In: *ECOS 2018 - Proceedings of the 31st International Conference on Efficiency, Cost, Optimization, Simulation and Environmental Impact of Energy Systems* (2018), pp. 1–12.

[72] ICEDD Institut de Conseil et d'Etudes en Développement Durable. "Bilan énergétique de la Wallonie 2012 - Consommation du secteur domestique". In: (2014).

[73] Simon Hilpert, Cord Kaldemeyer, Krien Uwe, Stephan Günther, clemens wingenbach, and Guido Pleßmann. "The Open Energy Modelling Framework (oemof) - A new approach to facilitate open science in energy system modelling". In: *Energy Strategy Reviews* 22 (July 2018), pp. 16–25. DOI: 10.1016/j.esr.2018.07.001.

[74] Mostafa Fallahnejad, Benedikt Eberl, and Maik Günther. *Long-Term Forecast of Residential and Commercial Gas Demand in Germany*. Mar. 2017.

[75] *Abwicklung von Standardlastprofilen Gas*. Accessed: 2021-10-21. URL: https://www.enwg-veroeffentlichungen.de/badtoelz/Netze/Gasnetz/Netzbeschreibung/LF-Abwicklung-von-Standardlastprofilen-Gas-20110630-final.pdf.

[76] Andreas Belderbos and Erik Delarue. "Accounting for flexibility in power system planning with renewables". In: *International Journal of Electrical Power Energy Systems* 71 (2015), pp. 33–41. ISSN: 0142-0615. DOI: https://doi.org/10.1016/j.ijepes.2015.02.033. URL: https://www.sciencedirect.com/science/article/pii/S0142061515001167.

[77] Fernando J. de Sisternes and Mort D. Webster. "Optimal selection of sample weeks for approximating the net load in generation planning problems optimal selection of sample weeks for approximating the net load in generation planning problems". In: *Massachusetts Institute of Technology. Engineering Systems Division* January (2013), p. 12. URL: https://dspace.mit.edu/bitstream/handle/1721.1/102959/esd-wp-2013-03.pdf?sequence=1{\&}isAllowed=y.

[78] A. K. Jain, M. N. Murty, and P. J. Flynn. "Data Clustering: A Review". In: *ACM Comput. Surv.* 31.3 (Sept. 1999), 264–323. ISSN: 0360-0300. DOI: 10.1145/331499.331504. URL: https://doi.org/10.1145/331499.331504.

[79] Paul Nahmmacher, Eva Schmid, Lion Hirth, and Brigitte Knopf. "Carpe diem: A novel approach to select representative days for long-term power system modeling". In: *Energy* 112 (2016), pp. 430–442. ISSN: 03605442. DOI: 10.1016/j.energy.2016.06.081.

[80] Samira Fazlollahi, Stephane Laurent Bungener, Pierre Mandel, Gwenaelle Becker, and François Maréchal. "Multi-objectives, multi-period optimization of district energy systems: I. Selection of typical operating periods". In: *Computers and Chemical Engineering* 65 (2014), pp. 54–66. ISSN: 00981354. DOI: 10.1016/j.compchemeng.2014.03.005.

[81] Fernando Domínguez-Muñoz, José M. Cejudo-López, Antonio Carrillo-Andrés, and Manuel Gallardo-Salazar. "Selection of typical demand days for CHP optimization". In: *Energy and Buildings* 43.11 (2011), pp. 3036–3043. ISSN: 03787788. DOI: 10.1016/j.enbuild.2011.07.024.

[82] C. H. Marton, A. Elkamel, and T. A. Duever. "An order-specific clustering algorithm for the determination of representative demand curves". In: *Computers and Chemical Engineering* 32.6 (2008), pp. 1365–1372. ISSN: 00981354. DOI: 10.1016/j.compchemeng.2007.06.010.

[83] Kris Poncelet, Hanspeter Hoschle, Erik Delarue, Ana Virag, and William Drhaeseleer. "Selecting representative days for capturing the implications of integrating intermittent renewables in generation expansion planning problems". In: *IEEE Transactions on Power Systems* 32.3 (2017), pp. 1936–1948. ISSN: 08858950. DOI: 10.1109/TPWRS.2016.2596803.

[84] Bram van der Heijde, Annelies Vandermeulen, Robbe Salenbien, and Lieve Helsen. "Representative days selection for district energy system optimisation: a solar district heating system with seasonal storage". In: *Applied Energy* 248.February (2019), pp. 79–94. ISSN: 03062619. DOI: 10.1016/j.apenergy.2019.04.030. URL: https://doi.org/10.1016/j.apenergy.2019.04.030.

[85] Hang Li and Dinh Phung. "Journal of Machine Learning Research: Preface". In: *Journal of Machine Learning Research* 39.2014 (2014), pp. i–ii. ISSN: 15337928.

[86] Gurobi. "Algorithms in Gurobi". In: (2016).

[87] Kevin Sartor, Vincent Lemort, and Pierre Dewallef. "Improved district heating network operation by the integration of high-temperature heat pumps". In: *International Journal of Sustainable Energy* 37.9 (2018), pp. 842–856. DOI: 10.1080/14786451.2017.1383409. eprint: https://doi.org/10.1080/14786451.2017.1383409. URL: https://doi.org/10.1080/14786451.2017.1383409.

[88] Charles F. Jekel and Gerhard Venter. *pwlf: A Python Library for Fitting 1D Continuous Piecewise Linear Functions*. 2019. URL: https://github.com/cjekel/piecewise_linear_fit_py.

[89] Björn Bahl, Theo Söhler, Maike Hennen, and André Bardow. "Typical Periods for Two-Stage Synthesis by Time-Series Aggregation with Bounded Error in Objective Function". In: *Frontiers in Energy Research* 5 (2018), p. 35.

[90] Leander Kotzur, Peter Markewitz, Martin Robinius, and Detlef Stolten. "Time series aggregation for energy system design: Modeling seasonal storage". In: *Applied Energy* 213.January (2018), pp. 123–135. ISSN: 03062619. DOI: 10.1016/j.apenergy.2018.01.023. arXiv: 1710.07593. URL: https://doi.org/10.1016/j.apenergy.2018.01.023.

[91] European Commission Joint Research Center. *Copernicus Database of the European Union's Earth observation programme*. https://www.copernicus.eu/en/research/project-database. Accessed: 2021-01-18. 2021.

[92] Amit Kumar Yadav and S.S. Chandel. "Tilt angle optimization to maximize incident solar radiation: A review". In: *Renewable and Sustainable Energy Reviews* 23 (2013), pp. 503 –513. ISSN: 1364-0321. DOI: https://doi.org/10.1016/j.rser.2013.02.027. URL: http://www.sciencedirect.com/science/article/pii/S1364032113001299.

[93] ADEME. "Les réseaux de chaleur et de froid – état des lieux de la filière". In: *2019* (2019), pp. 1–89.

[94] The Danish Energy Agency and Energinet. "Technology Data - Generation of Electricity and District heating". In: (2016), p. 414. URL: http://www.ens.dk/teknologikatalog.

[95] Numerique E T Experimentale and Frédéric Ransy. "Performances D ' Une M Ini Pompe À Chaleur Réversible Fonctionn Ant Sur L ' Air Extrai T : Étude". In: (2017), pp. 1–6.

[96] A. Bolther, R. Casari, E. Fleury, D. Marchio, and J. Millet. "Méthode De Calcul DES Consommations D'Énergie Des Bâtiments Climatisés Consoclim". In: (1999).

[97] S. Gendebien, E. Georges, and V. Lemort. "Projet Flexipac - Développement d'un modèle de pompe à chaleur destiné à l'intégration dans un modèle de bâtiment". In: (2014).

[98] *Emissions de polluants liés à la consommation énergétique*. Accessed: 2021-10-26. URL: https://energieplus-lesite.be/theories/consommation-energetique/les-emissions-de-polluants-liee-a-la-consommation-energetique/.

[99] Efficacity. *Efficacity - Institut de Recherche et Développement: Outils d'Efficacity*. Accessed: 2021-11-02. 2020. URL: https://www.efficacity.com/la-chaine-doutils-defficacity/.

[100] Stefano Moret, Michel Bierlaire, and François Maréchal. "Strategic Energy Planning under Uncertainty: a Mixed-Integer Linear Programming Modeling Framework for Large-Scale Energy Systems". In: *26th European Symposium on Computer Aided Process Engineering*. Ed. by Zdravko Kravanja and Miloš Bogataj. Vol. 38. Computer Aided Chemical Engineering. Elsevier, 2016, pp. 1899–1904. DOI: https://doi.org/10.1016/B978-0-444-63428-3.50321-0. URL: https://www.sciencedirect.com/science/article/pii/B9780444634283503210.

[101] Michael Wetter and Christoph van Treeck. *IEA EBC Annex 60: New Generation Computing Tools for Building and Community Energy Systems*. Sept. 2017. ISBN: 978-0-692-89748-5. URL: https://www.iea-annex60.org/pubs.html.

[102] Shady Attia and Erwin Mlecnik. "Principles for nearly zero energy building in Belgium". In: *World Sustainable Energy Days* (2012).

[103] Cyx W., Renders M., Van Holm M., and Verbeke S. "TABULA – Typology Approach for Building Stock Energy Assessment". In: August (2017). URL: http://webtool.building-typology.eu/.

[104] Queralt Altes-Buch, Sylvain Quoilin, and Vincent Lemort. "Greenhouses: A Modelica Library for the Simulation of Greenhouse Climate and Energy Systems". In: *Proceedings of the 13th International Modelica Conference, Regensburg, Germany, March 4–6, 2019* 157 (2019), pp. 533–542. DOI: 10.3384/ecp19157533.

[105] Thibaut Résimont, Queralt Altes-buch, Kevin Sartor, and Pierre Dewallef. "Economic and environmental comparison of a centralized and a decentralized heating production for a district heating network implementation". In: *10th International Conference on System Simulation in Buildings* (2018), pp. 1–17.

[106] Thibaut Résimont, Kevin Sartor, and Pierre Dewallef. "Thermo-economic evaluation of a virtual district heating network using dynamic simulation". In: *ECOS 2018 - Proceedings of the 31st International Conference on Efficiency, Cost, Optimization, Simulation and Environmental Impact of Energy Systems* 1 (2018).

[107] Eurostat. *Statistics Explained On Natural Gas Prices in the European Union*. Accessed: 2021-01-25. 2020. URL: https://ec.europa.eu/eurostat/statistics-explained/index.php?title=File%3ANatural_gas_prices_for_household_consumers%2C_first_half_2020_%28EUR_per_kWh%29_v3.png.

[108] Danish Energy Agency. *Danish Energy Agency website*. Accessed: 2020-10-26. 2020. URL: https://ens.dk/en/our-services/projections-and-models/technology-data/technology-data-individual-heating-plants.

[109] Danish Energy Agency. *Danish Energy Agency website*. Accessed: 2020-10-26. 2020. URL: https://ens.dk/en/our-services/projections-and-models/technology-data/technology-data-generation-electricity-and.

[110] Tatu Laajalehto, Maunu Kuosa, Tapio Mäkilä, Markku Lampinen, and Risto Lahdelma. "Energy efficiency improvements utilising mass flow control and a ring topology in a district heating network". In: *Applied Thermal Engineering* 69.1-2 (2014), pp. 86–95. ISSN: 13594311. DOI: 10.1016/j.applthermaleng.2014.04.041. URL: http://dx.doi.org/10.1016/j.applthermaleng.2014.04.041.

[111] László Dobos and János Abonyi. "Controller tuning of district heating networks using experiment design techniques". In: *Energy* 36.8 (2011), pp. 4633–4639. ISSN: 03605442. DOI: 10.1016/j.energy.2011.04.014. URL: http://dx.doi.org/10.1016/j.energy.2011.04.014.

[112] Pengfei Jie, Neng Zhu, and Deying Li. "Operation optimization of existing district heating systems". In: *Applied Thermal Engineering* 78 (2015), pp. 278–288. ISSN: 13594311. DOI: 10.1016/j.applthermaleng.2014.12.070. URL: http://dx.doi.org/10.1016/j.applthermaleng.2014.12.070.

[113] Elisa Guelpa, Giulia Barbero, Adriano Sciacovelli, and Vittorio Verda. "Peak-shaving in district heating systems through optimal management of the thermal request of buildings". In: *Energy* 137 (2017), pp. 706–714. ISSN: 03605442. DOI: 10.1016/j.energy.2017.06.107. URL: https://doi.org/10.1016/j.energy.2017.06.107.

[114] K. Sartor, S. Quoilin, and P. Dewallef. "Simulation and optimization of a CHP biomass plant and district heating network". In: *Applied Energy* 130 (2014), pp. 474–483. ISSN: 03062619. DOI: 10.1016/j.apenergy.2014.01.097. URL: http://dx.doi.org/10.1016/j.apenergy.2014.01.097.

[115] M. Wetter, C. Van Treeck, L. Helsen, A. Maccarini, D. Saelens, D. Robinson, and G. Schweiger. "IBPSA Project 1: BIM/GIS and Modelica framework for building and community energy system design and operation - Ongoing developments, lessons learned and challenges". In: *IOP Conference Series: Earth and Environmental Science* 323.1 (2019). ISSN: 17551315. DOI: 10.1088/1755-1315/323/1/012114.

[116] Irina Gabrielaitiene, Benny Bøhm, and Bengt Sunden. "Evaluation of approaches for modeling temperature wave propagation in district heating pipelines". In: *Heat Transfer Engineering* 29.1 (2008), pp. 45–56. ISSN: 01457632. DOI: 10.1080/01457630701677130.

[117] K. Sartor and P. Dewalef. "Experimental validation of heat transport modelling in district heating networks". In: *Energy* 137 (2017), pp. 961–968. ISSN: 0360-5442. DOI: https://doi.org/10.1016/j.energy.2017.02.161. URL: https://www.sciencedirect.com/science/article/pii/S0360544217303444.

[118] Kévin Sartor, David Thomas, and Pierre Dewallef. "A comparative study for simulating heat transport in large district heating networks". In: *ECOS 2015 International Conference* (2015). URL: http://orbi.ulg.ac.be/request-copy/2268/183406/247807/?step=4{\&}token=7e8b59730f22b74d262334d8d99ae256{\&}id=1.

[119] B. van der Heijde, M. Fuchs, C. Ribas Tugores, G. Schweiger, K. Sartor, D. Basciotti, D. Müller, C. Nytsch-Geusen, M. Wetter, and L. Helsen. "Dynamic equation-based thermo-hydraulic pipe model for district heating and cooling systems". In: *Energy Conversion and Management* 151.July (2017), pp. 158–169. ISSN: 01968904. DOI: 10.1016/j.enconman.2017.08.072. URL: http://dx.doi.org/10.1016/j.enconman.2017.08.072.

[120] Kevin Sartor and Pierre Dewallef. "Optimized Integration of Heat Storage Into District Heating Networks Fed By a Biomass CHP Plant". In: *Energy Procedia* 135 (2017). 11th International Renewable Energy Storage Conference, IRES 2017, 14-16 March 2017, Düsseldorf, Germany, pp. 317–326. ISSN: 1876-6102. DOI: https://doi.org/10.1016/j.egypro.2017.09.

523. URL: https://www.sciencedirect.com/science/article/pii/S1876610217346283.

[121] Michael Wetter, Wangda Zuo, Thierry S. Nouidui, and Xiufeng Pang. "Modelica Buildings library". In: *Journal of Building Performance Simulation* 7.4 (2014), pp. 253–270. ISSN: 19401493. DOI: 10.1080/19401493.2013.765506.

[122] Sartor Kevin. *Développement d'un outil de simulation et d'analyse technico-économique et environnementale d'un réseau de chaleur*. Accessed: 2020-10-28. 2018. URL: http://hdl.handle.net/2268/229271.

[123] SPF Economie, DG Statistique, and information économique. "Votre commune en chiffres: Herstal". In: (2012), p. 18. URL: http://ng3.economie.fgov.be/ni/municipalkeyfigures/FR/slide/slide{_}62051.pdf.

[124] Intradel. *Quand nos déchets deviennent source d'énergie*. http://www.uvelia.be/index.php?page=introduction. 2021.